



ICHA 2018

HARMFUL ALGAE 2018 – FROM ECOSYSTEMS TO SOCIO-ECOSYSTEMS

PROCEEDINGS OF THE 18TH INTERNATIONAL CONFERENCE ON HARMFUL ALGAE

21-26 October 2018, Nantes, France



Intergovernmental
Oceanographic
Commission

ISBN 978-87-990827-7-3

HARMFUL ALGAE 2018 – FROM ECOSYSTEMS TO SOCIO-ECOSYSTEMS

PROCEEDINGS OF THE 18TH INTERNATIONAL CONFERENCE ON HARMFUL ALGAE

21-26 October 2018, Nantes, France

Editor: Philipp Hess (Ifremer)

Graphic design : MCI France

Lay-out : H  l  ne Parfait (Ifremer)

Published by the International Society for the Study of Harmful Algae (ISSHA) and the Institut Francais de Recherche pour l'Exploitation de la Mer (Ifremer), in cooperation with the Intergovernmental Oceanographic Commission of the United Nations Educational, Scientific and Cultural Organization (IOC/UNESCO).

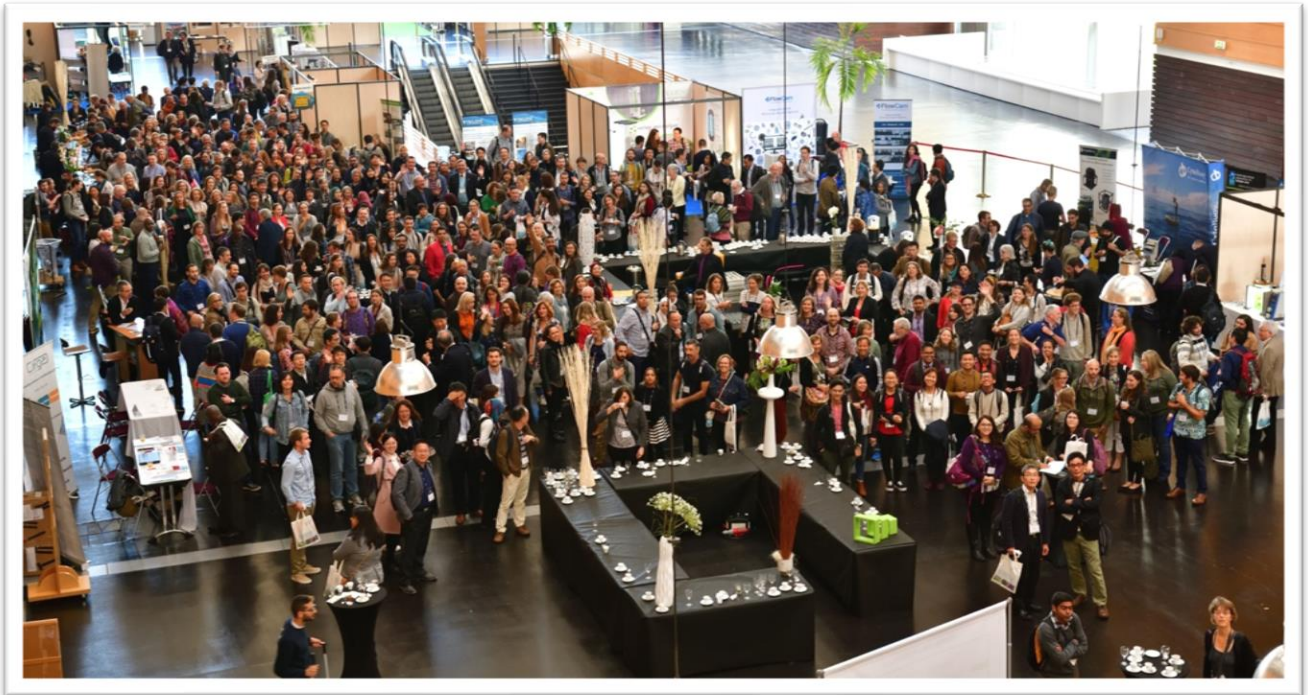
For bibliographic purposes, this document should be cited as follows:

Ph. Hess [Ed]. 2020. *Harmful Algae 2018 – from ecosystems to socioecosystems. Proceedings of the 18th Intl. Conf. on Harmful Algae*. Nantes. International Society for the Study of Harmful Algae. 214 pages. ISBN: 978-87-990827-7-3.

DISCLAIMER

Authors are responsible for the choice and the presentation of the facts contained in signed articles and for the opinions expressed therein, which are not necessarily those of ISSHA, IOC/UNESCO or Ifremer and do not commit these organizations.

The designations employed and the presentation of material throughout this publication do not imply the expression of any opinion whatsoever on the part of Ifremer, ISSHA or UNESCO concerning the legal status of any country, territory, city or area or of its authorities or concerning the delimitation of its frontiers or boundaries.



ICHA
2018
21 - 26 OCTOBER
NANTES, FRANCE

THE 18TH INTERNATIONAL CONFERENCE
ON HARMFUL ALGAE

The logo for ICHA 2018 features a stylized graphic of colorful dots (red, green, blue) arranged in a cluster to the left of the text. The text is in a clean, sans-serif font, with 'ICHA' and '2018' in large blue letters, and the dates and location in smaller blue letters. Below this, the full name of the conference is written in a smaller, all-caps blue font.

Hosted by

Institut Français de Recherche pour l'Exploitation de la Mer (Ifremer)

Convener

Philipp Hess, Ifremer Centre Atlantique, Nantes, France

Under the auspices of

The International Society for the Study of Harmful Algae (ISSHA)

COMMITTEES

Local organizing committee

Anthony MASSE

Université de Nantes, France

Maud LEMOINE

Ifremer, France

Sophie PILVEN

Ifremer, France

Gaël BOUGARAN,

Ifremer, France

Patricia THIBAUT-PRALIN

Ifremer, France

Véronique SECHET

Ifremer, France

Hélène PARFAIT

Ifremer, France

Philipp HESS

Ifremer, France

Zouher AMZIL

Ifremer, France

Scientific Committee (reviewers underlined)

Allan CEMBELLA

Alfred-Wegener-Institut, Germany

Claudia WIEGAND

Université de Rennes 1, France

Amel LATIFI

Aix Marseille Université, France

Clémence GATTI

Institut Louis Malardé, France

Anne THEBAULT

Agence nationale de sécurité sanitaire de l'alimentation, de l'environnement et du travail, France

Damien TRAN

Université de Bordeaux, France

Annick WILMOTTE

Université de Liège, Belgium

Delphine LATOUR

Université Blaise-Pascal de Clermont-Ferrand, France

Anthony MASSE

Université de Nantes, France

Felipe ARTIGAS

Université Littoral Côte d'Opale, France

Benjamin MARIE

Muséum National d'Histoire Naturelle, France

Gaël BOUGARAN

Ifremer, France

Catherine BELIN

Ifremer, France

Hélène HÉGARET

Université de Brest, France

Catherine DREANNO

Ifremer, France

Jean-François HUMBERT

Université Pierre et Marie Curie, France

Catherine QUIBLIER

Museum National d'Histoire Naturelle, France

Jean-Luc ROLLAND

Ifremer, France

Cécile BERNARD

Museum National d'Histoire Naturelle, France

Jordi MOLGO

Institut des Neurosciences Paris-Saclay, France

Juliette FAUCHOT

Université de Caen, France

Laure GUILLOU

Station biologique de Roscoff, France

Marc SOURISSEAU

Ifremer, France

Marie BONNIN

*Institut de Recherche pour le Développement,
France*

Marie-Yasmine DECHRAOUI-BOTTEIN

International Atomic Energy Agency, Monaco

Mathilde PALUSSIÈRE

*DGAI/Bureau des Produits de la Mer et de l'Eau
Douce, France*

Maud LEMOINE

Ifremer, France

Mélanie ROUE

*Institut de Recherche pour le Développement,
France*

Mireille CHINAIN

Institut Louis Malardé, France

Mohamed LAABIR

Université de Montpellier, France

Muriel GUGGER

Institut Pasteur, France

Myriam BORMANS

Université de Rennes 1, France

Nathalie ARNICH

*Agence nationale de sécurité sanitaire de l'alimen-
tation, de l'environnement et du travail, France*

Nicolas CHOMERAT

Ifremer, France

Philipp HESS

Ifremer, France

Philippe SOUDANT

Université de Brest, France

Raffaele SIANO

Ifremer, France

Rodolphe LEMÉE

*Observatoire océanologique de Villefranche sur
Mer, France*

Romulo ARAOZ

Commissariat à l'Energie Atomique, France

Ronel BIRÉ

*Agence nationale de sécurité sanitaire de l'alimen-
tation, de l'environnement et du travail, France*

Sophie PARDO

Université de Nantes, France

Valérie FESSARD

*Agence nationale de sécurité sanitaire de l'alimen-
tation, de l'environnement et du travail, France*

Véronique MARTIN-JEZEQUEL

Université de Nantes, France

Véronique SECHET

Ifremer, France

Zouher AMZIL

Ifremer, France

International Advisory Board (reviewers underlined)

Aifeng LI

China

Allan CEMBELLA

Germany

Ana GAGO

Spain

Asma HAMZA

Tunisia

Bastiaan Willem IBELINGS

Switzerland, Netherlands

Beatriz REGUERA*

Spain

Charles LUGOMELA

Tanzania

Christine BAND-SCHMITT

Mexico

Don ANDERSON

USA

Emanuela TESTAI

Italy

Esther GARCÈS*

Spain

Grant PITCHER

South Africa

Gustaaf HALLEGRAEF*

Australia

Henrik ENEVOLDSEN*

Denmark

Ian JENKINSON*

China, France

Lincoln MACKENZIE*

New Zealand

Lirong SONG

China

Luis BOTANA

Spain

Luis PROENCA

Brazil

Marie-Yasmine

DECHRAOUI-BOTTEIN

Monaco

Mitsunori IWATAKI

Japan

Patricia TESTER

USA

Philipp HESS*

France

Rainer KURMAYER

Austria

Rencheng YU

China

Robin RAINE*

Ireland

Sandra SHUMWAY

USA

Songhui LU

China

Sun Ju KIM

Republic of Korea

Takeshi YASUMOTO

Japan

Triantafyllos KALOUDIS

Greece

Vera TRAINER*

USA

**members of the ISSHA Council
Conference Organizing Sub-
committee*

ADDITIONAL PROCEEDINGS REVIEWERS

Adriana ZINGONE

*Stazione Zoologica Anton
Dohrn Napoli, Italy*

Antonella PENNA

*Università degli Studi di
Urbino Carlo Bo, Italy*

Bengt KARLSON

*Swedish Meteorological and
Hydrological Institute,
Sweden*

Elisa BERDALET

*Institut de Ciències del Mar,
Spain*

Fran VAN DOLAH

*National Oceanic and
Atmospheric
Administration, USA*

Keith DAVIDSON

*Scottish Association for
Marine Science, Scotland*

Leila BASTI

*Tokyo University of Marine
Science and Technology,
Japan*

Luiz MAFRA

*Universidade Federal do
Paraná, Brazil*

Øjvind MOESTRUP

*University of Copenhagen,
Denmark*

Patrice GUILLOTREAU

*Université de Nantes,
France*

Po Teen LIM

*University of Malaya,
Malaysia*

Raphael LE GARREC

*Université de Bretagne
Occidentale, France*

Raphe KUDELA

*University of California,
Santa Cruz, USA*

Robert HATFIELD

*Centre for Environment,
Fisheries and Aquaculture
Science, UK*

Urban TILLMANN

*Alfred Wegener Institute,
Germany*

Uwe JOHN

*Alfred Wegener Institute,
Germany*

Wayne LITAKER

*National Oceanic &
Atmospheric
Administration, USA*

PARTNERSHIPS

Bronze sponsors

French Research Project ANR OSS-Cyano
Marine Drugs
McLane
Phytoxigene
Synoxis Algae

Other sponsors

Cambridge Isotope Laboratories
Cifga
Cytobuoy B.V.
Fluid Imaging Technologies
IKA Werke GmbH & Co. KG
Jerico-Next
Marine Institute
Merck KGaA
Novakits Abraxis
Photon Systems Instruments
Statera Environmental
Station Ifremer Concarneau

French Institutional Support

Institut Français de Recherche pour l'Exploitation de la Mer (Ifremer)
GdR Phycotox (Ifremer – CNRS 3569)
Agence Française pour la Biodiversité (AFB)
Commissariat à l'énergie atomique et aux énergies alternatives (CEA)
Museum National d'Histoires Naturelles
Nantes Métropole
Université Bretagne Loire
Institut Universitaire Mer et Littoral (IUML)

International Institutional Cooperation

International Atomic Energy Agency (IAEA)
U.S. National Institute of Environmental Health Sciences (NIEHS)
Scientific Committee on Oceanic Research (SCOR)
U.S. National Oceanic and Atmospheric Administration (NOAA)

EDITOR'S PREFACE

The 18th International Conference on Harmful Algae (ICHA) was held at La Cité des Congrès, Nantes, France, 21-26 October 2018. After the last conference in the same spot 25 years earlier, this was the second time the conference was convened in France. The conference was hosted by Ifremer and was born from an initiative of the French marine HAB research community (GdR PHYCOTOX), with strong support by its sister organization for freshwater cyanobacteria (GIS Cyano). The theme of the conference “From Ecosystems to Socioecosystems” was chosen to stress the need to integrate natural sciences with social sciences to increase the impact of our science on society. A short summary of the event and a scientific summary have already been published in *Harmful Algae News* (pages 1-8, issue 62; June, 2019).

Compared to previous conferences, this edition has enjoyed record attendance (709 participants from 64 countries) and scientific contributions (613 abstracts, with 255 oral presentations and 358 posters, 45 of which were also presented as ignite talks). Out of nine plenary lectures, five were given by scientists not usually attending this conference. This is a testimony to our efforts in soliciting scientists from adjacent scientific fields. They gave us insights into recent developments regarding linkages between climate change and eutrophication (Anna Michalak), in human toxicology (Thomas Hartung), trait-based ecology (Elena Litchman), natural products chemistry (William Gerwick) and remediation (Eric Jeppesen). The four plenaries directly related to HAB science focused on HAB parasites (Laure Guillou), Ciguatera (Mireille Chinain), chemical ecology (Allan Cembella, Yasumoto award lecture 1) and analytical measurements (Michael Quilliam, Yasumoto award lecture 2). The other lectures, like the posters, were subdivided into 21 themes, 45 oral sessions and three lunch time seminars. Credit for this scientifically diverse and inspiring program largely goes to our

national scientific committee built on GdR Phycotox and GIS Cyano (43 people). Overall feedback on this ambitious program was very positive (87 participants (12%) replied to our feedback questionnaire: 80% of the respondents found the scientific program good or excellent). We heavily drew on the ISSHA council, our national scientific committee and other key scientific members of our community for our 53 session chairs – again, thank you all for helping us in this event!

I also acknowledge the help of our reviewers of the 47 submissions to the proceedings (> 90% reviewed by 2 referees). A frustrating aspect of conference proceedings is the change in publication attitude of conference attendees. While most participants contributed to the conference proceedings in 1989 (100 contributions), less than 8% of contributions to the conference in 2018 resulted in 47 submissions to the proceedings. This lack in participation to the proceedings obviously results from the need for “measurable outputs” in form of peer-reviewed papers in journals indexed in the “Web of Science”. Still, it also means that conference proceedings no longer actually reflect the science presented at the conference. For a comprehensive overview of the conference, please download the [final programme](#) or the [abstract book](#).

Participation and number of contributions has approximately doubled since the last conference in Nantes in 1993. The fourth *International Conference on Toxic Marine Phytoplankton* (26-30 June 1989, Lund, Sweden) was the first one to extend coverage beyond dinoflagellates to all kinds of marine microalgae, including benthic or epiphytic species. Since that time, the breadth of the conference has gradually increased which partly explains the increased participation. For instance, the 2018 edition also had a very strong component on cyanobacterial ecology, toxins and remediation. Another interesting example is the report of the structure of Ciguatoxin (= CTX1B = P-CTX1) by

Takeshi Yasumoto, which was one of the five contributions on *Gambierdiscus* and its toxins in 1989; comparatively, there were 49 contributions to this theme at the conference 30 years later, which is in line with recent IOC prioritization of this problem. Similarly, 7 contributions dealt with effects of HABs on aquatic organisms in 1989, shortly after a major bloom of *Chrysochromulina polyleptis* in the Skagerrat, while 23 contributions dealt with this theme in 2018, indicating an increased interest in this topic over time. The most striking paradox comparing these two conferences is that the 1989 event finishes its overview (Max Taylor, page 532 of the proceedings) with a major question dealt with during the conference: Are HABs increasing and are they spreading? As outlined by Gustaaf Hallegraeff in its HAN article (HAN 62, pages 9-11), 139 abstracts of the 2018 Nantes meeting dealt with the same question, formulated in the context of climate change. Thus, three major topics in the 2020s (ciguatera, fish kills and evolution of HABs in the context of climate change) have been subject of discussion by our community for several decades. However, there were also many more recent developments discussed at the conference, drawing on modern techniques. The three lunch time seminars were dedicated to (i) sensors and drones for surveillance of freshwater HABs, (ii) *in-situ* monitoring tools for marine HAB species, such as the *Imaging Flow CytoBot*, and (iii) molecular biology techniques such as qPCR for monitoring of species difficult to identify with light microscopy. These seminars were a clear testimony to our increased capacity to detect and monitor an ever wider range of species more efficiently.

Recent advances in the Omics field (43 contributions) also led to significant progress reported at this conference on toxin discovery (> 100 prymnesins & cyanotoxins), our understanding in toxin biosynthesis (domoic acid & polyketides) and interactions of HAB species with aquatic animals (copepodamides).

Overall, the conference was also financially viable since income provided by participants (72 %) and sponsors (20 %) covered 92 % of total costs incurred (455k€), while Ifremer recovered all direct expenses, excluding staff time. Thanks also go to H  l  ne Parfait, the secretary of the Phycotoxins Laboratory (Ifremer, Nantes), and C  cile Salaun (administrative project officer, Ifremer, Brest) who both accompanied me in managing the professional conference organizer and budgets on a daily basis. There was a reasonable equilibrium between public (14) and private (12) sponsors, who I thank for balancing our budget. Many, many thanks also to our Phycotoxins team in Nantes who lovingly helped during countless hours with logistics during the preparation and the event itself. Finally, I'd like to express my gratitude to our directorate at Ifremer for taking on the financial risk of this undertaking as early as 2014, at a time when nothing was known of Zika-virus, French protests against carbon taxes (yellow vests) or Corona-virus, to name but some of the risks conference organizers have to deal with. We wish our Mexican and Central American colleagues all the best of courage, patience and luck for the organization of the 19th ICHA in La Paz, which will be held in 2021 due to latest developments.

TABLE OF CONTENTS

Biomolecular methods for HAB species 13

- Satellite symposium on morpho-molecular methods to study harmful algae
Kenneth Neil Mertens, Nicolas Chomérat, Urban Tillmann, Dave Clarke, Lincoln MacKenzie, Kirsty F. Smith 14
- QPCR Assay for amphidomataceae: state of the art and new challenges
Urban Tillmann, Stephan Wietkamp, Haifeng Gu, Dave Clarke, Kirsty Smith 15
- PCR assays for the detection of ASP, DSP, PSP and AZP toxigenic producing phytoplanktonic species in Irish coastal waters
Dave Clarke, Rafael Salas, Paula Hynes, Annaclare McCarthy, Debbie Walsh, Joe Silke 19
- Application of gel-formatted qPCR assays for rapid diagnosis of shellfish toxin producing and fish-killing micro-algae in seawater
Lincoln MacKenzie, Jonathan Banks, Kirsty Smith..... 25

Eco-physiology & cellular biology of harmful algae and cyanobacteria 29

- The role of phosphatase activities during a bloom of *Ostreopsis cf. ovata* in the northern Adriatic Sea
Stefano Accoroni, Marisa Pasella, Tiziana Romagnoli, Emanuela Razza, Cecilia Totti, Neil Thomas William Ellwood 30
- Effects of selenium and light on the growth of the Mediterranean neurotoxic dinoflagellate *Gymnodinium catenatum* HW Graham responsible for recurrent PSP outbreaks in coastal waters of Morocco
HichamAboualaalaa, Benlahcen Rijal leblad, Hassane Riadi, Mouna Daoudi, Naima Maamour, Mohamed Marhraoui, Mohamed Ouelad Abdellah, Mohamed Laabir..... 34

Biological oceanography and limnology of HABs 37

- Algal blooms: how are they harming models used for climate management?
Ian R. Jenkinson, Elisa Berdalet, Wei-Chun Chin, Haibing Ding, Jizhou Duan, Florence Elias, Zhuo Li, Xavier Mari, Laurent Seuront, Jun Sun, Oliver Wurl, Tim Wyatt..... 38
- Operational tools to improve the prediction capacity of the HABs in Galician mollusc production areas
Yolanda Pazos, F.M BellasAlaez, Luis González Vilas, Jesús M T. Palenzuela 42
- Combination of machine learning methodologies and imaging-in-flow systems for the automated detection of Harmful Algae
Guillaume Wacquet, Alain Lefebvre, Camille Blondel, Arnaud Louchart, Philippe Grosjean, Nadine Neaud-Masson, Catherine Belin, Luis Felipe Artigas 46
- Automated techniques to follow the spatial distribution of *Phaeocystis globosa* and diatom spring blooms in the English Channel and North Sea
Arnaud Louchart, Reinhoud de Blok, Elisabeth Debuschere, Fernando Gómez, Alain Lefebvre, Fabrice Lizon, Jonas Mortelmans, Machteld Rijkeboer, Klaas Deneudt, Arnold Veen, Guillaume Wacquet, François G. Schmitt, Luis Felipe Artigas 51
- Predicting bloom initiation on the Texas (USA) coast: Combining satellite imagery with an individual-based model
Darren W. Henrichs, Michelle C. Tomlinson, Lisa Campbell 55

Ecology – from the ecological niche to population dynamics and biogeography 59

- Revealing the distribution and relative abundance of HABs species in the South China Sea using metagenomics analysis
Kieng Soon Hii, Ing Kuo Law, Winnie Lik Sing Lau, Zhen Fei Lim, Zhaohe Luo, Haifeng Gu, Chui Pin Leaw, Po Teen Lim..... 60

Relationships between environmental conditions and phytoplankton in the Mellah lagoon (south western Mediterranean, Algeria), with an emphasis on HAB species <i>Mohamed Anis Draredja, Hocine Frihi, Chahinez Boualleg, Anne Goffart & Mohamed Laabir</i>	64
Environmental factors leading to the occurrence of a harmful alga, <i>Vicicitus globosus</i> , in the center of the Seto-Inland Sea, Japan <i>Shizuka Ohara, Ryoko Yano, Etsuko Hagiwara, Hiroyuki Yoneyama, Setsuko Sakamoto, Kazuhiko Koike</i>	68
Diversity of <i>Pseudo-nitzschia H. Pergallo, 1900</i> along the Slovenian coast, Adriatic Sea, with insights into seasonality, toxicity and potential introductions <i>Timotej Turk Dermastia, David Stanković, Janja Francé, Magda Tušek Žnidarič, Andreja Ramšak, Patricija Mozetič</i>	72
Distribution patterns of toxic epibenthic microalgae <i>Prorocentrum lima</i> in the Gulf of Gabès (South-eastern Mediterranean Sea) <i>Lamia Dammak Walha, Fatma Abdmouleh, Moufida Abdennadher, Asma Hamza, Cherif Sammari</i>	76
Are harmful epibenthic dinoflagellates proliferating in Southern Mediterranean? A case study of the Bizerte Bay and Lagoon (North of Tunisia, Southern Mediterranean Sea) <i>Hela Ben Gharbia, Mohamed Laabir, Abdelouahed Ben Mhamed, Sonia KM Gueroun, Ons Kéfi - Daly Yahia</i>	80
Bloom of <i>Pyrodinium bahamense</i> in the Pacific coastal waters of Guatemala. <i>Josué García-Pérez, Leonel Carrillo-Ovalle, Maribelle Vargas-Montero, Elisa Blanda</i>	84
<i>Pseudo-nitzschia</i> biogeography combining Real-Time PCR analysis and oceanographic models to investigate 13 years trends of ASP toxicity <i>Angéline Lefran, Beatrix Siemering, Caroline Cusack, Dave Clarke, Joe Silke, Rafael Salas</i>	87
An exceptional summer bloom of <i>Dinophysis acuta</i> in a Chilean fjord <i>Patricio A. Díaz, Iván Pérez-Santos, Angela Baldrich, Gonzalo Álvarez, Francisco Rodríguez, Paulina Montero, Gabriela Igor, Giovanni Daneri, Miriam Seguel, Leonardo Guzmán, Gemita Pizarro, Luis Norambuena, Jorge I. Mardones, Pamela Carbonell, Beatriz Reguera</i>	91
Eco-physiology & cellular biology of harmful algae and cyanobacteria	95
Diversity and distribution of Harmful Algal Bloom (HAB) species in Coastal Waters of Ghana <i>Denutsui Dzifa, Marina Cabrini, Adotey K. Dennis, Gyingiri Achel, Kuranchie-Mensah H, Palm Linda, Beran Alfred, Serfor-Armah Yaw</i>	96
Taxonomy	100
Morphological, molecular and toxicological data on <i>Ostreopsis cf. siamensis</i> (Dinophyceae) from the Atlantic Iberian Peninsula <i>Helena David, Aitor Laza-Martínez, Mariana Santos, Maria Filomena Caeiro, Luciana Tartaglione, Fabio Varriale, Carmela Dell'Aversano, Antonella Penna, Ana Amorim</i>	101
Morphological and phylogenetic characterization of <i>Amphidinium</i> spp. (Dinophyceae) strains from the Bay of Biscay and the Mediterranean Sea <i>Louis-Josselin Lavier-Aydat, Sergio Seoane, Aitor Laza-Martínez</i>	105
First report of <i>Alexandrium</i> affine in Uruguay; molecular, morphological and toxicological study of a bloom during summer 2017 <i>Silvia M. Méndez, Francisco Rodríguez, Ana Martínez, Pilar Riobó, Maribelle Vargas-Montero</i>	109
Toxin analysis – Novel detection methods	113
Analysis of PSP toxins in Moroccan shellfish by MBA, HPLC and RBA Methods: Monitoring and Research <i>R. Abouabdellah, A. Bennouna, M.-Y. Dechraoui Bottein, H. Alkhatib, A. Mbarki, N. Imzilen, M. Alahyane</i>	114
Bioassays for detection and identification of cyclic imine toxins <i>Rómulo Aráoz, Jordi Molgó, Denis Servent</i>	118
Sea turtle mortality in El Salvador: Analysis by receptor binding assay confirms saxitoxin findings <i>Oscar A. Amaya, Marie-Yasmine Dechraoui Bottein, Rebeca Quintanilla, Gerardo Ruíz</i>	122

Boronate techniques for clean-up and concentration of the vic-diol-containing tetrodotoxins from shellfish <i>Daniel G. Beach, Elliott S. Kerrin, Pearse McCarron, Jane Kilcoyne, Sabrina D. Giddings, Thor Waaler, Thomas Rundberget, Ingunn A. Samdal, Kjersti E. Løvberg, Christopher O. Miles</i>	125
Risk assessment for algal and cyanobacterial toxins.....	129
Monitoring the invasive cyanobacterium <i>Cylindrospermopsis raciborskii</i> – a case of dispersion into northern Portuguese freshwater systems <i>Cristiana Moreira, Cidália Gomes, Vitor Vasconcelos, Agostinho Antunes</i>	130
Ciguatera and related benthic HAB organisms and toxins	134
Application of a Receptor Binding Assay to the Analyses of Ciguatera toxin in Reef fish, Thailand <i>Wutthikrai Kulsawat, Boonsom Porntepkasemsan, Phatchada Nochit</i>	135
Global distribution of the genera <i>Gambierdiscus</i> and <i>Fukuyoa</i> <i>Patricia. Tester, Lisa Wickliffe, Jonathan Jossart, Lesley Rhodes, Henrik Enevoldsen, Masao Adachi, Tomohiro Nishimura, Francisco Rodriguez, Mireille Chinain, Wayne Litaker</i>	138
Medical applications of algae, cyanobacteria and their toxins.....	144
Gambierol enhances evoked quantal transmitter release and blocks a potassium current in motor nerve terminals of the mouse neuromuscular junction <i>Jordi Molgó, Sébastien Schlumberger, Makoto Sasaki, Haruhiko Fuwa, M. Carmen Louzao, Luis M. Botana, Denis Servent, Evelyne Benoit</i>	145
Impact of microalgae/cyanobacteria on aquatic organisms (incl. fish kills and shellfish mortalities)	149
Contribution of the HAB _f INDEX for fish farm's risk analysis <i>Alejandro Clément, Thomas Husak, Sofia Clément, Francisca Muñoz, Marcela Saldivia, Carmen G. Brito, Roberta Crescini, Nicole Correa, Karenina Teiguel, César Fernández, Gustavo Contreras, Stephanie Saez</i>	150
Harmful Algal bloom species associated with massive Atlantic salmon mortalities while transported through the Gulf of Penas, southern Chile <i>Carolina Toro, Cesar Alarcón, Hernán Pacheco, Pablo Salgado, Máximo Frangopulos, Francisco Rodríguez, Gonzalo Fuenzalida, Roberto Raimapo, Gemita Pizarro and Leonardo Guzmán</i>	154
New major events & exploitation of longtime series (monitoring & case studies).....	158
Occurrence of Yessotoxins in Canadian Shellfish from 2012-2018 <i>Wade Rourke, Nicola Haigh</i>	159
Comprehensive study of the occurrence and distribution of lipophilic marine toxins in shellfish from production areas in Chile <i>Benjamín A. Suárez-Isla, Fernanda Barrera, Daniel Carrasco, Leonardo Cigarra, Américo M. López-Rivera, Ignacio Rubilar, Carmen Alcayaga, Víctor Contreras and Miriam Seguel</i>	163
Ichthyotoxic skeleton-forming silicoflagellates in British Columbia, Canada; Results from the Harmful Algae Monitoring Program, 1999 – 2017 <i>Nicola Haigh, Tamara Brown, and Devan Johnson</i>	167
New tools (omics, lab-on-a-chip, ecotron...)	171
Characterisation of azaspiracid producers in New Zealand waters using molecular tools <i>Julie Steynen, Kirsty Smith, Lesley Rhodes</i>	172
The Phosphopantetheinyl Transferases in Dinoflagellates <i>Ernest P Williams, Tsvetan R Bachvaroff, and Allen R Place</i>	176
Life without Chargaffs Rules: Mapping 5-hydroxymethyluracil in genomic DNA <i>Allen R Place, Ernest P Williams, Tsvetan R Bachvaroff and Robert Sabatini</i>	181

Mitigation of HABs and water treatment technologies 185

- Development of an information sharing system for broad harmful algal bloom distributions
Sou Nagasoe, Akiko Maeda, Takahisa Tokunaga, Yukihiro Matsuyama, Kazumaro Okamura, Kazuko Ichihashi, Katsunori Kimoto..... 186

Socio-economic impacts of HABs 190

- Saxitoxin and the Cold War
Patricia A. Tester, Julie Matweyou, Brian Himelbloom, Bruce Wright, Steven R. Kibler, R. Wayne Litaker 191
- Integrated management of Harmful Algal Blooms (HABs) along the French Channel area. A system approach to assess and manage socio-economic impacts of HABs
Pascal Raux, José Pérez Agundez and Sarra Chenouf 195

Optical sensors and drone systems for the monitoring of harmful blooms 199

- Development of a low cost optical sensor and of a drone system for the monitoring of cyanobacteria in freshwater ecosystems
Gabriel Hmimina, Kamel Soudani, Florence Hulot, Louise Audebert, Stéphane Buttigieg, Patrice Chatelier, Simon Chollet, Beatriz Decencièrre, François Derkx, Catherine Freissinet, Yi Hong, Bruno Lemaire, Alexis Millot, Aurélien Perrin, Catherine Quiblier, Gonzague Six, Jean-Luc Sorin, Kevin Tambosco, Viet Tran Khac, Brigitte Vinçon-Leite, Jean-François Humbert 200
- Coupling high-frequency measurements and predictive modelling for monitoring and an early warning system of cyanobacteria blooms..... 204
Brigitte Vinçon-Leite, Francesco Piccioni, Yi Hong, Viet Tran Khac, Bruno J. Lemaire, Denis Furstenau Plec, Chenlu Li, Philippe Dubois, Mohamed Saad, Gabriel Hmimina, Kamel Soudani, Catherine Quiblier, Kevin Tambosco, Gonzague Six, Catherine Freissinet, Brigitte Decencièrre, Jean-François Humbert 204

Networking activities around HABs: global HAB, global HAB status report, ICES-WGs and other initiatives 208

- Overview of New Zealand HAB species and HAEDAT Events, with a comparison to Australian events
Enora Jaffrezic, Lesley Rhodes, Lincoln Mackenzie, Laura Schweibold, Gustaaf Hallegraef 209



Biomolecular methods for HAB species

Satellite symposium on morpho-molecular methods to study harmful algae

Kenneth Neil Mertens¹ *, Nicolas Chomérat¹, Urban Tillmann², Dave Clarke³, Lincoln MacKenzie⁴, Kirsty F. Smith⁴

¹ Ifremer, LER BO, Station de Biologie Marine, Place de la Croix, BP40537, F-29185 Concarneau CEDEX, France; ² Alfred Wegener Institute, Am Handelshafen 12, 27570 Bremerhaven, Germany;

³ Marine Institute, Rinville, Oranmore, Galway H91 R673, Ireland;

⁴ Cawthron Institute, 98 Halifax Street East, Nelson, 7010 New Zealand.

* corresponding author's email: Kenneth.Mertens@ifremer.fr

Abstract

During ICHA 2018, a satellite symposium was organised to bring together scientists working on harmful algae, with an interest to develop molecular methods, such as probes and quantitative polymerase chain reaction (qPCR), and a focus on the genera *Azadinium*, *Alexandrium* and *Pseudo-nitzschia*. 261 persons subscribed to the symposium. There was a strong focus on discussing methodological issues.

Keywords: qPCR, toxigenic

Three studies were presented during the satellite symposium, held during ICHA 2018 on morpho-molecular methods, and all three are summarised in these proceedings.

Tillmann et al. (2020) evaluated the state of the art of Amphidomatacean qPCR assays, and highlighted the importance of continuous reassessment of the assays, given the increasing number of newly identified taxa in this group.

Clarke et al. (2020) demonstrated the use of PCR assays for several toxigenic species occurring in Irish waters, including three *Pseudo-nitzschia* species, one *Azadinium*, one *Amphidoma*, two *Dinophysis* and one *Alexandrium*, which allowed them to improve their risk assessment. Clarke et al. (2020) emphasized the need for continuous reassessment of the assays as well.

MacKenzie et al. (2020) presented qPCR assays in a solid-phase gel format that allow the rapid detection of harmful algal bloom (HAB) species in New Zealand waters. Although promising, the assays had variable performance, depending on the targeted species.

At least 261 persons participated in the satellite symposium, which shows the tremendous interest of HAB scientists in molecular probe and qPCR techniques, technologies which will surely continue to develop rapidly.

Acknowledgements

This workshop was financed by the Royal Society of New Zealand Catalyst: Seeding programme, grant number 16-CAW-004-CSG (“Cyst Risk: Assessment of Risk of Benthic Life Stages of Toxic Dinoflagellates to the Seafood Sectors of New Zealand and France”)

References

Clarke, D., Salas, R., Hynes, P. McCarthy, A., Walsh, D., Silke, J. (2020). Proceedings ICHA 2018.

MacKenzie, L., Banks, J., Smith, K. (2020). Proceedings ICHA 2018.

Tillmann, U., Wietkamp, S., Gu, H., Clarke, D., Smith, K. (2020). Proceedings ICHA 2018

qPCR Assay for amphidomataceae: state of the art and new challenges

Urban Tillmann^{1*}, Stephan Wietkamp¹, Haifeng Gu², Dave Clarke³, Kirsty Smith⁴

¹ Alfred Wegener Institute, Am Handelshafen 12, 27570 Bremerhaven, Germany;

² Third Institute of Oceanography, State Oceanic Administration, Xiamen 361005, China;

³ Marine Institute, Rinville, Oranmore, Galway H91R673, Ireland;

⁴ Cawthron Institute, Privat Bag 2, Nelson 7042, New Zealand.

* corresponding author's email: urban.tillmann@awi.de

Abstract

Azaspiracids (AZA) are a group of lipophilic toxins, which are produced by a few species of the marine nanoplanktonic dinoflagellate genera *Azadinium* and *Amphidoma* (Amphidomataceae). Amphidomataceae were found to be globally distributed in coastal waters and new areas of occurrence are regularly discovered. The AZA toxins accumulate mainly in shellfish and - when consumed by humans - may cause health problems. Given this serious threat, appropriate detection methods enabling a fast identification and quantification for these toxigenic species are needed. AZA-producing species are small and inconspicuous and difficult - if not impossible - to be identified by traditional microscopy. Therefore, a number of molecular detection and quantification assays have been developed and are in use. We here evaluate the current state of the art of amphidomatacean qPCR assays and identify new challenges, which are important to be continuously assessed for reliable qualitative and quantitative detection.

Keywords: *Azadinium*, *Amphidoma*, molecular detection, qPCR assays, ribotypes

Introduction

Amphidomataceae are a family of dinoflagellates which are known for the production of azaspiracids (AZA), a group of lipophilic polyketide toxins that can accumulate in shellfish and may cause human health problems (Twiner et al., 2014). Azaspiracids are a major problem in Ireland, where AZA concentrations in shellfish above the EU regulatory limit (0.16 µg g⁻¹ mussel flesh) are recurrently registered (Salas et al., 2011). The resulting long-lasting closures of shellfish farms lead to high economic losses and are a major threat for the Irish shellfish industry. In 2009, the first source organism of AZA, the small thecate dinoflagellate *Azadinium spinosum* was identified and described as a new species in a new genus within the family of Amphidomataceae (Tillmann et al., 2009). Since then, knowledge on the diversity of Amphidomataceae has increased rapidly, and currently there are 26 described species. Among the 13 Amphidomataceae species tested so far, only four have been found to produce AZA, i.e., *Az. spinosum*, *Az. poporum*, *Az. dexteroporum*, and *Amphidoma languida* (Krock et al., 2019), and based on phylogenetic data the toxigenic species do not represent a distinct clade (Tillmann et al., 2018). All species of Amphidomataceae show distinct morphological features, but morphological species identification in most cases requires

scanning electron microscopy. This, together with a high number of very similar and small non-toxic species in the group, makes routine detection and quantification of the toxigenic Amphidomatacean species in field samples challenging and almost impossible using light microscopy. Thus, other alternative and innovative methods are needed for a more routine and fast identification and enumeration of Amphidomataceae in field samples.

State of the art and new challenges

Card-fish probes using *in situ* hybridization are available for a few *Azadinium* species (Toebe et al., 2013), but have never been applied in the field, probably because of the complex sample treatment protocol.

In contrast, molecular qPCR assays for detection and quantification are now commonly used for a large number of toxic microalgae (e.g. Engesmo et al., 2018; Ruvindy et al., 2018) and a number of assays are also available for Amphidomataceae (**Tab. 1**). In 2016, Smith et al. designed one SYBR Green real-time PCR assay targeting the common intergenic transcribed spacer (ITS) regions of all species of *Azadinium* and *Amphidoma*.

Furthermore, species-specific TaqMan qPCR assays are available for four species: The non-toxicogenic *Az. obesum* and the toxicogenic species *Az. spinosum*, *Az. poporum* and *Am. languida* (Toebe et al., 2013; Wietkamp et al., 2019). These assays are now regularly used by the Marine Institute in Galway/Ireland, where the *Az. spinosum* assay is now an integrated part of the Irish monitoring program, which has recently undergone in-house validation and is now accredited to ISO 17025 standards. The assays have also been tested for the Scottish monitoring program (Paterson, 2018) and used in various field sample surveys, including the Puget Sound area (Kim et al., 2017), the Norwegian coast (Tillmann et al., 2018), Irish coastal waters (Wietkamp et al., 2019) or in Argentinean coastal waters (Tillmann et al., 2019). One general and major challenge of all qPCR assays is a reliable quantification (Bonk et al.,

microorganisms have been observed for a number of dinoflagellate species (Perini et al., 2011; Macé et al., 2018) and thus needs to be carefully assessed for Amphidomataceae as well. Variability of copy number for Amphidomataceae is not well known yet and definitely has to be determined using multiple strains and different physiological stages of toxicogenic species in the near future, as has been recently performed for *Amphidoma languida* (Wietkamp et al., 2019).

Another general problem and challenge of using the qPCR for detection and enumeration of target cells is the assay specificity, which needs to be extensively tested using non-target species and strains to reduce false positive signals. However, there is also the risk of false negative results. This is especially important in the Amphidomataceae, where new species and new strains are almost continuously discovered and established. When the

Table 1: Available real-time PCR assays for Amphidomataceae detection and quantification.

Target species	Target gene	Oligonucleotide type	Sequence (5'-3')	Product size (bp)	Reference
<i>Azadinium</i> and <i>Amphidoma</i> genera	ITS				
Amp240F		F-Primer	CAACTTTCAGCGACGGATGTCTCG	179	Smith <i>et al.</i> 2016
Amp418R		R-Primer	AAGCYRCWGGCATKAGAAGGTAGWGGC		
<i>Azadinium spinosum</i>	LSU				
Asp48F		F-Primer	TCGTCTTTGTGTCAGGGAGATG	72	Toebe <i>et al.</i> 2013
Asp120R		R-Primer	GGAAACTCCTGAAGGGCTTGT		
Aspin77T		TaqMan MGB probe	6FAM-CGCCAAAAGGACTCCT-MGB		
<i>Azadinium poporum</i>	LSU				
Apop62F		F-Primer	GATGCTCAAGGTGCCTAGAAAAGTC	68	Toebe <i>et al.</i> 2013
Apop148R		R-Primer	CCTGCGTGTCTGTTGCA		
Apop112		TaqMan MGB probe	6FAM-TTCCAGACGACTCAAAA-MGB		
<i>Azadinium obesum</i>	LSU				
Aob134F		F-Primer	AGG GAT CGA TAC ACAAAT GAG TAC TG	74	Toebe <i>et al.</i> 2013
Aob208R		R-Primer	AAA CTC CAG GGACAT GGT AGT CTT A		
Aob163		TaqMan MGB probe	6FAM-AAG ACA TTC GAC CTA CCG T-MGB		
<i>Amphidoma languida</i>	LSU				
Alan509F		F-Primer	CGGTTACAGGCGAGGAT	60	Wietkamp <i>et al.</i> 2019
Alan569R		R-Primer	GACATTCACCTCCGTGGAA		
		TaqMan MGB probe	6FAM-CTTCTGAGGACATGGTAAC-MGB		

2018). Quantification in qPCR is based on standard curves prepared using the DNA of target species cells and can either be dilution series of target DNA or of the amplified PCR product of the specific target gene. Therefore, any variability in these numbers (i.e. DNA copy number) between species and strains will bias the quantification of field populations (Galluzzi et al., 2010; Eckford-Soper and Daugbjerg, 2016; Nishimura et al., 2016). Intra- and inter-specific differences in the number of target molecules for the qPCR in the genome of

original assays were designed, the known species and available strains were quite limited compared to what we have just a few years later. For one of the toxicogenic species, *Az. poporum*, the qPCR assay was designed based on the only three Danish strains available at that time. With now more than 70 described strains, we know that *Az. poporum* has a very wide distribution, and a high intraspecific variability in sequence data with three major ribotypes and some significant further sub-groups is evident. The parent strains for the assay from

Denmark belong to ribotype A1 and there are significant differences to the other ribotypes. Variation also occurs in the large subunit (LSU) region of the rDNA, the target of the qPCR respective assay, where all other ribotypes have 1 – 3 base pair mismatches with the forward primer of the current specific *Az. poporum* assay (**Fig. 1 A**). Therefore, new primers and probes need to be tested in order to quantitatively catch all ribotypes of *Az. poporum* that we now are aware of.

The same problem becomes evident for another important toxigenic species, *Az. spinosum*. The qPCR assay was designed based on two strains from the North Sea, but in the meantime many new strains revealed intraspecific variability as well, and currently three ribotypes of *Az. spinosum* are defined. Importantly, not only the DNA sequences, but also AZA toxin profiles differ among ribotypes. Strains from ribotype A produce AZA-1, -2 and -33, strains from ribotype B produce either AZA-11

important toxigenic species. In this particular case, it may also be advised to specifically design new primers and probes, which enable the user to target ribotypes A and B (AZA producing strains), but not ribotype C (non-AZA producing strains).

Conclusion

In conclusion, the Amphidomataceae family, which includes only a few toxigenic species, is an obvious case, where molecular tools are needed for routine detection and quantification. A number of qPCR assays for this group have been published and are in use, but it is important to continuously assess those assays for reliable quantitative detection, especially in light of a still increasing number of newly identified species, strains and ribotypes in this group.

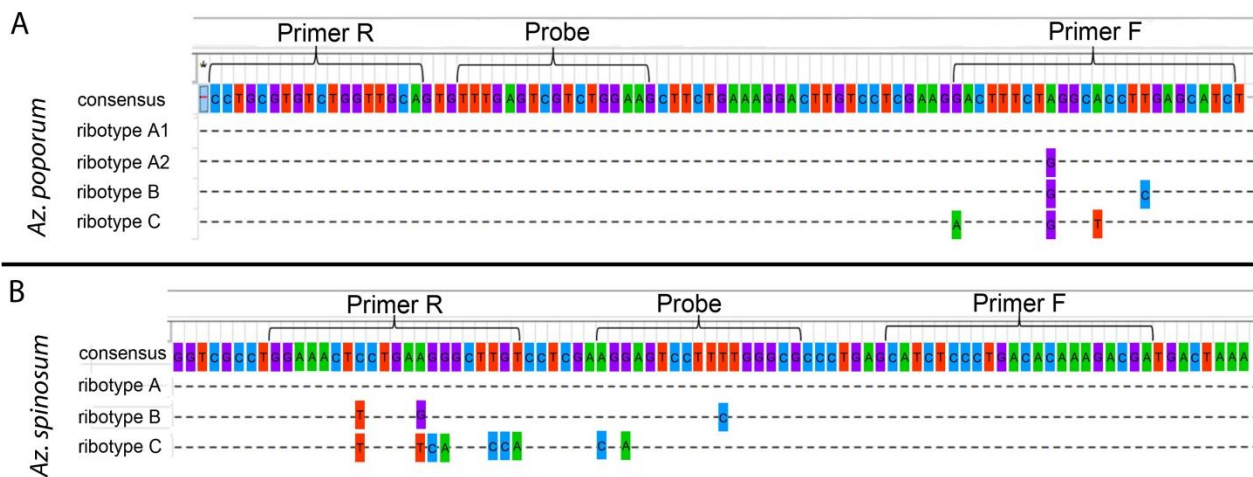


Fig. 1: Base pair mismatches between the ribotypes of (A) *Az. poporum* and (B) *Az. spinosum* with the primers and probe of the respective TaqMan qPCR assays.

and AZA-51 or just AZA-2, and strains of ribotype C lack any detectable AZA (Tillmann et al., 2019). As it is the case for *Az. poporum*, there are base pair mismatches with primers and probe of the qPCR assay for *Az. spinosum* ribotypes as well. Strains of the AZA producing ribotype B have two mismatches with the reverse primer and one with the probe, and the non AZA-producing ribotype C has six mismatches with the reverse primer (**Fig. 1 B**). Preliminary laboratory tests (Smith and Tillmann, unpublished) confirmed the concern that new strains of *Az. spinosum* are not detected efficiently, and this has a serious impact for monitoring programs, which rely on the currently used *Az. spinosum* qPCR assay. Therefore, there is a need to re-design the *Az. spinosum* assay in order to fully capture and quantify more strains of this

Acknowledgements

This work was supported by funding of the German Ministry for Education and Research (project RIPA ZA, 03F0763A) and by the PACES research program of the Alfred-Wegener-Institute as part of the Helmholtz Foundation initiative in Earth and Environment.

References

- Bonk, F., Popp, D., Harms, H., Centler, F. (2018). *J. Microbiol. Methods* 153, 139-147.
- Eckford-Soper, L.K., Daugbjerg, N. (2016). *J. Phycol.* 52, 174-183.
- Engesmo, A., Strand, D., Gran-Stadniczeňko, S., Edvardsen, B., Medlin, L.K., Eikrem, W. (2018). *Harmful Algae* 75, 105-117.

- Galluzzi, L., Bertozzini, E., Penna, A., Perini, F., Garces, E., Magnani, M. (2010). *J. Appl. Phycol.* 22, 1-9.
- Kim, J.W., Tillmann, U., Adams, N.G., Krock, B., Stutts, W.L., Deeds, J.R., Han, M.S., Trainer, V.L. (2017). *Harmful Algae* 68, 152-167.
- Krock, B., Tillmann, U., Tebben, J., Trefaults, N., Gu, H. (2019). *Harmful Algae* 82, 1-8.
- Macé, A., Kutalik, Z., Valsesia, A. (2018). In: Evangelou, E. (Ed.) *Genetic Epidemiology*. Humana Press, New York, pp. 231-258.
- Nishimura, T., Hariganeya, N., Tawong, W., Sakanari, H., Yamaguchi, H., Adachi, M. (2016). *Harmful Algae* 52, 11-22.
- Paterson, R.F. (2018). PhD Thesis, Univ. of Aberdeen, Scotland. 286 pp.
- Perini, F., Casabianca, A., Battocchi, C., Accoroni, S., Totti, C., Penna, A. (2011). *PLoS One* 6, e17699.
- Ruvindy, R., Bolch, C.J., MacKenzie, L., Smith, K.F., Murray, S.A. (2018). *Frontiers in Microbiology* 9, 3153
- Salas, R., Tillmann, U., John, U., Kilcoyne, J., Burson, A., Cantwell, C., Hess, P., Jauffrais, T., Silke, J. (2011). *Harmful Algae* 10, 774-783.
- Smith, K.F., Rhodes, L., Harwood, D.T., Adamson, J., Moisan, C., Munday, R., Tillmann, U. (2016). *J. Appl. Phycol.* 28, 1125-1132.
- Tillmann, U., Elbrächter, M., Krock, B., John, U., Cembella, A. (2009). *Eur. J. Phycol.* 44, 63-79.
- Tillmann, U., Edvardsen, B., Krock, B., Smith, K.F., Paterson, R.F., Voß, D. (2018). *Harmful Algae* 80, 15-34.
- Tillmann, U., Gottschling, M., Krock, B., Smith, K.F., Guinder, V. (2019). *Harmful Algae*, 84, 244-260.
- Toebe, K., Joshi, A.R., Messtorff, P., Tillmann, U., Cembella, A., John, U. (2013). *J. Plankton Res.* 35, 225-230.
- Twiner, M., Hess, P., Doucette, G.J. (2014). In: Botana, L.M. (Ed.) *Seafood and Freshwater Toxins*. CRC Press, Boca Raton, USA, pp 823-855.
- Wietkamp, S., Tillmann, U., Clarke, D., Toebe, K. (2019). *J. Plankton Res.* 41, 101-113.

PCR assays for the detection of ASP, DSP, PSP and AZP toxigenic producing phytoplanktonic species in Irish coastal waters

Dave Clarke*, Rafael Salas, Paula Hynes, Annaclaire McCarthy, Debbie Walsh, Joe Silke.

Marine Institute, Rinville, Oranmore, Galway H91 R673, Ireland

*corresponding author's email: dave.clarke@marine.ie

Abstract

The Marine Institute, Ireland have established a dedicated phytoplankton molecular unit employing real time qPCR assays in the targeted detection of phytoplankton toxigenic species responsible for causing toxic events in Irish shellfish. DSP, PSP, ASP & AZP events are a common occurrence and are often observed on an annual basis in Ireland. As many of these causative species cannot be identified to species level by light microscopy, the real time PCR assays in use by the unit, have proven to be useful and invaluable tools as a confirmatory method to support and compliment the routine method for species identification and enumeration via microscopy in samples from the national monitoring programme and surveys. These qPCR assays are primarily used in determining the presence and quantifying the following toxigenic species in water samples, ASP - *Pseudo-nitzschia australis*, *P. multiseriata*, *P. seriata*; AZP – *Azadinium spinosum*, *Amphidoma languida*; DSP – *Dinophysis acuta*, *D. acuminata*; PSP – *Alexandrium minutum*. In addition, these assays have provided supplemental information in determining the biogeography of species and also in discriminating between toxigenic and non-toxigenic species in field samples containing mixed species compositions. The resulting information has been used in making improved risk management decisions during toxic events.

Keywords: Molecular, PCR assay, *Dinophysis*, *Azadinium*, *Amphidoma*, *Alexandrium*, *Pseudo-nitzschia*

Introduction

Since the 1990's, the Marine Institute's (MI) Phytoplankton unit has been operating a national monitoring programme for the observation of the presence of toxigenic and harmful/nuisance phytoplanktonic species in Irish coastal waters. Over the past 3 decades, with the growth of the Irish aquaculture industry, the unit and the programme has expanded to analysing in excess of 3000 water samples per year by light microscopy. All aquaculture sites which are actively harvesting are sampled and analysed on a weekly basis throughout the year. Throughout this period, the knowledge and methodologies of determining the toxin profile in Irish shellfish and the identification and enumeration of the causative toxigenic species present in water samples has been extensively developed to provide a comprehensive and robust monitoring programme.

However, the monitoring of toxic events and the scientific advice given to industry and regulatory agencies during closure periods can be challenging, in particular, toxin accumulation can occur rapidly in shellfish above regulatory levels, including Amnesic Shellfish Poisoning (ASP), Azaspiracid Shellfish Poisoning (AZP) and Paralytic Shellfish Poisoning (PSP). The causative toxigenic species

associated with these toxin groups can be problematic to identify at species level by light microscopy, and are often reported at the genus level. These genera can contain both non-toxic and toxic species, which are indistinguishable by traditional microscopic methods, and in the case of *Azadinium* species, which can look extremely similar morphologically to species of closely related genera. Unfortunately, from both scientific and aquaculture production points of view, this does not give the full information required for industry and regulatory agencies to operate on a daily basis, particularly if the species observed cannot be determined and could potentially give rise to a toxic event in shellfish.

This occurred in 2005, where an unprecedented ASP event occurred in the SouthWest of Ireland and caused numerous closures of mussel (*M. edulis*) and pacific oyster (*C.gigas*) production areas. Whilst the microscopic method, which is used as an early warning of the onset of toxic events in shellfish, can give cell counts of *Pseudo-nitzschia seriata* group complex, the causative toxigenic species can not be identified or discriminated from samples composed of mixed non-toxic and toxic *Pseudo-nitzschia* species. The

conclusion after this event was that if the presence of the causative *Pseudo-nitzschia* species (*P. australis*) could have been identified and reported, it would have provided valuable advice, in addition to the microscope results, as a pre-warning of the potential ASP event. Since 2005, ASP events have been an annual occurrence in the SW and also occasionally along the West coast. Therefore in the mid 2000's, complimentary and confirmatory methodologies were investigated to determine if these problematic hard to identify species by microscopy could indeed be identified and enumerated at species level in order to provide additional information to industry and regulatory agencies of the onset, and during, shellfish toxin events. Molecular assays targeting specific DNA gene regions to discriminate between different species were chosen as a promising technique which could meet these requirements.

In 2007, the Marine Institute established the Phytoplankton Molecular unit, which to date has developed and validated a number of in-house and externally published molecular assays in determining the qualitative and quantitative concentrations of both toxicogenic and non-toxicogenic

species of the genera; *Alexandrium*, *Amphidoma*, *Azadinium*, *Dinophysis* and *Pseudo-nitzschia*. The unit predominantly focuses on real time qPCR assays using molecular probes as the primary tool of analysis. The high specificity of target DNA detection, high throughput of samples and rapid result turnaround times, make these assays suitable for incorporating into the national monitoring programme and supplementing the existing analysis via microscopy. Other molecular methodologies including FISH probes (Touzet et al. 2009) and microarrays (McCoy et al. 2013) have been previously assessed as suitable as a means of analysis, but not for routine use where rapid result turnaround times are required for reporting in monitoring programmes.

The unit employs the use of four main molecular probe/assay types (Table 1), including TaqMan Minor Groove Binding (MGB) hydrolysis probes, Fluorescence Resonance Energy Transfer (FRET) hybridisation probes, Universal Probes, and SYBR Green assays. These assays are used as confirmatory analysis when a suspected toxic species is observed in routine samples, but cannot be identified at species level with microscopy.

Table 1. Overview of qPCR assays employed in the MI Phytoplankton Molecular Unit.

Toxin Group	Target Genus/Species	Assay/Probe Type	References
DSP	<i>Dinophysis acuminata</i> * <i>Dinophysis acuta</i> *	FRET Hybridisation	Kavanagh <i>et al.</i> 2010
ASP	<i>Pseudo-nitzschia australis</i> * <i>Pseudo-nitzschia delicatissima</i> <i>Pseudo-nitzschia fraudulenta</i> <i>Pseudo-nitzschia pungens</i> <i>Pseudo-nitzschia multiseriata</i> * <i>Pseudo-nitzschia seriata</i> *	FRET Hybridisation	Kavanagh (unpublished) Keady (2010)
PSP	<i>Alexandrium minutum</i> * <i>Alexandrium tamarense</i> <i>Alexandrium tamutum</i> <i>Alexandrium ostenfeldii</i>	TaqMan (MGB)	Toebe <i>et al.</i> 2013 Collins <i>et al.</i> 2009
AZP	<i>Amphidoma languida</i> * <i>Azadinium spinosum</i> * <i>Azadinium obesum</i> <i>Azadinium poporum</i> <i>Azadinium/Amphidoma</i>	TaqMan (MGB) SYBR Green	Wietkamp <i>et al.</i> 2019 Toebe <i>et al.</i> 2013 Smith <i>et al.</i> 2016

Materials and Methods

Dinophysis species assay

A FRET hybridisation probe assay (Kavanagh et al. 2010) was developed as part of the Phytotest project targeting and distinguishing between two

causative *Dinophysis* species, *D. acuminata* and *D. acuta*, responsible for the production of the DSP compounds, Okadaic acid (OA) and Dinophysistoxin-2. These compounds accumulate in shellfish on an annual basis in Ireland and Clarke (2019). This assay was developed by sequencing the

D1-D2 LSU region from isolated cells of *D. acuta* and *D. acuminata* from Irish coastal water samples. Alignments of the Irish rDNA sequences were performed with all LSU *Dinophysis* sequences available at the time in GenBank, where primers (DIN_F and DIN_R) and hybridisation probes (LSU_1 and LSU_2) were designed from the alignments. The designed primers amplify a 270-bp product internal to the LSU D1-D2 region, whereas the probes compliment a 43-bp sequence within the target region of the Irish isolates of *D. acuta* and the LSU_2 probe was designed to have a 4-bp mismatch to Irish isolates of *D. acuminata*. To distinguish between the potential presence of co-occurrence of cells of both *D. acuta* and *D. acuminata*, a melt curve analysis is performed after amplification. The observed melt peaks T_m for *D. acuminata* is 61°C and for *D. acuta* 48°C (Fig. 1). These melt peaks are used to simultaneously detect and discriminate between the presence of *D. acuta* and *D. acuminata* cells.

The sensitivity of the assay was assessed by serial dilutions of plasmids where detection limits of < 10 copies per target were consistently obtained. The detection limit of the assay was established to be between 1-5 cells for *D. acuminata*.

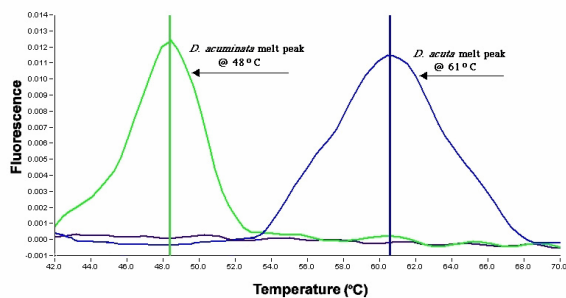


Fig. 1. Melt curve analysis showing the T_m's of the presence of *D. acuminata* and *D. acuta* (Kavanagh et al. 2008).

Pseudo-nitzschia species assay

A series of FRET hybridisation probe assays (Kavanagh, unpublished) were developed as part of the Phytotest project, (Maher et al. 2007, Kavanagh et al. 2008), targeting *P. australis*, *P. delicatissima*, *P. fraudulenta* and *P. pungens*. Two further FRET probes were developed as part of the EU SPIES DETOX project targeting *P. seriata* and *P. multiseriata* (Keady, 2010; Keady et al. 2009). These two species in addition to *P. australis* are known Domoic Acid (DA) toxin producers in Irish coastal waters responsible for ASP events in shellfish. The developed assays for all 6 *Pseudo-nitzschia* species target the internal transcribed spacer 1 (ITS-1) region of rRNA gene. For *P. multiseriata* and *P. seriata*, the assay specificity was assessed on 25 non-target species of varying

diatom and dinoflagellate species, including nine *Pseudo-nitzschia* species. Similar to the *Dinophysis* species assay, a melt curve analysis to determine the melt peak (T_m) is performed after the cycle amplification to confirm the target species. For *P. multiseriata*, the T_m is 66°C, and for *P. seriata* the T_m is 56°C. The sensitivity of the two assays were assessed through serial dilutions of known cell concentrations and verified in spiked field samples, where the limit of detection was determined of both assays to 10 cells/25ml of sample for both assays.

The remaining four assays, PCR primers and species-specific hybridisation probes were designed from the ITS-1 region and the following species specific T_m's were observed: *P. australis* 62°C (Fig. 2), *P. fraudulenta* 55°C, *P. delicatissima* 58°C and *P. pungens* 60°C. The assay for *P. pungens* was also able to detect *P. australis* (T_m 49°C), *P. fraudulenta* (T_m 42°C) and *P. multiseriata* (T_m 53°C). These 4 assays were tested for their specificity using various *Pseudo-nitzschia* species and a number of dinoflagellate species in culture and in field samples. There was no cross reactivity for any of the assays with non-target species. The limit of detection was consistently established at <10 copies for each target which equates to approximately one cell.

Performance evaluations and results of the FRET assays were compared to the microscopic method results for the determination of cells of both *Dinophysis* and *Pseudo-nitzschia* species in field samples (n=137) from the national monitoring programme. Overall there was a very good correlation between the 2 methods, with no false positives (n=17) being observed.

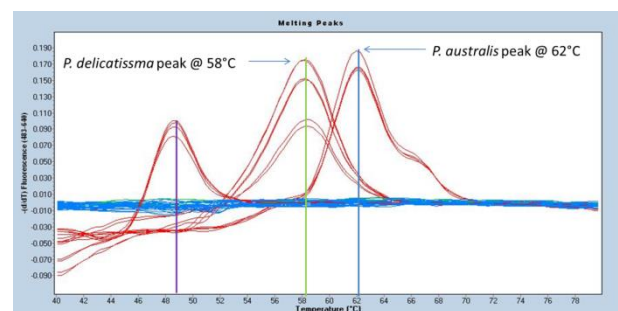


Fig. 2. Melt curve analysis showing the T_m's of the presence of *P. delicatissima* and *P. australis*.

Alexandrium species assay

TaqMan MGB probes are employed for the detection of *A. minutum*, *A. tamarense*, *A. tamutum* (Toebe et al. 2013) in monitoring programme samples, survey samples and sediments. Oligonucleotide primers and TaqMan MGB probes were designed to target the small sub-unit (SSU) of *A. minutum* and the variable D1-D2 LSU region of

A. tamarense and *A. tamutum*. The assays were demonstrated to have a high efficiency of qPCR reactions, to be highly species-specific, group specific and showed no cross-reaction with other *Alexandrium* species. Therefore, these probes were deemed suitable for the monitoring and determining the species composition of *Alexandrium* blooms which occur for a short period on an annual basis in the South of Ireland, where all 3 species can be present, co-occurring or one species more dominant at different periods during a bloom event. *Alexandrium ostenfeldii* also occurs to a lesser extent in Ireland in terms of distribution and occurrence, the TaqMan MGB assay designed (Collins et al. 2009) has been used in monitoring this species.

Azadinium species and *Am. languida* assay

Oligonucleotide primers and TaqMan MGB probes were designed to target the LSU region for the detection of *A. obesum*, *A. poporum* and *A. spinosum* (Toebe et al. 2013). The primers and probes designed for these 3 species were demonstrated to be highly specific and shown to have no cross-reactivity with non-target or co-occurring species. Recent testing of the *A. spinosum* assay for newly discovered ribotypes has demonstrated that the original assay is too specific and not suitable for detecting all ribotypes of *A. spinosum*, (Tillmann et al. 2018; Tillmann et al. 2019) this is a potential issue as one of the ribotypes is observed to be non-toxic. Therefore, there is a requirement for the re-design of this probe to distinguish between the AZA producing and non-toxic ribotypes of *A. spinosum* for the use of this assay in monitoring programmes.

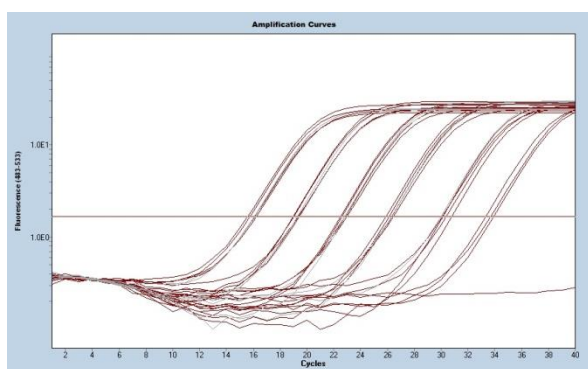


Fig. 3. Standard curve dilution series for the quantification of *A. spinosum* cells.

The original *A. spinosum* assay has been optimised and fully validated by the MI to ISO 17025 standards where all aspects of validation requirements have been met and assessed, including reproducibility, repeatability, sensitivity, limit of detection, selectivity, specificity, robustness, matrix effects and linearity (Clarke et

al. 2019). This assay is regularly used within the national monitoring programme to determine the presence of and quantify *A. spinosum* cells (Fig. 3) in water samples to provide information for management decisions during AZA events in shellfish.

Additionally, the unit also uses a qPCR assay for the detection and quantification of *Amphidoma languida* (Wietkamp et al. 2019), a species which also produces Azaspiracids (AZA's 38, 39). This assay was successfully tested on field samples from a 2017 survey from Irish Coastal waters. This TaqMan MGB probe assay has been demonstrated to be species specific and highly sensitive.

Azadinium / *Amphidoma* genus assay

A real time SYBR Green PCR assay for the detection of species of the genera *Azadinium* and *Amphidoma* (family Amphidomataceae) was developed (Smith et al. 2016). Primers were designed based on the ITS region of *Azadinium* species and *Am. languida*, and the assay specificity checked with extracted DNA from these species. A melt curve analysis is performed after amplification, where a T_m of approximately 83°C (Fig. 4) is observed for the presence of *Azadinium* and *Am. languida* species. The assay was determined to be highly sensitive and specific.

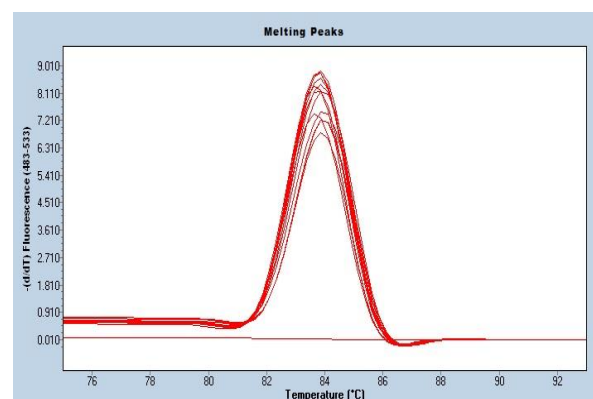


Fig. 4. Melt curve analysis showing the T_m 's of the presence of *Az. spinosum*, *Az. poporum* and *Am. languida* in field samples.

Results and Discussion

These developed and validated qPCR assays have been proven to be an invaluable complimentary and confirmatory monitoring tool in species identification and enumeration in routine samples from the Irish national monitoring programme. The high sensitivity of these assays, coupled with the high specificity of the probes, the high throughput and rapid turnaround times give vital information regarding the onset of potential toxin events, and the monitoring of ongoing toxic events. Results can now be disseminated to the regulatory agencies and

industry within the same day as sample receipt. To further increase the volumes of analysis and shorten result report turnaround times, the unit also uses automated instrumentation for DNA extraction and transfer to 96 well plates. The unit has also developed a number of multiplex assays which allows for the simultaneous detection of two or more target species. These assays have also been employed in analysing sediment samples, in particular for the presence of *A. minutum* cysts.

For the monitoring of *A. spinosum*, which is the main causative species responsible for AZA's in shellfish, this PCR assay has become a powerful monitoring tool. AZA events in shellfish are an annual occurrence in Ireland and result in numerous production area closures. Over the last number of years, the unit has optimised and in-house validated the assay, and in 2018 was successful in accrediting the method to ISO 17025 standards, the first laboratory internationally to have a PCR method for the detection of this species accredited.

Due to the fact that identifying *Dinophysis* cells to species level is achievable by light microscopy, the developed *Dinophysis* species probes are not regularly used in routine monitoring. However, they have been used in survey samples as a screening method confirming the presence or absence of cells of *Dinophysis* species. This has proven to be an effective screening tool in filtering out negative samples from large numbers of samples in a short time frame.

For ASP and PSP monitoring of shellfish flesh samples in Ireland, this is triggered on the presence of the associated causative species observed via light microscopy. Now with the ability of these molecular assays to target and identify down to species levels, distinguishing between toxic and non-toxic species, and also determining the composition of mixed species populations, affords the volume of testing of flesh samples to be increased or decreased as appropriate, therefore leading to increased laboratory efficiencies for shellfish testing.

The developed *Pseudo-nitzschia* species probes are assisting in our better understanding of species composition in samples and assemblage succession, spatially and temporally, making these PCR assays powerful ecological tools. Over time, this information greatly contributes in the ability to make improved risk management decisions. In the MI, the *Pseudo-nitzschia* species and *Azadinium/Amphidoma* species and genus assays are currently used in a number of biogeography projects (LeFran et al. 2019), affording a valuable insight into how species composition and distribution changes throughout an event.

However, there a number of points to consider with the use of these PCR assays, particularly in the areas of specificity, cross reactivity and detection. There is a danger that assays can be too specific or not specific enough to the desired target DNA region to identify to species level and potential species ribotype. The specificity and design of these assays should be continuously reassessed with the emergence of new species, strains and ribotypes. The use of standard curves, positive and negative extraction controls, internal process controls to assess potential sample inhibition, and negative template controls are necessary in running these assays to ensure the correct results and the optimal assay efficiencies are obtained.

Acknowledgements

The Phytotest project was supported and funded through the Strategic Marine RTDI Programme-Advanced Technologies (Project Ref AT/04/02/02)

The development of the *P. multiseriata* and *P. seriata* assays was supported and funded through the 6th EU Framework Programme (SPIES-DETOX 0302790-2).

Thanks to Kerstin Toebe, Urban Tillmann, Uwe John in AWI, Bremerhaven, Germany for original training, guidance and post-advice on the *Azadinium* species assays.

MI staff, contractors and students, past and present who have worked within the Phytoplankton Molecular Unit.

References

- Clarke, D., Salas, R., Tillmann, U., Toebe, K. (2019). In prep.
- Collins, C., Graham, J., Brown, L., Bresnan, E., Turrell, E. (2009). Ifremer. Proceedings of the seventh International Conference on Molluscan Shellfish Safety: <http://www.symposcience.eu/exl-php/articles/683-article.htm> .
- Kavanagh, S., Brennan, C., Lyons, C., Chamberlain, T., Salas, R., Moran, S., Silke, J., Maher, M. (2008) Marine Institute, Marine Environment and Health Series No. 33: 36-43.
- Kavanagh, S., Brennan, C., O'Connor, L., Moran, S., Salas, R., Lyons, J., Silke, J., Maher, M. Mar Biotechnol (NY). 2010 Oct;12(5):534-42.
- Keady, E. (2010). National University of Ireland, Galway, Theses ; 9213.
- Lefran, A., Siemerling, B., Cusack, C., Silke, J., Salas, R. (2019) Proceeding of the Eighteenth

- International Conference on Harmful Algae, Nantes, France. In prep.
- Maher, M., Kavanagh, S., Brennan, C., Moran, S., Salas, R., Lyons, J., Silke, J. (2007) Marine Institute, Marine Environment and Health Series No. 27: 70-77.
- McCoy, G., Touzet, N., Flemming, G.T., Raine, R. (2013) Environ Sci Pollut Res Int. Oct;20(10):6751
- Salas, R.; Clarke, D. (2019). Toxins 2019, 11, 61
- Smith, K.F., Rhodes, L., Harwood, D.T., Adamson, J., Moisan, C., Munday, R., Tillmann, U. (2016). J. Appl. Phycol. 28, 1125-1132.
- Tillmann, U., Edvardsen, B., Krock, B., Smith, K.F., Patterson, R.F., Voss, D. (2018). Harmful Algae, 80, 15-34.
- Tillmann, U., Gottschling, M., Krock, B., Smith, K.F., Guinder, V.(2019) Harm Algae. In Press.
- Toebe, K., Tilman, A.J., Tillmann, U., Krock, B., Cembella, A., Jown, U. (2013). Eur. J. Phycol. 48:1, 12-26.
- Toebe, K., Joshi, A.R., Messtorff, P., Tillmann, U., Cembella, A., John, U. (2013). J. Plankton Res. 35, 225-230.
- Touzet, N., Keady, E., Raine, R., Maher, M. (2009). FEMS Microbiol Ecol. 67, 329-341
- Wietkamp, S., Tillmann, U., Clarke, D., Toebe, K. (2019). J. Plankton Res. In press.

Application of gel-formatted qPCR assays for rapid diagnosis of shellfish toxin producing and fish-killing micro-algae in seawater

Lincoln MacKenzie, Jonathan Banks, Kirsty Smith

Cawthron Institute, 98 Halifax Street, Nelson, 7010 New Zealand
corresponding author's email: lincoln.mackenzie@cawthron.org.nz

Abstract

The establishment of large-scale offshore fin-fish and shellfish aquaculture presents new challenges for harmful algal bloom (HAB) monitoring, especially in areas where blooms of toxic and noxious species (e.g. *Alexandrium pacificum*, *Heterosigma akashiwo*) commonly occur. Monitoring methods need to provide identification and enumeration of problematic species from multiple samples collected over large areas in as near real-time as possible. To accomplish this, a quantitative polymerase chain reaction (qPCR) assay in a solid phase gel format (Aquila Diagnostics Hydrogels) was evaluated for the routine screening of seawater samples for the presence and abundance of several species of toxic and noxious micro-algae. The aim was to carry out trials of this rapid, low-cost method and evaluate its suitability for application by industry. Samples collected from natural blooms and cell cultures were used to evaluate the assays. The assays had good sensitivity for *Alexandrium pacificum*, and *Alexandrium minutum*, although the precision of quantification was low. The Hydrogel assay for *Karenia brevisulcata* performed well, but poorly for *Heterosigma akashiwo* and not at all for *Pseudochattonella verruculosa*. All assays had a relatively high proportion of results that exhibited non-specific amplification that confounded accurate quantification. The Hydrogel assays potentially provide an excellent practical monitoring option, but their reliability and accuracy need improvement.

Keywords: Toxic and noxious micro-algae, quantitative polymerase chain reaction (qPCR) methods, Hydrogel assay

Introduction

In New Zealand, early warning of impending blooms of micro-algae responsible for the contamination of shellfish, or direct harmful effects on fin-fish in sea cages, currently relies on the manual microscopic examination of water samples to identify and estimate the abundance of potentially harmful species. This approach requires skilled analysts, is slow and tedious, and can be difficult to definitively identify some species after sample preservation. Advanced autonomous instruments such as the Environmental Sample Processor (ESP) and Imaging FlowCytobot (IFCB) that use DNA sandwich hybridisation assays, quantitative polymerase chain reaction (qPCR), immunoassays, and image analysis technologies to provide real-time *in situ* analysis of water samples to detect harmful phytoplankton have been developed (Anon, 2014). However, these are sophisticated and expensive machines that are technically and financially beyond the reach of most aquaculture monitoring situations that require data of high spatial and temporal resolution.

There is a need for simple, rapid, sensitive, accurate, high-throughput and inexpensive methods for the identification and enumeration of harmful species that can provide data in near real-time in real-world aquaculture settings. Pre-formatted qPCR assays targeting specific DNA sequences in combination with rapid DNA extraction methods, provide a potential means of achieving this aim. In this study we have carried out trials of solid phase qPCR assays (Aquila Diagnostics Hydrogel assay) targeting two shellfish toxin producing dinoflagellates (*Alexandrium pacificum* and *A. minutum*) and three species hazardous to fin-fish in sea cages (*Pseudochattonella verruculosa*, *Heterosigma akashiwo*, and *Karenia brevisulcata*) to evaluate their potential as routine monitoring tools. The Hydrogel system is a patented, customised product which has all the PCR reagents stabilised in a gel format. User input is simply to load extracted DNA on to the hydrogels, run the qPCR assay on a thermocycler and interpret the results.

Materials and Methods

DNA samples

Cell concentrates from natural water samples and microalgal cultures were prepared by filtration through 13 mm, 8 µm cellulose mixed ester membrane filters using a 50-100 mL syringes and Swinnex filter holders (Millipore). Up to 200 mL of natural sea water was filtered after prefiltration through a 100 µm screen. Depending on the cell density 250 – 1,000 µL of cultured cells were filtered. DNA was extracted from the filters using BioGX bead lysis tubes (product # 800-1000) for 10 minutes at 2,850 rpm on a vortex shaker with a horizontal microtube adapter. The extracts were applied directly to the Hydrogels without any further purification.

Hydrogel assays

SYBR Green based hydrogel assay units were custom made by Aquila Diagnostic Systems Inc. (Edmonton, Canada). Primer sequences (D1-D2 region of the large subunit ribosomal DNA; (LSU rDNA) for *A. pacificum* and *A. minutum* as described by Rendy et al. (2018). LSU rDNA primers targeting *K. brevisulcata*, *H. akashiwo* and *P. verruculosa* were as described by Smith et al. (2014), Coyne et al. (2005) and Eckford and Daugbjerg (2016) respectively. The assays in the lab and in the field were run on a MyGo Mini thermocycler (IT-IS Life Science Ltd.) using the following conditions: an initial step of 95°C for 10 minutes followed by 40 cycles of 95°C for 20 seconds, 60°C for 30 seconds and 72°C for 30 seconds. Fluorescence was measured at the end of each extension step. At the completion of the PCR cycling a high-resolution melt curve analysis was conducted, from 65°C to 95°C in increments of 0.5°C with each temperature held for five seconds. The assays were calibrated using serial dilutions of the DNA extracts of cultures with known cell concentrations. All assays were run in triplicate. The specificity of the assays was determined by running assays on a number of cultured isolates from the Cawthron Institute Culture Collection of Micro-algae (<http://cultures.cawthron.org.nz>) of various closely related species to check for cross reactivity.

Results and Discussion

Quantitative PCR assays of serial dilutions of extracted cultured cells (Figs 1, 2) of *A. pacificum*, *A. minutum*, and *H. akashiwo* had acceptable amplification efficiencies (96-107%) however the

K. brevisulcata assay (Fig. 2B) only had an efficiency of 83%. The assay targeting *P. verruculosa* failed to produce any consistent PCR product.

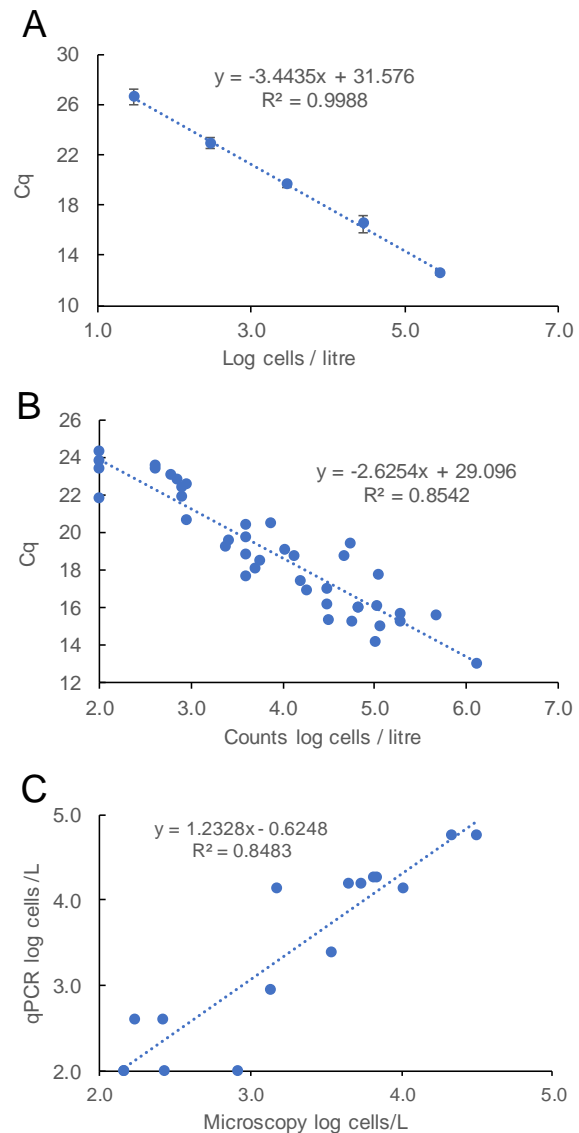


Fig. 1. (A) Hydrogel assays of cultured cells of *A. pacificum*. (B) Cq values versus counts of cell numbers of *A. pacificum* in seawater samples from Nydia Bay, Pelorus Sound. (C) Comparison of estimates of *A. pacificum* cell abundance by microscopy and the Hydrogel qPCR assay.

The specificity of the target sequence amplification was confirmed by examination of the product melt curves (Fig. 3). Unfortunately, the performance of the Hydrogels was variable with >20% (against all species) showing evidence of a high level of primer-dimer and other non-specific amplification that confounded quantification in affected assay tubes.

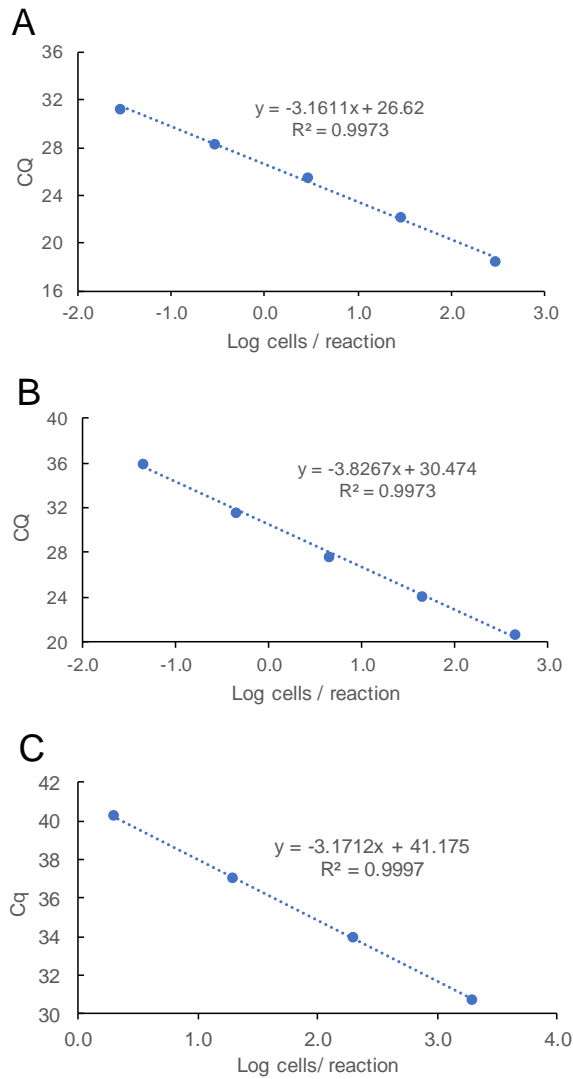


Fig. 2. Hydrogel assay calibration curves established from extracts of cultured species. A. *Alexandrium minutum*. B. *Karenia brevisulcata*. C. *Heterosigma akashiwo*.

Elimination of assays that failed to amplify properly resulted in a general agreement between quantification by microscopy and qPCR of *A. pacificum* in natural sea-water samples (Fig. 1B, 1C) although precision was relatively poor. The sensitivity of the assays was acceptable with a level of detection for *A. pacificum* of about 10 cells /L with filtration of a 100 mL seawater sample.

Cross-reactivity experiments showed that the *A. pacificum* and *A. minutum* assays (Table 1) did not cross react with other closely related species.

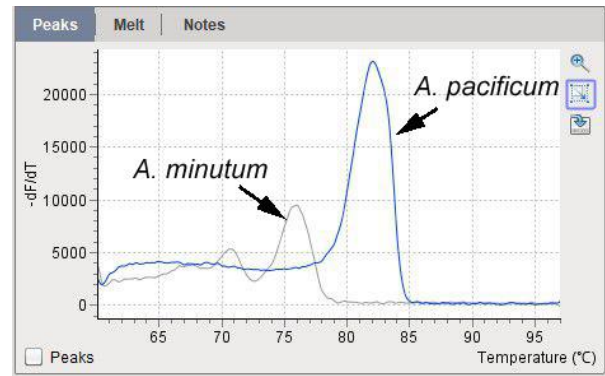


Fig. 3 Melt curves of *A. pacificum* and *A. minutum* amplification products run on an *A. pacificum* targeted hydrogel.

Table 1. Cross reactivity of *Alexandrium* spp. hydrogels

Cultured isolates	Hydrogels	
	<i>A. minutum</i>	<i>A. pacificum</i>
<i>A. pacificum</i> CAWD 235	-	+
<i>A. minutum</i> CAWD 11	+	-
<i>A. minutum</i> CAWD 12	+	-
<i>A. minutum</i> CAWD 273	+	-
<i>A. fraterculus</i> CAWD 52	-	-
<i>A. margalefii</i> CAWD 10	-	-
<i>A. ostenfeldii</i> CAWD 136	-	-
<i>A. pseudogonyaulax</i> CAWD 20	-	-

Table 2. Cross reactivity of *Karenia brevisulcata* hydrogels.

Cultured isolates	Hydrogel
	<i>K. brevisulcata</i>
<i>Karenia brevisulcata</i> CAWD 82	+
<i>Karenia selliformis</i> CAWD 79	+
<i>Karenia umbella</i> CAWD 131	-
<i>Karenia brevis</i> CAWD 122 (Florida)	-
<i>Karenia papilionacea</i> CAWD 91	-
<i>Karenia mikimotoi</i> CAWD 192	-
<i>Karenia bidigitata</i> CAWD 92	-

The *K. brevisulcata* assay (Table 2) cross-reacted strongly with *K. selliformis* but not with other *Karenia* species. However, when the primers are used with the additional specificity of a hydrolysis probe the assay shows no cross-reactivity with *K. selliformis* (Smith et al. 2014). These two dinoflagellates are morphologically very similar and in practise this cross-reactivity is not likely to be a problem since both species are equally hazardous to fin-fish in sea cages.

Table 3. Cross reactivity of *Heterosigma akashiwo* hydrogels

Cultured isolates	Hydrogel <i>H. akashiwo</i>
<i>Heterosigma akashiwo</i> CAWR 04 (Australia)	+
<i>Heterosigma akashiwo</i> CAWR 06 (NZ)	+
<i>Heterosigma akashiwo</i> CAWR 08 (NZ)	+
<i>Heterosigma akashiwo</i> CAWR 09 (NZ)	+
<i>Heterosigma akashiwo</i> CAWR 13 (NZ)	+
<i>Heterosigma akashiwo</i> CAWR 15 (Canada)	+
<i>Chattonella marina</i> CAWR 18 (NZ)	-
<i>Fibrocapsa japonica</i> CAWR 19 (NZ)	-

The *H. akashiwo* assay (Table 3) reacted with all other isolates of this species in the collection, including Australian and Canadian isolates. It did not react with other raphidophytes (*Chattonella marina*, *Fibrocapsa japonica*).

The Hydrogel assays, coupled with cell concentration with syringe filters and the BioGX cell lysis/DNA extraction kit, are simple and rapid to carry out, with results available in less than two hours from the time of sample collection. All the qPCR reagents are incorporated into the reaction gel and remain stable for long term storage at room temperature. In our study assays were successfully carried out in the field on a small (7 metre) sampling vessel. The MyGo Mini thermocycler can analyse 16 samples simultaneously (including standards and controls) and throughput would be easily scalable using multiple instruments or other instruments capable of simultaneously running a larger number of samples. In sampling excursions to remote areas, the results of multiple assays can be available before the vessel returns to port. The assay format is eminently suitable for use on fish farms or in processing plants with rudimentary laboratory facilities. These assays potentially offer an excellent practical monitoring option that in terms of cost is highly competitive with microscopy monitoring methods. They have an advantage in providing near real time data from multiple samples with minimal labour input. Unfortunately, the assays for all the species evaluated here had a high proportion of results with unacceptably high levels of amplification of non-target DNA. This impacted on the accuracy of quantification. The cause of this is unknown. It could be an artefact created during polymerisation of the gels or issues related to primer design. In the case of the *P. verruculosa* assay no evidence of amplification of the target DNA was apparent and further work on the design of the primer sequences is clearly necessary.


An important consideration for accurate quantification of qPCR assays is the stability of target gene copy number within populations of the species in question. Year to year variations in the LSU rRNA gene copy number in populations of *Alexandrium fundyense* in the Gulf of Maine (D. Anderson pers. com.) has been observed that have made a substantial difference to estimates of absolute abundance. This is an issue that will need to be addressed and corrections applied if it is identified as a problem. A further improvement to the assays would be the inclusion of an internal amplification control to identify potential inhibition effects that might occur with the simple DNA extraction procedure (BioGX bead lysis tubes) used in this study.

Acknowledgements

This research has been funded through the “Seafood Safety Platform” (MBIE contact # CAWX1801) and the National Science Challenge, Sustainable Seas Innovation Fund (Contract C01X1515). This project was endorsed under the GlobalHAB programme.

References

- Anon. (2014). Environ. Health Perspect. 122 (8). 207-213
- Coyne, k.J., Handy, S.M., Whereat, E.B., Huchins, D.A., Portune, K.J., Doblin, M.A., Cary, S.C. (2005). Limnol. Oceanogr. Meth. 3. 381-391.
- Eckford-Soper, L.K., Daugbjerg, N. (2016) J. Phycol. 52. 174-183.
- Erdner, D.L., Percy, L., Keafer, B., Lewis, J., Anderson, D.M. (2010). Deep-Sea Res. II 57. 279-287.
- Rendy, R., Bolch, C.J., MacKenzie, L., Smith, K.F., Murray, S.A. (2018). Front. Microbiol. doi:10.3389/fmicb.2018.03153
- Smith, K.F., de Salas, M., Adamson, J., Rhodes, L.L. (2014). Mar. Drugs 12. 1361-1376. Doi:10.3390/md12031361.



Eco-physiology & cellular biology of harmful algae and cyanobacteria

The role of phosphatase activities during a bloom of *Ostreopsis cf. ovata* in the northern Adriatic Sea

Stefano Accoroni^{1*}, Marisa Pasella¹, Tiziana Romagnoli¹, Emanuela Razza¹, Cecilia Totti¹, Neil Thomas William Ellwood²

¹Dipartimento di Scienze della Vita e dell'Ambiente, Università Politecnica delle Marche, via Brecce Bianche, 60131 Ancona, Italy;

²Dipartimento di Scienze, Università Roma Tre, Viale G. Marconi 446, 00146 Roma.

* corresponding author's email: s.accoroni@univpm.it

Abstract

Increased organic nutrient loads deriving from anthropogenic activities and natural processes frequently cause eutrophication of coastal waters. An increasing number of phototrophs have been shown to make use of organic nutrients. The potential utilization of dissolved organic phosphorus (DOP) by microbial-mats associated with the toxic dinoflagellate *Ostreopsis cf. ovata*, was investigated throughout a full cycle of a bloom that occurred in 2015 in the Conero Riviera (N Adriatic Sea). Measurements of phosphomonoesterase (PMEase) and phosphodiesterase (PDEase) activities of the epiphytic mats (including cells and exopolymeric substances) and chemical-physical parameters were made weekly from late summer to early autumn.

Analyses of ambient inorganic nutrient fractions revealed very low filterable reactive P (FRP) concentrations, however, DOP concentrations were on average 85% of the total dissolved P. A rapid increase in PMEase and PDEase activities in the microbial community was recorded, coinciding with the onset of a proliferation of the *Ostreopsis* population. Chromogenic staining of samples showed that activity was closely associated with the *Ostreopsis* cells, located both extracellularly (cell surface and within the EPS) and intracellularly (ventral cytoplasm). The increase in both PMEase and PDEase activities indicates that the *Ostreopsis*-mat community can utilize a wide range of DOP types. Tests in laboratory confirmed that *O. cf. ovata* can utilize both phosphomonoester (D-Fructose 1,6-disphosphate, β -Glycerophosphate, α -D-Glucose 1-phosphate, Guanosine 5'-monophosphate and Phytic acid) and phosphodiester (DNA and RNA) sources to grow.

The experiments also demonstrated that PMEase and PDEase were strongly influenced by water temperature, with maximum values recorded at 30-35 °C.

Based on the present findings, *O. cf. ovata* seems to have adaptations that allow it to thrive in P-limited environments where organic P is the main source of P, as long as water temperature is high enough to maintain elevated PMEase and PDEase activities.

Keywords Organic phosphorus, *Ostreopsis*, Phosphorus limitation

Introduction

In the Mediterranean Sea, the benthic marine dinoflagellate *Ostreopsis* has gained particular attention because of the summer-autumn blooms it forms in almost all rocky coasts (Jauzein et al., 2018). These phenomena are often associated with noxious effects on human health (e.g. fever, cough, dyspnea, sore throat, rhinorrhea, skin irritation, etc.), through marine aerosol inhalation and direct contact (Migliaccio et al., 2016; Vila et al., 2016). To date, three *Ostreopsis* species have been reported from the Mediterranean Sea: *O. cf. ovata*, *O. cf. siamensis* and *O. fattorussoi*, (Penna et al., 2012; Accoroni et al., 2016a). *O. cf. ovata* produces a large array of palytoxin analogues, i.e. isobaric palytoxin (isobPLTX) and ovatoxins

(OVTXs) namely OVTX-a to -h (Brissard et al., 2015; García-Altare et al., 2015).

Despite the number of studies concerning the environmental influence on *Ostreopsis* blooms, the complexity of their development is still far from being understood. Particularly confounding is the ability of *Ostreopsis* to form blooms, in the P-limited waters of the northern Adriatic Sea (Cozzi & Gianni, 2011).

In response to a lack of information on the, potentially bioavailable, dissolved organic phosphorus fractions in this area, it was decided to investigate the potential utilization of DOP by microbial-mats associated with *Ostreopsis cf. ovata*. In a previous *in situ* study, the phosphatase

activities of *O. cf. ovata* throughout a full cycle of a bloom that occurred in 2015 in the Conero Riviera (NW Adriatic Sea) was performed, suggesting a high ability of *Ostreopsis*-mats to use organic P. In this study, this ability was further investigated incubating *O. cf. ovata* with different DOP sources in laboratory conditions. These observations should shed further light on how, temperature and nutrients affect the bloom dynamics of *O. cf. ovata*.

Materials and Methods

A strain of *Ostreopsis cf. ovata* (OOAPS0810/S3) was isolated from microphytobenthos community growing epiphytically on seaweeds during a bloom occurred at the Passetto station in the Conero Riviera (Ancona, NW Adriatic Sea). The cells were isolated using a capillary pipette (Hoshaw & Rosowski, 1973) into filtered seawater at 21 ± 0.1 °C under a 12:12 h LD photoperiod with an irradiance of $90\text{--}100 \mu\text{mol m}^{-2}\text{s}^{-1}$, in modified f/4 medium (Guillard, 1975).

The ability of *O. cf. ovata* to utilize DOP was investigated using a modified f/4 medium replacing orthophosphate with a phosphomonoester (D-Fructose 1,6-disphosphate, β -Glycerophosphate, α -D-Glucose 1-phosphate, Guanosine 5'-monophosphate and Phytic acid) or a phosphodiester (DNA and RNA). Cell counts were made every 3 d for 39 d in total, to evaluate *O. cf. ovata* growth on each P source.

The analogue substrates *para*-nitrophenyl phosphate (*p*NPP) and bis-*para*-nitrophenyl phosphate (bis-*p*NPP) were used in the assays of phosphomonoesterase (PMEase) and phosphodiesterase (PDEase) activities, respectively. The activities of the cultured *O. cf. ovata* strain were measured at eight different temperatures (5, 10, 15, 20, 25, 30, 35 and 40 °C). The procedure used broadly followed that of Turner *et al.* (2001). The chromogenic stain BCIP-NBT (5-bromo-4-chloro-3'-indolylphosphate-nitro blue tetrazolium) was used to visualize the location of PMEase as it produces a blue-purple precipitate at the site of the hydrolysis. Staining was carried out using the same conditions as the enzyme assays.

Results and Discussion

Ostreopsis cf. ovata blooms occurring along the Conero Riviera, a strongly P-limited area, were among the most intense in the entire Mediterranean basin, with maximum abundances reaching 10^4 cells cm^{-2} (10^6 cells g^{-1} fw, 10^7 cells g^{-1} dw) in late summer (Accoroni *et al.*, 2015).

Calm conditions are recognized as a prerequisite for bloom onset, and hydrodynamics strongly influence the proceeding bloom dynamics (Accoroni *et al.*, 2015). For example, in 2015 there was a temporary decrease of abundance observed from mid-to late-September, when moderate to high hydrodynamic events occurred (Douglas scale ≥ 2). The bloom finally declined rapidly by mid-October in correspondence of further moderate to high hydrodynamic conditions (Fig. 1A, Accoroni *et al.*, 2017).

Ostreopsis blooms are generally considered to be summer events in Mediterranean Sea, but it has been repeatedly shown that the highest abundances of *Ostreopsis* do not occur with the highest water temperature in all areas (Mangialajo *et al.*, 2011).

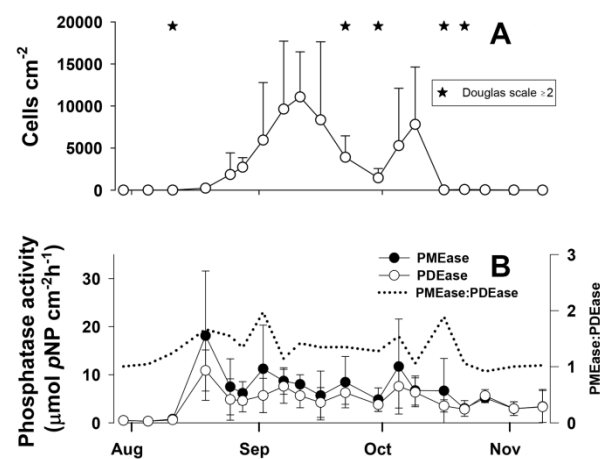


Fig. 1. Changes in (A) *Ostreopsis cf. ovata* abundance on macroalgae (cells cm^{-2}) (B) and phosphatase (PMEase, PDEase) activity ($\mu\text{mol pNP cm}^{-2}\text{h}^{-1}$) and their ratio in Passetto station in 2015. * marks heavy sea dates (Douglas scale ≥ 2) (figure 2 in Accoroni *et al.*, 2017).

A temperature threshold seems to be important to trigger a bloom; for example, the Conero Riviera bloom consistently peaked in late summer (between 18.8 and 24 °C), but the bloom onset occurred at maximum summer temperatures (from 25 to 28.6 °C). It was hypothesized that *Ostreopsis* may need to reach a high temperature threshold to initiate cyst germination, generally around 25 °C (Accoroni *et al.*, 2014). However, in the northern Adriatic Sea the bloom onset is often observed about 30 days after the reaching the 25 °C-temperature threshold, suggesting that other environmental factors, besides temperature, may affect the development of *O. cf. ovata* blooms. In fact, our studies showed that *O. cf. ovata* blooms appear to be triggered by a combination of optimal temperature and nutrient concentration: the temperature threshold plays a key role on the

germination of *O. cf. ovata* cysts and optimal nutrient conditions are necessary to allow cell proliferation (Accoroni *et al.*, 2015).

Although no clear relationship was found between nutrient concentrations and *O. cf. ovata* abundances in the Conero Riviera, it was shown that during bloom onset, inorganic P (FRP) and N:P ratios were significantly lower than in the rest of the study period implying that P-limitation may be involved somehow. Interestingly, there was a corresponding increase in DOP concentrations, on average 85% of the total dissolved P (Accoroni *et al.*, 2017). At the same time, a rapid increase in the PMEase and PDEase activities of the microbial community was also recorded, which also corresponded with the onset of *O. cf. ovata* proliferation and were also maintained at elevated levels for the duration of the bloom (Fig. 1B, Accoroni *et al.*, 2017). PMEase and PDEase are specific for ester bonds and not for the organic moiety, so an increase in both their activities suggests that the *Ostreopsis*-mat community can utilize a wide range of DOP types. This was somewhat confirmed in the culture study, where growth was noted in all of the phosphomonoesters (D-Fructose 1,6-disphosphate, β -Glycerophosphate, α -D-Glucose 1-phosphate, Guanosine 5'-monophosphate and Phytic acid) and the phosphodiester (DNA and RNA) that were tested (Table. 1). Significantly higher maximum yields were observed using Guanosine 5'-monophosphate than in the other conditions ($p < 0.01$).

Table 1. Growth rates (μ) and maximum yield (max-yld) of *Ostreopsis cf. ovata* with various phosphorus sources.

Growth medium	μ (day ⁻¹)	max-yld (cells ml ⁻¹)
<u>Inorganic P</u>		
Ortho-P	0.16	718 \pm 278
<u>PME</u>		
FDP	0.13	721 \pm 103
Glycero-P	0.21	901 \pm 382
G1P	0.22	1487 \pm 211
GMP	0.25	3179 \pm 282
Phy-Acid	0.23	1550 \pm 403
<u>PDE</u>		
DNA	0.20	1629 \pm 929
RNA	0.31	2433 \pm 1224

Staining of samples with BCIP-NBT showed that activity was closely associated with the *Ostreopsis*

cells, located both extracellularly (cell surface and within the EPS) and intracellularly (ventral cytoplasm) (Fig. 2).

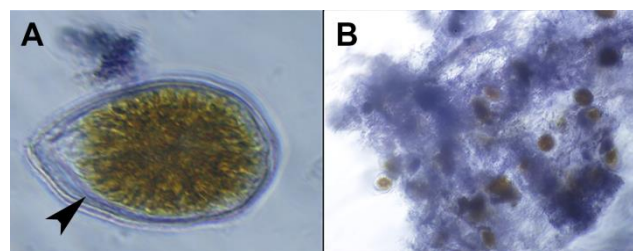


Fig. 2. Staining of PMEase activity of *Ostreopsis cf. ovata* and EPS: (A) cell surface associated (black arrow); (B) within the EPS (figure 4C and E in Accoroni *et al.*, 2017).

Laboratory tests showed that phosphatase activities were strongly influenced by water temperature. Both phosphatases displayed significant positive correlation with temperature (PMEase: $r^2 = 0.88$, $n = 24$, $p < 0.001$; PDEase: $r^2 = 0.64$, $n = 24$, $p < 0.001$) and PMEase was significantly lower at 5 °C than at 30, 35 and 40 °C ($p < 0.01$, Fig. 3). This may explain why in N Adriatic Sea *Ostreopsis* blooms can persist until autumn with temperatures down to 15 °C, while in winter with temperatures down to ~ 5 °C no *O. cf. ovata* cells are observed (Accoroni *et al.*, 2016b): *O. cf. ovata* can maintain a sizeable population by utilizing the relatively more abundant DOP in the environment as long as water temperature values are high enough.

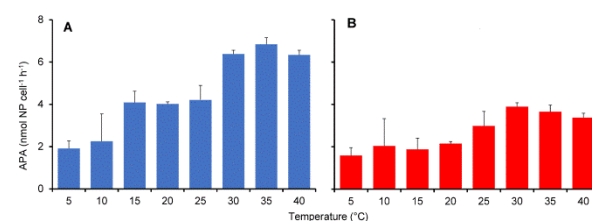


Fig. 3. PMEase (A) and PDEase (B) activities (nmol NP cell⁻¹ h⁻¹) of *Ostreopsis cf. ovata* grown at different temperature (5, 10, 15, 20, 25, 30, 35 and 40 °C). The values represent mean and the error bars indicate the standard deviation.

In conclusion, this study has elucidated many of the environmental aspects involved in *Ostreopsis* bloom formation and development in the northern Adriatic Sea. The synergic effects of hydrodynamics, temperature and nutrient availability, particularly both inorganic and organic phosphorus, are possibly the main factors triggering the bloom. The ability to use organic P in a strongly P-limited area where organic P can make up most of the TP, can explain the success of this benthic dinoflagellate.

Acknowledgements

This study was partially supported by ISPRA-Italian Ministry of the Environment, MURST (PRIN 2007), and ENPI CBCMED M3-HABs projects.

References

- Accoroni, S., Romagnoli, T., Pichierri, S., Totti, C. (2014). *Harmful Algae* 34, 7–16.
- Accoroni, S., Glibert, P.M., Pichierri, S., Romagnoli, T., Marini, M., Totti, C. (2015). *Harmful Algae* 45, 14–25.
- Accoroni, S., Romagnoli, T., Penna, A., Capellacci, S., Ciminiello, P., Dell’Aversano, C., Tartaglione, L., Abboud-Abi Saab, M., Giussani, V., Asnaghi, V., Chiantore, M., Totti, C. (2016a). *J. Phycol.* 52, 1064–1084.
- Accoroni, S., Romagnoli, T., Pichierri, S., Totti, C. (2016b). *Harmful Algae* 55, 179–190.
- Accoroni, S., Totti, C., Razza, E., Congestri, R., Campanelli, A., Marini, M., Ellwood, N.T.W. (2017). *Water Res.* 120, 272–279.
- Brissard, C., Hervé, F., Sibat, M., Séchet, V., Hess, P., Amzil, Z., Herrenknecht, C. (2015). *J. Chromatogr. A* 1388, 87–101.
- Cozzi, S., Giani, M. (2011). *Cont. Shelf Res.* 31, 1881–1893.
- García-Altare, M., Tartaglione, L., Dell’Aversano, C., Carnicer, O., de la Iglesia, P., Forino, M., Diogène, J., Ciminiello, P. (2015). *Anal. Bioanal. Chem.* 407, 1191–1204.
- Guillard, R.R.L. (1975). In: Smith, W.L., Chanley, M.H. (Eds.), *Culture of Marine Invertebrate Animals*. Plenum Press, New York, pp. 26–60.
- Hoshaw, R.W., Rosowski, J.R., 1973. In: Stein, J.R. (Ed.), *Handbook of Phycological Methods*. Cambridge University Press, New York, pp. 53–67.
- Jauzein, C., Açaf, L., Accoroni, S., Asnaghi, V., Fricke, A., Hachani, M.A., Abboud-Abi Saab, M., Chiantore, M., Mangialajo, L., Totti, C., Zaghmouri, I., Lemée, R. (2018). *Ecol. Indic.* 91, 116–127.
- Langner, C.L., Hendrix, P.F. (1982). *Water Res.* 16, 1451–1454.
- Mangialajo, L., Ganzin, N., Accoroni, S., Asnaghi, V., Blanfuné, A., Cabrini, M., Cattaneo-Vietti, R., Chavanon, F., Chiantore, M., Cohu, S., Costa, E., Fornasaro, D., Gossel, H., Marco-Miralles, F., Masó, M., Reñé, A., Rossi, A.M., Sala, M.M., Thibaut, T., Totti, C., Vila, M., Lemée, R. (2011). *Toxicon* 57, 408–420.
- Migliaccio, O., Castellano, I., Di Cioccio, D., Tedeschi, G., Negri, A., Cirino, P., Romano, G., Zingone, A., Palumbo, A. (2016). *Sci. Rep.* 6, 26086.
- Penna, A., Fraga, S., Battocchi, C., Casabianca, S., Perini, F., Capellacci, S., Casabianca, A., Riobo, P., Giacobbe, M., Totti, C., Accoroni, S., Vila, M., Reñé, A., Scardi, M., Aligizaki, K., Nguyen-ngoc, L., Vernesi, C. (2012). *Cryptogam. Algol.* 33, 153–163.
- Turner, B.L., Baxter, R., Ellwood, N.T.W., Whitton, B.A. (2001). *Plant Cell Environ.* 24, 1165–1176.
- Vila, M., Abós-Herrándiz, R., Isern-Fontanet, J., Álvarez, J., Berdalet, E. (2016). *Sci. Mar.* 80, 107–115.

Effects of selenium and light on the growth of the Mediterranean neurotoxic dinoflagellate *Gymnodinium catenatum* HW Graham responsible for recurrent PSP outbreaks in coastal waters of Morocco

HichamAboualaalaa^{1,2,3*}, Benlahcen Rijal leblad², Hassane Riadi¹, Mouna Daoudi², Naima Maamour², Mohamed Marhraoui², Mohamed Ouelad Abdellah², Mohamed Laabir³

¹ Applied Botanical Laboratory, Abdelmalek Essaadi University, Faculty of Sciences, Tetouan, Morocco

²ToxicMicroalgaeLaboratory, Institut National de Recherche Halieutique, Tanger, Morocco,

³ MARBEC, Montpellier University, CNRS, IRD, Ifremer, Montpellier, France,

* corresponding author's email: Hichamaboulaala@gmail.com

Abstract

The chain-forming dinoflagellate *Gymnodinium catenatum* is responsible for outbreaks of paralytic shellfish poisoning (PSP) worldwide. In Morocco, shellfish poisoning events were recorded early in 1969. Since then, numerous intoxications and deaths were reported in Moroccan Atlantic waters. Moreover, the Mediterranean coastline of Morocco is recurrently and severely impacted by PSPs affecting the exploited mollusks and in particular the cockle *Acanthocardia tuberculatum* which showed persistent high levels of PSPs exceeding the threshold level. The causative species has been identified as *G. catenatum*. In our study, several strains of *G. catenatum* were isolated from M'diq Bay located in Western Moroccan Mediterranean Sea and monoclonal cultures were established. The isolated strains were identified as *G. catenatum*. To determine the optimal conditions for *G. catenatum* growth, this species was cultivated at 23±2 °C in L1 medium, using different selenium concentrations (0, 10⁻⁸, 10⁻⁷ and 10⁻⁶ M) and light intensities (15, 20, 30 μmole.m⁻².s⁻¹). Results showed that the growth of *G. catenatum* varied significantly with these environmental factors. The maximum growth (0.16 day⁻¹) was recorded with 10⁻⁸M of selenium with cell yield of 9000 cells.ml⁻¹. In the absence of this oligo-element growth rate decreased (0.1 day⁻¹) with a cell yield of 1400 cells.ml⁻¹. Increasing light intensity led to the increase of the growth rate from 0.11 day⁻¹ with cell yield of 4000 cells.ml⁻¹ for the irradiance 15 μmol m⁻² s⁻¹ to 0.17 day⁻¹ with cell yield of 13000 cells.ml⁻¹ for the irradiance 30 μmole m⁻² s⁻¹. Altogether, our results confirm the key role of selenium and light in the growth of the Moroccan strain of *G. catenatum*.

Keywords: *Gymnodinium catenatum*, Selenium, light, Mediterranean, Morocco

Introduction

Among HAB species, the dinoflagellate *Gymnodinium catenatum* is distributed worldwide (Hallegraeff et al., 2012). This neurotoxic dinoflagellate also develops in Moroccan and Mediterranean coastal marine ecosystems and caused several cases of human intoxications and even death of human consumers of contaminated mollusks (Tahri-Joutei, 1998). In Western Mediterranean, this species proliferates at the beginning of winter and during autumn (Rijal leblad, 2012). It produces Paralytic Shellfish Toxins (PSTs) which often accumulates in the exploited mollusks inducing a closure of shellfish harvesting for several months each year. The development of *G. catenatum* is determined by complex environmental conditions. Studies on the influence of the culture medium and origin of the water used for cultivation on the growth of

dinoflagellates highlighted specific requirements regarding some trace elements as selenium (Se) (Band-Schmidt et al., 2004). Doblin et al. (1999) demonstrated that *G. catenatum* from Australian waters have obligate requirement for Se, this element is known to be required for growth of several organisms at low level concentrations, but can induce toxicity at high doses (Gojkovic et al., 2014; Schiavon et al. 2017). Irradiance is an other important environmental factor that influences algal physiology. The growth rate is reduced under low irradiance. Our objective was to isolate *G. catenatum* cells, to establish monoclonal cultures and to study the effect of Se and irradiance on the growth of the Moroccan strain of this neurotoxic dinoflagellate.

Materials and Methods

Sampling site

Seawater was sampled at depth of 0.5 m at the M'diq bay located in the western Mediterranean Moroccan sea (35 ° 41'646 N - 05 ° 19'075 W), sampling location depth is 15 m. This was performed during blooming period (March 2016) of *G. catenatum*



Fig. 1: Geographical location of sampling site (M'diq bay)

Isolation, identification and culture establishment of *G. catenatum* strain

In the laboratory, single cells of *G. catenatum* were isolated using a pasteur pipette and a monoclonal culture was established. The identification was based on morphological characteristics using photonic microscope observations. The culture of *G. catenatum* was grown in our laboratory using L1 medium based on natural seawater from the Mediterranean (Guillard and Hargraves 1993), a temperature of 23 ± 1 °C, a salinity of 36 and cool white fluorescent illumination ($30 \mu\text{mole.m}^{-2}.\text{s}^{-1}$) under a 12 h:12 h light:dark cycle.

Ecophysiology experiments

Controlled laboratory experiments were carried out to test the effects of Se (H_2SeO_3) and irradiance level on the growth and cell yield (maximum cell density reached) of *G. catenatum*. Flasks were filled with 200 ml of L1 medium enriched with increasing concentrations of selenium (0 M, 10^{-8}M , 10^{-7}M , 10^{-6}M) with irradiance of $30 \mu\text{mol.m}^{-2}.\text{s}^{-1}$. In the second set of experiments, the flasks were exposed to increasing irradiances of 15, 20, 30 $\mu\text{mol.m}^{-2}.\text{s}^{-1}$, with an enrichment of 10^{-8}M of Se. Each flask was inoculated at t0 with *G. catenatum* cells to obtain an initial concentration of 50 cells. ml^{-1} . All the experiments were conducted in triplicates. Cell concentration was monitored every 3 to 7 days by direct microscopic counts using a Sedgewick counting chamber. The maximum growth rate was calculated following Guillard (1973) method. Growth was monitored for at least

53 days or until the maximum cell concentration (cell yield) was reached.

Results and discussion

Effect of Selenium

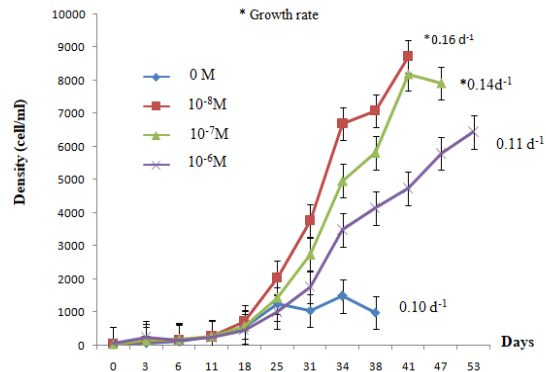


Fig. 2: Evolution of *Gymnodinium catenatum* densities as a function of Se concentration

The isolated strain was named GCMBM16 (*G. catenatum* from M'diq Bay, Morocco 2016). It forms chains of up to 20 cells. The morphology of our strain corresponds to that described by Fukuyo *et al.* (1990) and Rees *et al.* (1991) referring to *G. catenatum* HW Graham 1943.

Results showed that Se affected the growth of GCMBM16. An absence of added Se (0 M) resulted in a cell density of 1400 cells. ml^{-1} which suggests its requirement for the growth of this strain. Se enrichment of 10^{-8}M seems to be the optimal concentration for the growth (0.16 d^{-1}) of the Moroccan strain *G. catenatum* which reached a cell yield of 9000 cells. ml^{-1} . Fu *et al.* (2002) showed that sodium selenite induce GPX activity in *Chlamydomonas reinhardtii*, this enzyme (GPX) is known to prevent oxidative stress by catalyzing the reduction of hydrogen peroxide. Doblin *et al.* (1999) demonstrated that Se stimulates the cell division. In our experiments, when increasing the Se concentrations (10^{-7} and 10^{-6}M), the growth rate and cell yield decreased suggesting an adverse effect of Se given at high concentrations ($\geq 10^{-6}\text{M}$), becoming toxic to cells, this inhibition of growth at high doses of Se may result from impaired photosynthesis (Geoffroy *et al.* 2007).

Effect of irradiance

The growth of GCMBM16 increased with increasing irradiance level, from 0.11 day^{-1} for 15 $\mu\text{mol.m}^{-2}.\text{s}^{-1}$ to 0.17 day^{-1} for 30 $\mu\text{mol.m}^{-2}.\text{s}^{-1}$. This is in accordance with the results of De-bashan (2008).

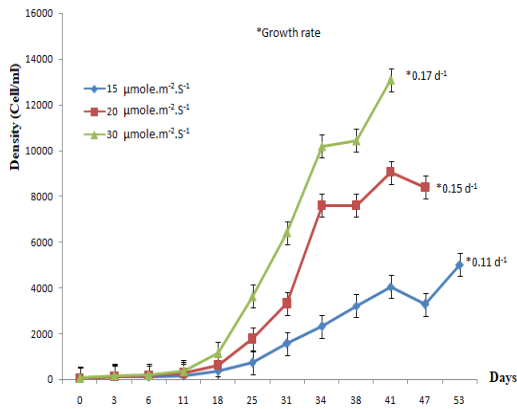


Fig. 3: Evolution of *Gymnodinium catenatum* densities (cells.ml⁻¹) and growth rate (d⁻¹) in function of irradiance level ($\mu\text{mol.m}^{-2}\text{s}^{-1}$)

Our data suggest that the increase of growth rate is related to irradiance level. This is probably due to the increase of photosynthetic activity and carbon fixation which promotes cell division.

Conclusion

Our results showed that the Moroccan strain of *G. catenatum* was a slow growing species considering the tested laboratory conditions. Low amounts of Selenium triggered the growth of this dinoflagellate. *G. catenatum* growth increased with light intensity. These laboratory experiments have to be completed by testing other environmental factors as temperature, salinity and macro-nutrients on the physiology of the Mediterranean strain of *G. catenatum*. A field survey is undergoing to examine the relationship between these main environmental factors and *G. Catenatum* bloom dynamic in the coastal Moroccan Mediterranean waters.

Acknowledgements

I would like to sincerely thank MARBEC laboratory who funded my stay in Montpellier, IAEA (International Atomic Energy Agency) and the GDR Phycotox for funding ICHA 2018 registration and accommodation in Nantes.

References

- Band-Schmidt, C. G., Morquecho, L., Jechuga-devéze, C. H., Anderson, D. M. (2004). *J. plankton Res.* 14, 1459–1470
- De-Bashan, L. E., Trejo A., Huss, V.A.R., Hernandez, J.P., Bashan, Y (2008). *Bioresource Technology* 99, 4980-4989.
- Doblin, M.A., Blackburn, S.I., Hallegraeff, G.M. (1999). *J. Plankton. Res.* 21, 1153-1169

Fu, L. H., Wang, X. F., Eyal, Y., She, Y. M., Donald, L. J., Standing, K. G. & Ben-Hayyim, G. (2002). *J. Biol. Chem.* 277, 25983–91.

Fukuyo, Y., Takano, H., Chihara, M., Matsuoka, K. (1990). Uchida Rokakuho, Co., Ltd., Tokyo. 407

Geoffroy, L., Gilbin, R., Simon, O., Floriani, M., Adam, C., Pradines, C., Cournac, L.,

Garnier-Laplace, J., 2007. *Aquat. Toxicol.* 83, 149-158.

Gojkovic, Z., Garbayo, I., Luis, J., Ariza, G., , Márová, I., Vílchez, C., (2015) *Algal Research* 7 106–116

Guillard, R. R. L. (1973) In: Stein J. R. (ed). Cambridge University Press, Cambridge, 289 – 320

Guillard, R.R.L. Hargraves, P.E. (1993). *Phycologia* 32, 234-236.

Hallegraeff, G. M., Blackburn, S.I., Doblin, M.A., Bolch, C.J.S. (2012) *Harmful Algae* 14. 130–143

Rees, A.J.J., Hallegraeff, G.M., (1991). *Phycologia* 30, 90-105

Rijal-leblad, B. (2012). Abdelmalek Essaadi University, Tanger. Thesis N° 57

Schiavon, M., Ertani, A., Parrasia, S., DallaVecchia, F., (2017) *Aquatic Toxicology* 189 1–8.

Tahri-Joutei, L. (1998). *Harmful Algae*. Xunta de Galicia & Intergovernmental Oceanographic Commission of UNESCO, Santiago de Compostela. 66-6.



Biological oceanography and limnology of HABs

Algal blooms: how are they harming models used for climate management?

Ian R. Jenkinson^{1, 2, *}, Elisa Berdalet³, Wei-Chun Chin⁴, Haibing Ding⁵, Jizhou Duan⁶, Florence Elias⁷, Zhuo Li^{8, 9}, Xavier Mari^{10, 11}, Laurent Seuront¹², Jun Sun¹³, Oliver Wurl¹⁴, Tim Wyatt¹⁵

¹ Chinese Academy of Sciences Institute of Oceanology, CAS Key Laboratory of Marine Ecology and Environmental Sciences, 7 Nanhai Road, Qingdao 266071, China;

² Agence de Conseil et de Recherche Océanographiques, 19320 La Roche Canillac, France;

³ Institute of Marine Sciences (CSIC), Passeig Marítim de la Barceloneta, 37-49, E-08003, Barcelona, Catalonia, Spain;

⁴ Department of Bioengineering, University of California, Merced, CA, USA;

⁵ Ocean University of China, Key Laboratory of Marine Chemistry Theory and Technology, Qingdao, China;

⁶ Chinese Academy of Sciences Qingdao Science and Education Park, West Coast New Area of Qingdao 266400, China;

⁷ Laboratoire Systèmes et Matières complexes, Université Paris Diderot, CNRS UMR 7075, Paris, France;

⁸ State Key Laboratory of Pollution Control and Resource Reuse, Tongji University, Shanghai 200092, China;

⁹ Shanghai Institute of Pollution Control and Ecological Security, Shanghai, China;

¹⁰ Aix-Marseille Université, CNRS/INSU, Université de Toulon, IRD, Mediterranean Institute of Oceanography (MIO) UM 110, Marseille, France;

¹¹ Institute of Marine Environment and Resources (IMER), Vietnam Academy of Science and Technology (VAST), Haiphong, Vietnam;

¹² CNRS UMR 8187, Laboratoire d'Océanologie et de Géoscience, Wimereux, France;

¹³ Tianjin Key Laboratory of Marine Resources and Chemistry, Tianjin University of Science and Technology, Tianjin, China;

¹⁴ Carl von Ossietzky Universität Oldenburg, Institute for Chemistry and Biology of the Marine Environment, 26382 Wilhelmshaven, Germany;

¹⁵ Barrio A Tomada, Borreiros, Gondomar, 36378 Pontevedra, Spain.

* corresponding author's email: ian.jenkinson@ocean-expert.org

Abstract

Microalgae blooms are generally associated with bacterial secondary producers. They produce organic matter (OM), some of which associates with the sea surface microlayer (SML). OM in the SML below the actual surface reduces fluxes of energy, including heat and momentum, and substances, including greenhouse gases, aerosols, algae, bacteria and viruses.

In addition to the SML-associated OM, another OM fraction, foam (including whitecaps), often lies above the primary SML when windspeeds exceed about 5 m s^{-1} , trapping gas bubbles. Such foam also dramatically increases albedo, reflecting solar radiation back into space, thus reducing solar heating and penetration of photosynthetically active radiation. Mean coverage of the ocean surface by foam has been measured to range between 1-6%, particularly in zones of Trade Winds.

Different types of OM, and particularly their mechanical properties, depend on ambient algal abundance, as well as on taxonomic composition, as do the dynamics of foam formation and decay. Air-sea fluxes may thus be influenced by genomic control through the blooming microalgae and Darwinian-type evolution. Bacteria may also play a role. In addition, foam patches on the ocean's surface serve as a unique microbial habitat. Such blooms, particularly when their taxonomic composition changes unpredictably, are likely to be harming the usefulness of climate models. Some of this harm might be mitigated by studying the relevant effects of these blooms on fluxes, and incorporating these effects into climate models.

Introduction

Algae (here including cyanobacteria) bloom in ocean waters. They produce and consume CO₂ and other greenhouse gases, of which the concentrations and fluxes are incorporated into models of climate. Algae are the primary producers of most of the organic matter (OM) in aquatic ecosystems (Hansell et al., 2009). Some of this OM, as well as OM from secondary production by

bacteria (Kurata et al., 2016; Howe et al., 2018) and other plankton, accumulate in the surface microlayer (SML). The mechanical effects of microalgal OM in the SML are still absent in models of how air-water fluxes of gases, particles and heat, affect climate. Here we propose some avenues for correcting this absence, and validating the effects empirically.

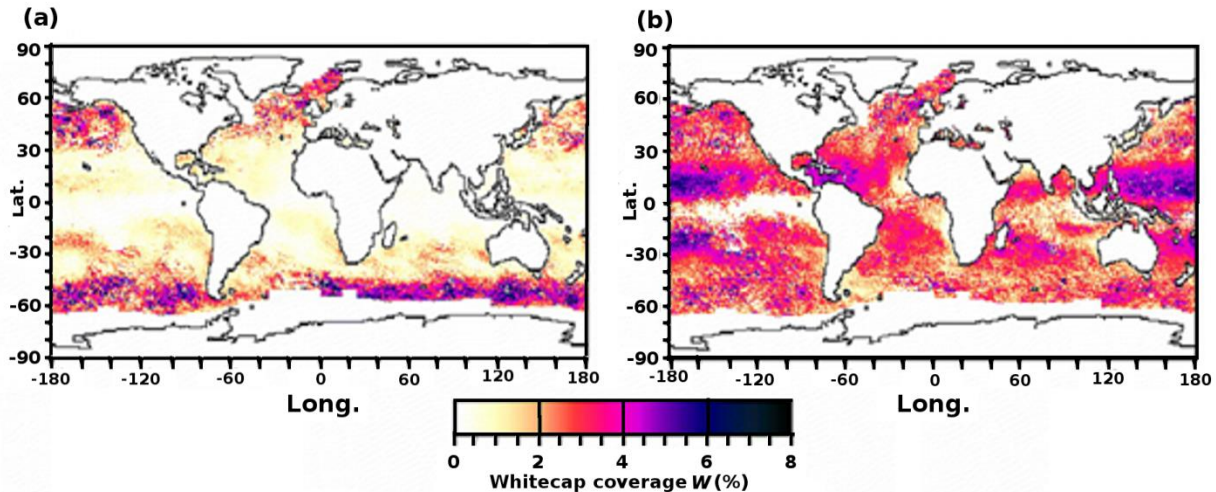


Fig. 1: Whitecap coverage (W) computed from models using daily fields of wind speed (a) and measured values of W observed from satellites (b), both for March 1998 (average of 31 daily maps of W). Redrawn from Anguelova & Webster (2006), as in Jenkinson et al. (2018). Note how in the Tropical areas, particularly the Trade Winds areas, observed values of W are higher than modelled values, while W values at around 60°S are smaller.

Fluxes modified by OM variation not modelled in climate models

The abundance, chemical composition and physical properties of OM secreted by blooming microalgae depend on algal abundance, taxonomic composition and physiological state (Seuront et al, 2006, 2010; Jenkinson & Sun, 2010, 2014; Jenkinson et al, 2018). Variation in the quality and quantity of algae-produced OM in the SML is not included in International Panel on Climate Change models (IPCC, 2018). However, such surface-associated OM reduces exchange of O₂, CO₂ and other greenhouse gases (GHG) (Goldman et al, 1998; Calleja et al, 2009), and may also reduce exchange of salts, humidity, aerosols and both thermal and mechanical energy, which are all important inputs to storm formation (Veron, 2015). In addition, OM in the surface film can damp ripples, gravity waves (Alpers & Hühnerfuss, 1989) and even low-frequency ocean swell (Henderson & Segur, 2013). In ocean cyanobacterial slicks (relative to nearby non-slicked water) both increase in temperature and

reduction in salinity have been measured during daytime in and just below the SML (Wurl et al., 2018), indicating reduction in evaporation over slick areas. Furthermore, at low windspeeds in some oligotrophic ocean regions, CO₂ fluxes measured by Calleja et al. (2009) were up to 2.7 times more than in water of higher productivity under otherwise similar conditions.



Fig. 2: Massive coastal foam events. (a) Foam event at Audresselles, Pas de Calais, France, associated with bloom of *Phaeocystis globosa*. Note the flying foam to the right of the hotel, and also that the hotel roof is partly white, from wind-blown and sticky foam (insert is enlarged to show wind-blown foam aggregates); (b) Foam at Cape Silleiro, Galicia, Spain, about a fortnight after gales in early February 2009. Such foam is produced by the action of breaking waves, entraining

air into seawater, itself containing polymeric organic matter produced mainly by algae. Photos by Laurent Seuront (a) and Tim Wyatt (b), as in Jenkinson et al, (2018).

Measurements of air-sea gas fluxes in relation to OM have so far been made only under calm to moderate winds (0-13 m s⁻¹), but not in heavy weather (Goldman et al, 1998; Calleja et al, 2009; Mari et al, 2017). Such studies, however, rarely report its tertiary polymeric structure or rheological properties of the OM. Algal-produced OM, however, shows huge inter- and intra- taxon variations in its rheological properties (Jenkinson et al, 2018). This suggests that sudden shifts in the taxon composition of microalgae, particularly in large offshore areas, could lead to abrupt changes in ocean modulation of climate.

Foam-production by algal blooms

OM produced by algae and bacteria, through its mechanical and surface-active properties, interacts with turbulence produced by wind, waves and other processes to produce whitecaps (Fig. 1a, b) and more persistent (>~1h) foam (Fig.2a, b). High levels of near-surface dissolved organic matter (DOM) in the Trade Winds areas are associated with ~3-8%, which is more than that in the Southern Ocean (~2-4% coverage), even though winds there are much stronger (Anguelova & Webster, 2006).

The higher foam coverage in the Trade Winds zones despite lower wind speeds may be caused by higher mean levels of DOM in the top 30 m (~50-75 $\mu\text{mol kg}^{-1}$ in Trade Winds zones compared to only ~45-55 $\mu\text{mol kg}^{-1}$ in the Southern Ocean) (Hansell et al, 2009). A supplementary explanation may be that the DOM in these different areas likely varies in molecular composition reflecting production by taxonomically different blooming microalgae as well as different OM histories after production.

Increase in ocean albedo

Change in albedo (i.e. proportion of radiation reflected) of the ocean can moderate global warming: increasing the albedo of the low-albedo ocean surface by about 5% could compensate the entire greenhouse gas (GHG)-driven perturbation of the Earth's radiation balance (Gattuso et al, 2018). The albedo of ocean foam is ~0.5 (Stabeno & Monahan, 1986). The present ocean-wide average albedo of about 2.5% \times 0.5 = 1.25%. This therefore represents enough albedo to counter ¼ of current GHG perturbation and thereby seriously harm models of global warming through production of DOM and foam. At certain times and

places, some algal blooms, such as those of *Phaeocystis* spp. (Seuront et al, 2006) (Fig. 2a, b) produce huge amounts of persistent foam with the potential to increase albedo much more. Adding "surfactants" to the ocean surface to produce persistent foam is being proposed to increase albedo and reduce global warming (Evans, 2010; Garciadiego Ortega & Evans, 2019). While concern about secondary ecological effects may preclude this (Crook et al, 2016), the ecological effects of foam coverage should also be studied.

Smaller-scale effects

At the scales of coastal blooms, modification of air-water gas exchange needs to be incorporated into models of aerosols responsible for respiratory distress in humans in HABs including those of *Ostreopsis* spp. (Vila et al, 2016) and *Karenia brevis* (Heil et al, 2014).

Conclusions

OM in the SML derives from primary and secondary production mainly by algae and bacteria. There is a need to characterize the tertiary chemical structure of OM especially in the surface film, in relation to its rheological and surface properties, and to the taxonomic composition of blooming microalgae throughout the oceans at all seasons and in all weathers. Such characterization should be combined with measurements of gas exchange and foam production. Algal blooms that somewhat invalidate (i.e. harm) the power of models to predict weather and climate represent a new type of HAB. The harm they do can be mitigated by conceiving and validating climate models incorporating biological modulation of marine foam production and longevity.

Funding

JS is supported by National Nature Science Foundation of China grant (41876134) and the Changjiang Scholar Program of Chinese Ministry of Education.

References

- Alpers W, Hühnerfuss H. 1989.. J geophys Res, 94(C5), 6251-6265.
- Anguelova MD, Webster F. 2006. J geophys Res, 111, C03017.
- Calleja ML, Duarte CM, Prairie YT, Agustí S, Herndl G J, 2009. Biogeosciences, 6, 1105-1114. .
- Crook JA, Jackson LS, Forster PM. 2016. J geophys Res Atmospheres, 121, 1549-1558.

- Evans JRG, Stride EPJ, Edirisinghe MJ, Andrews DJ, Simon, RR. 2010 *Climate Res*, 42, 155-160.
- Garciaadiego Ortega E, Evans JRG. 2019.. *J Eng marit Env*, 233, 388-397.
- Gattuso, JP et al. 2018. *Frontiers mar Sci*, 5, 337.
- Goldman JC, Dennett MR, Frew NM, 1998. *Deep-Sea Res*, 35, 1953-1970.
- Hansell DA, Carlson CA, Repeta DJ, Schlitzer R. 2009. *Oceanography*, 22(4), 202-211.
- Henderson DM, Segur H. 2013. *J geophys Res Oceans*, 118, 5074-5091.
- Heil CA et al. 2014. *Harmful Algae*, 38, 127-140.
- Howe KL, Dean CW, Kluge J, Soloviev AV, Tartar A, Shivji M, Lehner S, Perrie W. 2018. *Elem Sci Anth*, 6, 8.
- IPCC. 2018. Global Warming at 1.5°C. <https://www.ipcc.ch/sr15/> (Consulted 23 Jul 2019)
- Jenkinson IR. 1986. *Nature*, 323, 435-437.
- Jenkinson IR, Sun J. 2010. *J mar Sys*, 83, 287-297.
- Jenkinson IR, Sun J. 2014. *Deep Sea Res II*, 101, 216-230.
- Jenkinson IR, Seuront L, Ding H, Elias F. 2018. *Elem Sci Anth*, 6, 26.
- Kurata N, Vella K, Hamilton B, Shivji M, Soloviev A, Matt S, Tartar A, Perrie W. 2016. *Sci Rep*, 6, 19123.
- Mari X, Passow U, Migon C, Burd AB, Legendre L. 2017. *Prog Oceanogr*, 151, 13-37.
- van Oss CJ, Giese RF, Docoslis A. 2005. *J disp Sci Technol*, 26, 585-590.
- Seuront L, Vincent D, Mitchell JG. 2006. *J mar Sys*, 61, 118-133.
- Seuront L, Leterme SC, Seymour JR, Mitchell JG, Ashcroft D, Noble W, Thomson PG, Davidson AT, Van den Enden R, Scott FJ, Wright SW, Schapira M, Chapperon C, Cribb N. 2010. *Deep-Sea Res II*, 57, 877-886.
- Stabeno PJ, Monahan EC. 1986. In Monahan EC, Mac Niocaill G (eds), *Ocean Whitecaps*, D Riedel & Galway Univ Press, p. 261-266.
- Veron F. 2015. *Ann Rev Fluid Mech*, 47, 507-538.
- Vila M, Abós-Herrándiz R, Isern-Fontanet J, Àlvarez J, Berdalet E. 2016. *Scientia Marina*, 80, 107-115.
- Wurl O, Ekau W, Landing WM, Zappa CJ. 2017. *Elem Sci Anth*, 5, 3
- Wurl O, Bird K, Cunliffe M, Landing WM, Miller U, Mustaffa NIH, Ribas-Ribas M, Witte C, Zappa CJ. 2018. *Geophys Res Lett*, 45, 4230-4237.

Operational tools to improve the prediction capacity of the HABs in Galician mollusc production areas

Yolanda Pazos¹, F.M BellasAlaez², Luis González Vilas², Jesús M T. Palenzuela²

¹ Intecmar, Oceanography and Phytoplankton Unit, Peirao de Vilaxoán, 36611, Vilagarcía, Po. Spain;

² Applied Physics Dep., Biology Faculty, University of Vigo, Lagoas Marcosende 36310, Vigo, Spain;

* corresponding author's email: jesu@uvigo.es

Abstract

Galician *rias* represent a highly productive area which is located along the northern boundary of the Northeast Atlantic Upwelling System. Hence, the area supports important fishing and aquaculture activities, mainly mollusc culture in rafts, which are seriously hindered by harmful algae blooms (HABs). The study of HABs in this area requires an understanding of the ocean processes over the continental shelf, the effects of rivers and freshwater runoff, the anthropogenic pressure and the biology of species. In addition to the weekly oceanography and phytoplankton monitoring program aimed at shellfish safety, satellite images could provide information about the spatial distribution of phytoplankton blooms using regional-based algorithms for chlorophyll *a* concentration, which is considered to be a good estimator of phytoplankton biomass, or species indicators. Finally, statistical techniques and machine learning methods have proven to be useful tools for predicting HABs using both environmental parameters and distribution patterns of toxic species. In this work we introduce the European (EU H2020) project CoastObs, which explores the potential use of the new Sentinel satellites to monitor coastal water environments by developing a set of innovative high-level products, including HABs. The approach is based on combining map products (chlorophyll *a* or species indicators) derived from Ocean and Land Colour Instrument (OLCI) on-board Sentinel 3 satellite with a set of physical and biological parameters in order to develop predictive models of HABs on the Galician coast based on Support Vector Machines (SVM).

Keywords: harmful algae blooms (HABs), monitoring, remote sensing, Sentinel 3, OLCI, machine learning

Introduction

In terms of food security and biodiversity preservation, Harmful Algal Blooms (HABs) are considered one of the most dangerous threats to coastal ecosystems worldwide. HABs are caused by temporary increases of the abundance of toxic phytoplankton species (Anderson *et al.*, 2017).

Galician *rias* waters are optically very complex because of their regional characteristics: local freshwater inputs rich in organic and inorganic material and periodical upwelling events associated with northern winds introducing deep, cold, nutrient-rich waters. The area is highly productive and supports an intensive exploitation of fish and shellfish resources, including mollusc (mainly mussels) culture using floating rafts (or *bateas*). These activities are seriously hindered by HABs, which cause an important ecological, social and economic impact since they can even force the closure of production areas (Spyrakos *et al.*, 2011).

The HABs monitoring program in Galicia is conducted by INTECMAR. This program includes analysis of biotoxins and toxic phytoplankton in both water and mollusc samples, study of oceanographic conditions leading to potential HABs and decision-making about the closure of production areas (Gonzalez Vilas *et al.*, 2014).

Prediction in advance of HABs is very important for mollusc producers in terms of organization and logistic, as well as for the social policies related to one of the main economic driving forces in the region (Gonzalez Vilas *et al.*, 2014).

Due to its complexity, operational prediction of HABs (or closures/reopenings) in Galicia presents a great challenge. Remote sensing and machine learning methods could be a valuable tool for both prediction and complementing data based on samplings from monitoring programs (Spyrakos *et al.*, 2011; Gonzalez Vilas *et al.*, 2014).

Remote Sensing

Chlorophyll *a* (chl_a) concentration derived from different optical satellite images is suitable for detecting and monitoring HABs because it is related to phytoplankton biomass and is common to almost all taxonomic groups. Unfortunately, it does not provide information about the species or its toxicity (Spyrakos *et al.*, 2011).

As a consequence of the strong increase in phytoplankton biomass, phytoplankton blooms show distinct spectral signatures as compared to clean waters: significant absorption bands around 500 nm and 675 nm and reflectance peaks at 550 nm and 700 nm. Moreover, some HABs show a chlorophyll fluorescence peak at 683 nm that is useful for an effective separation from other complex water types. However, for some HABs this peak is shifted towards 700 nm because of the contribution of the elevated backscattering related to the high biomass concentration diminish the fluorescence effect, or the peak is the result of a combination of both fluorescence and backscattering effects (Anderson *et al.*, 2017).

Specific toxic species can also show distinct spectral characteristics, allowing the development of species indicators, i.e. algorithms which are aimed at detecting a toxic species directly from satellite images (Blondeau-Patissier *et al.*, 2014). For instance, Anderson *et al.* (2009) developed statistical models for *Pseudo-nitzschia* spp. abundance in Santa Barbara channel incorporating ocean color and sea surface temperature data.

As compared to traditional sampling methods, satellite methods are more cost-effective and produce map outputs providing more information about the spatial distribution of the HABs (Blondeau-Patissier *et al.*, 2014).

Machine Learning Methods

Different methods, varying in modelling approach and complexity, have been applied to the prediction of phytoplankton blooms. Unlike statistical or regression models, machine learning methods are able to provide high accuracies even when dealing with complex, non-linear and/or noisy datasets (Anderson *et al.*, 2017).

Machine learning methods that have been applied to HABs prediction include fuzzy logic, Artificial Neuronal Networks (ANN) and Support Vector Machines (SVM). Machine learning models can also incorporate data derived from satellite images into the prediction of HABs (Gonzalez Vilas *et al.*, 2014).

Materials and Methods

In this work, we introduce the methodology proposed within the European (EU H2020) funded project CoastObs (<http://coastobs.eu/>) to monitor and predict HABs in Galicia. The approach is based on combining maps products derived from Sentinel-3 data and a set of physical and biological parameters using machine learning methods to generate predictive models of HABs.

Maps products proposed within CoastObs include chl_a and species indicators. In both cases, the first step is the development of regional cluster-specific algorithms for the retrieval of a specific parameter (chlorophyll *a*, species abundance or bloom/no bloom) by adapting the methodology proposed by Gonzalez Vilas *et al.* (2011), but using OLCI instead of MERIS.

In situ data collected in a field campaign developed in summer 2018 were used in the development and validation of these algorithms. For each one of the 68 sampling stations, water-leaving reflectance spectra were measured using two field radiometers: TrioOS and Water Insight Spectrometer, or WISP-3. Profiles of water temperature, pH and dissolved oxygen were monitored by a portable meter (HI 9829, Hanna instruments), while chl_a fluorescence was measured using a Turner designs CYCLOPS-7 submersible fluorimeter. Vertical profiles of temperature, salinity, fluorescence and depth of water column were collected from a Seabird Model 25 CTD. Triplicate water samples from surface to 4 meters were collected at each station using an integrated polycarbonate tubular water sampler and then filtered in the laboratory to estimate several optical parameters. Chl_a concentration was determined using an HPLC method applying a reversed phase C8 for the separation of the pigments.

Predictive models are based on SVM, which have already been proven to be a powerful tool for predicting blooms of *Pseudo-nitzschia* spp. in Galicia (Gonzalez Vilas *et al.*, 2014). Models are based on a set of physical and biological parameters. Models use as input temperature and salinity data from the INTECMAR monitoring program, chlorophyll data derived from both INTECMAR and satellite images, and upwelling indices routinely distributed by the Fleet Numerical Meteorology and Oceanography Center (FNMOC) and available from a dedicated web page of the Spanish Oceanographic Institute (IEO). As output, models can use bloom/no bloom of a specific species or taxonomic group (e.g. *Pseudo-nitzschia*

spp.), or closures/reopenings of production areas due to paralytic toxins (PSP) or amnesic toxins (ASP). Output data are available from INTECMAR.

Results and Discussion

Figure 1a shows a picture of the application of WISP-3 field radiometer. Spectra measured from WISP-3 were used for validating Sentinel-3 data and select the optimal atmospheric correction for the development of *chl a* regional algorithms and species indicators (see Gonzalez Vilas *et al.*, 2011 for more details).

Figure 1b shows a *chl a* map derived from a Sentinel-3 image acquired on 15 July 2017. Patches of relative high chlorophyll are observed inside the *rias* and in the adjacent platform as a consequence of an upwelling event.

Chl a concentration is considered to be a good estimator of phytoplankton biomass, since it is common to almost taxonomic groups. In fact, *chl a* maps have already proven to be useful for detecting and monitoring HABs using MERIS images (Spyrakos *et al.*, 2011). *Chl a* maps from Sentinel-3 provide a good spatial resolution (300 m) and an excellent temporal resolution with an image per day since December 2018. The main disadvantages are that maps can only be obtained under cloud-free conditions and the lack of information about species and toxicity.

Figure 1c shows the results of SMV models developed for the prediction of *Pseudo-nitzschia* spp. blooms using data from 1992. Input variables include temperature, salinity, chlorophyll and upwelling indices in the previous days.

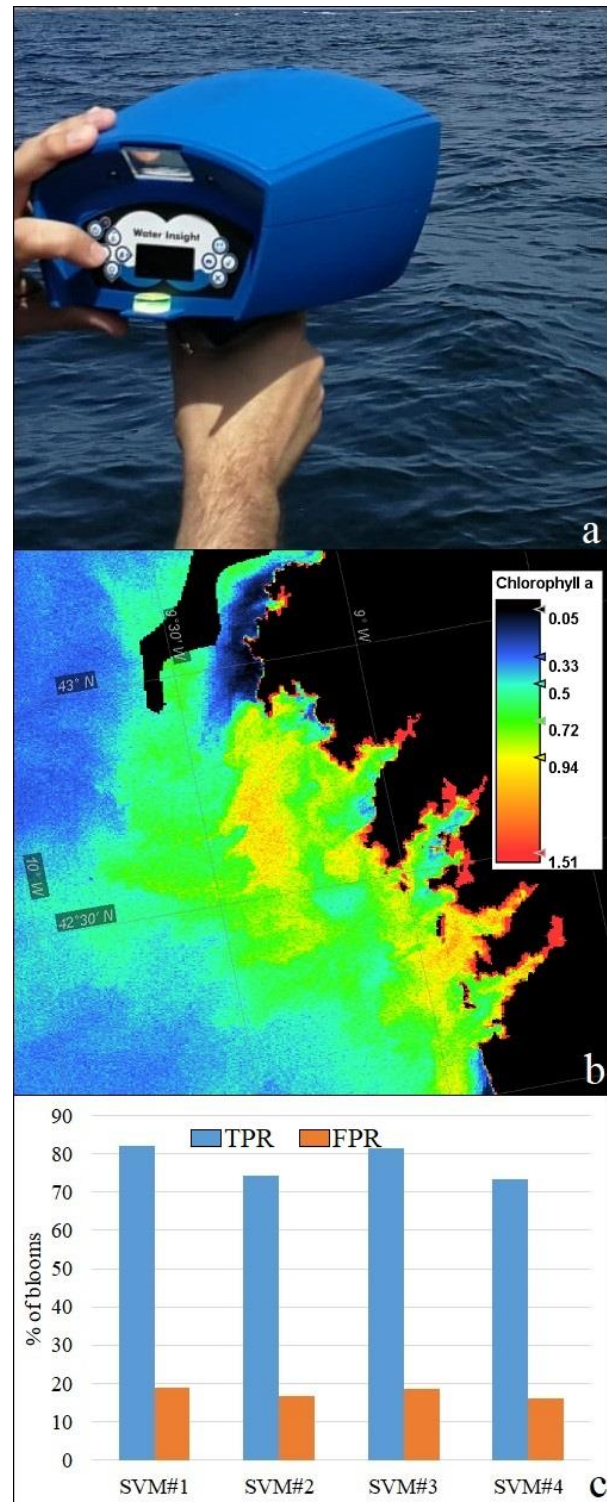


Fig. 1. a) WISP-3 radiometer; b) *chl a* map derived from the Sentinel-3 image acquired on 15 July 2017; c) results of SVM models for predicting *Pseudo-nitzschia* spp. blooms (TPR: true positive rate; FPR: false positive rate).

The percentage of blooms correctly classified (true positive rate or TPR) and the false positive rate (FPR) were computed for each model using an independent dataset. TPR varies between 73 % and 82 % while FRP is lower than 20 % in all the models.

SVM models were compared to other modelling approaches based on machine learning methods. Results of the best model for each technique are shown in Table 1.

Table 1: Classification results obtained from the best models using three modelling approaches.

Model	TPR	FPR
SVM	82.0 %	18.9 %
AdaBoost	72.4 %	18.0 %
RandomForest	46.9 %	4.7 %

RandomForest shows a low FPR, but at expense of a low TPR. On the other hand, AdaBoost shows a similar FPR as SVM, but with a lower TPR. Hence, SVM provides the best balance between FPR and TPR.

Results suggest a robust method with a good generalization capability. The approach is limited because these models do not distinguish between toxic and non-toxic events.

The approach proposed within CoastObs integrates both methodologies by using map products derived from Sentinel-3 images as input of machine learning methods. CoastObs started in November 2017 and it is expected to conclude in September 2020. In September 2019, HAB products had already been developed and were being validated and evaluated by the users.

Despite of the Galician *rias* are a highly dynamic environment, monitoring program is based on weekly samplings, which could lead to miss some short-term events. However, traditional monitoring

program might help testing and improving the approach proposed in this work, which could complement it by providing data about prediction and spatial distribution of HABs with a higher spatial coverage on a daily basis.

Acknowledgements

This work was supported by the European Union's Horizon 2020 research and innovation programme project CostObs (grant agreement n° 776348). The authors thank INTECMAR by providing biological and oceanographic data for algorithm development. We also thank The Regulatory Council of Mussel from Galicia and The Cooperative of Shipowners of the Port of Vigo (ARVI) for sharing their knowledge and experience.

References

- Anderson, D.M., Boerlage, S.F.E. and Dixon, M.B. (2017) Harmful Algal Blooms (HABs) and Desalination: A Guide to Impacts, Monitoring, and Management. Paris: Intergovernmental Oceanographic Commission of UNESCO 2017.
- Anderson, C.R., Siegel, D.A., Kudela, R.M. and Brzezinski, M.A. (2009). Harmful Algae, 8, 478-492.
- Blondeau-Patissier, D., Gower, J., Dekker, A., Phinn, S. and Brando, V. (2014). Prog. Oceanogr., 123, 123–144.
- González Vilas, L., Spyrakos, E., Palenzuela, J.M.T and Pazos, Y. (2014). Prog. Oceanogr., 124, 66–77.
- González Vilas, L., Spyrakos, E. and Palenzuela, J.M.T. (2011). Remote Sens. Environ., 115, 524–535.
- Spyrakos, E., González Vilas, L., Palenzuela, J.M.T. and Barton, E.D. (2011) Remote Sens. Environ, 115, 2471–2485.

Combination of machine learning methodologies and imaging-in-flow systems for the automated detection of Harmful Algae

Guillaume Wacquet^{1,2,3,*}, Alain Lefebvre², Camille Blondel², Arnaud Louchart¹, Philippe Grosjean³, Nadine Neaud-Masson⁴, Catherine Belin⁴, Luis Felipe Artigas^{1,*}

¹ Laboratory of Oceanology and Geosciences (UMR 8187 LOG), CNRS, ULCO, ULille, Wimereux, France

² Ifremer, Environment and Resources Laboratory (LER), Boulogne-sur-Mer, France

³ Univ. Mons, Complexys Institute, Laboratory of Numerical Ecology of Aquatic Systems, Mons, Belgium

⁴ Ifremer, Information System for Integrated Management and Monitoring (VIGIES), Nantes, France

* corresponding authors: guillaume.wacquet@univ-littoral.fr; felipe.artigas@univ-littoral.fr

Abstract

In recent years, improvements in data acquisition techniques have been carried out to sample, characterize and quantify phytoplankton communities at high temporal and geographical resolution, with a special focus on potential harmful algae, during oceanographic campaigns or in the frame of monitoring networks (to support knowledge but also for EU Directives and Regional Sea Convention needs). These acquisition and digitization techniques, including "imaging-in-flow" systems, allow to process a high number of samples and, consequently, generate an important quantity of data in which the presence of target events might not be detected. Indeed, as for traditional samples analysis with inverted microscope, a full manual quantification of the particles based on a simple visual inspection can be time-consuming, tedious and consequently lead to erroneous or wrong identifications.

For this purpose, the ZooImage R-package was and is still being developed to allow greater automation in data classification and analysis while also permitting some user-interaction during the process. The proposed methodology consists in combining few expert knowledge and machine learning algorithms at different levels: (i) to classify particles into different groups based on the definition and the adaptation of a specific training set through the use of "contextual data"; (ii) to detect and partially validate the "most suspect" predictions, based on a probability of misclassification; (iii) to estimate the number of cells for each colonial form thanks to the building of specific predictive models.

These different semi-automated tools were applied to the *in vivo* image dataset acquired with the FlowCam instrument during the September-October CAMANOC 2014 (Ifremer) cruise in the English Channel, in order to evaluate their operational ability to monitor the diversity of samples for the microphytoplankton, and especially to detect, track and count the most frequent potentially harmful algae found in this area at that period, like species belonging to *Pseudo-nitzschia*, *Dinophysis*, *Prorocentrum* and *Phaeocystis* genera. A distribution of these target groups was computed which highlights different sub-regions in the English Channel during the late summer-fall transition.

Keywords: Machine learning, User-interaction, Semi-automated classification, English Channel, HABs

Introduction

Since 2000, phytoplankton is defined as a biological parameter for marine quality assessment by the Water Framework Directive (WFD) and in 2008, the European Marine Strategy Framework Directive (MSFD) confirms this capacity. Today, about 7000 different species have been identified worldwide of which about 70 are potentially harmful (toxins or foam producers). Because of the consequences they have on the ecosystems goods and services, their economic and health impacts,

the occurrence of these toxic events contributed to renewed interest towards studies on marine ecosystem, including ecological, climatic and economic domains.

The traditional technique to determine the phytoplankton composition of a sea water sample, is the identification and enumeration by inverted microscopy method after sedimentation (Utermöhl, 1958). However, this method is time consuming and requires experts specialized in phytoplankton

taxonomy. Moreover, it cannot detect spatial and temporal changes in the marine ecosystem combining high frequency and quality of information obtained without competent human participation to collect and classify these samples. Recent advances in image analysis and pattern recognition have made possible to estimate microphytoplankton concentration without hard numerical process, directly on living samples (Tang *et al.*, 1998). These approaches, using digital imaging of phytoplankton particles measured by image analysis and classified using machine learning algorithms, reduce the analysis time, improve the counting accuracy and can carry out a lot of measurement providing opportunities for microbiologists to get new insights into the functioning of communities in the nano-microplankton size range (Benfield *et al.*, 2007). Over the past few decades, different specialized systems coupling digitization devices and data processing software have been developed for enumeration and measurements of particles in the nano-microplankton size range, like the Imaging FlowCytoBot instrument (IFCB) coupled to a specific data processing and classification software (Olson and Sosik, 2007), or the FlowCam® system (Fluid Imaging Technologies, Inc.¹) associated to the VisualSpreadSheet® software (Sieracki *et al.*, 1998). Unfortunately, these software systems are designed for specific devices and are not always compatible with other imaging systems. Additionally, recent optimization of plankton imagers leads to faster digitization, multiplication of analyses and accumulation of a large quantity of data and images.

In this context, we propose to develop, to test and to prove the added-value of a semi-automated identification system for phytoplankton classification. This system could improve our knowledge of the ecology of phytoplankton by allowing semi-automated analyses to be applied to a higher temporal/spatial resolution than traditional techniques, due to time saving during data acquisition and processing steps (including validation of the results). These analyses are thus better adapted to study the frequencies of phenomena that control this biological compartment (Cloern, 1996). The proposed tool consists in coupling the FlowCam device for acquiring the digital images of phytoplankton particles in a sample, with the ZooImage R-package², which allows identifying and counting

phytoplankton in a semi-automated way (Grosjean and Denis, 2013).

Materials and Methods

Sampling strategy

The CAMANOC cruise was a multidisciplinary survey within the framework of an ecosystem approach to fisheries. It was conducted from September 16 to October 12, 2014, in the Western and Central English Channel, on-board the R/V “Thalassa” (IFREMER). Water samples were collected at 89 sampling stations at subsurface (<0.5m), using a 5-L Niskin bottle. These samples were maintained cold (4°C) and in the dark until their analysis.

Imaging-in-flow system

Samples were digitized using an 8-bit grayscale benchtop FlowCam® VS with the pump speed set to 1.8 ml.min⁻¹. A 4X objective (40X overall magnification) coupled with a 300µm-depth flow-cell was used and samples were run in “AutoImage” operation mode. As described by Zarauz *et al.* (2007), all particles in the field of view of the camera (phytoplankton, zooplankton and inorganic particles) are imaged and captured at a regular user-defined interval, which allows an accurate estimation of imaged volume and consequently of particle concentration.

The specific software program, provided with the FlowCam device and named VisualSpreadSheet, is essential for all the major aspects of analysis: setup for data acquisition through the context settings for controlling the device, managing files and setting preferences, data acquisition and post-processing of collected data. For each particle, we obtain a set of 26 image parameters: 8 basic shape parameters (area, length, width, etc.), 13 advanced morphological parameters (circularity, convexity, roughness, etc.) and 5 grayscale measurements (intensity, transparency, etc.). The rest of the process, from image processing to statistical analysis, is done using the version 5.5.2 of the ZooImage R-package.

Training set and classifier

Building a training set is a crucial step in the automated recognition of plankton. Indeed, it represents the database used to generate a tool for automated or semi-automated recognition. Within this study, a training set representative of each plankton community met in the English Channel,

¹ <https://www.fluidimaging.com/>

² <https://cran.r-project.org/web/packages/zooimage/>

was built using samples taken throughout 2013 (in the frame of the Ifremer Regional Nutrients Monitoring network) and 2014 (in the frame of the CNRS LOG DYPHYRAD monitoring transect). A total of 3582 images were manually classified in 28 plankton groups. Moreover, instead of manually removing detrital particles and artefacts as is commonly done (Zarauz *et al.*, 2007), we added 12 groups for floating dark and light dead particles, bubbles, fibers, etc. to the 28 plankton groups in order to automatically identify and then eliminate them from the statistics. Finally, 5154 images were sorted into 40 groups. From this training set, a classifier is trained using the “Random Forest” algorithm (Breiman, 2001). Global error measured by using 10-folds cross-validation is equal to 25% for this training set.

Adaptive learning

Phytoplankton communities are sensitive to environmental and climate changes and modifications in their composition can occur at fast rates, which can lead to significant prediction errors when a static training set is used. Indeed, the representativeness and the variability of the particles into each group in the training set can have an important impact on the classification results. However, in order to build an ideal training set, a large number of labelled particles is needed, but also requires a lot of time, human resources and skills. To overcome this problem, adaptive learning improves a simple training set by adding labelled items taken from a pool of candidates.

This pool is composed of particles belonging to samples taken in the same experimental conditions than the studied one, and already validated by an expert. These “contextual” data allow to adapt the training set temporally and geographically to the phytoplankton communities generally encountered in the studied area and consequently to reduce the initial prediction error by 20-30%. In this study, one sample was selected every 2 days and all particles were manually labelled and validated. These particles were added to the initial training set in order to build an adapted recognition tool which is then used to classify the samples of the next 2 days.

Semi-automated validation

Performance scores obtained by completely automated classification are often considered too low to provide relevant abundances for all groups. Therefore, it is necessary to validate these predictions (Gorsky *et al.*, 2010). However, the

validation of all predictions can be tedious and time-consuming if the sample size is important. In the ZooImage package, sophisticated techniques for semi-automated recognition are proposed. This allows a less biased estimation of abundance without having to manually validate all images.

In this context, the images which must be validated are detected by the automated classification system on the basis of a probability of a correct prediction for each particle. Once the images validated, the error can be modelled in order to perform statistical corrections. This approach offers an ideal trade-off between the full-automated method and the total manual validation while guaranteeing similar or better performances of recognition within an acceptable time. Moreover, the statistical correction of the remaining errors associated to the adaptive learning method, allows decreasing the global error more rapidly than with the initial training set.

Single cell counts

Usually, with automated acquisition systems like FlowCam, IFCB, flow cytometry, etc., colonies are considered and subsequently counted as one single particle, the same as single cells. Moreover, although colonies contribute largely to annual productivity, all biomass estimators are essentially calibrated on abundance in terms of single cells per volume unit. That is why the automated counting of the number of single cells in the various colonial forms represents a real challenge.

The proposed method consists in building specific predictive models for each studied group, based on the manual counts made on images contained in the training set. For this, a multivariate analysis was performed thanks to a simple linear modelling.

Results and Discussion

HABs distribution in the English Channel

An important spatial heterogeneity in microphytoplankton distribution was observed all along the sampling area. In order to highlight specific areas for the potential HABs and the associated spatial distribution, a clustering method was applied to their abundances. The Partitioning Around Medoids algorithm (PAM) showed 3 distinct areas (Figure 1):

- Western English Channel (WEC) where HABs were essentially characterized by *Pseudo-nitzschia* genus;

- Central English Channel (CEC) with high abundances of dinoflagellates (*Prorocentrum* genus) and haptophytes (*Phaeocystis* genus);
- Bay of Seine (BOS) where the highest abundances of *Pseudo-nitzschia* and *Prorocentrum* genera were observed.

Microscopy comparison and single cell counts

In order to validate these results, a comparison with the abundances obtained by microscopic counts was performed in some stations in the WEC, and especially for the most abundant genus which is *Pseudo-nitzschia*. As shown on Figure 2, the raw abundance (*i.e.* with colonial forms) estimates obtained with the FlowCam were always lower than counted with the inverted microscope, for which all cells were counted, whether they be in a colonial or a single cell form.

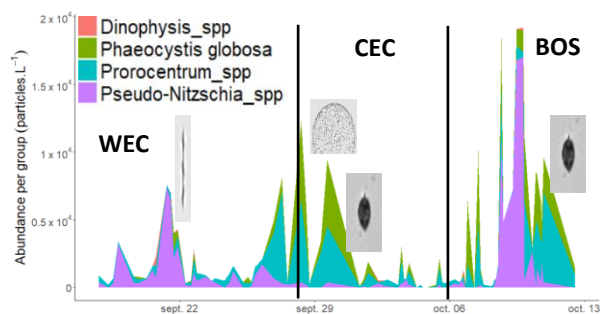


Fig. 1. Variability of the abundances (particles.L⁻¹) of each harmful genera during the CAMANOC cruise.

However, despite this under-estimation, a significant Spearman's rank correlation coefficient was found between *Pseudo-nitzschia* FlowCam and microscopic counts (Table 1).

After application of the specific predictive model for *Pseudo-nitzschia*, the overall dynamics of abundance obtained by microscopy and FlowCam were similar (Figure 2). In addition, an increase of the correlation coefficient was observed.

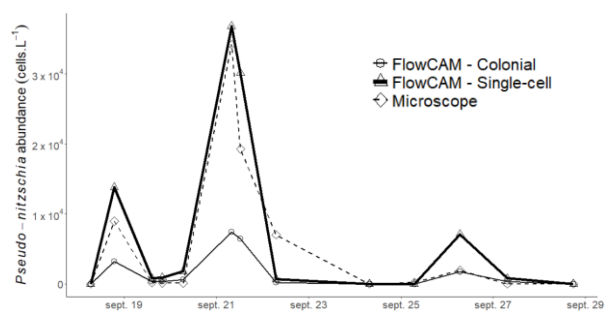


Fig. 2. Comparison between cell abundance obtained by microscopy (dashed line) and FlowCam with () and without single cell enumeration for *Pseudo-nitzschia* genus in some stations in WEC.

The results presented in this study highlight the need and the relevance of the combination of the automated process and the integration of some expert knowledge. However, in order to lead to more accurate discrimination, an optimization of training sets and algorithms, associated with the improvement of the resolution of the digital images, is still needed. Moreover, it is important to note that the ZooImage package, and consequently all the (semi-)automated tools presented in this study, can also be used on images acquired by various automated systems, like ZooScan, IFCB, etc.

Table 1. Spearman's rank correlation coefficient between *Pseudo-nitzschia* abundances obtained by microscopy and by FlowCam analysis, considering colonial forms or single cells counting.

Comparison	Spearman	p-value
Colonial form	0.74	< 0.05
Single cell	0.79	< 0.05

Acknowledgements

The authors thank the P.I. of the CAMANOC cruise (Morgane Travers-Trollet), as well as the captain and crew of R/V "Thalassa". Guillaume Wacquet was supported by post-doctoral grants funded by the Complexys Institute of the University of Mons and by the "Conseil Régional des Hauts-de-France" and is currently supported by the Centre National de la Recherche Scientifique (CNRS) in the frame of the MSFD convention (n°2101893310) with the French Ministry for an Ecological and Inclusive Transition (MTES), for the monitoring programme for pelagic habitats.

References

Benfield M. C., Grosjean Ph., Culverhouse P. F., Irigoien X., Sieracki M. E., Lopez-Urrutia A., Dam H. G., Hu Q., Davis C. S., Hansen A., Pilskaln C. H., Riseman E. M., Schultz H., Gorsky G. (2007). *Oceanography* 20, 172-187.

Breiman, L. B. (2001). *Mach. Learn* 45, 5-32.

Cloern, J.E. (1996). *Geophysics* 34(2), 127-168.

Gorsky G., Ohman M.D., Picheral M., Gasparini S., Stemmann L., Romagnan J.-B., Cawood A., Pesant S., García-Comas C., Prejger F. (2010). *Plankton Research* 32(3), 285–303.

Grosjean Ph., Denis K. (2013). *Data Mining Applications with R*, Elsevier, 978-0-12-411511-8, Chapter 12.

Olson R.J., Sosik H.M. (2007). *Limnol. Oceanogr.* 5, 195-203.

Sieracki C. K, Sieracki M. E., Yentsch C. S. (1998). *Mar. Ecol. Prog. Ser.* 168, 285-296.

Tang X., Stewart W. K., Vincent L. U. C., Huang H. E., Marra M., Gallager S. M., Davis C. S. (1998). *Artificial Intelligence Review* 12, 177-199.

Utermöhl H. (1958). *Mitt. Int. Ver. Limnol.* 9, 1-38.

Zarauz L., Irigoien X., Urtizberea A., Gonzalez M. (2007). *Mar. Ecol. Prog. Ser.* 345, 27–39.

Automated techniques to follow the spatial distribution of *Phaeocystis globosa* and diatom spring blooms in the English Channel and North Sea

Arnaud Louchart^{1*}, Reinhoud de Blok², Elisabeth Debuschere³, Fernando Gómez¹, Alain Lefebvre⁴, Fabrice Lizon¹, Jonas Mortelmans³, Machteld Rijkeboer⁵, Klaas Deneudt³, Arnold Veen⁵, Guillaume Wacquet¹, François G. Schmitt¹, Luis Felipe Artigas^{1*}

¹ CNRS, Univ. Littoral Côte d'Opale, Univ. Lille, UMR 8187, LOG, Laboratoire d'Océanologie et de Géosciences, 62930 Wimereux, France;

² Laboratory of Protistology & Aquatic Ecology, Department of Biology, Ghent University, Ghent, Belgium;

³ Flanders Marine Institute (VLIZ), Ostend, Belgium;

⁴ IFREMER, LER/BL, Boulogne sur mer, France;

⁵ Laboratory for Hydrobiological Analysis, Rijkswaterstaat (RWS), Zuiderwagengplein 2, 8224 AD Lelystad, The Netherlands;

*corresponding authors: arnaud.louchart@etu.univ-littoral.fr; felipe.artigas@univ-littoral.fr

Abstract

Two innovative automated techniques were used to track phytoplankton spatial and temporal variability in the Eastern English Channel (EEC) and Southern North Sea, during three consecutive cruises in spring 2017, in the frame of local/national monitoring programmes in France, Belgium and the Netherlands. The cruises started after the onset of spring blooms in the EEC and followed their development along the EEC towards the southern North Sea, during one month. Our study aimed at: (i) applying multi-spectral fluorometry (MSF) and pulse shape-recording flow cytometry (PSFCM) to characterize *Pseudo-nitzschia* spp. and *Phaeocystis globosa*, which contribute to spring blooms in the area; (ii) highlighting the patchiness and sharp variability in abundance and chlorophyll a fluorescence (used as a proxy of biomass) of these species; (iii) studying the relation between nutrient loads and the extension of these potential HABs.

Both MSF and PSFCM revealed spatial heterogeneity in the distribution of phytoplankton groups. The MSF detected *Phaeocystis globosa* up to 80% of the total biomass in the French Region of Freshwater Influence (ROFI) named as the “Coastal flow”, the Dover Strait and the Dutch estuarine plumes whereas “brown Algae” (diatoms and dinoflagellates) represented always more than 60% of the total biomass in the Bay of Seine and the Thames estuary. PSFCM showed high abundance (7.0×10^4 cell mL⁻¹) of *P. globosa* life stages along the French coast, the Dutch coastal and estuarine waters, up to the Wadden Sea. *Pseudo-nitzschia* spp. were very abundant in the “coastal flow”, from the Bay of Somme to the Dover Strait and along the Dutch ROFI (under the direct influence of Westerschelde and Rhine estuaries), reaching up to 3.0×10^3 cell mL⁻¹. Validation of the results was carried out by microscopic observations and counts.

Keywords: Automated pulse shape-recording flow cytometry, Multispectral fluorometry, Harmful Algal Blooms, High Frequency phytoplankton monitoring, *Pseudo-nitzschia* spp., *Phaeocystis globosa*, North Sea, Eastern English Channel

Introduction

The Eastern English Channel (EEC) and the Southern North Sea (SNS) are influenced by Atlantic waters entering from the West into the English Channel. Several rivers bring freshwaters with nutrients inputs defining Regions of Freshwater Influence (ROFI) along the French, Belgian, U.K. and Dutch coastal systems. Some of these estuarine waters flow towards the North Sea (residual current) along the French coast resulting in a brackish “coastal flow” (Brylinski et al., 1991). During spring, important nutrient loads together

with the increase in irradiance are responsible of outbursts of phytoplankton species. In the EEC and SNS, spring blooms are characterized by diatoms and, in most locations, by *Phaeocystis globosa*. Thus, two potential HAB forming species were characterised in these areas: *Phaeocystis globosa* (foam-aggregates) and some species of the genus *Pseudo-nitzschia* (toxin producers). These areas benefit of long-term monitoring at fixed stations coupled with seasonal cruises. Unfortunately, the techniques used are most of the time applied at low

frequency (monthly or bi-monthly) and can miss occurrences and patches or extreme events.

For a decade, automated and innovative techniques including pulse shape-recording automated flow cytometry (PSFCM) and multi-spectral fluorometry (MSF) have allowed continuous recording/profiling in coastal and open sea systems as a complement of the existing monitoring in the area (*e.g.* Bonato et al., 2015; 2016). They lead to higher resolution (spatial and/or temporal) than those which can be achieved by applying reference techniques (*i.e.* microscopy, HPLC).

Automated techniques were applied to characterize HABs and monitor changes in abundance and biomass in phytoplankton communities. These automated approaches therefore represent a significant improvement for implementing the monitoring programme of the European Marine Strategy Framework Directive (MSFD).

Materials and Methods

Study area

Samples were collected during three cruises in spring 2017: April 21st to 30th, PHYCO-CNRS cruise on board the R/V “*Côtes de la Manche*”, May 4th to 8th, LifeWatch-VLIZ-cruise on board the R/V “*Simon Stevin*” and May, 12th to 15th, RWS Spring cruise on board the R/V “*Zirfaea*”.

These cruises were planned in the frame of local programmes as the CPER MARCO French project, European projects JERICO-Next H2020 and LifeWatch as well as part of the Dutch national monitoring of coastal and marine waters and French national preliminary work for implementing the monitoring of pelagic habitats in the frame of the MSFD. According to phytoplankton observations from current monitoring within the partners involved, spring blooms start earlier in the EEC than in the SNS (Lancelot et al., 1987). Our sampling strategy followed the same chronology. Water was pumped continuously from approximately 3 m-depth and passed through an automated pulse shape-recording flow cytometer (PSFCM, CytoSense, CytoBuoy b.v.) to record and count particles every 10 min. Depending on the speed of the ship, we obtained a spatial resolution from 1.5 to 3.7 km. At 94 stations, water column was also investigated by reference measurements (pigments, nutrients), multi-spectral fluorometry (MSF, FluoroProbe, bbe Moldaenke) profiles or discrete surface and bottom measurements, as for PSFCM.

Multispectral fluorometry (FluoroProbe, bbe Moldaenke).

Because the water column is well-mixed, we focused on the sub-surface data. The MSF aims at discriminating spectral groups of algae based on their pigment's composition following the specific excitation spectrum (composed of 6 Leds) and corresponding emission of chlorophyll *a* fluorescence. Here, the FluoroProbe was set up to discriminate four spectral groups: “BlueGreen algae” (phycocyanin-containing cells such as Cyanobacteria), “Cryptophytes” (phycoerythrin-containing cells mainly Cyanobacteria and Cryptophytes), *Phaeocystis* (Haptophytes) and “Brown algae” (cells with fucoxanthin-derived pigments including diatoms and dinoflagellates). The *Phaeocystis* fingerprint was defined on cultures and during a massive bloom of the recorded in the EEC (Houliez et al., 2012).

Automated flow cytometry (CytoSense, CytoBuoy b.v.)

The PSFCM characterize particles according to their optical signature from 1 μm to 800 μm (width) and a few mm (length). The intersection of the 5 μm laser beam (488 nm) and each particle generate a pulse shape, itself composed of five signals according to the internal and/or external composition of the particles. The Forward Scatter (FWS) is associated with the size of the particle by calculating the length of this FWS. Size calibration was done using 3 and 10 μm fluorescent beads. The Sideward Scatter (SWS) is related to internal and/or external component such as chloroplast, vacuole, nucleus or calcites plates. The signal is also composed of three types of fluorescence: Red as a proxy of chlorophyll *a*, Orange and Yellow for phycoerythrin and phycocyanin proxy. We set a low trigger level on the red fluorescence in order to separate photosynthetic-active seston and the detritus and non-living particulate matter. The discrimination of each group was processed taking into account the amplitude and the shape of the five signals. The discrimination between groups was processed manually with CytoClus® software (CytoBuoy b.v.). The software provides also several mathematical features on each signal (*e.g.* Length, Total, Average...) increasing the number of possible combinations.

Results and Discussion

Deployments of the MSF showed high chlorophyll *a* concentration in the French brackish coastal waters (“coastal flow”), from the north of the Bay of Seine until the Dover Strait, the Dutch estuarine plumes and the Wadden Sea, where *Phaeocystis* represented more than 80% of the total biomass (Figure 1). At some places (*e.g.* French coast of the EEC, Dutch estuarine plumes), the *Phaeocystis*

fingerprint could be considered as a quasi monospecific bloom formation (Anderson et al., 1998).

In the Thames and the Seine plumes, chlorophyll *a* estimated concentration was lower than in the “coastal flow”. Those estuarine influenced areas were characterized by Brown Algae (diatoms and dinoflagellates) representing always more than 60% of the total biomass (Figure 1) and the *Phaeocystis* proportion was higher in the Thames plume than the Bay of Seine.

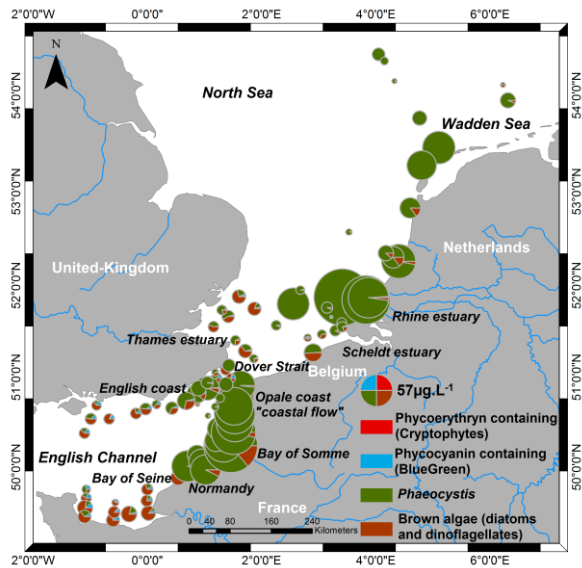


Fig. 1: Spatial distribution of the 4 spectral groups identified by MSF during the spring 2017 cruises.

Up to seven groups were characterized by PSFCM during the three cruises (Table 1): two of those groups concerned potential HAB: *Phaeocystis globosa*-like, *Pseudo-nitzschia* spp.

Previous work enabled us to characterize the optical cytometric signature of *P. globosa* in the EEC/SNS during massive spring blooms (Rutten et al. 2005, Guiselin 2010, Bonato et al. 2016). As observed by Guiselin (2010), *P. globosa* can be subdivided into three groups, two haploid groups with a size around 3µm and two kinds of red fluorescence (low and high) and one diploid stage with very high red fluorescence content and a size around 4-6µm. In our study, those three life stages were grouped together to form *P. globosa*-like group. All nanophytoplankton was defined as *Phaeocystis* in our study, even though other nanoeukaryotes were most probably present too.

In our study, a supplementary group was characterized, showing two symmetric chloroplasts based on the signature profile. This optical signature was compared with culture of *Pseudo-nitzschia* spp. shape file, which were similar to those collected during the cruise.

Table 1: Cytometry groups discriminated by PSFCM and their estimated size (after calibration with beads).

Group	Size ± sd (µm)
<i>Synechococcus</i>	1.99 ± 0.45
Picoeukaryotes	3.01 ± 0.42
<i>Phaeocystis globosa</i> -like	5.40 ± 1.22
Cryptophytes	5.27 ± 2.47
Coccolithophores	7.06 ± 2.31
<i>Pseudo-nitzschia</i> spp.	18.87 ± 4.78
Microphytoplankton	33.45 ± 10.25

Significant correlations were found between optical microscopy and PSFCM for *Pseudo-nitzschia* spp. ($r = 0.39^{***}$ considering samples from PHYCO and RWS cruises and $r = 0.77^{***}$ only for RWS cruise), *P. globosa* ($r = 0.75^{***}$) and between *Phaeocystis* red fluorescence and *Phaeocystis* by CHEMTAX ($\rho = 0.70^{***}$ for LifeWatch-VLIZ cruise). The spring blooms were clearly dominated, in terms of abundance, by nanophytoplankton groups, especially *P. globosa* (data not shown).

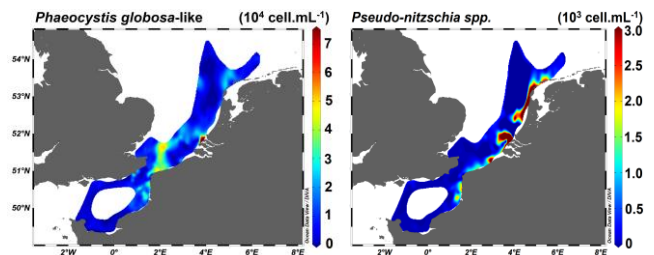


Fig. 2: Spatial distribution of the potential HABs discriminated groups by the PSFCM during the spring 2017 cruises

High total abundance and biomass was evidenced along the French coast, starting from the Bay of Somme and then going towards offshore waters of the SNS, but also off along the Dutch estuaries and coast up to the Wadden Sea.

P. globosa-like was very abundant nearby the Rhine estuarine mouth. Abundance reached more than 7.0×10^4 cell mL⁻¹ and the cells were mainly from the haploid stages. Along the French coast of the EEC, *P. globosa*-like reached 4.0 to 5.0×10^4 cell mL⁻¹. Drifted by the residual current through the Strait of Dover we found the same range of abundance in offshore waters of the southern North Sea (Figure 2). Therefore, populations of the Rhine estuarine mouth and the French coast do not seem to be connected.

Pseudo-nitzschia spp. was very abundant in the French “coastal flow”, from the Bay of Somme to the Dover Strait and along the Dutch ROFI and

coast (Figure 2). Abundance was higher along the Dutch coast than in the Strait of Dover. However, we found a succession of high and low abundance generating patchiness of abundance along the coast, from the Bay of Somme to Wadden Sea.

High Si:DIN (Dissolved Inorganic Nitrogen) ratios were measured in the coastal area of the Rhine and Scheldt ROFI. Thus, silicate oversupplies the area and can be taken up by *Pseudo-nitzschia* spp. This suggests a potential limitation of nitrate for the development of *Phaeocystis globosa*.

Along the French coast, the Bay of Seine and Normandy coasts were characterized by a high Si:P ratio whereas at the Opale coast (“coastal flow”), phosphorus was limited over DIN (High DIN:P). High Si:P is suitable for diatoms development whereas the potential phosphorus limitation in the French EEC favors a bloom of colonial *P. globosa* form (Veldhuis and Admiraal, 1987).

In summary, innovative techniques successfully characterized *Pseudo-nitzschia* genus and/or *P. globosa* outbursts, which contribute greatly to the spring blooms in the EEC-SNS area. They were able to highlight patchiness and sharp variations in abundance and fluorescence of potential HABs. A major improvement will focus in the future on the automated identification of more HABs taxa. Identifying optical signatures can lead to a better and/or an automated characterization of particles by semi-supervised classification based on PSFCM features and optical profiles (R package « RclusTool³ » Wacquet *et al.*, this volume). Thus, coupling those tools and implementing automated techniques (*e.g.* PSFCM improved with automated image acquisition and MSF) during cruises on Research Vessels, ships of opportunity and/or automated moorings or fixed platforms could increase the detection of HABs and better understand the fine spatial and temporal dynamics (JERICO-NEXT project). By increasing the sampling frequency, automated techniques would represent early warning systems of HAB blooms for environmental management.

Acknowledgements

Arnaud Louchart benefits of a PhD grant from the French government (Ministère de l'Enseignement Supérieur et de la Recherche/ Université du

Littoral-Côte d'Opale) and the French Region Hauts-de-France. The cruise and lab work were funded by the JERICO-NEXT project, the European Union (ERDF), the Flemish contribution to the LifeWatch ESFRI by Flanders Marine Institute, the French Government, the French Region Hauts-de-France and Ifremer, in the framework of the project CPER MARCO 2015-2020 and the French Ministry for the Ecological and Inclusive Transition in the frame of its convention with CNRS (n°2101893310) for the implementation of the Marine Strategy Framework Directive (MSFD). We thank the Captains and the crews on board the R/V « *Côtes de la Manche* », « *Simon Stevin* » and « *Zirfaea* » as well as of scientific and technical staffs of RWS, VLIZ and CNRS-LOG.

References

- Anderson DM, Cembella AD, Hallegraeff GM (1998). *Physiological Ecology of Harmful Algal Blooms*. Springer.
- Bonato S, Christaki U, Lefebvre A, Lizon F, Thyssen M, Artigas LF (2015). *Estuarine, Coastal and Shelf Science*. 154:214-223
- Bonato S, Breton E, Didry M, Lizon F, Cornille V, Lécuyer E, Christaki U, Artigas LF (2016). *Journal of Marine Systems*. 156:76–85
- Brylinski JM (1991). *Oceanology Acta*. 11:197-203
- Guiselin N (2010). Ph.D. Thesis. Université du Littoral-Côte d'Opale. 237pp
- Houliez E, Lizon F, Thyssen M, Artigas LF, Schmitt FG (2012). *Journal of Plankton Research* 34:136–151
- Lancelot C, Billen G, Sournia A, Weisse T, Colijn F, Veldhuis MJW, Davies A, Wassman P. (1987) *Ambio* 1:38-46
- Rutten TPA, Sandee B, Hofman ART (2005). *Cytometry Part A* 64:16–26
- Veldhuis MJW, and Admiraal W (1987). *Marine Biology* 95:47-54

³ <http://mawenzi.univ-littoral.fr/RclusTool/>

Predicting bloom initiation on the Texas (USA) coast: Combining satellite imagery with an individual-based model

Darren W. Henrichs^{1*}, Michelle C. Tomlinson², Lisa Campbell^{1,3}

¹ Department of Oceanography, Texas A&M University, College Station, Texas, USA;

² NOAA, National Centers for Coastal Ocean Science, Silver Spring, Maryland, USA;

³ Department of Biology Texas A&M University, College Station, Texas, USA.

* corresponding author's email: dhenrichs@tamu.edu

Abstract

A key question when modeling harmful algal blooms is: where do blooms start? Here we combined a previously developed, spatially explicit individual-based model (IBM) for *Karenia brevis* with a satellite imagery ensemble model to identify patches of *K. brevis* that may serve as seed populations in the southern Gulf of Mexico. We focused on the region north of the Yucatan peninsula, Yucatan, Mexico to identify potential *K. brevis* populations, which were then used to seed the IBM and track the cells through time. Individuals were tracked from ~1 Jul through 31 Dec (~180 days) and the arrival of a sustained presence of cells (i.e. consecutive days with cells present) at the coast of Texas was compared with a 10-year time series of abundance captured with an Imaging FlowCytobot (IFCB) at Port Aransas, Texas, USA. The IFCB captures images of all phytoplankton cells (10-150 μm) and has provided early warning for 8 harmful algal blooms, specifically *Dinophysis ovum* and *K. brevis*. Modeled cells were allowed to vertically migrate in the water column to maximize their access to light and nutrients, but there was no cell division and no cell death. Two different, highly simplified, nutrient fields were tested, one based on salinity (nutrient concentration increases with decreasing salinity) and one based on mixed layer depth (nutrient concentration increases with depth; MLD). To account for randomness associated with each individual cell, each year was tested with multiple model runs and the results averaged. In 2015, a bloom of *K. brevis* was identified at Port Aransas on 14 Sept. Retrospective analysis of the satellite imagery indicated the potential presence of a patch of *K. brevis* north of the Yucatan Peninsula on 12 July. Cells were seeded in this region of Mexico and tracked forward in time. The first sustained presence of modeled cells in the region near Port Aransas occurred between 7 - 18 Sept, dependent upon how the nutrient field was derived. Model runs utilizing the MLD-based nutrient field were better at capturing the timing of arrival while those utilizing the salinity based nutrient field appeared to better capture the bloom dynamics once the bloom had arrived. Results varied by year, with the starkest difference being 2010, when no large bloom of *K. brevis* was observed along the coast of Texas. Results from the model utilizing a salinity based nutrient field indicated a large bloom, with cells arriving in mid-September. In contrast, the results utilizing a MLD-based nutrient field indicated no cells until mid-November, well beyond the typical start period for a bloom in Texas (September-October). As the true nutrient field is much more complex than those used here, the incorporation of better nutrient fields could greatly improve future results and the potential for forecasting of blooms.

Keywords: individual-based model, *Karenia brevis*, *Dinophysis ovum*, harmful algal bloom, Gulf of Mexico

Introduction

In the Gulf of Mexico, harmful algal blooms (HABs) are predominantly caused by *Karenia brevis* and *Dinophysis* spp. (Campbell et al. 2010; Steidinger et al. 1998.). Additionally, other toxic phytoplankton exist in the Gulf of Mexico (e.g. *Pseudo-nitzschia* spp. and *Prorocentrum* spp.) but are not as prevalent, or have not, to date, formed a HAB, (Henrichs et al. 2013; Parsons et al. 2013). *K. brevis* is a toxic dinoflagellate capable of forming large blooms that can last for >1 year. The neurotoxin produced by *K. brevis*, brevetoxin, can

become aerosolized at the coast, resulting in respiratory irritation in humans as well as mortality of fish and marine mammals. Identifying the source of blooms could provide useful information about the conditions necessary for bloom formation. In particular, blooms of *K. brevis* occur in both Florida and Texas but the coastal dynamics of each coast differ greatly. Previous modelling results from a spatially explicit, individual-based model (IBM), developed specifically for *K. brevis*, indicated that *K. brevis* blooms in Texas originate

from the southern Gulf of Mexico in the Bay of Campeche region (Henrichs et al. 2015). This is consistent with historical records of *K. brevis* occurrence in Mexican waters ranging from the northern Yucatan peninsula all the way to the Mexico/U.S. border (Magaña et al. 2003).

Satellite imagery has predominantly been used to provide information about the chlorophyll content of the ocean over a wide spatial range. An ensemble model of satellite imagery based on three different optical methods was developed by Tomlinson et al. (2009) for detection of *K. brevis* in the Gulf of Mexico. Results from the ensemble model indicated that *K. brevis* could be present in the southern Gulf of Mexico during the summer months. To determine whether these patches of possible *K. brevis* could be transported north toward the Texas coast we utilized the previously developed IBM for *K. brevis* to track cells across the Gulf of Mexico. In 2015, a bloom of *K. brevis* was identified at Port Aransas on 14 September. Retrospective analysis of the satellite imagery indicated the potential presence of a patch of *K. brevis* north of the Yucatan Peninsula on 12 July. Unfortunately, there are no *in situ* field data available for the central Gulf of Mexico and it is unknown whether *K. brevis* was present on the northern coast of the Yucatan. Using results from the IBM with cell counts collected by the Imaging FlowCytobot (IFCB; McLane Research Laboratories) station in Port Aransas, Texas, which has been deployed since 2007 (Campbell et al. 2010, 2013), we evaluated whether the IBM can be combined with satellite imagery to produce a longer term early warning forecast for *K. brevis* at the Texas coast.

Materials and Methods

Satellite imagery

Data products from the ensemble model for *K. brevis* were evaluated and regions of suspected *K. brevis* patches identified. The model uses three different optical methods to identify patches of suspected *K. brevis* including a chlorophyll anomaly, relative particulate backscatter, and the changes in spectral shape of the 490nm wavelength. Based on image outputs from the ensemble model, early July was identified to be an important time for patches of suspected *K. brevis*

near the Yucatan peninsula. However, satellite imagery was not consistently available for this exact time period each year (e.g. cloud cover). Therefore, we focused on identifying regions where cells are frequently identified and seeded this same region for each model year run (blue box; Fig. 1).

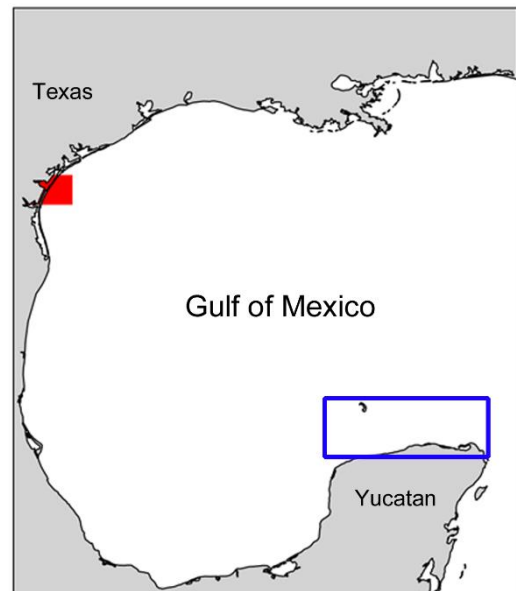


Fig. 1. Map of the study region in the western Gulf of Mexico. The filled red box indicates the Port Aransas, Texas region where cells were counted for the time series produced by the individual-based model. The blue box marks the bounding area for cells seeded in the model. All cells started the model within this region.

Individual-based model

The IBM of Henrichs et al. (2015) was used for hindcasting blooms of *K. brevis*. The model tracks individual cells that are capable of swimming vertically in the water column in order to maximize access to nutrients (nutrient uptake) and light (photosynthetic rate). Cell death and cell division were turned off for all of the model runs in order to track all of the cells from start to end. Seven years of data were modelled to see if differences in cell tracks between bloom years and non-bloom years could be identified. Model runs began ~ 1 July and ran until 31 December. A time series of cell abundance from the IFCB at Port Aransas, Texas was compared with a time series of abundance produced by the IBM. Cells were seeded inside the blue box (Fig. 1) at several starting depths and tracked forward through time. Any cell entering the filled red box near Port Aransas, Texas were counted toward the total cell abundance for as long as the cell remained within the red box (Fig. 1). The time step of the model was 3 minutes and cell

abundance data were summarized once per model day.

Two different nutrient profiles were tested in the model, one based on the mixed layer depth (MLD) and one based on salinity. The MLD profile contains low nutrient concentration at the surface, increasing concentration with depth, and a nutricline at the MLD. The salinity based profile contains higher nutrient concentrations at lower salinities, in order to approximate incoming river discharge, and background nutrient concentrations at higher salinities.

Tracks of cells were maintained and used to visualize the path taken by each cell during the model run. Since individual cell parameters stochastically vary among cells, replicate runs ($n=3$) were conducted for each nutrient profile, for each year. Time series of cell abundance indicate the mean \pm 1 SD.

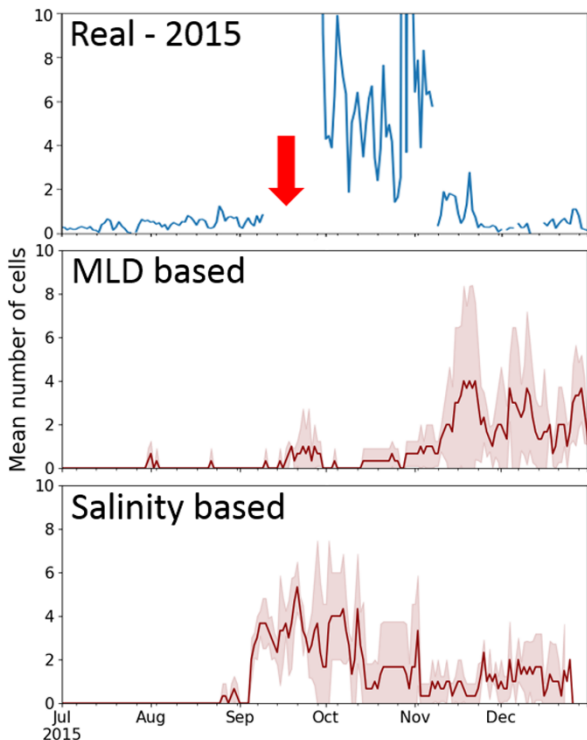


Fig. 2. Time series of *Karenia brevis* cell abundance at Port Aransas, Texas in 2015 from data collected by the IFCB (top), model runs using a mixed layer depth nutrient profile (middle), and model runs using a salinity based nutrient profile (bottom). Red arrow indicates the timing of actual cell arrival (data is off-scale). Dark red lines and light red shading indicate the mean \pm 1 SD, respectively, for modelled data.

Results and Discussion

The modelled time series of cell abundance at Port Aransas, Texas varied from year to year with the largest difference in timing of arrival observed with the nutrient profile based on MLD.

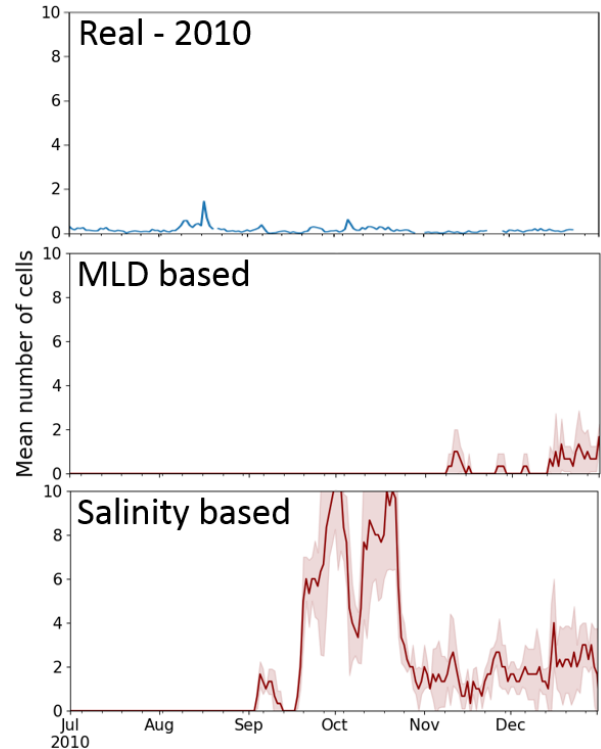


Fig. 3. Time series of *Karenia brevis* cell abundance at Port Aransas, Texas in 2010 from data collected by the IFCB (top), model runs using a mixed layer depth nutrient profile (middle), and model runs using a salinity based nutrient profile (bottom). Dark red lines and light red shading indicate the mean \pm 1 SD, respectively, for modelled data.

In 2015, a bloom year for *K. brevis* in Texas, cells of *K. brevis* were first observed in Port Aransas, on 14 September (red arrow; Fig. 2). The timing of arrival of cells was captured well using the MLD based nutrient profile while the salinity based nutrient profile showed cells arriving approximately two weeks early (Fig. 2). One striking difference between the two model runs was the abundance of cells indicated. While the model is not designed to capture the absolute magnitude of the true bloom abundance, the relative magnitude of the peaks within a model run should be informative. The salinity-based run indicated a high abundance bloom early on (September – mid-October) with cells decreasing after mid-October. The MLD based run indicated the opposite result, with cells arriving in low abundance early on and increasing in abundance during the November – December.

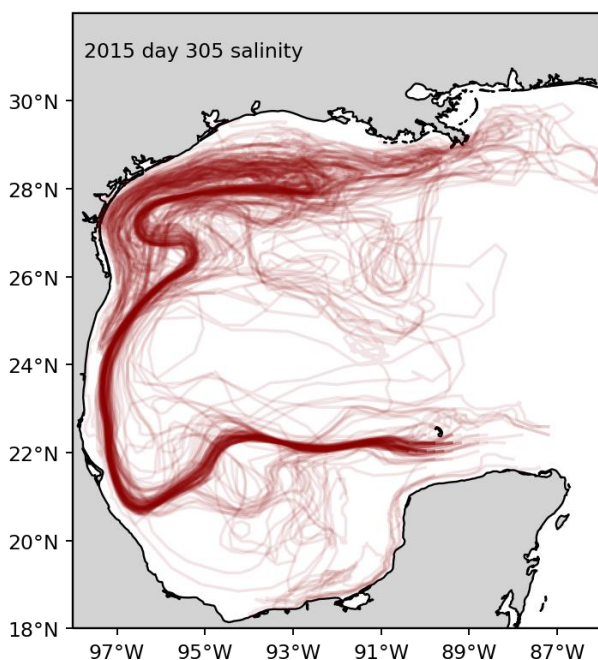


Fig. 4. Tracks of cells whose path passed through the region near Port Aransas, Texas at any point during the 2015 model run. Darker areas indicate more cells passed over that region.

In 2010, a non-bloom year for *K. brevis* in Texas, the IFCB data indicated no *K. brevis* present at Port Aransas, Texas. The timing of arrival of cells from the MLD based run was in mid-November (Fig. 3), well after the typical initiation window in Texas based on historical data (August - early October). The salinity-based run indicated cells arriving in early September and a bloom occurring from late September through October. However, no bloom occurred. Satellite SSH imagery from August 2010 indicated an eddy near the Mexico/U.S. border that could have moved cells into the central Gulf of Mexico, away from Texas (data not shown). There remains the possibility that cells were present offshore of Texas in 2010 and therefore not captured by the IFCB. Overall, the MLD based runs captured the timing of arrival (or not) of cells at the Texas coast better than the salinity-based runs. In contrast, during bloom years, the salinity-based runs captured the dynamics (increases/decreases in abundance) of the bloom once the bloom had arrived at Port Aransas, Texas. In 2015, the ensemble satellite imagery model indicated patches of likely *K. brevis* off the northern coast of the Yucatan peninsula. Figure 4

shows the tracks of cells from that region whose path passed through the red box near Port Aransas, Texas (Fig. 1) at any point. Modelled cells starting from a small region (approx. 90°W, 22°N) north of the Yucatan were transported to the Texas coast and arrived near Port Aransas, Texas ~3 days prior to the actual bloom (Figs. 3, 4). Further work is needed to better parameterize the nutrient profile for the model domain and *in situ* data on bloom occurrence in Mexico is necessary to validate the imagery and improved model initiation. Additional coastal observatories throughout the western Gulf of Mexico would greatly aid in model validation and early warning.

Acknowledgements

This work was funded in part by Gulf of Mexico Coastal Ocean Observing System (GCOOS), NOAA/PCM HAB NA15NOS4780173.

References

- Campbell, L., Olson, R.J., Sosik, H.M., Abraham, A., Henrichs, D.W., Hyatt, C.J., and Buskey, E.J. (2010) *J Phycology* 46: 66-75.
- Campbell, L., Henrichs, D.W., Olson, R.J., and Sosik, H.M. (2013) *Environmental Science and Pollution Research* 20: 6896-6902.
- Henrichs, D.W., Scott, P.S., Steidinger, K.A., Errera, R.M., Abraham, A., Campbell, L. (2013). *J Phycology* 49: 143-155.
- Henrichs, D.W., Hetland, R.D., and Campbell, L. (2015) *Ecological Modelling* 313: 251-258.
- Magaña, H.A., Contreras, C., Villareal, T.A. (2003). *Harmful Algae* 2:163-171.
- Parsons, M.L., Dortch, Q., Doucette, G.J. (2013). *Harmful Algae* 30: 65-77.
- Steidinger, K.A., Vargo, G.A., Tester, P.A., and Tomas, C.R. (1998) In *Physiological Ecology of Harmful Algal Blooms*. Anderson, D.M., Cembella, A.D., and Hallegraeff, G.M. (eds). New York: Springer, pp. 135-153.
- Tomlinson, M.C., Wynne, T.T., Stumpf, R.P. (2009). *Remote Sensing of Environment*. 113: 598-609.



Ecology – from the ecological niche to population dynamics and biogeography

Revealing the distribution and relative abundance of HABs species in the South China Sea using metagenomics analysis

Kieng Soon Hii¹, Ing Kuo Law¹, Winnie Lik Sing Lau¹, Zhen Fei Lim¹, Zhaohe Luo², Haifeng Gu², Chui Pin Leaw^{1*}, Po Teen Lim^{1*}

¹Bachok Marine Research Station, Institute of Ocean and Earth Sciences, University of Malaya, Bachok, Malaysia;

²Thrid Institute of Oceanography, Xiamen, China.

*Corresponding authors' emails: cpleaw@um.edu.my, ptlim@um.edu.my

Abstract

Harmful algal blooms (HABs) are related to the proliferation of micro-algae in marine ecosystems. HABs are increasingly reported over wider geographical regions including the South China Sea. To gain more insight about the distribution of HABs species along the east coast of the Malaysian peninsular, a metagenomic approach was adopted in this study. A total of 30 subsurface water samples were collected by a submersible pump and filtered through a 15-micron net from 30 sampling sites during a 10-day research cruise on *RV Discovery* in August 2016. Saline-ethanol preserved samples were used to extract the environmental genomic DNA and analyzed using an Illumina MiSeq platform. Phytoplankton community composition was assessed by metagenomic analysis from the sequences of the V9 region of the 18S ribosomal DNA. A total of 69 taxa of phytoplankton species were identified. HABs species were identified from these locations. The paralytic shellfish toxin-producer *Alexandrium tamiyavanichii* was found to be widely distributed in the region. Nine species of *Alexandrium* were newly identified in the area (*A. affine*, *A. andersonii*, *A. fraterculum*, *A. leei*, *A. margalefii*, *A. monilatum*, *A. ostenfeldii*, *A. insuetum*, and *A. tamerense*). Several ichthyotoxic species were confirmed genetically, these included *Margalefidinium polykrikoides*, *Karlodinium veneficum*, and *Chattonella* sp. *Azadinium dexteroporum* and *Protoceratium* sp. were found but with low relative abundances at selected sites. This study provides useful baseline data on the distribution and occurrence of HAB species along the east coast of the Malaysian peninsular.

Keywords: *Alexandrium*, *Azadinium*, *Karlodinium*, small subunit ribosomal DNA, South China Sea

Introduction

The occurrence of harmful algal blooms (HABs) increased worldwide (Hallegraeff, 2003), the South China Sea is also concerned. These events are threatening human health and socio-economic activities. In Malaysia, HABs events are mainly associated with paralytic shellfish poisoning (PSP) and blooms of *Pyrodinium bahamense* have been reported almost every year in the west coast of Sabah, Malaysia Borneo (Lim et al., 2012; Usup et al., 2012).

Two other PSP-toxins producing dinoflagellate species were observed in the waters of Malaysia, viz. *Alexandrium tamiyavanichii* and *Alexandrium minutum*. The species *A. tamiyavanichii* was first reported to cause intoxication in mussel farms in 1991 (Usup et al., 2002) and it was subsequently reported to cause PSP incidents in 2013 and 2014 (Mohd Noor et al., 2018).

In 2001, a bloom of *A. minutum* was observed that caused six victims that were hospitalized and a death (Lim et al., 2004). An unprecedented bloom of this species recurred in 2015 (Lau et al., 2017). Algal blooms that caused massive fish kill events in aquaculture farms have also been documented in Malaysian waters, such as a *Karlodinium australe* bloom in the western Johor Strait in 2014 and 2015 (Lim et al., 2014; Teng et al., 2016) and blooms of *Margalefidinium polykrikoides* in Sabah (Anton, et al., 2008).

Current monitoring efforts in the country have relied on conventional microscopic observation of the harmful algae in selected sites of Malaysian water. This is labor-intensive, time-consuming and required expertise in microalgal identification, which may be insufficient and often required further evidence to provide a definitive conclusion.

Over the past decades, molecular tools, with increased accuracy and throughput rate, have been developed to substitute the conventional microscopy methods (Medlin 2013). Among the molecular techniques applied in HAB monitoring, metagenomic approaches are reliable and fast, and have been widely used for comprehensive taxonomic profiling and elucidation of functional genes of microbial communities in the environment (Kunin et al., 2008), as well the marine and freshwater ecosystems (Logares et al., 2014; Sze et al., 2018; Reza et al., 2018).

In this study, the distribution and relative abundance of HAB species along the east coast of the Malaysian peninsular, offshore of the South China Sea, was investigated by a metagenomic survey using the Illumina Miseq system.

Materials and Methods

Samples collection

Phytoplankton samples were collected from 30 stations during the National Scientific Cruise Expedition aboard the *RV discovery* in August 2016. The Sampling route covered coastline of the east coast of the Malaysian peninsular towards the offshore of South China Sea. Subsurface seawater samples (225 L) were collected by using the submersible water pumping system with the water flow rate of 0.9 L/s. Phytoplankton samples were concentrated with a 15 µm-mesh plankton net, followed by filtration with a 0.2 µm pore-size nylon membrane filters. The filters were preserved in 10 mL of modified saline ethanol (Miller and Scholin, 2000) and kept at -20° C until further analysis.

Environmental DNA extraction, amplification, and sequencing

The saline ethanol-preserved samples (1 mL) were used for environmental genomic DNA isolation (Toyobo Mag Extractor Plant Genome kit, Japan). The V9 region of the small subunit ribosomal rDNA was amplified with a pair of eukaryotes specific primers, 1391F (Lane, 1991) and EuKB (Medlin et al., 1988). The gene was amplified (PEQlab, Germany) and paired-end sequencing was performed on the Illumina Miseq platform.

Bioinformatics analysis

The paired-end reads of the sequences were trimmed with cutadapt (Marcel, 2011) and assembled using PEAR (Zhang et al., 2014), followed by Prinseq (Schmieder and Edwards, 2011). The operational taxonomic units (OTUs) were clustered (at least 20 reads) using SEARCH (Edgar, 2017) at a similarity threshold of 97%. Chimeric sequences were removed in this analysis.

Taxonomic assignment for the OTUs was performed using NCBI Blast+ (Altschul, et al., 1990) against Silva (<https://www.arb-silva.de>) and an E-value cut off of 10^{-3} was used.

Phylogenetic analyses were performed to determine the relationships amongst OTUs. Multiple sequence alignments were performed using the Clustal-X program (Thompson, et al., 1997) and BioEdit sequence alignment editor ver. 6.0.7 (Hall, 1999). Phylogenetic analyses were carried out using MrBayes ver. 3.2.6 (Huelsenbeck and Ronquist, 2001) for Bayesian inference to estimate the phylogeny.

Results and Discussion

The paired-end sequencing performed in this study generated a total of 1,831,822 assembled paired-end reads that were corresponding to 1,784,115 unique sequences. Following the sequence filtering and chimera removal analyses, the result yielded 1,541,770 unique sequences. Taxonomy clustering with Blast analysis clustered 9,265 OTUs with 110 to 500 bp in range.

A total of 69 taxa of phytoplankton species were identified from the OTUs. Several known and potential HAB species were identified from this study. The PST-producer *A. tamiyavanichii* was found to be widely distributed offshore of the east coast of the Malaysian peninsular (Figs. 1, 2). This species is considered a highly toxic species among the PST-producing dinoflagellates due to its high toxin quota ($200 \text{ fmol cell}^{-1}$, Ogata et al., 1990; Lim et al., 2006). The cell density of only 20-40 cells L^{-1} of *A. tamiyavanichii* in the water column is sufficient to pose a warning of shellfish poisoning. The results also revealed the distributions of nine additional species of *Alexandrium* including *A. affine*, *A. andersonii*, *A. fraterculum*, *A. leei*, *A. margalefii*, *A. cf. monilatum*, *A. ostenfeldii*, *A. cf. insuetum* and *A. cf. tamarensis* (Fig. 1). This discovery brings the currently known number of *Alexandrium* species in Malaysian waters to at least twelve (Usup et al., 2002; Lim et al., 2005; Leaw et al., 2005).

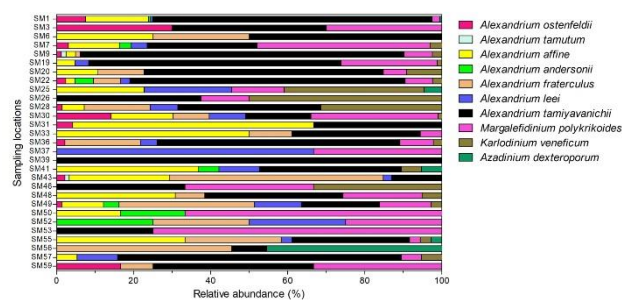


Fig. 1. Species composition of *Alexandrium* and other harmful species.

It is interesting to note that *A. minutum* which commonly bloomed in the Geting Lagoon, Tumpat, a semi-enclosed lagoon (Lim, et al., 2004; Lau et al., 2017), was not detected in the dataset of this study. This result showed that the species is likely to occur only in semi-enclosed coastal waters as reported by other studies (MacKenzie and Berkett, 1997; Matsuoka, et al., 1997; Maguer, et al., 2004; Lim, et al., 2004) or in other seasons.

Several ichthyotoxic micro-algal species were also found in the dataset: *Margalefidinium polykrikoides*, *Karlodinium veneficum*, and *chattonella* sp. The azaspiracid toxin-producer *Azadinium dexteroporum* was also found, but with low relative abundances (Fig. 1) and was only detected on stations SM25, 41, 53, and 55.

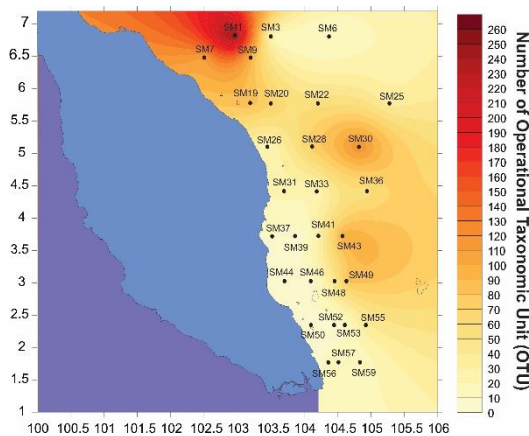


Fig. 2. Distribution and relative abundances of OTUs in the east coast of the Malaysian peninsular.

The highest relative OTU abundance of HAB species was found at the northeastern coast of the Peninsula (SM1). The results revealed considerably lower relative OTU abundance of HAB species at the coastline of Pahang (SM37, SM44, and SM39) as compared to some offshore areas. The patchy distribution of HAB species in this study could be explained by the hydrographic conditions in the South China Sea (Kok et al., 2015).

The Bayesian phylogenetic tree of the OTUs (Fig. 4) was supported by the V9 18S rDNA dataset in NCBI Genbank sequence database. Beside the recognized species, the results of this study also highlighted several unidentified ribotypes of *Alexandrium* (OTU 4623, OTU 13833, OTU 4449, and OTU 1020) and *Azadinium* (OTU 1283 and OUT 6510) from Malaysian water (Fig. 3).

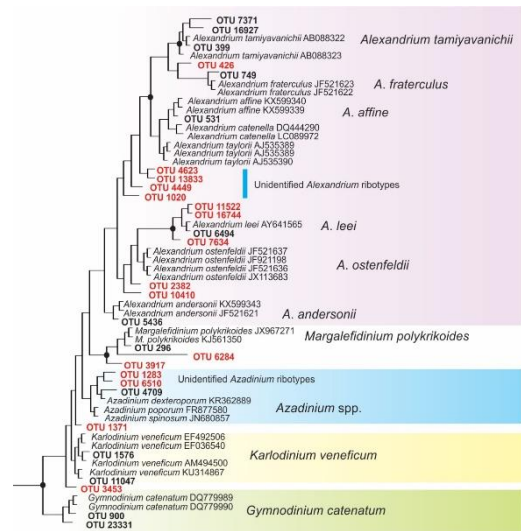


Fig. 3. Bayesian phylogenetic tree showing the relationship amongst the OTUs (in red bold).

Conclusion

Metagenomic data from this study have provided a fast and reliable tool for risk assessment of HABs, and the data obtained in this study constitutes a useful baseline inventory of the distribution and occurrence of HABs species along the east coast of the Malaysian peninsular. Environmental factors regulating the distribution and dispersion of HABs species in the water have to be investigated.

Acknowledgments

This work was supported by the Malaysian Government through MESTECC EPSK16, ICF [CF001-2018], MOE HiCoE [IOES-2014C], UM-RU fund [TU001A-2018] to PT Lim; [RU003A-2017] to KS Hii; and the National Key Research and Development Program of China [2016YFE0202100] to H Gu.

References

- Altschul, S.F., Madden, T.L., Schaffer, A.A., Zhang, J., Zhang, Z., Miller, W., Lipman, D.J., 1990. Journal Molecular Biology 215, 403-410.
- Anton, A., Teo, P.L., Shaleh, S.R.M.S., Normawaty, M.N., 2008. Harmful Algae 7, 331-336.
- Edgar, R.C., 2017. bioRxiv.
- Hall, T., 1999. Nucleic Acids Symposium Series 41, 95-98.
- Hallegraeff, G.M., 2003. UNESCO, Paris, pp. pp. 25-49.
- Huelsenbeck, J., Ronquist, F., 2001. Bioinformatics 17, 754-755.

- Kunin, V., Copeland, A., Lapidus, A., Mavromatis, K., Hugenholtz, P., 2008. *Microbiology and molecular biology reviews: MMBR* 72, 557-578.
- Lane, D.J., 1991. Wiley, New York, pp. 115-175.
- Lau, W.L.S., Law, I.K., Liow, G.R., Hii, K.S., Usup, G., Lim, P.T., Leaw, C.P., 2017. *Harmful Algae* 70, 52-63.
- Leaw, C.P., Lim, P.T., Ng, B.K., Cheah, M.Y., Ahmad, A., Usup, G. 2005. *Phycologia* 40, 550-565.
- Lim, H.C., Leaw, C.P., Tan, T.H., Kon, N.F., Yek, L.H., Hii, K.S., Teng, S.T., Razali, R.M., Usup, G., Iwataki, M., Lim, P.T., 2014. *Harmful Algae* 40, 51-62.
- Lim, P.T., Leaw, C.P., Usup, G., 2004. In: Phang, S.M., Chong, V.C., Ho, S.S., Mokhtar, N., Ooi, J.L.S. (Eds.). University of Malaya Maritime Research Centre, Kuala Lumpur, Malaysia, pp. 661-667.
- Lim, P.T., Usup, G., Leaw, C.P., Ogata, T. 2005. *Harmful Algae* 4, 391-400.
- Lim, P.T., Leaw, C.P., Usup, G., Kobiyama, A., Koike, K., Ogata, T., 2006. *J. Phycol.* 42, 786-799.
- Lim, P.T., Usup, G., Leaw, C.P., 2012. *Sains Malaysiana* 41, 1509–1515.
- Logares, R., Sunagawa, S., Salazar, G., Cornejo-Castillo, F.M., Ferrera, I., Sarmiento, H., Hingamp, P., Ogata, H., Vargas, C., Lima-Mendez, G., Raes, J., Poulain, J., Jaillon, O., Wincker, P., Kandels-Lewis, S., Karsenti, E., Bork, P., Acinas, S.G., 2014. *Environmental Microbiology* 16(9), 2659-2671.
- MacKenzie, L., Berkett, N., 1997. *N. Z. J. Mar. Freshwater Res.* 31, 403-409.
- Maguer, J.F., Wafar, M., Madec, C., Morin, P., Erard-Le Denn, E., 2004. *Limnology and Oceanography* 49, 1108-1114.
- Marcel, M., 2011. EMBnet 17, 10-12 DOI: <http://dx.doi.org/10.14806/ej.14817.14801.14200>.
- Matsuoka, K., Fukuyo, Y., Yoshida, M., 1997. In: Sudara, S. (Ed.). Chulalongkorn University, Chiangrai, Thailand, pp. 85-94.
- Medlin, L., Elwood, H.J., Stickel, S., Sogin, M.L., 1988. *Gene* 71, 491-499.
- Miller, P.E., Scholin, C.A., 2000. *J. Phycol.* 36, 238 - 250.
- Mohd Noor, N., Adam, A., Lim, P.T., Leaw, C.P., Lau, W.L.S., Liow, G.R., Muhamad-Bunnori, N., Hamdan, H., Md-Nor, A., Kemat, N., Muniandi, D. 2018. *Phycological Research* 66, 37-44.
- Reza, M.S., Kobiyama, A., Yamada, Y., Ikeda, Y., Ikeda, D., Mizusawa, N., Ikeo, K., Sato, S., Ogata, T., Jimbo, M., Kudo, T., Kaga, S., Watanabe, S., Naiki, K., Kaga, Y., Mineta, K., Bajic, V., Gojobori, T., Watabe, S., 2018. *Gene* 665, 192-200.
- Schmieder, R., Edwards, R., 2011. *Bioinformatics (Oxford, England)* 27, 863-864.
- Sze, Y., Miranda, L.N., Sin, T.M., Huang, D., 2018. *Metabarcoding and Metagenomics* 2.
- Teng, S.T., Leaw, C.P., Winnie, L.S.L., Law, I.K., Lim, P.T., 2016. *Harmful Algae News* 52, 5.
- Thompson, J.D., Gibson, T.J., Plewniak, F., Jeanmougin, F., Higgins, D.G., 1997. *Nucleic Acids Research* 25, 4876-4882.
- Usup, G., Leaw, C.P., Ahmad, A., Lim, P.T., 2002. *Harmful Algae* 1, 265-275.
- Usup, G., Ahmad, A., Matsuoka, K., Lim, P.T., Leaw, C.P. 2012. *Harmful Algae* 14, 301-312.

Relationships between environmental conditions and phytoplankton in the Mellah lagoon (south western Mediterranean, Algeria), with an emphasis on HAB species

Mohamed Anis Draredja^{1,4*}, Hocine Frihi², Chahinez Boualleg¹, Anne Goffart³ & Mohamed Laabir⁴

¹ Laboratory of Aquatic and Terrestrial Ecosystems, University of Souk Ahras, Algeria

² Laboratory of Marine Bioresources, University of Annaba, Algeria

³ University of Liege, Oceanology, FOCUS Research Unit, MARE Centre, Liege Sart-Tilman, Belgium

⁴ MARBEC, IRD, Ifremer, CNRS, University of Montpellier, France

* corresponding author's email: anisdraredja@yahoo.fr

Abstract

A bi-weekly monitoring of environmental parameters and microphytoplankton assemblages was conducted in the well-preserved Mellah lagoon ecosystem (south western Mediterranean). Sampling was performed at 3 stations in 2016. We aimed to study the evolution of the phytoplankton community with a focus on harmful species in relation with the environmental characteristics. Phytoplankton of Mellah Lagoon was characterized by a mixture of marine, brackish-water and freshwater taxa. In all of the stations, 227 species of phytoplankton were identified (160 diatoms and 53 dinoflagellates). The overall mean phytoplankton abundance was higher at station A ($2.24 \cdot 10^5$ cells l^{-1} , early September) and B ($2.98 \cdot 10^5$ cells l^{-1} , early October) near of marine inputs, compared to station C ($1.73 \cdot 10^5$ cells l^{-1} , early June) located in the south of the lagoon. Diatoms dominated in spring and dinoflagellates developed in summer and early autumn in the Mellah. The dynamic of the phytoplankton in Mellah was influenced by temperature and salinity. For the first time, a number of potentially toxic species have been identified, including 2 diatom species: *Pseudo-nitzschia delicatissima*-group (max.: $2.52 \cdot 10^3$ cells l^{-1}), *Pseudo-nitzschia seriata*-group (max.: 700 cells l^{-1}) and 6 dinoflagellate species: *Alexandrium minutum* (max.: $1.42 \cdot 10^3$ cells l^{-1}), *Alexandrium tamarense/catenella* (max.: $1.35 \cdot 10^3$ cells l^{-1}), *Dinophysis acuminata* (max.: 180 cells l^{-1}), *Dinophysis sacculus* (max.: 120 cells l^{-1}), *Akashiwo sanguinea* (max.: $7.20 \cdot 10^3$ cells l^{-1}), *Prorocentrum lima* (max.: 110 cells l^{-1}). Even the abundances of the HABs species were relatively low in Mellah lagoon, they could potentially form blooms in the coming decades at the favor of warming and trophic status changes observed in Mediterranean marine systems. Monitoring program of HABs species must be established to gain more insight in the development of potentially toxic species and the toxins produced.

Keywords: phytoplankton, HABs species, structure, Mellah lagoon, south western Mediterranean

Introduction

The lagoons are singular ecosystems, zones of transition between land and sea. Lagoon environments constitute about 13% of the world's coastlines (Larras 1964; Barnes 1994).

The intensity and frequency of harmful phytoplankton blooms in coastal ecosystems has continued to increase (Glibert et al., 2005; Anderson et al., 2008; Heisler et al., 2008). The multiplication of episodes of toxic algal blooms and their health and economic consequences justify the rise of research on this phenomenon. In recent years, harmful algal blooms have caused great economic loss to fisheries and aquaculture because of public health problems caused by toxic dinoflagellates (Matsuoka & Fukuyo, 2000). The development of toxic species leads each year to the

closure of many aquaculture plants (mussels, oysters, clams). Indeed, some phytoplankton species (mainly dinoflagellates) produce powerful toxins that can be concentrated in the food chain mainly by filtering molluscs. The toxins accumulate in the tissues of filtering bivalves up to sometimes lethal concentrations for humans.

The Mellah Lagoon, the only lagoon ecosystem in Algeria with its environmental and economic interests, is a site to explore further. Fish and shellfish farming are practiced in this lagoon. The phytoplankton of this ecosystem has been studied only in one occasion (Draredja, 2007). The objective of this work is to study the evolution of the microphytoplankton community with a focus

on Harmful Algal Blooms (HABs) species in relation to the environmental conditions.

Materials and Methods

The Mellah lagoon is located in the northeast of Algeria (36°54'N 8°20'E) far of all sources of pollution, within a protected natural reserve (Fig. 1). The lagoon (8.65 km²) communicates with the sea by a long and narrow channel. During 2016, a monitoring program of microphytoplankton and physico-chemical parameters (temperature, salinity, dissolved oxygen, pH and suspended matter) was carried out fortnightly in 3 representative stations in the lagoon (Fig. 1).



Fig. 1. Location of the Mellah lagoon and position of sampling stations.

Nutrient (NO₃, NO₂, NH₄, PO₄) and Chlorophyll-*a* analyses, were carried out by spectrophotometry. Microphytoplankton was sampled in surface waters, where a volume of 50 liters of water was filtered through a plankton net (20 μm mesh size) and fixed with neutralized formalin (4%). Both the identification and counting of phytoplankton (cells l⁻¹) were performed with an inverted light microscope (Leika 750 PM). Statistical analyses were performed using R, version 3.4.2 (R Core Team, 2017) developed for Windows by (Ihaka & Gentleman 1996).

Results and Discussion

The seasonal values of environmental parameters are reported in Table 1. Unlike most

Mediterranean lagoons (Dell'Anno et al., 2002; Bernardi-Aubry et al., 2004; Ifremer, 2006), Mellah appears less rich in nutrients. So we class it among Mediterranean lagoons meso oligotrophic (OECD, 1982). The low level of nutrients of the of the Mellah lagoon waters results in a moderate seasonal biomass in chlorophyll-*a* (between 0.70 and 5.45 μg l⁻¹) (Table 1), compared to other Mediterranean lagoons (Triantafyllou et al., 2000; Nuccio et al., 2003; Bernadi Aubry & Acri, 2004; Solidoro et al., 2004).

Table 1. Seasonal extremes of physico-chemical parameters and chlorophyll-*a* of the Mellah lagoon waters (2016).

	Winter		Spring		Summer		Autumn	
	Min.	Max.	Min.	Max.	Min.	Max.	Min.	Max.
Temperature (°C)	12.26	16.98	18.89	25.25	25.80	29.00	14.30	24.80
Salinity	24.00	27.42	27.41	28.84	30.40	35.44	30.65	36.23
Dissolved oxygen (mg l ⁻¹)	6.89	8.38	5.73	8.59	5.25	7.88	5.71	7.88
pH	7.88	8.23	7.75	8.55	7.95	8.35	7.95	8.51
Suspended matter (mg l ⁻¹)	17.36	34.38	8.28	23.85	6.25	20.02	5.12	16.00
Ammonium (NH ₄) (μmoles l ⁻¹)	0.05	6.60	1.12	3.75	0.00	4.12	0.00	3.37
Nitrites (NO ₂) (μmoles l ⁻¹)	0.12	0.53	0.02	1.08	0.05	0.24	0.07	0.46
Nitrates (NO ₃) (μmoles l ⁻¹)	0.23	1.15	0.04	3.20	0.01	3.84	0.10	1.37
DIN* (μmoles l ⁻¹)	1.27	8.09	0.92	6.14	0.54	5.65	0.38	5.81
Phosphate (P04) (μmoles l ⁻¹)	0.11	1.55	0.08	1.57	0.14	0.99	0.02	1.68
Chlorophyll- <i>a</i> (μg l ⁻¹)	0.26	1.78	0.62	5.59	0.27	5.58	0.08	5.59

(*) Dissolved inorganic nitrogen (DIN = NH₄ + NO₂ + NO₃).

In total, 227 microphytoplankton species belonging mainly to diatoms (160 species) and dinoflagellates (53 species), were inventoried in the Mellah lagoon. In this list of species, we found height potentially HAB species (2 diatoms and 6 dinoflagellates) (Table 2). The lagoon was characterized by a clear dominance of diatoms (63%) compared to dinoflagellates (37%). This trend is observed in many Mediterranean lagoons (Tolomio et al., 1999; Bernardi Aubry & Acri, 2004), but also in Algerian coastal marine waters

(Frehi, 1995; Illoul, 2014). The overall mean phytoplankton abundance was higher at St.A ($223.99 \cdot 10^3$ cells l^{-1} , early September) and St.B ($298.41 \cdot 10^3$ cells l^{-1} , early October) near marine inputs, compared to St.C ($173.13 \cdot 10^3$ cells l^{-1} , early June) under land influence (Fig. 2, I).

Proliferations of harmful species as *Akashiwo sanguinea* at St.C ($7.20 \cdot 10^3$ cells l^{-1} , end of June), were noted in summer (Fig. 2, II). This species is toxic to several models with a hemolytic effect (Xu et al., 2017). Other potentially neurotoxic species as *Alexandrium minutum* at St.B ($1.42 \cdot 10^3$ cells l^{-1} , early June) and *A. tamarense/catenella* at St.A ($1.35 \cdot 10^3$ cells l^{-1} , early February) were observed in winter and spring respectively (Fig. 2, II). The abundance of these HAB species remained relatively low, but they could potentially form blooms in the future at the favor of warming and trophic status changes affecting Mediterranean waters (Benedetti, 2016; Karidis & Kitsiou, 2011). Other HAB species were present (Table 2) but poorly represented (< 700 cells l^{-1}). They included *Prorocentrum lima*, *Dinophysis* sp. and *Pseudo-nitzschia* spp., responsible of DSP and ASP syndromes. The distribution of these HAB species is very similar in the three stations prospected (Fig. 2, II), hence the role of the hydrodynamic action in the lagoon.

The Pearson analyses showed that the microphytoplankton densities in the Mellah lagoon were positively correlated with temperature (0.46 to 0.56) and salinity (0.16 to 0.43), $p < 0.05$. Finally, unlike the majority of Mediterranean lagoons, which are eutrophic, the Mellah lagoon is distinguished by its meso oligotrophy, due to its remoteness from any source of pollution.

Despite the meso oligotrophy of the Mellah lagoon specific microphytoplankton richness (227 species) is higher than some eutrophic Mediterranean lagoons.

The proliferation of dinoflagellates coincides with the warming of the waters and the increase of the Mellah waters salinity during the summer season.

A regular dredging of the channel must be established to improve the water exchange between the Mellah and Mediterranean Sea to stabilize the quality of lagoon waters and to increase phytoplankton species diversity.

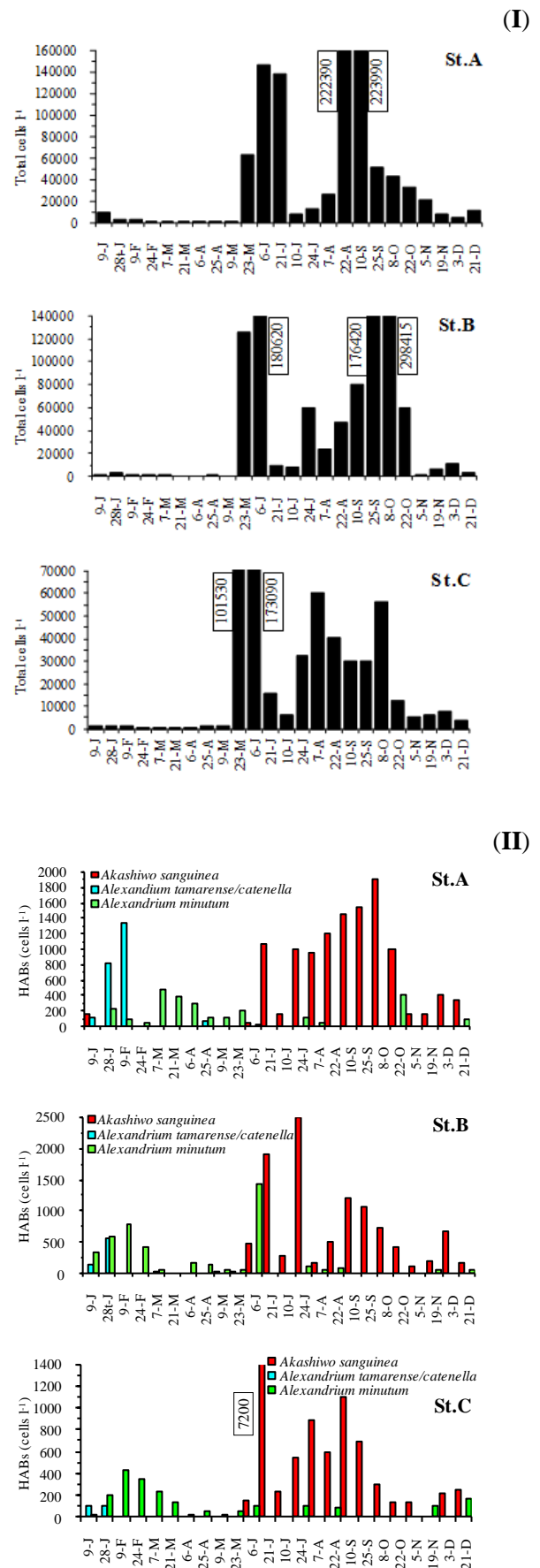


Fig. 2. Abundance (cells l^{-1}) of total microphytoplankton (I) and harmful species (HABs) (II) in the Mellah waters (2016).

Table 2. Check list of potentially harmful species (HABs) encountered in Mellah lagoon (2016). (M: marine species, L: lagoon species).

DIATOMOPHYCEAE (Rabenhorst, 1864)

PENNATE DIATOMS

Bacillariaceae Ehrenberg, 1831

Pseudo-nitzschia delicatissima-group (Cleve) Heiden, 1928 (M)

Pseudo-nitzschia seriata-group (Cleve) H. Peragallo, 1899 (M)

DINOPHYCEAE (G.S. West & Fritsch, 1927)

DINOPHYSALES (Lindemann, 1928)

Dinophysiaceae Stein, 1883

Dinophysis acuminata Claparède & Lachmann, 1859 (M)

Dinophysis sacculus Stein, 1883 (M)

GYMNODINIALES Lemmermann, 1970

Gymnodiniaceae Lankester, 1885

Akashiwo sanguinea (K. Hirasaka) G. Hansen & Ø. Moestrup, 2000 (M, L)

PERIDINIALES Haeckel, 1894

Gonyaulacaceae Lindemann, 1928

Alexandrium tamarense/catenella (Lebour, 1925) Balech, 1995 / (Whedon & Kofoid) Balech, 1985 (M)

Alexandrium minutum Halim, 1960 (M)

PROOCENTRALES Lemmermann, 1910

Prorocentraceae Stein, 1883

Prorocentrum lima (Ehrenberg) F. Stein, 1878 (M)

Microphytoplankton of the Mellah lagoon is dominated by diatoms. The presence of HABs species related to PSP, DSP and ASP syndromes stresses the need to implement a monitoring program to detect the related toxic species order to prevent any human intoxication due to the consumption of contaminated shellfish.

Acknowledgements

I would like to sincerely thank MARBEC laboratory who funded my stay in Montpellier, IAAE (International Atomic Energy Agency for) and the GDR Phycotox for funding ICHA 2018 registration and accommodation in Nantes.

References

Anderson, D.M., Burkholder, J.M., Cochlan, W.P., Glibert, P.M., Gobler, C.J, Heil, C.A., Kudela, R.M., Parsons, M.L., Rensel, J.E.J., Townsend, D.W., Trainer, V.L., Vargo, G.A. (2008). *Harmful Algae*, 8, 39-53.

Barnes, R.S.K. (1994). *Estuar. Coast. Shelf Sci.*, 38, 41-48.

Benedetti, F. (2016). In: Moatti J.P, Thiébaud, S. (ed. IRD), Marseille, pp. 211-217.

Bernardi Aubry, F., Acri, F. (2004). *J. Mar. Syst.*, 51, 65-76.

Bernardi-Aubry, F., Breton, A., Bastianini, M., Socal, G., Acri, F. (2004). *Cont. Shelf Res.*, 24, 97-115.

Dell'Anno, A., Mei, M.L., Pusceddu, A., Danovaro, R. (2002). *Mar. Pollut. Bull.*, 44, 611-622.

Draredja, B. (2007). PhD thesis. Univ. Annaba (Algeria), 225pp.

Fréhi, H. (1995). PhD thesis. Univ. Annaba (Algeria), 160 pp.

Glibert, P.M., Anderson, D.M, Gentien, P., Granéli, E., Sellner, K.G. (2005). *Oceanography*, 18, 130-141.

Heisler, J., Glibert, P., Burkholder, J., Anderson, D.M., Cochlan, W., Dennison, W.C, Dortch, Q., Gobler, C.J., Heil, C., Humphries, E., Lewitus, A., Magnien, R., Marshall, H., Sellner, K., Stockwell, D., Stoecker, D., Suddleson, M. (2008). *Harmful Algae*, 8, 3-13.

Ifremer (2006). Rapport RSL-06/2006, 450pp.

Xu, N., Wang, M., Tang, Y., Zhang, Q., Duan, S., Gobler, C.J. (2017). *Aquat. Microb. Ecol.*, 80, 209-222.

Illoul, H. (2014). PhD thesis. Univ. USTHB, Algiers (Algeria), 181 pp.

Ihaka, R., Gentleman, R. (1996). *J. Comput. Graph. Stat.*, 5, 299-314.

Karidis, M., Kitsiou, D. (2011). *Environ. Monit. Assess.* 184, 4931-84.

Larras, J. (1964). Ed. Eyrolles, 172 pp.

Matsuoka, K., Fukuyo, Y. (2000). WESTPAC-HAB/WESTPAC/IOC, Japan Society for the Promotion of Science, Tokyo, 29 pp.

Nuccio, C., Melillo, C., Massi, L., Innamorati, M. (2003). *Oceanol. Acta*, 26, 15-25.

OECD (1982). Organisation for Economic and Cooperative Development (OECD), Paris, France, 154 pp.

R Core Team (2017). R Foundation for Statistical Computing, Vienna, Austria. <http://www.r-project.org/>

Solidoro, C., Pastres, R., Cossarini, G., Ciavatta, S. (2004). *J. Mar. Syst.*, 51, 7-18.

Tolomio, C., Moschin, E., Moro, I., Andreoli, C. (1999). *Vie Milieu*, 49, 25-37.

Triantafyllou, G., Petihakis, G., Dounas, C., Koutsoubas, D., Arvanitidis, C., Eleftheriou, A. (2000). *ICES ICES J. Mar. Sci.*, 57, 1507-1516.

Environmental factors leading to the occurrence of a harmful alga, *Vicicitus globosus*, in the center of the Seto-Inland Sea, Japan

Shizuka Ohara^{1*}, Ryoko Yano², Etsuko Hagiwara³, Hiroyuki Yoneyama³, Setsuko Sakamoto⁴, Kazuhiko Koike¹

¹ Graduate School of Biosphere Science, Hiroshima University, 1-4-4 Kagamiyama, Higashi-hiroshima 739-8528, Japan;

² Faculty of Applied Biological Science, Hiroshima University, 1-4-4 Kagamiyama, Higashi-hiroshima 739-8528, Japan;

³ Hiroshima Prefectural Agriculture, Forestry and Fisheries Bureau, 10-52 Motomachi, Naka-ku, Hiroshima 730-8511, Japan;

⁴ National Research Institute of Fisheries and Environment of Inland Sea, Japan Fisheries Research and Education Agency, 2-17-5 Maruishi, Hatsukaichi 739-0452, Japan.

* corresponding author's email: oharashizu@hiroshima-u.ac.jp;

Abstract

Monthly monitoring conducted from May 2014 to March 2018 at the center of the Seto-Inland Sea of Japan revealed a dominant occurrence of the harmful alga *Vicicitus globosus*, mostly in May. This alga was most abundant in 2014, and absent in 2016 when diatoms dominated. To understand the factors that might lead to *V. globosus* bloom, a principal component analysis (PCA) was conducted, using data sets collected in May for four years. In the PCA biplot, a cluster of data obtained in 2014, in which *V. globosus* dominated, and that obtained in 2016, in which diatoms dominated, were distantly separated. The 2014 biplot cluster was associated with increases in salinity and light intensity on the sea surface, while the 2016 cluster was negatively associated with these variables, but positively correlated with PO₄-P and *Fv/Fm*. Precipitation was highest in 2016 and lowest in 2014, resulting in higher riverine PO₄-P and higher *Fv/Fm* in the plankton community. These conditions were favorable for diatoms and unfavorable for *V. globosus*. The opposite result was observed in 2014, where conditions unfavorable for diatoms mainly due to decrease in riverine nutrients input, which may have created an ecological niche for *V. globosus* domination.

Keywords: diatoms, oligotrophication, precipitation, principal component analysis, PO₄-P

Introduction

The Seto-Inland Sea of Japan is the largest inland sea stretching over the western part of Japan (Fig. 1a) and was once heavily eutrophicated. As a result, severe red tides had occurred and caused serious fish kills (SFCO, 2018). Recently, nutrients that cause eutrophication, including inorganic nitrogen, have been decreased due to a strict law, and now the sea has been reported to be undergoing an oligotrophication process (Tanda et al., 2014). Red tide incidences have constantly decreased from peak period during the 1970s of 200–300 cases per year down to approximately 100 cases per year currently. However, incidences of fish mortality have not been reduced as expected, and 7–19 cases were reported in the recent decade (SFCO, 2018).

The silicoflagellate *Vicicitus globosus* was once recognized as a raphidophycean species, *Chattonella globosa*, but is now classified as Dictyochophyceae (Chang et al., 2012). This flagellate co-occurred with other harmful red tide species, e.g., *Pseudochattonella verruculosa* or *Heterosigma akashiwo*, and has been suspected to cause negative impacts onto the fisheries of New Zealand and Norway (Chang and Mullan, 2014; Lømsland et al., 2013). In the center of the Seto-Inland Sea of Japan, Bingo Nada, *V. globosus* formed a red tide with *Pseudochattonella verruculosa* (*Chattonella verruculosa*) in 2006 associated to fish kills (Kawaguchi et al., 2007). Recently, in this area, *V. globosus* has occurred from late spring through early summer, with

suspected negative effect on fisheries observed in 2006.

In this study, a statistical analysis by using four years of data sets obtained from our sampling was carried out to reveal which environmental factors could lead to *V. globosus* bloom in this region.

Materials and Methods

Field sampling

Monthly monitoring has been conducted in Bingo Nada (Fig. 1a) at stations shown in Fig. 1b from May 2014 to March 2017. At each station, vertical profiles of water temperature, salinity and upward photosynthetically active radiation (PAR) were measured by sensors installed in a CTD (DS5, Hydrolab) at 0.5 m depth intervals. Based on the upward PAR versus depth, a diffuse attenuation coefficient (k) was determined. Water samples from 1, 3 and 10 m depths were collected with a Van Dorn water sampler and subjected to chemical analysis (i.e., inorganic nutrients) or biological analysis (i.e., chlorophyll *a*, phytoplankton occurrence and photosynthesis activity of phytoplankton community). Dissolved inorganic nitrogen (DIN; $\text{NO}_3+\text{NO}_2+\text{NH}_4\text{-N}$), $\text{PO}_4\text{-P}$ and $\text{SiO}_2\text{-Si}$ were analyzed using a nutrient autoanalyzer (SWAAT, BLTEC) in the laboratory. Extracted chlorophyll *a* concentrations were determined fluorometrically. Populations of each phytoplankton species were counted under a light microscope. Maximum quantum yield of Photosystem II (PS II) (F_v/F_m) of phytoplankton communities was measured by a pulse amplitude modulation fluorometer (Water-PAM, Heinz Walz).

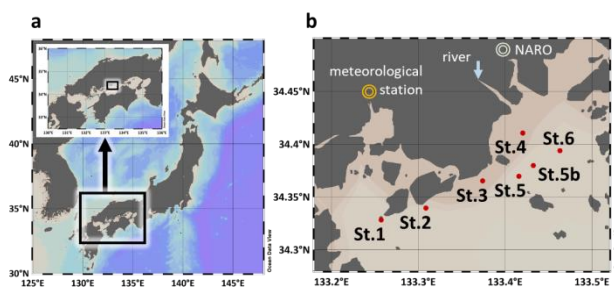


Fig. 1. (a) A map of Japan showing the Seto-Inland Sea and Bingo Nada; (b) A map of Bingo Nada showing locations of the stations. The maps were created by using Ocean Data View (Schlitzer, 2018).

Meteorological data

Based on hourly global solar radiation recorded at the Western Region Agricultural Research Center, the National Agriculture and Food Research Organization (NARO, Fig. 1b), an averaged PAR

value for each month was calculated and then used to represent potential PAR reaching the sea surface. Monthly hours of sunlight and precipitation were obtained from the meteorological station at Fukuyama City, Hiroshima (Fig. 1b).

Data analysis

A principal component analysis (PCA) was performed using R statistical software (ver. 3.5.1, R Core Team, 2018). Eight environmental variables [i.e., water temperature, salinity, diffuse attenuation coefficient, inorganic nutrients (DIN, $\text{PO}_4\text{-P}$, $\text{SiO}_2\text{-Si}$), monthly averaged PAR], chlorophyll *a* concentration and F_v/F_m were used in this analysis.

Results and discussion

Population dynamics of *V. globosus*

V. globosus occurred from April to September in Bingo Nada, predominantly in May. The maximum cell density was 117 cells mL^{-1} on May 13, 2014, which was lower but similar to that recorded in 2006 (145 cells mL^{-1}) when notable fish kills had occurred (Kawaguchi et al., 2007).

Proportions of *V. globosus*

Fig. 2 shows the proportions of phytoplankton taxa in May, consisting of diatoms, dinoflagellates, raphidophytes, and others as well as *V. globosus* obtained by using Ocean Data View (Schlitzer, 2018). In May 2014, *V. globosus* dominated at all the stations, and its cell density was highest among the four years (34–117 cells mL^{-1}). Similarly, except at St.3 in 2015, *V. globosus* cell density surpassed other taxa at all the stations in 2015 and 2017, while it was low (0–2 cells mL^{-1}) in May 2016 when diatoms dominated at all the stations with higher cell densities compared to those of other years (18–184 cells mL^{-1}). Consequently, *V. globosus* seemed to be competing with diatoms in Bingo Nada.

Environmental factors

Table 2 shows the environmental parameters recorded in May when the dominant occurrences of *V. globosus* were observed. There were no obvious variations in water temperature, salinity, k or chlorophyll *a* (chl. *a*) even in comparison between the years. However, slightly lower salinities were observed in 2015 and 2016 than in

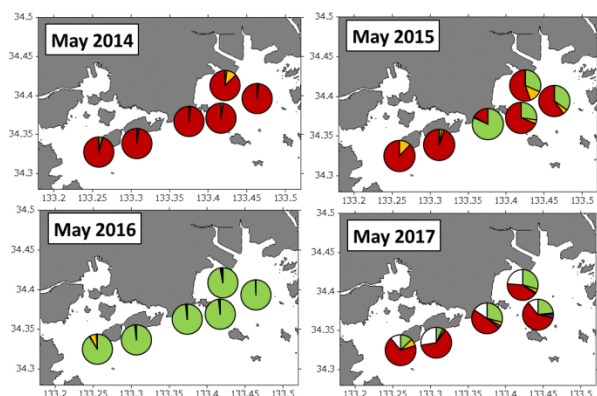


Fig. 2. Proportions of cell density (sum of the water column) for phytoplankton taxa in May from 2014 to 2017. Diatoms, green; dinoflagellates, orange; raphidophytes, purple; *V. globosus*, red; others, white.

Table. 2. Range (minimum – maximum) of environmental parameters recorded at 5 or 6 stations in May, from 2014 to 2017 when dominant occurrences of *V. globosus* were observed.

	2014	2015	2016	2017
temperature (°C)	16.16 – 17.30	16.91 – 18.70	16.45 – 17.16	16.56 – 18.04
salinity	32.51 – 33.04	31.22 – 32.23	31.36 – 32.42	32.24 – 33.15
<i>k</i>	0.30 – 0.44	0.29 – 0.55	0.19 – 0.44	0.31 – 0.69
DIN (μmol L ⁻¹)	0.4 – 12.6	0.9 – 19.2	0.3 – 15.2	0.4 – 4.9
PO ₄ -P (μmol L ⁻¹)	0.0 – 0.2	0.0 – 0.2	0.0 – 0.4	0.0 – 0.2
SiO ₂ -Si (μmol L ⁻¹)	8.4 – 22.9	16.7 – 29.7	12.7 – 31.1	12.0 – 25.0
chl. <i>a</i> (μg L ⁻¹)	3.54 – 13.91	1.78 – 6.50	1.88 – 7.91	2.53 – 14.71
<i>Fv/Fm</i>	0.40 – 0.63	0.42 – 0.62	0.63 – 0.80	0.41 – 0.66

the other years, indicating that levels of inflowing river water to the sampling sites were higher. Due to this riverine water, levels of DIN were higher in these two years than those in other years, and PO₄-P levels were higher in 2016. Silicate levels were sufficient for diatoms; Si/N ratios were constantly higher than the consensus level of 1. *Fv/Fm* values of the phytoplankton community were notably high in 2016 when diatoms dominated, which may have been caused by increased inorganic nutrients due to greater riverine inflow.

Principal component analysis

Fig. 3 shows a principal component analysis biplot loaded with data obtained at every sampling depth of the stations or surface light (S-Light; monthly averaged PAR) and *k* of the water

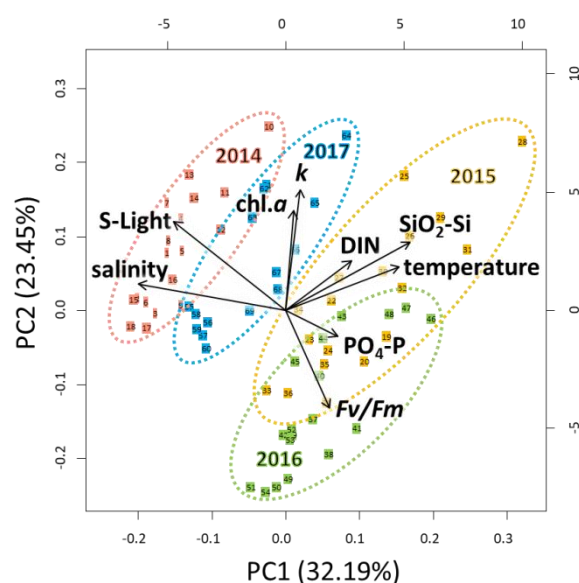


Fig. 3. Principal component analysis biplot of a certain depth of stations, recorded in May of 2014 (red circle), 2015 (blue circle), 2016 (green circle) and 2017 (orange circle), including eigenvectors of environmental factors, chl. *a* and *Fv/Fm*.

columns at the stations, which were recorded in May in 2014 (red circle), 2015 (blue circle), 2016 (green circle) and 2017 (orange circle). PC1 (32.19% of the variance) is positively correlated with water temperature and SiO₂-Si, and negatively correlated with S-Light and salinity, which may show the degrees to which riverine water causes increases in SiO₂-Si loading and decreases in salinity and influence of cloudy weather (decrease in S-Light).

In this biplot, the clusters of the sampling station or depth are each discriminated by years. In particular, the cluster of 2014, in which *V. globosus* dominated, and that of 2016, in which diatoms dominated, are distantly separated. The clusters of 2015 and 2017 were positioned between those of 2014 and 2016. Such obvious discrimination of the clusters, which extend horizontally in the biplot, is associated with interannual differences on precipitation and sunshine hours in April and May of each year (Fig. 4). The year 2014 was characterized with longer sunlight hours (Fig. 4a) and less precipitation (Fig. 4b), while 2016 had shorter sunlight hours and greater precipitation in April. As a result, the cluster of 2014 in the biplot was positively associated with increases in salinity and S-light, while the cluster of 2016 was negatively correlated with these variables. Higher precipitation in 2016 brought riverine PO₄-P and resulted in higher *Fv/Fm* of the plankton

community. These conditions were favorable for diatoms to grow and unfavorable for competitors, such as *V. globosus*. The year 2014 was the opposite of 2016; conditions were unfavorable for diatoms, mainly due to the decrease in riverine nutrients, and they created an ecological niche for *V. globosus* domination.

The relationships between the occurrence of *V. globosus* and nutrient concentrations or the occurrence of diatoms have previously been little studied (Kawaguchi et al., 2007; Chang and Mullan, 2014; Lømsland et al., 2013). If indeed such environmental conditions lead to the decline of diatoms, causing a bloom of the harmful flagellate *V. globosus*, more flexible wastewater management of the Seto Inland Sea than the current control, for example, changing regulation values of nutrients by season, might be required. Needless to say, further investigation of the factors associated with blooming of *V. globosus* is required.

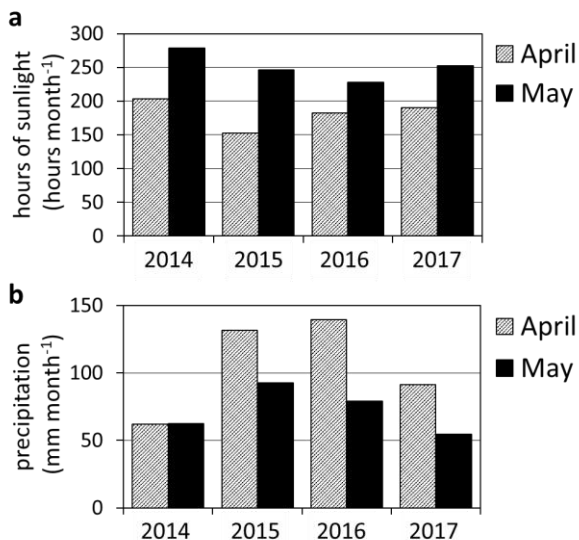


Fig. 4. (a) Hours of sunlight and (b) precipitation in April and May from 2014 to 2017.

Acknowledgements

We thank members of a Tashima fishery cooperative and crew of Toyoshio-maru for supporting us at samplings.

References

Chang, F. H., Mcveagh, M., Gall, M., Smith, P. (2012). *Phycologia* 51, 403-420.

Chang, F. H., Mullan, A. B. (2014). In: Kim, H.G., Reguera, B., Hallegraeff, G.M., Lee, C.K.,

Han, M.S., Choi, J.K. (Eds), Proceedings of the 15th International Conference on Harmful Algae. International Society for the Study of Harmful Algae, 199-202.

Kawaguchi, O., Takatsuji, H., Murakami, T., Iida, Y. (2007). Bulletin of the Hiroshima Pref. Fisheries & Marine Technology Center 2, 21-27. (in Japanese).

Lømsland, E. R., Johnsen, T. M., Eikrem, W. (2013). In: Pagou, K. A. and Hallegraeff, G. M. (Eds), Proceedings of the 14th International Conference on Harmful Algae, International Society for the Study of Harmful Algae and Intergovernmental Oceanographic Commission of UNESCO, 126-128.

Tanda, M., Akashige, S., Ariyama, H., Yamanoi, H., Kimura, H., Dan, A., Sakamoto, H., Saiki, Y., Ishida, Y., Kotobuki, H., Yamada, T. (2014). *Journal of Fisheries Technology*, 7, 37-46 (in Japanese).

R Core Team (2018). R Foundation for Statistical Computing, Vienna, Austria. URL <https://www.R-project.org/>.

Schlitzer, R., (2018) Ocean Data View, <https://odv.awi.de>.

SFCO (Setonaikai Fisheries Coordination Office, Fisheries Agency, Japan) (2018). Red Tide in the Seto Inland Sea (in Japanese).

Diversity of *Pseudo-nitzschia* H. Pergallo, 1900 along the Slovenian coast, Adriatic Sea, with insights into seasonality, toxicity and potential introductions

Timotej Turk Dermastia¹, David Stanković¹, Janja Francé¹, Magda Tušek Žnidarič², Andreja Ramšak¹, Patricija Mozetič¹

¹ National Institute of Biology, Marine Biology Station, Fornace 40, 6330 Piran, Slovenia

² National Institute of Biology, Department of Biotechnology and Systems Biology, Večna pot 111, 1000 Ljubljana, Slovenia

Abstract

The diatoms species belonging to *Pseudo-nitzschia* H. Pergallo, 1900 genus are extensively studied because many of them are responsible for amnesic shellfish poisoning (ASP) via the production of domoic acid (DA). *Pseudo-nitzschia* species are important members of the phytoplankton community and are regularly reported in the Adriatic Sea. We present first results from an 18-month study, in which cultures were established from single cells sampled monthly in the northernmost part of the Adriatic Sea, the Gulf of Trieste (GOT). Thirty-five cultures were identified morphologically with transmission electron microscopy (TEM) and molecularly by screening the *rbcL* region of the chloroplast genome. Based on the phylogenetic reconstruction seven species were identified: *P. calliantha*, *P. fraudulenta*, *P. pungens*, *P. mannii*, *P. delicatissima*, *P. galaxiae* and *P. multistriata*. This is the first genetic recognition of *P. multistriata* in this region, thus we speculate it has spread from southern and neighbouring regions in the Adriatic where it was previously identified as an introduced species. Most cultured strains belonged to the *P. calliantha* clade. Toxicity tests were carried out on five strains and low toxin concentration (0.22 fg DA/cell) was detected in a single strain of *P. multistriata*. We revealed some seasonal patterns of *Pseudo-nitzschia* distribution in the GOT. While some species tend to occur only in particular seasons (i.e. *P. multistriata* from early autumn to late winter, *P. fraudulenta* and *P. delicatissima* mainly in spring), others, such as *P. calliantha*, seem to be present throughout the year.

Keywords: *Pseudo-nitzschia*, domoic acid, seasonality, phylogeny, Gulf of Trieste

Introduction

Some species of the genus *Pseudo-nitzschia* show cosmopolitan distribution while others are more localized (Bates et al., 2018). With increasing marine traffic and environmental change, species that are generally developed to particular localities may proliferate in other regions via anthropogenic introduction / bio-invasion (Mozetič et al., 2017). Inter-annual and seasonal dynamics of *Pseudo-nitzschia* spp. have been studied for decades in the Gulf of Trieste (GOT) (Cabrini et al., 2012) but the formal species identification is still lacking due to morphological similarities between members of the genus and limitations of optical microscopy used in routine monitoring surveys. Precise identification can only be achieved with dedicated investigation using electron microscopy and/or genetic identification. Moreover, the genus' genetics and phylogenetic relationships are proving to be complicated, with many cases of cryptic species within distinct clades (Amato et al., 2007; Lelong et al., 2012; Lundholm et al., 2006). In the northern Adriatic, *Pseudo-nitzschia* species occur

throughout the year with recognizable seasonal peaks in late autumn and early spring and recently also in summer (Cabrini et al., 2012; Ljubešić et al., 2011). Shellfish monitoring schemes from different coastal areas of the northern Adriatic, including Slovenian sites of aquaculture (unpublished data) have occasionally reported the presence of domoic acid (DA) in shellfish, however it was always found at low concentrations and the source was not identified (Marić et al., 2011; Pistocchi et al., 2012). The true causative agent of the toxicity has not been yet identified, since the community is usually not monospecific and many species are known to produce DA toxin under some conditions. The most commonly reported species is *P. calliantha* that has also been linked to the production of DA (Marić et al., 2011), however this was not proved in culture experiments. Other species that have been reported include *P. delicatissima*, *P. pseudo-delicatissima*, *P. mannii*, *P. pungens*, *P. fraudulenta*, *P. subfraudulenta*, *P. galaxiae* and *P. multistriata* (Cabrini et al., 2012;

Pistocchi et al., 2012). The Adriatic strain of *P. multistriata* was also found to produce DA, albeit at low concentrations of 0.003pg/cell (Pistocchi et al., 2012), however given its small size and relatively low numbers in the natural environment it is unlikely that this species is contributing to toxicity found in shellfish.

While phytoplankton abundance seems to be declining in the GOT, which is linked to oligotrophication due to decreased river runoff and the improvement of waste water treatments (Mozetič et al., 2010), *Pseudo-nitzschia* abundance seems to be increasing throughout whole NA according to a 30-year long time series data (Maric Pfannkuchen et al., 2018). Here we report a comprehensive study of *Pseudo-nitzschia* in the GOT based upon morphological and genetic characteristics revealed by transmission electron microscopy (TEM), and screening of the *rbcL* gene. Insights in the toxicity and seasonality are presented as well and potential introduction ways are discussed.

Materials and Methods

Sampling, culturing and microscopy

Sampling was carried out monthly between October 2016 and March 2018 in the south-eastern part of the GOT. Cultures were established from isolates obtained from 20µm phytoplankton net tows. Nets were hauled five times vertically from the sea bottom (17m) at the sampling station near a Slovenian shellfish farm (Figure 1). The concentrated sample was observed under the Zeiss Axio Observer Z1 inverted light microscope, from which cells or cell chains were serially diluted in order to obtain a monoclonal culture. The isolates were kept in 50 ml Erlenmeyer flasks at a 12:12 photoperiod regime at 70 µmol m⁻²s⁻¹ and 20°C. Cultures were transferred into fresh media (which media ??) every 2 weeks throughout the study period. Some strains also died off due to natural progression. In parallel to net hauls, seawater samples were also taken and analysed under inverted light microscope (LM) for monitoring purposes (National monitoring program of toxic phytoplankton in Slovenian shellfish farms). Cultures were cleaned and prepared for TEM using nitric and sulphuric acid as described in the Assemble protocol by Percopo & Sarno (<http://www.assemblemarine.org/assets/Uploads/Documents/tool-box/>).

Cleaned cultures were loaded onto carbon coated copper grids and examined under TEM (Philips CM 100). Images were taken using the Bioscan CCD camera Gatan, using Digital Micrograph software. Despite little species resolution based on

cell counts of *Pseudo-nitzschia* spp., we were able to report on seasonal patterns that were resolved from field observations and culturing attempts.

DNA processing

During the first fortnight the growth of the strains was monitored and when the growth curve reached the stationary phase 10 mL of the culture was collected and DNA was extracted using the E.Z.N.A Mollusc DNA kit (Omega Bio-Tek). DNA quality and quantity were checked with electrophoresis and measured fluorimetrically. DNA was stored at -20°C until further processing. Primers for the *rbcL* region Rbc11_mod and RbcL7_mod (Jones et al., 2005) were used in PCR under standard conditions. Both the forward and reverse strands were sequenced in all samples using 11F and 11R primers (Amato et al., 2007). PCR products were visualised on an agarose gel against a standard ladder. Successful amplicons were purified and sent for sequencing to Macrogen Inc.

Phylogenetic inference

Contigs were assembled using ChromasPro (v. 2.1.8) and subjected to BLAST searches. Phylogenies were reconstructed using MrBayes v.3.2.6 (Ronquist et al., 2012).

Toxicity

Toxin (DA) analyses of four selected strains were carried out using the Liquid Chromatography-Mass Spectrometry (LC-MS) method by the National Reference Laboratory for Marine Biotoxins, Cesenatico, Italy.

Results and Discussion

The sampling campaign resulted 38 strains that were isolated and cultured. At least one strain of each species reported here was investigated using TEM, to confirm its morphological identity. The exception is *P. galaxiae*, of which DNA was extracted and sequenced, however TEM was not used due to the early death of cultured strains and the inability to obtain sufficient material. We were able to obtain 32 *rbcL* sequences.

While the best barcoding marker is ITS2 (Moniz & Kaczmarska, 2009) because of its smaller size relative to *rbcL*, highly populated database and the fact that it can be used as a mating compatibility predictor based on compensating base changes (Amato et al., 2007), our data shows very good species resolution even with *rbcL*. Furthermore, ITS is usually subjected to lower amplification and sequencing success, which could be connected with intragenomic variability of this marker (Orsini et al., 2004) or contamination of cultures with small

chlorophytes, which was also often observed in our samples.

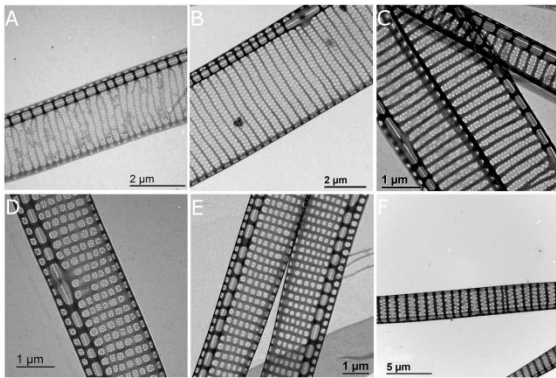


Fig. 1 TEM micrographs of the identified species. A) *P. multistriata* (strain 51216), 13500x. B) *P. fraudulenta* (strain 217-A1), 10500x. C) *P. delicatissima* (strain 240417), 19000x. D) *P. calliantha* (strain 281016-A2), 19000x, E) *P. mannii* (strain 817-C1), 13500x. F) *P. pungens* (strain 41217-A1), 4600x.

The phylogenetic tree (Fig. 2) revealed that our strains belong to seven species. The well described variability in *P. pungens* (Lim et al., 2014) is captured by our analysis and it places our *P. pungens* strains in clade I *sensu* Lim et al., (2014), which is expected. Likewise, strains belonging to the *P. delicatissima* group cluster into the widely-distributed clade A/2 *sensu* Quijano-Scheggia et al., (2009). Perhaps the most interesting is the clustering of the two *P. galaxiae* strains isolated in the GOT, which are placed into two distinct clusters (*P. galaxiae* III and *galaxiae* V, this study), although they both have low posterior probabilities. The exceptionally high intraspecific diversity of this species is well known (Cerino et al., 2005; McDonald et al., 2007; Ruggiero et al., 2015). Ruggiero et al. (2015) identified 45 distinct ribotypes, forming four ribogroups. Here we see that there are five clusters present, although they do not all have high support. It is worth noting that the two strains A1G and A2G, separated by four base changes, were isolated on the same day. Therefore, we predict these strains to be reproductively isolated. Unfortunately, we were unable to obtain sequences of these strains, nor were the differences distinguishable with LM and thus we cannot provide further morphological variability. Peculiarly, the two strains were both representative of the medium morphotype (*sensu* Cerino et al. 2005). In accordance, they were both found to produce chains. Strain A2G was somewhat smaller and thinner; however, the culture was in a bad shape and is therefore difficult to draw conclusions from this. They both

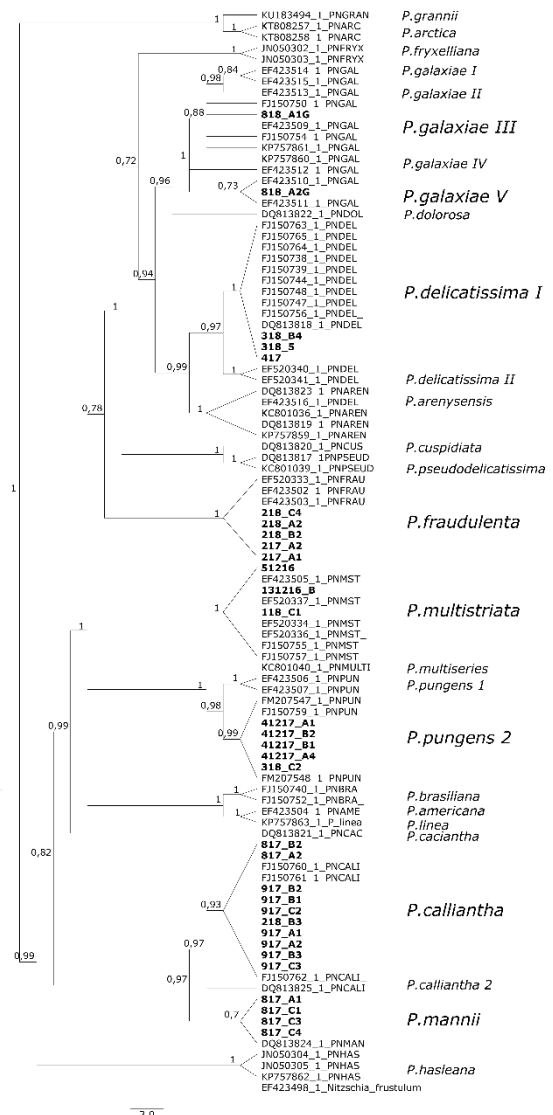


Fig. 2 Bayesian inference phylogeny of the *rbcL* marker (GTR + I + G, ngen =500000). Numbers in nodes represent posterior probabilities of the branches.

share the same LSU sequence (not shown), but are distinct in *rbcL*, which is in accordance with Ruggiero et al., (2015).

We can draw some conclusions on seasonality based on observations and isolation dates (strain names are named after the isolation date coupled with a strain identifier). Particularly, for *P. multistriata*, which is easily identifiable with LM, and was only observed and isolated in the winter months (from November to February). This is in accordance with the clonal libraries constructed in Ruggiero et al., (2015) in the Gulf of Naples, although they also reported summer peaks of this species, which we have not registered. The isolation of *P. fraudulenta* was successful only in February in two successive years, which is in total compliance with Ruggiero et al., (2015) who also registered this species only in February. Similar species were observed with TEM also in other seasons; however, no successful cultures were

established. Finally, a toxic strain of *P. multistriata* (131216_C) was identified with TEM and 28S (not shown). The domoic acid content in culture was low but detectable (0.2 fg/cell). This is an order of magnitude less than the previously identified toxic *P. multistriata* in the Adriatic (3fg/cell; Pistocchi et al., 2012). This is the first genetic confirmation of *P. multistriata* in the region, albeit it is not surprising as it was reported from nearby areas as well as northern Adriatic ports before (Mozetič et al., 2017). This work represents the first comprehensive survey of the *Pseudo-nitzschia* species diversity in the GOT and will be followed by more detailed examinations in population genetics, ecology and seasonal patterns.

Acknowledgements

This work was funded by the Young Researcher grant of the Slovenian research agency (ARRS) to Timotej T.D. We would like to thank Silvia Pigozzi (Fondazione Centro Ricerche Marine, Cesenatico, IT) for kindly analysing our samples for toxicity.

References

- Amato, A., Kooistra, W. H. C. F., Levaldi Ghiron, J. H., Mann, D. G., Pröschold, T., & Montresor, M. (2007). *Protist*, 158(2), 193–207.
- Bates, S. S., Hubbard, K. A., Lundholm, N., Montresor, M., & Leaw, C. P. (2018). *Harmful Algae*, (October), 1–41.
- Cabrini, M., Fornasaro, D., Cossarini, G., Lipizer, M., & Virgilio, D. (2012). *Estuarine, Coastal and Shelf Science*, 115, 113–124.
- Cerino, F., Orsini, L., Sarno, D., Dell’Aversano, C., Tartaglione, L., & Zingone, A. (2005). *Harmful Algae*, 4(1), 33–48.
- Jones, H. M., Simpson, G. E., Stickle, A. J., & Mann, D. G. (2005). *European Journal of Phycology*, 40(1), 61–87.
- Lelong, A., Hégaret, H., Soudant, P., & Bates, S. S. (2012). *Phycologia*, 51(March), 168–216.
- Lim, H. C., Lim, P. T., Teng, S. T., Bates, S. S., & Leaw, C. P. (2014). *Harmful Algae*, 37, 142–152.
- Ljubešić, Z., Bosak, S., Viličić, D., Borojević, K. K., Marić, D., Godrijan, J., ... Dakovac, T. (2011). *Harmful Algae*, 10(6), 713–722.
- Lundholm, N., Moestrup, Ø., Kotaki, Y., Hoef-Emden, K., Scholin, C., & Miller, P. (2006). *Journal of Phycology*, 42(2), 464–481.
- Marić, D., Ljubešić, Z., Godrijan, J., Viličić, D., Ujević, I., & Precali, R. (2011). *Estuarine, Coastal and Shelf Science*, 92(3), 323–331.
- Maric Pfannkuchen, D., Smodlaka Tankovic, M., Baricevic, A., Kuzat, N., & Pfannkuchen, M. (2018). In ICHA2018 Abstract book.
- McDonald, S. M., Sarno, D., & Zingone, A. (2007). *Harmful Algae*, 6(6), 849–860.
- Moniz, M. B. J., & Kaczmarska, I. (2009). *Molecular Ecology Resources*, 9(SUPPL. 1), 65–74.
- Mozetič, P., Cangini, M., Francé, J., Bastianini, M., Bernardi Aubry, F., Bužančič, M., ... Skejić, S. (2017). *Marine Pollution Bulletin*, (December).
- Mozetič, P., Solidoro, C., Cossarini, G., Socal, G., Precali, R., Francé, J., ... Fonda Umani, S. (2010). *Estuaries and Coasts*, 33(2), 362–375.
- Orsini, L., Procaccini, G., Sarno, D., & Montresor, M. (2004). *Marine Ecology Progress Series*, 271(May), 87–98.
- Pistocchi, R., Guerrini, F., Pezzolesi, L., Riccardi, M., Vanucci, S., Ciminiello, P., ... Riccardi, E. (2012, January). *Marine Drugs*. Multidisciplinary Digital Publishing Institute (MDPI).
- Quijano-Scheggia, S. I., Garcés, E., Lundholm, N., Moestrup, Ø., Andree, K., & Camp, J. (2009). *Phycologia*, 48(6), 492–509.
- Ronquist, F., Teslenko, M., van der Mark, P., Ayres, D. L., Darling, A., Höhna, S., ... Huelsenbeck, J. P. (2012). *Systematic Biology*, 61(3), 539–542.
- Ruggiero, M. V., Sarno, D., Barra, L., Kooistra, W. H. C. F., Montresor, M., & Zingone, A. (2015). *Harmful Algae*, 42(1), 15–24.

Distribution patterns of toxic epibenthic microalgae *Prorocentrum lima* in the Gulf of Gabès (South-eastern Mediterranean Sea)

Lamia Dammak Walha^{1,2,*}, Fatma Abdmouleh^{1,2}, Moufida Abdennadher¹, Asma Hamza¹, Cherif Sammari¹

¹Laboratoire Milieu Marin, Institut National des Sciences et Technologies de la Mer,

²Faculté des Sciences de Sfax, Université de Sfax, Sfax, Tunisia

* corresponding author's email: lamia.dammak@gmail.com

Abstract

Blooms of toxic epibenthic are associated with harmful effects on human health and the environment. In the Gulf of Gabès (south-eastern Mediterranean Sea), the toxic epibenthic dinoflagellate *Prorocentrum lima* was recorded as a common component of epiphytic assemblages, observed in the water column and attached on various substrates. The present work provides the spatiotemporal survey of *P. lima* on different substrata (*Ulva rigida*, stones, sediment and biofilm) during one-year observation from March 2015 to February 2016, in five stations at five stations selected among the regular monitoring sites along the Gulf of Gabès coast. The relationships between physico-chemical parameters and *P. lima* abundance were investigated. A post-hoc test (SNK) revealed a significant difference between stations and substrates. *P. lima* was most abundant at the Skhira site (S6). This station was characterized by high ammonium concentration. At S6, it was most abundant in the biofilm in March, September and January, on the stones during February and August and in the sediment in January and March. High relative abundance of *P. lima* was preferentially hosted by stones for all sampling sites. The seasonal variability of *P. lima* was influenced by temperature and nutrients particularly ammonium.

Keywords: *P. lima*, *Ulva rigida*, stone, sediment

Introduction

Prorocentrum lima (Ehrenberg) Stein is the most commonly reported benthic species of *Prorocentrum*. It has been reported as cosmopolitan and has been identified at various locations ranging from temperate to tropical latitudes (Nagahama et al., 2011). *P. lima* is a toxic species, it was described to produce okadaic acid (OA) and its related derivatives (dinophysins toxins, DTXs) (Hoppenrath et al., 2013). In the Gulf of Gabès, *P. lima* was a common component of epiphytic assemblages. It was observed in the water column (Loukil-Baklouti et al., 2017) and attached to various substrates such as angiosperms and macroalgae (Ben Brahim et al., 2013; Moncer et al., 2017). This study aims to examine the spatiotemporal distribution of *P. lima* on different substrates (sediment, biofilm, *U. rigida* and stones) during one year of sampling at five monitoring sites along the Gulf of Gabès coast.

Materials and Methods

Study area

This study was carried out in the Gulf of Gabès (South-eastern Mediterranean) extending from Ras Kapoudia to the Tunisian-Libyan border. Samples (sediment, biofilm, macroalgae (*U. rigida*) and

stone) were collected monthly from March 2015 to February 2016 at five monitoring sites along the Gulf of Gabès (S1, S2, S6 for Sfax and G2, G3 for Gabès) (Fig. 1).

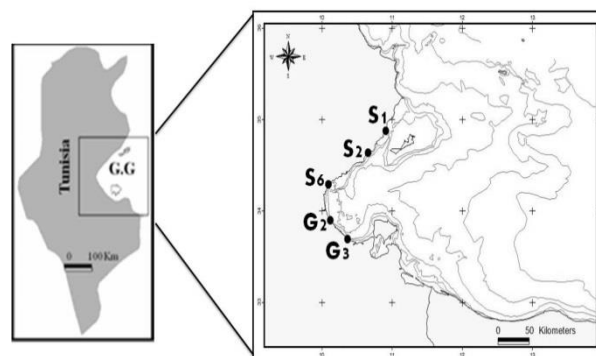


Fig. 1. Location of sampling stations (S1: El Aouabed; S2: Tabia; S6: Skhira; G2: Gabès Harbour; G3: Zarrat).

Sampling and water analyses

Biofilm and sediment were sampled by means of a plastic core sampler (5 cm diameter). The top cap from the core was removed and the biofilm was put in a bottle. 1 g sediment was suspended in 100 mL of filtered seawater and then filtered using 0.45- μ m filter membranes (Loukil Baklouti et al., 2017). *U. rigida* was collected and placed in a plastic bag.

The collected materials, 200 g of *U. rigida* were washed in 1L of filtered seawater (Ben Brahim et al., 2013). Stones with a diameter between 15-20 cm and without filamentous algae were selected. The upper parts of the stone were brushed with a toothbrush and were washed with 200 mL of filtered seawater (Çolak Sabanci, 2013). All recuperated water samples were fixed with formaldehyde (3%). Microalgal enumeration was conducted according to Utermöhl (1958) using 10 mL sedimentation chamber under an inverted microscope (Nikon Eclipse TS100). Temperature, pH, and salinity were measured *in situ* using a kit (Multi 3400 i/SET). Inorganic nutrients (nitrite, nitrate, ammonium, orthophosphate and silicate) were analyzed with a BRAN-LUEBBE type 3 autoanalyser (APHA, 1992).

Data analysis

The Student-Newman-Keuls (SNK) post hoc test was performed for post hoc multiple comparisons of means). Cochran's C test was used before each analysis to check the homogeneity of the variance and data; were log (x+1) transformed when necessary (Underwood, 1997). The similarity of *P. lima* abundance between different substrates was analyzed using cluster analysis. The hierarchical agglomerative clustering analysis (Clarke and Warwick, 2001) used the routine "CLUSTER" of Excel Abundance of *P. lima* was related to environmental factors by means of principal component analysis (PCA).

Results and Discussions

Spatiotemporal distribution of *P. lima*

The Spatiotemporal distribution of *P. lima* in different substrates is illustrated in figure 2. *P. lima* abundance varied in function of stations and substrates along the studied period. The highest abundance was recorded in the biofilm and the sediment during January, on stone during February and on *U. rigida* during November and December (fig. 2). During spring, *P. lima* was not fixed on the stones.

On the stones, the maximum abundance of *P. lima* was (850 ± 108 cells cm^{-2}) at S6.

P. lima was present with low abundance in the Biofilm (100 ± 82 cells L^{-1}), collected at Skhira in July and December, whereas its maximal abundance (833 ± 94 cells L^{-1}) (mean \pm SD) was recorded during March at the same station. In the sediment *P. lima* maximal abundance was at S6 station in January (3800 ± 455 cells g^{-1} FW). Loukil-Baklouti et al. (2018) recorded *P. lima* as present mostly in the biofilm rather than in

sediment at S2 (91 ± 42 cells L^{-1}) and S6 (18 ± 39 cells L^{-1}).

For *U. rigida*, the maximum abundance of *P. lima* (733 ± 170 cells g^{-1} FW) was detected at G3 in December. *P. lima* was present at low abundance (80 ± 33 cells g^{-1} FW) at S6 probably caused by the ability of *Ulva* to inhibit the proliferation of harmful microalgae. Indeed, Tang and Gobler (2011) and Ben Gharbia et al. (2017) showed negative allelopathic effect of *U. rigida* on *P. lima* in co-culture laboratory experiments.

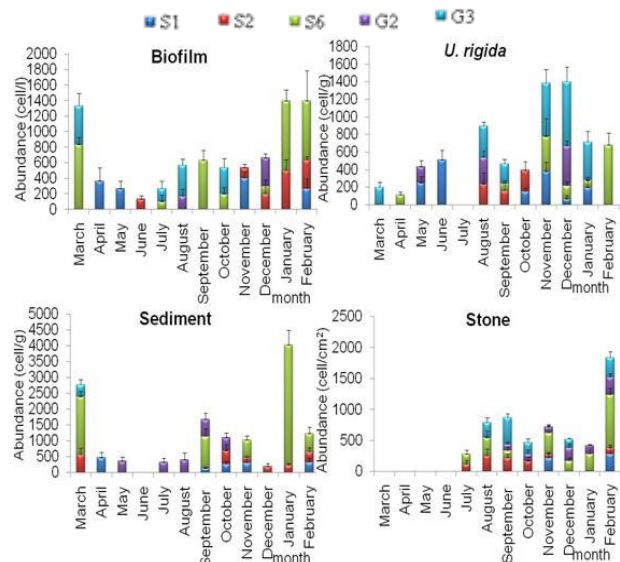


Fig. 2. Spatiotemporal distribution of *P. lima* in study area in different substrates

Cluster analysis

The cluster analysis between different stations showed 3 groups (fig. 3 A): the first group GI was composed of stations S1, S2 and G2; the second group GII was encompassed only one station (G3) with the maximum concentration recorded on *U. rigida*. The third group GIII was composed of station S6 with the maximum abundance of *P. lima* in sediment, biofilm and stone.

In fact, stations S2, G2 were influenced by industrial activity involving the manufacture, storage, use of chemicals including petrochemicals phosphate treatment, tannery, and plastic plants (Bejaoui et al., 2004), while station S6 was affected by petroleum pollution from the transport harbor (Loukil-Baklouti et al., 2018).

The foreshore of G3 is very extensive without evident anthropogenic source of pollution and is considered as not polluted (El Zrelli et al., 2018).

The cluster analysis between substrates (fig. 3 B) showed 3 groups. The first group GI was composed of stone and biofilm. The second group GII was represented by the sediment. The third group GIII was corresponded to *U. rigida*. This classification depends of the affinity of *P. lima* to the host

support. For instance, macroalgae can inhibit microalgae by creating competition for nutrients and by allelochemical effects (Tang and al., 2014).

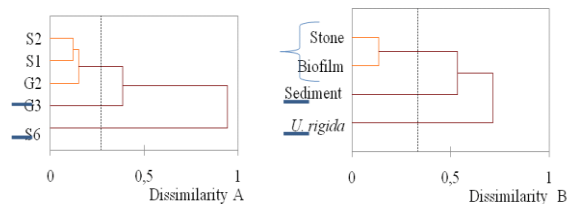


Fig. 3. Degree of similarity between (A) different stations and (B) substrates in terms of mean abundance of *P. lima*.

SNK test on the distribution of *P. lima* in different substrates

Post-hoc test (Table 1) was used to classify the order of affinity of *P. lima* to all stations with substrates. It revealed a significant difference between stations and substrates. The station 6 was discriminated from the all sampled stations where the highest abundance was recorded for sediment, biofilm and stone. For *U. rigida*, the station G3 was distinguished from the others stations by its relatively high abundance of *P. lima* caused by their allelopathic properties.

Table 1: SNK test on the distribution of *P. lima* in different substrates

Biofilm		<i>U. rigida</i>		Sediment		Stone	
Sites	Subset for $\alpha=0.05$	Sites	Subset for $\alpha=0.05$	Sites	Subset for $\alpha=0.05$	Sites	Subset for $\alpha=0.05$
	1 2		1 2		1 2		1 2
G2	4.44	G2	155.00	G3	30.55	S1	41.66
S1	108.33	S2	161.11	S2	76.38	G2	79.16 79.16
S2	111.11	S6	249.44 249.44	S1	125.00	S2	105.55 105.55
G3	116.66	S1	258.88 258.88	G2	169.44	G3	108.33 108.33
S6	429.44	G3	425.55	S6	647.22	S6	184.72
Sig.	.53 1.00	Sig.	.130	Sig.	.676 1.000	Sig.	.370 .054
G2<S1<S2<G3<S6		G2<S2<S6=S1<G3		G3<S2<S1<G2<S6		S1<G2<S2=G3<S6	

Means for groups in homogeneous subsets are displayed. a. Uses Harmonic Mean Sample Size = 36.00

Relation: physico-chemical parameters and *P. lima* abundance

The PCA plot illustrates two groups (A and B) surrounding the F1 and F2 component axes, both explaining 72.21% of the variance. F1 component axis extracts 44.79% and F2 27.42% of the variability (fig. 4).

The first group A included stations S6, S2 and G2, three substrates (biofilm, sediment and stone) and all physico-chemical variables. F1 component axis, was selected negatively the group B (S1, G3 and *U. rigida*). *P. lima* proliferation was controlled by substrates and environmental conditions in G2, S2 and S6 (fig. 4). In G3 and S1, *P. lima* proliferated on *U. rigida* without apparent links to environmental parameters. *P. lima* showed a

positive correlation with temperature ($r = 0.914$, $p < 0.05$) and salinity ($r = 0.59$, $p < 0.05$). A similar result was already reported in the water column of the Gulf of Gabès (Loukil-Baklouti et al., 2017), the Gulf of Tunis (Turki, 2005) and in the western Adriatic (Ingarao et al., 2009). In addition, Laabir et al., (2011) highlighted that temperature, salinity and irradiance are the most important environmental factors influencing the growth of toxics species. A positive correlation was also found between ammonium concentration and *P. lima* abundance ($r = 0.915$, $p < 0.05$) corroborating the results of Aissaoui et al., (2014) in the Gulf of Tunis showing a strong effect of ammonium on the proliferation of *P. lima*.

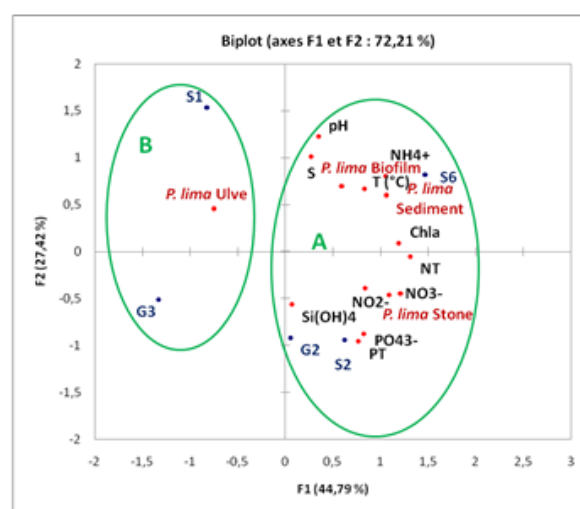


Fig. 4: Principal Component Analysis (PCA) between environmental parameters and abundance of *P. lima*

Conclusions

The Seasonal variability of *P. lima* was influenced by physico-chemical parameters particularly the temperature and the ammonium concentrations. *P. lima* was preferentially hosted by stones in all sampling sites whereas *U. rigida* was not a preferential substratum for this species. This result confirms that the substrate is a key element for the proliferation of *P. lima*. The mechanism by which the substrate affects the species abundance has to be elucidated.

References

- Aissaoui A., Armi Z., Akrouf F., Ben Hassine O.K. (2014). Water Environ. Res. 86, 2256–2270.
- Bejaoui B., Rais S. et Koutitonsky V. (2004). Bull. Inst. Natn. Scien. Tech. Mer Salammbô 31, 103-109

- Ben Brahim M., Hamza A., Ben Ismail S., Mabrouk L., Bouain A., Aleya L. (2013). *Mar. Poll. Bull.* 71(1–2), 286–298.
- Ben Gharbia H., Keafi-Daly Yahia O., Cecchi P., Masseret E., Amzil Z., Herve F., Rovillon G., Nouri H., M'Rabet C., Couet D., Zmerli Triki H., Laabir M. (2017). *Journal. Pone.* .
- Clarke K.R., Warwick R.M. (2001). *Change in Marine Communities: An Approach to Statistical Analysis and Interpretation*. 2nd Edition, PRIMER-E, Plymouth: 172 pp.
- Çolak Sabanci F. (2013). *Medit. Mar. Sci.* 14/1, 129–140.
- El Zrelli R., Rabaoui L., Ben Alaya M., Daghbouj N., Castet S., Bessona P., Michel S., Bejaoui N., Courjault-Radé P. (2018). *Mar. Poll. Bull.* 127, 445–452.
- Hoppenrath M., Chomérat N., Horiguchi T., Schweikert M., Nagahama Y., Murray S. (2013). *Harmful Algae* 27, 1–28.
- Ingarao, C., Lanciani, G., Verri, C., Pagliani, T. (2009). *Mar. Poll. Bull.* 58, 596–600.
- Laabir M.; Jauzein C.; Genovesi B.; Masseret E.; Grzebyk D.; Cecchi P.; Vaquer A.; Perrin Y.; Collos Y. (2011). *J. Plankton Res.* 33, 1550–1563.
- Loukil-Baklouti A., Feki-Sahnoun W., Hamza A., Abdennadher M., Mahfoudhi M., Bouain A., Jarboui O. (2018). *Cont. Shelf Res.* 52, 62–70.
- Moncer M., Hamza A., Feki-Sahnoun W., Mabrouk L., Bel Hassen M. (2017). *Scient. Mar.* 81(4).ISSN-L: 0214-8358
- Nagahama Y., Murray S., Tomaru A., Fukuyo Y. (2011). *J. Phycol.* 47, 178–189.
- Tang Y.Z., Gobler C.J. (2011). *Harmful Algae* 10, 480–488.
- Tang Y.Z., & Kang Y. & Berry D.Gobler Ch. J. J (2015). *Appl Phycol* 27:531–544.
- Turki, S., 2005. *Cah. Biol. Mar.* 46, 29–34.
- Underwood A.J. (1997). *Experiments in ecology: their logical design and interpretation using analysis of variance*. Cambridge Univ Press.
- Utermöhl H. (1958). *Mitt Int. Ver Theor. Angew. Limnol.*, 9, 1–38.

Are harmful epibenthic dinoflagellates proliferating in Southern Mediterranean? A case study of the Bizerte Bay and Lagoon (North of Tunisia, Southern Mediterranean Sea)

Hela Ben Gharbia^{1,2*}, Mohamed Laabir², Abdelouahed Ben Mhamed³, Sonia KM Gueroun⁴, Ons Kéfi - Daly Yahia¹

¹ Research Group on Oceanography and Plankton Ecology, Tunisian National Institute of Agronomy (INAT), 43 Avenue Charles Nicolle, Tunis 1082, IRESA-Carthage University Tunisia. LR18ES41 Marine Biology (University of Tunis El Manar, Tunisia).

² Center for Marine Biodiversity, Exploitation and Conservation (MARBEC), Institut de Recherche pour le Développement (IRD), Institut Français de Recherche pour l'Exploitation de la Mer (IFREMER), Centre National de la Recherche Scientifique (CNRS), Montpellier University, Place Eugène Bataillon, CC093, Montpellier Cedex 5 F-34095, France.

³ National Institute for Fisheries Research, Central laboratories, Bd Sidi Abderrahmane Ain Diab 2, Casablanca, Morocco.

⁴ Faculty of Sciences of Bizerte, Laboratory of Aquatic Systems Biodiversity and Functioning, Tunisia.

*corresponding author's e-mail: hela.bg@hotmail.fr

Abstract

Harmful events associated with benthic algal blooms (BHABs), have been reported more frequently over the last decades. Many epibenthic dinoflagellates are known to produce potent biotoxins that can accumulate in the food chain or even be released as marine aerosols. Nevertheless, reports on these benthic species are particularly scarce along the Southern Mediterranean coasts. A monthly monitoring of potentially toxic benthic dinoflagellates, associated with *Cymodocea nodosa* fronds, was performed over one year in the Bizerte bay and lagoon (North of Tunisia, Southern Mediterranean Sea). This important Tunisian aquaculture area is dominated by dense *C. nodosa* meadows and is subject to recurrent eutrophication and high anthropogenic pressures. Several potentially toxic dinoflagellate species, belonging to the genera *Prorocentrum*, *Ostreopsis*, *Coolia* and *Amphidinium*, were identified. The highest epibenthic dinoflagellate abundances were recorded on *C. nodosa* fronds from the Bizerte bay, while lower densities were associated with this magnoliophyte in the Bizerte lagoon. The highest mean cell abundances were reached by *Ostreopsis* cf. *ovata* in the Bizerte bay. Results revealed significant positive correlations between this toxic dinoflagellate and temperature. Our study suggests that high sea water temperatures are likely to promote the occurrence of *Ostreopsis* blooms in the Mediterranean basin.

Keywords: Harmful epibenthic dinoflagellates, *Cymodocea nodosa* fronds, *Ostreopsis* cf. *ovata* Southern Mediterranean Sea

Introduction

Harmful epibenthic dinoflagellates live attached to various substrates (macrophytes, rocks, corals and detritus) and can also be found in water bodies and sediments (Aligizaki and Nikolaidis, 2006; Hoppenrath et al., 2014). Benthic dinoflagellate assemblages usually include species of the genera *Prorocentrum*, *Ostreopsis*, *Coolia*, *Amphidinium* and *Gambierdiscus* (Morton and Faust, 1997; Vila et al., 2001a; Parsons and Preskitt, 2007; Blanfuné et al., 2015). Several toxins produced by these species are still uncharacterized. Proliferation of these microorganisms can have dramatic consequences in terms of public health and

inherent economic losses (GEOHAB, 2012). Confined areas such as harbors, small bays and semi-enclosed coastal lagoons are particularly prone to the proliferation of toxic phytoplankton species (Vila et al., 2001b). Harmful events associated with benthic algal blooms (BHABs) are showing a widening geographical range from their endemic tropical-subtropical areas toward temperate waters and higher latitudes. In the Northern Mediterranean Sea, *Ostreopsis* cf. *ovata* has represented a major cause of toxic blooms since 2005 (Ciminiello et al., 2006). *Ostreopsis* outbreaks showed the apparent range expansion of

epibenthic dinoflagellates and sounded the alarm about the potential risks that are threatening the Mediterranean waters.

Given the limited data available on potentially harmful benthic dinoflagellates in the Southern Mediterranean Sea, we performed a survey of the epibenthic dinoflagellate community associated with the magnoliophyte *Cymodocea nodosa* from the Bizerte bay and lagoon (North of Tunisia). The present work aims to determine the species composition and abundances of epiphytic dinoflagellates associated with *C. nodosa* fronds, and to identify the main environmental factors promoting their proliferation.

Materials and Methods

This study was carried out in the Bizerte bay and lagoon, located in the north of Tunisia (Southern Mediterranean Basin). Fresh fronds of the macrophyte *C. nodosa* were collected from 0.5-1m depth. Samples were harvested from four sites (Fig. 1): The Bizerte Bay (**BB**: 37°16'7"N 9°52'59"E), Menzel Abderrahmane (**L1**: 37°13'56"N 9°51'39"E), Menzel Jemil (**L2**: 37°13'24"N 9°56'0"E) and Menzel Bourguiba (**L3**: 37°10'30"N 9°47'18"E). Stations were sampled monthly between May 2015 and April 2016. Sampling was conducted during the first half of each month (between the 06th and the 15th) according to the weather conditions. Twenty grams of leaves were placed into a jar containing 250 ml of the *in situ* seawater (previously filtered through 180 µm). Leaves were then vigorously shaken to allow the dislodgement of epiphytic cells. Samples were then sieved (mesh size 180 µm), placed in brown glass bottles of 250 ml and fixed with neutralized formaldehyde (5%, final concentration). Temperature, salinity, pH and dissolved oxygen were measured at each station with a multiparameter HACH (HQ40d multi) sensor. NO₂⁻, NO₃⁻, NH₄⁺, PO₄³⁻ and Si(OH)₄ concentrations were analyzed with an automated channel Technicon autoanalyzer (Seal Analytical continuous flow AutoAnalyzer AA3).

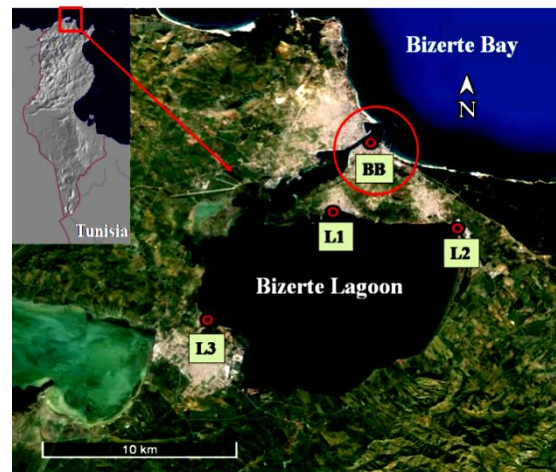


Fig. 1. Sampling sites in the Bay and Lagoon of Bizerte (North of Tunisia, Southern Mediterranean).

Identification of epiphytic dinoflagellate species was performed according to several keys and estimation of cell abundances was carried out using the Utermöhl method (1958). Cells were counted after settling for 24 hours in 25 ml sedimentation chambers. Dinoflagellate abundances on macrophyte leaves were expressed as the number of cells per 100 grams of fresh weight (cells.100g⁻¹ FW). Potential relationships between the abiotic environmental variables and the epibenthic dinoflagellate that reached the highest cell density were analyzed by Spearman's correlation coefficient.

Results and Discussion

Eight epibenthic dinoflagellate species belonging to the genera *Prorocentrum*, *Ostreopsis*, *Coolia* and *Amphidinium* were identified. For some *Amphidinium* species, the identifications were limited to the genera and these dinoflagellates were grouped under *Amphidinium* spp. Over our sampling period, the most common potentially toxic epibenthic dinoflagellates observed on *C. nodosa* fronds were *Ostreopsis* cf. *ovata*, *Prorocentrum lima*, *Coolia monotis* and *Amphidinium carterae*. The maximum cell density (194 688 cells.100g⁻¹ FW) was registered, in the Bizerte bay, for *O. cf. ovata* in October 2015 (Fig. 2).

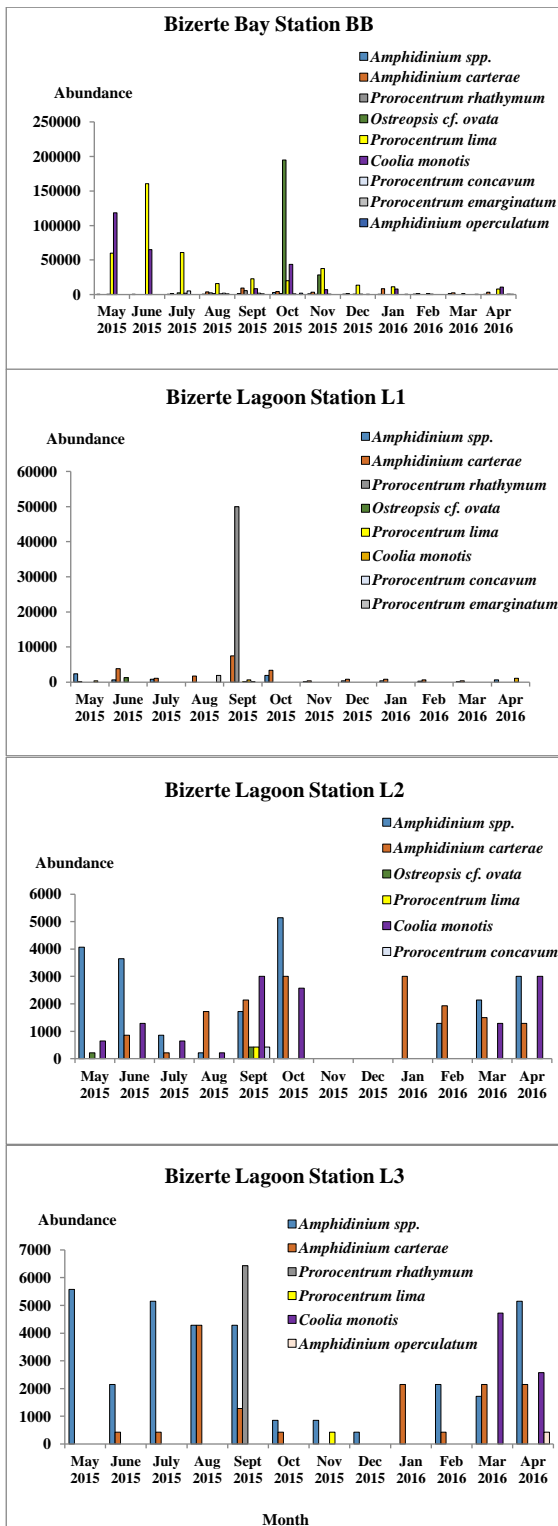


Fig. 2. Mean abundances of epibenthic dinoflagellates on *Cymodocea nodosa* fronds at the four sampling stations and for each month (expressed as cells.100g⁻¹ FW).

The maximum concentrations recorded for *O. cf. ovata* cells were in agreement with those reported by Moncer et al. (2017) in Tunisia (1.85 x 10³ cells.g⁻¹ FW on *Posidonia oceanica*), but much lower than those observed on other macroalgae from bloom areas of the northern Mediterranean:

2.8 x 10⁶ cells.g⁻¹ FW in Monaco (Cohu et al., 2011), 1.7 x 10⁶ cells.g⁻¹ FW (Totti et al., 2010) and 1.3 x 10⁶ cells.g⁻¹ FW (Accoroni et al., 2011) in the Adriatic Sea.

Spearman's analyses showed significant positive correlations between *O. cf. ovata* and temperature (Fig. 3). It has been reported that *O. cf. ovata* bloom events occurred when seawater temperatures were around 25 °C (Ciminiello et al., 2006; Ingarao and Pagliani, 2014). In the Bizerte Bay, *O. cf. ovata* maximum cell density was reached in October, when water temperature was about 24.6°C. Data from this study suggest that water warming may be considered among the major factors promoting *Ostreopsis* blooms and expansion in the Mediterranean basin. Results also showed negative correlations between *O. cf. ovata* and NO₂⁻ as well as NO₃⁻. Previous studies have reported negative (Ungaro et al., 2010; Carnicer et al., 2015) or non significant (Vila et al., 2001a; Parsons and Preskitt, 2007; Accoroni et al., 2011; Cohu et al., 2011; Dhib et al., 2013) correlations between epibenthic species and some/all nutrients. The way by which nutrient concentrations may affect epibenthic dinoflagellate bloom dynamics is still unclear.

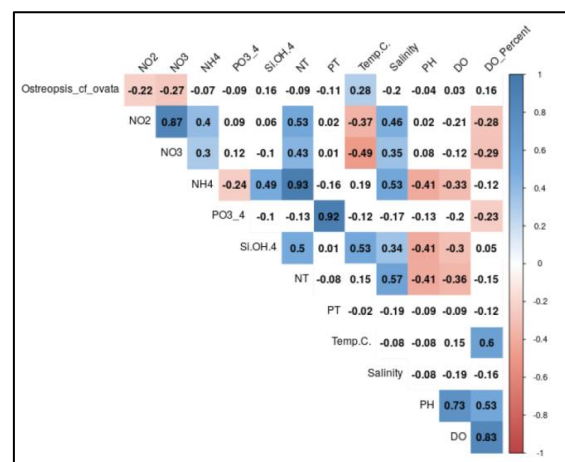


Fig. 3. Spearman's correlation coefficient (colored boxes = significant correlations: p < 0.05).

The diversity and the abundance of the epibenthic dinoflagellates varied according to the collection site. The highest epibenthic dinoflagellate abundances were recorded on *C. nodosa* fronds from the Bizerte Bay, while lower densities were associated with this magnoliophyte in the lagoon. Considering the current degradation of the environmental quality of the Bizerte Lagoon, we can hypothesize the low diversity and abundance of epibenthic dinoflagellates may be linked to an enhanced turbidity or to high pollutant levels. Toxic contaminants have been shown to inhibit epiphytic dinoflagellate development by altering

different physiological processes (Couet et al., 2018).

Macrophytes could release bioactive substances (allelochemicals) in order to reduce frond colonization by their competitors. Macrophyte-dinoflagellate allelopathic interactions may explain *in situ* observations and host preference trends. Several harmful and/or toxic species were detected on *C. nodosa* fronds in the Bizerte bay and lagoon. Thus, *C. nodosa* seems to offer a suitable substrate for the settlement of tychopelagic dinoflagellates (Turki, 2005; Mabrouk et al., 2014). This corroborated previous co-incubation laboratory experiments showing that *C. nodosa* has a relatively low negative allelopathic effect (Ben Gharbia et al., 2017).

Even if epibenthic dinoflagellate abundances in the Bizerte Bay and Lagoon were lower than those usually observed along Northern Mediterranean coasts, a regular monitoring of these epibenthic dinoflagellates and their biotoxins seems mandatory, in order to protect human health and marine ecosystems from the potential hazards.

Acknowledgements

This work was supported by the LAGUNOTOX project funded by Foundation TOTAL. H. Ben Gharbia thanks IRD and LMI COSYS-Med for funding her Ph.D. We would also like to thank the Tunisian National Institute of Agronomy for providing all necessary support for field trips, and Z. Hentati for her help during sampling.

References

Accoroni, S., Romagnoli, T., Colombo, F., Pennesi, C., Di Camillo, C.G., Marini, M., Battocchi, C., Ciminiello, P., Dell'Aversano, C., Dello Iacovo, E., Fattorusso, E., Tartaglione, L., Penna, A., Totti, C. (2011). *Mar. Pollut. Bull.* 62(11), 2512-2519.

Aligizaki, K., Nikolaidis, G. (2006). *Harmful Algae* 5, 717-730.

Ben Gharbia, H., Kéfi-Daly Yahia, O., Cecchi, P., Masseret, E., Amzil, Z., Herve, F., Rovillon, G., Nouri, H., M'Rabet, C., Couet, D., Zmerli Triki, H., Laabir, M. (2017). *PLoS ONE* 12(11), e0187963.

Blanfuné, A., Boudouresque, C.F., Gossel, H., Thibaut, T. (2015). *Environ. Sci. Pollut. R.* 22, 12332-12346.

Carnicer, O., Guallar, C., Andree, K.B., Diogène, J., Fernández-Tejedor, M. (2015). *Environ. Res.* 143, 89-99.

Ciminiello, P., Dell'Aversano, C., Fattorusso, E., Forino, M., Silvana Magno, G., Tartaglione, L., Grillo, C., Melchiorre, N. (2006). *Anal. Chem.* 78, 6153-6159.

Cohu, S., Thibaut, T., Mangialajo, L., Labat, J.P., Passafiume, O., Blanfuné, A., Simon, N., Cottalorda, J.M., Lemee, R. (2011). *Mar. Pollut. Bull.* 62, 2681-2691.

Couet, D., Pringault, O., Bancon-Montigny, C., Briant, N., Elbaz Poulichet, F., Delpoux, S., Kéfi-Daly Yahia, O., Ben Gharbia, H., M'Rabet, C., Hervé, F., Rovillon, G., Amzil, Z., Laabir, M. (2018). *Aquat. Toxicol.* 196, 154-167.

Dhib, A., Ben Brahim, M., Turki, S., Aleya, L. (2013). *Mar. Pollut. Bull.* 76, 116-127.

GEOHAB (2012). IOC of UNESCO and SCOR, Paris and Newark 64, 37-41.

Hoppenrath, M., Murray, S.A., Chomérat, N., Horiguchi, T. (2014). Schweizerbart'sche Verlagsbuchhandlung, Stuttgart, 276 pp.

Ingarao, C., Pagliani, T. (2014). *Harmful Algae News* 48, 2-3.

Mabrouk, L., Ben Brahim, M., Hamza, A., Mahfoudhi, M., Bradai, M.N. (2014). *J. Mar. Biol.* 2014, 1-10.

Moncer, M., Hamza, A., Feki-Sahnoun, W., Mabrouk, L., Bel Hassen, M. (2017). *Sci. Mar.* 81(4), 487-498.

Morton, S.L., Faust, M.A. (1997). *B. Mar. Sci.* 61 (3), 899-906.

Parsons, M.L., Preskitt, L.B. (2007). *Harmful Algae* 6, 658-669.

Totti, C., Accoroni, S., Cerino, F., Cucchiari, E., Romagnoli, T. (2010). *Harmful Algae* 9, 233-239.

Turki, S. (2005). *Cah. Biol. Mar.* 46, 29-34.

Utermöhl, H., 1958. *Mitteilungen internationalen Vereinigung für theoretische und angewandte Limnologie* 9, 1-38.

Ungaro, N., Pastorelli, A.M., Di Festa, T., Galise, I., Romano, C., Assennato, G., Blonda, V., Perrino, V. (2010). *Biol. Mar. Mediterr.* 17, 183-184.

Vila, M., Camp, J., Garcés, E., Masó, M., Delgado, M., 2001b. *J. Plankton Res.* 23, 497-514.

Vila, M., Garcés, E., Masó, M., 2001a. *Aquat. Microb. Ecol.* 26, 51-60.

Bloom of *Pyrodinium bahamense* in the Pacific coastal waters of Guatemala

Josué García-Pérez^{1*}, Leonel Carrillo-Ovalle¹, Maribelle Vargas-Montero², Elisa Blanda¹

¹Centro de Estudios del Mar y Acuicultura, Universidad de San Carlos de Guatemala

²Centro de Investigación en Estructuras Microscópicas, Universidad de Costa Rica.

* corresponding author's email: josgar85@gmail.com

Abstract

In Guatemala very little information exists on HAB events although, in recent decades, it is reported worldwide that there has been an increase in alarming mortality events of aquatic organisms and intoxications in humans, caused by toxins produced by microalgae. Therefore, a monthly monitoring program was established to investigate the presence of harmful algal blooms in the Pacific coastal waters of Guatemala, to prevent intoxication events. During the sampling from June to October 2011, high concentration of *Pyrodinium* genus was detected. To be able to confirm the toxic species, morphological analysis was carried out with photographs through scanning electron microscopy (SEM). The results confirmed a bloom of *P. bahamense* (Gonyaulacales) in co-occurrence with *Dinophysis caudata* and *Dinophysis acuminata*. According to the registry of National Laboratory of Health in Guatemala, the concentration of Saxitoxin during this bloom, ranged from 1,022 – 2,560 M.U / 100 g, which exceeded the regulatory limit for human consumption of molluscs.

Keywords: Saxitoxin, HABs, scanning electron microscopy, *Dinophysis caudata*, *Dinophysis acuminata*

Introduction

Harmful Algal Blooms (HABs) consists of a natural event where one or more species of microalgae, usually dinoflagellates, diatoms or cyanobacteria, increase in abundance, and produce chemicals in their normal metabolism (toxins), which affect other organisms in the aquatic environment and human health (Smayda, 1997; Herrera-Sepúlveda, Sierra-Beltran, & Hernández Saavedra, 2008; Band-Schmidt, Bustillos-Guzmán, López-Cortez, Nunez-Vasquez, & Hernández-Sandoval, 2011). Besides, the intensity and frequency of harmful algal blooms recently showed a rise and has been a growing concern for coastal waters worldwide: those blooms can cause an impact to human health in general and food security (Alkawri, Abker, Qutaei, Alhag, Qutaei, & Mahdy, 2016).

The *Pyrodinium* genus was previously described as a single species with two morphotypes or varieties, both proven to be toxic. *P. bahamense* was originally described from the Atlantic, specifically from New Providence Island (Bahamas) by Plate (1906). Thereafter, Bohm (1931) observed *P. bahamense* samples from the Arabian Gulf, while Wall and Dale (1969) indicated that *P. bahamense* was found generally confined to subtropical and tropical waters, and occurred throughout the Indo-Pacific and the tropical Atlantic. Later on,

Steidinger, Tester, & Taylo (1980) recognized the two varieties from this species: *bahamense* and *compressum*. However, recent studies have proven that there are no significant morphological differences between the two morphotypes (Mertens et al., 2015).

Pyrodinium bahamense is a very important dinoflagellate among Central America waters (Vargas-Montero & Freer, 2003), and it is a member of the paralytic shellfish toxin producers (PSP), which can cause one of the most well-known and problematic poisoning. Due to the ingestion of bivalve molluscs contaminated with PSP toxins, the most common of which are Saxitoxins, serious muscle paralysis can occur that might result into death in humans (Mertens et al., 2015).

Thus, the aim of this study was to document the bloom of *P. bahamense* and describe the bloom arisen off the Pacific coast of Guatemala.

Materials and Methods

Phytoplankton samples were collected at three sites: BTX Station, BRC Station, and BDR station, in the Pacific coastal waters of Guatemala (Fig. 1) from July to October 2011. Surface and vertical tows were made with a 25 cm diameter, 20 µm mesh plankton net. Samples were immediately fixed with acid Lugol solution. General

phytoplankton composition and abundance was determined using the Sedgewick-Rafter counting chamber, expressed as cell L⁻¹. Samples were analysed through light microscopy to identify specimens to the higher taxon, based on the available literature (Steidinger & Jagen, 1997). To identify the planktonic dinoflagellates, some samples were analysed at the University of Costa Rica, by using scanning electron microscopy (SEM). Shellfish toxicity was determined by standard mouse bioassay (AOAC International, 1995) performed by the National Laboratory of Health in Guatemala.

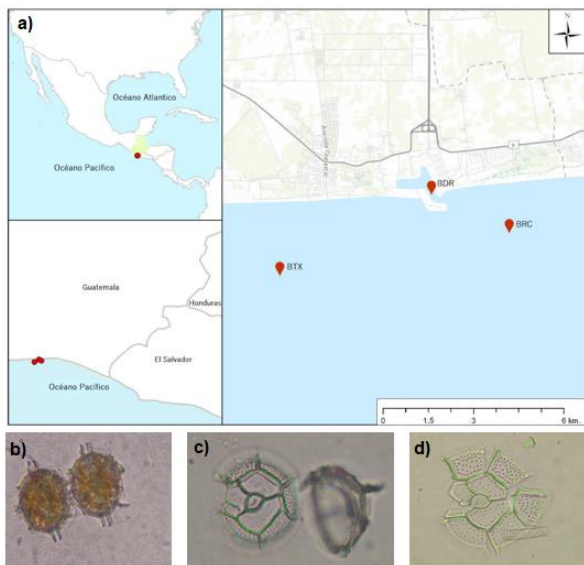


Fig. 1. Pyrodinium bloom, a) Sampling stations from the Guatemala Pacific coastal waters (b) Paired vegetative cells. (c) Empty cell showing apical horn and antapical horn (d) Close-up of the apical view plate.

Results and Discussion

This study shows that blooms of *P. bahamense* have a very wide distribution range and are able to proliferate along the Pacific, considering that it is one of the main species causing harmful algal blooms along the tropical Pacific.

From July to October 2011 a high concentration of chlorophyll *a* was observed and ranged from 4 to 35 mg/m³ according with AQUA MODIS. The bloom was observed from 1 m depth to the surface and was dominated by *P. bahamense*, which reached densities up to 4,000 cell L⁻¹ between July and September. However, in October 2011, the concentration of *P. bahamense* increased and a higher density was observed (>6,845 cell L⁻¹). According to the registry of National Laboratory of Health in Guatemala, during the *Pyrodinium* boom, only in July 2011 the concentrations of the Saxitoxin exceeded the regulatory limit for human consumption of molluscs. The concentration ranged from 1,022 – 2,560 M.U / 100 g.

P. bahamense has been described as producing paralytic toxins (Gedaria, Luckas, Reinhardt, & Aznza, 2007; Usup et al., 2012), and it has a highly toxic profile due to the STX and Neo-STX toxins (some of the toxins with highest toxicity), which forms 85 to 98% of the total composition (Gedaria et al., 2007). During the Bloom of *P. bahamense*, there were no human intoxications thanks to the rapid response of the public health authorities in Guatemala.

According with the SEM pictures analyses, some individuals of *P. bahamense* showed a semi-round shape, slightly compressed antero-posteriorly. This morphology occurred as individual cells, two-cell and four-cell chains. Cells size in average was $49.16 \pm 3.31 \mu\text{m}$ in length and $43.63 \pm 7.59 \mu\text{m}$ in height (n=10). The structure of the apical pore did not present any prolongation, however two spines with almost the same size were observed at the hypotheca (Fig. 2 A-C).

On the other hand, some vegetative cells of *P. bahamense* were found with a more rounded shape and showed apical and antapical horns (Figure 2 D-F). Moreover, those vegetative cells were larger, and their size was in average $48.71 \pm 2.22 \mu\text{m}$ in length and $56.85 \pm 7.67 \mu\text{m}$ in height (n = 5). The morphological differences among the vegetative cells of *P. bahamense* could be a response to environmental conditions and not genetically based, as described in Mertens et al., (2015).

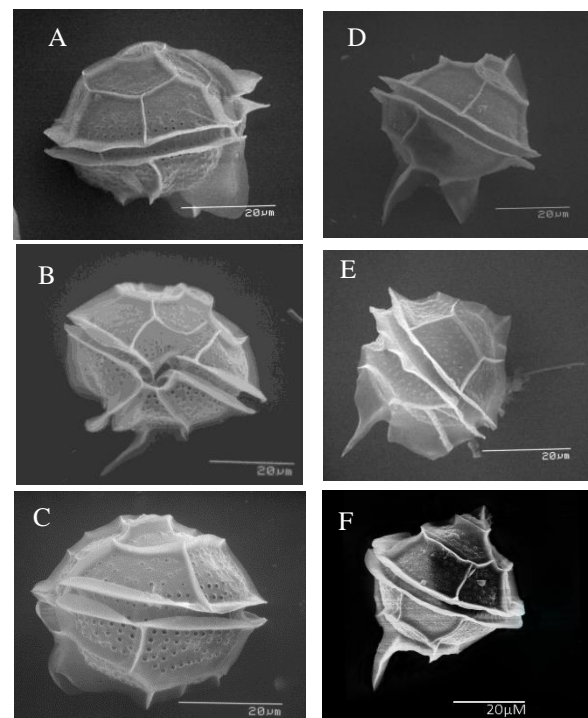


Fig. 2. Scanning electron micrographs of the vegetative cell of *P. bahamense*. A-C: semi-round shape, D-F: more rounded shape

The assemblage of the blooms in July-October 2011, was clearly dominated by *P. bahamense* which reached up to 90% of the total phytoplankton abundance. In general, the main dinoflagellates species abundance consisted of *P. bahamense*, *Dinophysis caudata* and *Dinophysis acuminata*.

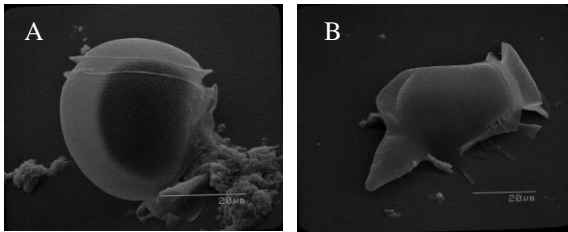


Fig. 3. Scanning electron micrographs of the vegetative cell of A) *Dinophysis acuminata* and B) *Dinophysis caudata*.

Because of the increasing events of phytoplankton blooms off the Pacific coast of Guatemala, in particular blooms of *Pyrodinium bahamense*, it is necessary to continue monitoring phytoplankton abundance and biodiversity in a monthly manner, for a better understanding of such events. Considering the risk that harmful algal blooms events can cause to human health, the monitoring will be extremely useful for the adequate management of marine-coastal resources in Guatemala.

References

Alkawri, A., Abker, M., Qutaei, E., Alhag, M., Qutaei, N., & Mahdy, S. (2016). Turkish Journal of Fisheries and Aquatic Sciences, 16: 275-282.

Band-Schmidt, C.J., Bustillos-Guzmán, J.J., López-Cortés, D.J., Nunez-Vasquez, E. & Hernández-Sandoval, F.E. (2011). Hidrobiologica, 21(3), 381-413.

Bohm, A. (1931). Peridineen aus dem Persischen Golf und dem Golf von Oman. Archiv für Protistenkunde 74:188–197.

Gedaria, A.I., Luckas, B., Reinhardt, K., & Azanza, R.V. (2007). Toxicon, 50, 518–529.

Herrera-Sepúlveda, A., Sierra-Beltrán, A. & Hernández-Saavedra, N. (2008). BioTecnología, 12(1), 23-40.

Mertens, K.N., Wolny, J., Carbonell-Moore, C., Bogus, K., Ellegaard, M., Limoges, A., De Vernal, A., Gurdebeke, P., Omura, T., Al-Muftah, A., Matsuoka, K. (2015). Harmful Algae, 41: 1-24.

Plate, L. (1906). *Pyrodinium bahamense* n.g., n. sp. die Leucht-Peridinee des "Feuersees" von Nassau, Bahamas. Archiv für Protistenkunde, 7, 411-442.

Smayda, T. (1997). Limnology and Oceanography, 42(5-II), 1137-1153.

Steidinger, K.A., (1979). Collection, enumeration and identification of free living marine dinoflagellates. In: Taylor, D.L., Seliger, H.H. (Eds.), Toxic Dinoflagellate Blooms. (pp. 435–442). New York: Elsevier.

Steidinger, K.A., Tester, L.S., & Taylor, F.J.R. (1980). Phycologia 19(4), 329–337.

Usup, G., Ahmad, A., Matsuoka, K., Lim, P. & Leaw, C. P. (2012). Harmful Algae, 14: 301 –312.

Vargas-Montero, M. & Freer, E. (2003). Co-occurrence of different morphotypes of *Pyrodinium bahamense* during an extensive bloom in the Gulf of Nicoya, Costa Rica. In: Villalba, A., Reguera, B., Romalde, J.L. & Beiras, R. (Eds.), Molluscan shellfish safety. (pp. 211–217). Vigo España, París Francia: Xunta de Galicia and IOC-UNESCO.

Wall, D. & Dale, B. (1969). Journal of Phycology, 5: 140-149.

***Pseudo-nitzschia* biogeography combining Real-Time PCR analysis and oceanographic models to investigate 13 years trends of ASP toxicity**

Angéline Lefran^{1&2}, Beatrix Siemering¹, Caroline Cusack¹, Dave Clarke¹, Joe Silke¹, Rafael Salas^{1*}

¹ Marine Institute, Oranmore, Ireland;

² Ifremer, LERN, Av. Général De Gaulle, 14520 Port-en-Bessin-Huppain, France;

* corresponding author's email: Rafael.Salas@marine.ie

Abstract

In situ, Harmful Algal Blooms (HAB) data revealed a strong variability in intensity and toxicity of *Pseudo-nitzschia* blooms between 2005-2017 in Killary Harbour and Bantry Bay, the most important production areas for rope grown mussels in Ireland. To study species successions and environmental interactions, a combination of different methods is used, including qPCR analysis, statistical analysis and a Lagrangian particle model. The biotoxin analyses from blue-mussels tissues and *Pseudo-nitzschia* spp. abundances results over a 13 years period suggest no relationship between ASP toxic episodes and major blooms in both Bantry Bay in spring (March-April) and in Killary Harbour, where toxic events occur in summer (May-July). In both cases, Real-Time PCR analysis shows that *Pseudo-nitzschia australis* is the species involved in these toxic events and is then succeeded by *P. pungens* in Bantry Bay. Although the causative organism *P. australis* is detected in Killary Harbour, Domoic Acid (causing ASP) concentrations in mussels did not rise above the EC regulatory closure limit (20 µg.g⁻¹). The particle tracking model shows a high level of variability in advective transport of cells within bays and along the coastline, suggesting that even small environmental changes in spring could have dramatic effects on bloom transport and development. A second *Pseudo-nitzschia* spp. bloom occurs in late summer-autumn in both Killary Harbour and Bantry Bay. These blooms did not result in shellfish toxicity over the period studied, indicating that another non-toxin producing species dominated the *Pseudo-nitzschia* spp. assemblage at this time. Comparison of the relative abundance of *Pseudo-nitzschia* spp. in water samples against other diatoms and dinoflagellates suggest that ASP toxic episodes are not explained by large monospecific blooms of these toxic species alone. In Bantry Bay, toxins can be detected when *Pseudo-nitzschia* spp. represent only 20-25% of the total microphytoplankton community abundance.

Keywords: Real-Time PCR, *Pseudo-nitzschia* spp., ASP, relative abundance

Introduction

In order to forecast events and prevent the consumption of contaminated shellfish, Ireland has had a national monitoring programme in place since the 1980s supervised by the Marine Institute. As part of this programme, a weekly HAB bulletin describing the current situation and immediate risk is freely available online (www.marine.ie/habs). Amongst other harmful algal bloom (HAB) species (*Dinophysis* sp., *Azadinium* sp. and *Alexandrium* sp.), the bulletin keeps track of the diatom *Pseudo-nitzschia* sp. which is known to produce Domoic Acid (DA) that causes Amnesic Shellfish Poisoning (ASP) syndrome. DA was first detected in Irish shellfish (scallops) in 1999 (James et al., 2005). The number of species in the genus is constantly increasing; from 37 identified species in 2012 (Lelong et al., 2012) to at least 48 species

currently reported in AlgaeBase (Guiry & Guiry, 2018). However, not all of the *Pseudo-nitzschia* sp. are toxic (Lelong et al., 2012). Cusack found six main species in offshore waters to the south of Ireland, with *P. pungens*, *P. fraudulenta* and *P. australis* the most frequently observed (Cusack, 2002). *Pseudo-nitzschia multiseriata* has been identified as a DA-producing species (Bates et al., 1998), and historically *P. australis* was responsible for ASP events in Scottish waters (Campbell et al., 2001), however the results are unclear for other species, as many produce DA at low concentrations worldwide (Cusack, 2002).

Like all diatoms, *Pseudo-nitzschia* sp. has a silica frustule. Characterised as a pennate diatom, this genus is naturally joined in colonies, making chains by overlapping cells ends (Horner, 2002). The

identification to the species level is difficult for routine light microscopy, therefore the species are recorded under two groups based on the cell width; *P. seriata* complex (>3µm) and *P. delicatissima* complex (<3µm) (Hasle & Syvertsen, 1997). This is why the Real-Time PCR (Polymerase Chain Reaction) assays is an invaluable methodology that can be used in monitoring programs to identify and discriminate this genus by targeting the DNA sequence of ribosomal sub-unit (LSU) (Andree et al., 2011; Fitzpatrick et al., 2010).

Ireland is characterised by two contrasting coastlines, the western Atlantic coastline and the eastern Irish Sea coastline. Most of the shellfish farms are situated on the western side of the country according to the national seafood agency Bord Iascaigh Mhara (BIM). Interestingly, the west coast was the most affected by toxic events in the past. *Mytilus edulis* is the best biological indicator for toxicity as it responds rapidly to any change in the phytoplankton composition (Bates et al., 1998). Hence, numerous closures of mussel production areas happened in 2005 and 2012 mostly in the south west sites of Ireland, where the toxins content was above 200µg.g⁻¹ in 2012 (Bantry Bay). During those periods, no closure was encountered in Killary Harbour, another important rope mussel area also on the west coast, 220 km north of Bantry. This work aims to examine differences between Killary and Bantry Bay which seem to be affected by the blooms of *Pseudo-nitzschia* spp. in distinct ways. Is the impact of the blooms on shellfish farms cell density dependant? Was there any significant succession among *Pseudo-nitzschia* species during the year 2017?

Materials and Methods

Sample background

Samples are sent to the Marine Institute from different shellfish and finfish farming sites across Ireland. Farmers collect water samples once a week or more in case of high toxicity risk. The samples are stored in 50mL labelled sample tubes. Lugol's Iodine is added soon after sampling. For the monitoring programme purpose the phytoplankton laboratory team takes 25 mL of every sample received and carries out an identification and quantification of the phytoplankton in the sample (Utermöhl, 1958). In parallel, the biotoxins within corresponding flesh samples of farmed mussels are quantified.

For this study, water samples that contain *Pseudo-nitzschia* cells were run on the qPCR. For 2017, a total of 81 samples from Killary and 87 samples

from Bantry were analysed to investigate the presence of six *Pseudo-nitzschia* species, namely *P. australis*, *P. delicatissima*, *P. fraudulenta*, *P. multiseriata*, *P. pungens* and *P. seriata*.

Real-Time Polymerase Chain Reaction (qPCR)

1) DNA extraction

25 mL of the samples were analysed by qPCR. Samples were centrifuged at 4,200 revolutions per minute (rpm) for 15 min to form a cell pellet where the supernatant was removed (approximately 23 mL) and discarded. The cell pellet was transferred to a 1.5 mL microtube and centrifuged for 5 min at 13,500 rpm. The supernatant was removed and discarded leaving approx. 0.2 mL of liquid and cells pellet. A double extraction process was used to disrupt the cells, a 5 cycles freeze-thaw (80°C) process with liquid nitrogen, followed by the addition of glass beads and a run of a bead mill mixer (Retsch) for 2 min at a frequency of 25 s⁻¹. DNA lysis and extraction were conducted with a modified protocol of the manufacturer's instructions using the DNeasy Plant Mini kit (QIAGEN). This kit binds extracted DNA to silica spin columns, which was then washed with buffers to remove inhibitory substances, resulting in a final eluted volume 100 µL of extracted DNA in buffer solution.

In addition to each batch of samples extracted, a known positive control (derived from spikes of mono-specific cell cultures for each species into sterile seawater) and a negative control (sterile seawater) were also extracted with the sample batch. Positive controls for *P. seriata* and *P. multiseriata* were unavailable for this investigation.

2) Master mixes preparations

The developed assays used Fluorescence Resonance Energy Transfer (FRET) hybridisation probes and forward and reverse primers which target the internal transcribed spacer 1 (ITS-1) region of rRNA gene (Clarke et al., 2019).

The Master mix was a solution of 10X LightCycler® FastStart DNA master hybridization probe mix (Roche), MgCl₂, Forward (25 µM) and Reverse Primers (25 µM), species specific FRET probes (2 µM) and molecular biology grade water adjusted to a final volume proportional to 18 µL per sample reaction.

3) Template preparation and run protocol

Using a 96 well plate, to each well, 18 µL of Master mix and 2 µL of an extracted sample / control were added. Each sample and control was run in duplicate in a separate well. The plates were sealed

with adhesive film, and centrifuged for 1 min at 1100 rpm.

Assays were run on real time PCR instruments (Roche LightCycler 480 Vr I and Vr II) with the following cycling parameters; 10 min at 95°C; 40 cycles of 10 s at 95°C, 15 s at 50°C and 10 s at 72°C; followed by a continuous melt curve analysis from 40°C to 80°C with a ramp rate of 1°C.s⁻¹.

4) Analysis process

To discriminate between each species present in a sample, a specific melt peak temperature (Tm) was obtained for each species; *P. multiseriata* 66°C, *P. seriata* 56°C, *P. australis* 62°C, *P. fraudulenta* 55°C, *P. delicatissima* 58°C and *P. pungens* 60°C. The assay for *P. pungens* was also able to detect *P. australis* (Tm 49°C), *P. fraudulenta* (Tm 42°C) and *P. multiseriata* (Tm 53°C).

The Tm for the peaks observed for the samples were checked with the references to attest the presence of the targeted species. Then, to show the presence/absence of each species per date, a table on which a colour was associated with a species and a square corresponded to a place and a date was made. Each square was divided and coloured by the number of species that were found for the considered time and place but did not give any quantitative proportion.

Results and Discussion

First, a look at the time series highlighted three facts (Fig.1); (A) In both bays, high *Pseudo-nitzschia seriata* complex densities were not correlated with high DA concentrations. (B) The six species-specific probes used in the qPCR analyses could not identify all *Pseudo-nitzschia* sp. present in the autumn blooms. (C) There were four significant ASP events in Bantry Bay over a period of 13 years (DA > 50 µg.g⁻¹) in April 2005, 2010, 2011 and 2012. The event in 2012 reached a DA level record of more than 200 µg DA.g⁻¹. During those ASP events, the relative abundance of *Pseudo-nitzschia seriata* complex was not at its highest; only reaching 30% of the microphytoplankton community (Fig.2). Whereas in Killary Harbour the maximum cells density was two times lower than reported in Bantry Bay and the DA level never exceeded the sanitary level. This could be due to the complex physical dynamic of this narrow shape area and the nutrient availability that is known to influence this genus and trigger DA production when limited (Parsons & Dortch, 2002; Siemering et al., 2016).

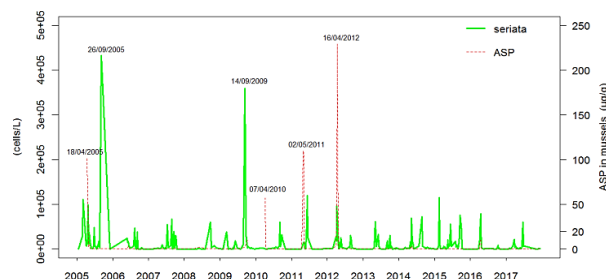


Fig.1. Bantry Bay historic records on *P. seriata* complex cell concentrations and associated toxicity through DA concentration found in mussels tissue.

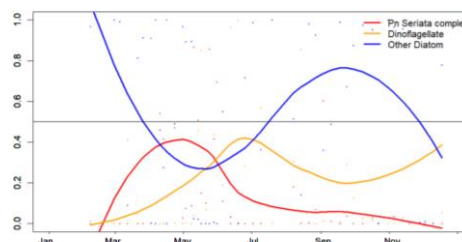


Fig.2. Bantry Bay Inner relative abundance of *Pseudo-nitzschia seriata* complex, Dinoflagellates and other diatoms for the year 2012.

Secondly, in Killary Harbour, detection at the outer part of the fjord comprised of a mix of *Pseudo-nitzschia* species occurred from the end of March (Fig.3). *Pseudo-nitzschia fraudulenta* was only seen during April and May at the outer part and the community changed in June when species detected throughout the fjord, from outer to inner sites, were predominated by *P. pungens* and *P. australis*.

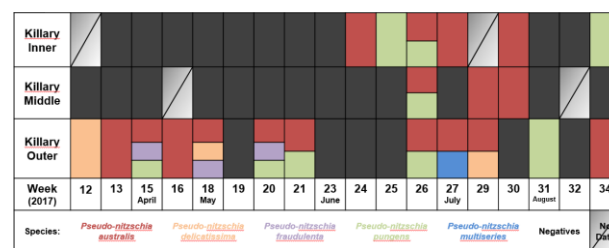


Fig.3. Compilation of Killary Harbour 2017's PCR results. Crossed cases indicate the absence of sample; dark boxes indicate negatives results.

Bantry Bay showed two distinct bloom patterns (Fig.4). One was characterised by *P. australis* presence from February to April followed by another period marked by *P. pungens* presence (April to July). *Pseudo-nitzschia delicatissima* was only observed during the first period, *P. fraudulenta* was present during this period as well. North and South Chapel sites (inner parts of the Bay) had a diverse *Pseudo-nitzschia* community make-up. The ASP events were recorded during

week 13, at the beginning of the decline of *P. australis* in favour of *P. pungens*, confirming the identity of the species associated with the toxicity in Bantry to be *P. australis*.

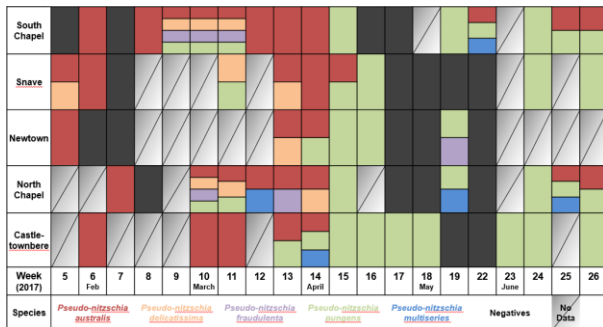


Fig. 4. Compilation of Bantry Bay 2017's PCR results. Note that toxins were spotted in week 13.

Lastly, the transport of HABs into the Bay was driven by changes in the direction and speed of local winds. During blooms, *Pseudo-nitzschia* sp. cells were observed in the inner parts of the bay first before reaching outer sites (according to particle tracking models of past events). This was likely to be associated with the advection of *Pseudo-nitzschia* blooms into Bantry Bay during upwelling events when colder bottom water enters the Bay and surface water exits. Upwelling events entering the Bay, may also have led to nutrient delivery from offshore shelf waters, triggering the blooms of *Pseudo-nitzschia*.

Acknowledgements

Thank you to the management and staff of the Marine Environment and Food Safety unit of the Marine Institute where this work was hosted in 2018. This work was one of the outputs of a student during her master's degree from the European Marine Institute University (IUEM, UBO, France) thanks to the DEI grant support.

References

Andree, K. B., Fernández-Tejedor, M., Elandaloussi, L. M., Quijano-Scheggia, S., Sampedro, N., Garcés, E., et al. (2011). Applied and Environmental Microbiology, 77(5), 1651–1659.

Bates, S. S., Garrison, D. L., & Horner, R. A. (1998). NATO ASI Series G Ecological Sciences, 41, 267–292.

Campbell, D. A., Kelly, M. S., Busman, M., Bolch, C. J. S., Wiggins, E., Moeller, P. D. R., et al. (2001). National Shellfisheries Association.

Clarke, D., Salas, R., Hynes, P., McCarthy, A., Walsh, D., & Silke, J. (2019). Proceeding of the Eighteenth International Conference on Harmful Algae, Nantes, France. In prep.

Cusack, C. K. (2002). National University of Ireland, Galway.

Fitzpatrick, E., Caron, D. A., & Schnetzer, A. (2010). Marine Biology, 157(5), 1161–1169.

Guiry, M. D., & Guiry, G. (2018). AlgaeBase. www.algaebase.org

Hasle, G. R., & Syvertsen, E. E. (1997). Academic Press, San Diego, CA (p. p 5-385). C.R. Thomas.

Horner, R. A. (2002). BioPress Ltd. Bristol UK 195pp

James, K. J., Gillman, M., Amandi, M. F., López-Rivera, A., Puente, P. F., Lehane, M., et al. (2005). Toxicon, 46(8), 852–858.

Lelong, A., Hégaret, H., Soudant, P., & Bates, S. S. (2012). Phycologia, 51(2), 168–216.

Parsons, M. L., & Dortch, Q. (2002). Limnology and Oceanography, 47(2), 551–558.

Siemering, B., Bresnan, E., Painter, S. C., Daniels, C. J., Inall, M., & Davidson, K. (2016). PloS One, 11(10), e0164482.

Utermöhl, H. (1958). Internationale Vereinigung Für Theoretische Und Angewandte Limnologie: Mitteilungen, 9(1), 1–38.

An exceptional summer bloom of *Dinophysis acuta* in a Chilean fjord

Patricio A. Díaz^{1,2*}, Iván Pérez-Santos^{1,3}, Angela Baldrich⁴, Gonzalo Álvarez⁵, Francisco Rodríguez⁶, Paulina Montero^{3,7}, Gabriela Igor^{3,7}, Giovanni Daneri^{3,7}, Miriam Seguel⁸, Leonardo Guzmán⁹, Gemita Pizarro¹⁰, Luis Norambuena⁹, Jorge I. Mardones⁹, Pamela Carbonell⁹, Beatriz Reguera⁶

¹ Centro i~mar, Universidad de Los Lagos, Casilla 557, Puerto Montt, Chile

²CeBiB, Universidad de Los Lagos, Casilla 557, Puerto Montt, Chile

³ Centro de Investigación Oceanográfica COPAS Sur-Austral, Universidad de Concepción, Chile

⁴ Programa de Doctorado en Ciencias mención Conservación y Manejo de Recursos Naturales, Universidad de Los Lagos, Puerto Montt, Chile

⁵ Facultad de Ciencias del Mar, Depto. de Acuicultura, Universidad Católica del Norte, Coquimbo, Chile

⁶ Centro Oceanográfico de Vigo, Instituto Español de Oceanografía (IEO), Vigo, España

⁷ Centro de Investigaciones en Ecosistemas de la Patagonia (CIEP), Coyhaique, Chile

⁸Centro Regional de Análisis de Recursos y Medio Ambiente (CERAM), Universidad Austral de Chile, Puerto Montt, Chile

⁹ Centro de Estudios de Algas Nocivas (CREAN), Instituto de Fomento Pesquero, Puerto Montt, Chile

¹⁰ Centro de Estudios de Algas Nocivas (CREAN), Instituto de Fomento Pesquero, Enrique Abello 0552, Punta Arenas, Chile

*corresponding author's email: patricio.diaz@ulagos.cl

Abstract

Diarrhetic shellfish poisoning (DSP) toxins and pectenotoxins (PTX) produced by endemic species of the genus *Dinophysis*, mainly *D. acuta* and *D. acuminata*, pose a big threat to public health, artisanal fisheries and the mussel industry in Southern Chile. Nevertheless, little is known about the environmental factors controlling these outbreaks in the Chilean Patagonian fjords and channels. During summer-autumn (January–April) 2018, several cruises were carried out in Puyuhuapi fjord (44.65°S–72.79°W) to characterize fjord conditions associated with bloom development and fine-scale distribution of *Dinophysis* populations. Here we present results from the survey carried out on February 16, 2018 along nine sampling stations in a 25-km long transect. This sampling coincided with the onset of an exceptional bloom of *D. acuta* in the Patagonian fjords. Vertical profiles of density (kg m^{-3}), temperature ($^{\circ}\text{C}$), in vivo fluorescence ($\mu\text{g equiv. Chl a L}^{-1}$) and dissolved oxygen (mL L^{-1}) (CTD casts) as well as water samples at 2 m intervals from surface to 20 m depth (Niskin bottles) for microphytoplankton analyses were collected at each station. Vertical hauls (0–20m) with a 20- μm mesh net were collected for lipophilic toxin analyses. Our results showed a strong thermohaline stratification along the fjord transect. *Dinophysis acuta* was present as a sub surface thin layer with a cell maximum of 118,000 cells L^{-1} . Due to the overwhelming dominance of *D. acuta*, the bloom gave a strong fluorescence signal coinciding with the fluorescence maximum (rather unusual with the typical low biomass blooms of *Dinophysis*) at 6 m depth, within the layer of maximal water column stability. Further, *D. acuta* seemed to avoid the low salinity values from Puyuhuapi fjord surface waters, because no cells were detected above the 16 psu isohaline at 2 m depth. Toxins analysis of the haul samples showed the presence of OA, dinophysistoxin-1 (DTX1) and PTX2 in addition to yessotoxins (YTX) associated with the co-occurrence of *Protoceratium reticulatum*. This exceptional summer bloom of *D. acuta* observed in Puyuhuapi fjord, represents one of the highest density blooms ever reported worldwide for this species and a record for Chile. The identification and parameterization of the key factors that triggered this intense bloom are discussed here.

Keywords: *Dinophysis acuta*, exceptional blooms, lipophilic toxins, Chilean fjords

Introduction

Harmful Algal Blooms (HAB) in Chile have followed the global trend of “apparent” increase of toxic events (Hallegraeff, 1993; Hallegraeff, 2010),

becoming the main threat to public health and the fishing industry in the Patagonian fjords system (Díaz et al., 2019). Diarrhetic shellfish poisoning

(DSP) toxins and pectenotoxins (PTX) produced by endemic species of the genus *Dinophysis* (Reguera et al. 2012; Reguera et al. 2014), mainly *D. acuta* and *D. acuminata*, pose a big threat to public health, artisanal fisheries and the mussel industry in Southern Chile, that include the area (Los Lagos region) where more than 95% of the national production of mytilids ($29 \times 10^4 \text{ t y}^{-1}$) takes place (Sernapesca, 2016).

Microscale physical-biological interactions—both in time and space—in fjords and semi-enclosed systems are modulated by processes such as turbulence, tidal cycles and circadian rhythms (GEOHAB, 2010). In the case of *Dinophysis* species, microscale variability of their vertical distribution hinders their detection and/or underestimates their density (Escalera et al., 2012). This variability can be exacerbated in highly heterogeneous systems, as it is the case with the Patagonian fjords, where multiple niches promote development or aggregation of different species (Díaz et al., 2011; Alves de Souza et al., 2014). In this context, a good understanding of this short-term variability is a key aspect for the development of operational models and improved risk assessment of shellfish poisoning and other hazardous events in Southern Chile. This paper describes the spatial distribution of *D. acuta* along nine sampling stations in a 25-km long Chilean fjord transect in February 2018, which coincided with the onset of an exceptional bloom of this species in the Patagonian fjords (Fig. 1).

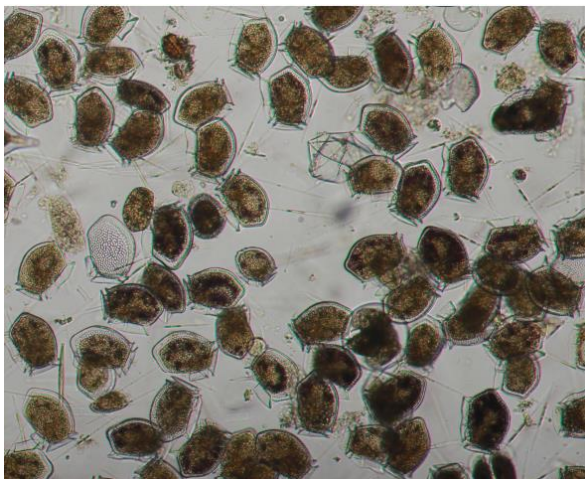


Fig. 1. Micrographs of *Dinophysis acuta* fixed in Lugol's solution collected at station 1 using a 20- μm mesh net in the Puyuhuapi fjord, during a bloom in February 16, 2018.

Materials and Methods

The survey was carried out on board R.V. *Queen* during one-day cruise along a Puyuhuapi fjord transect (25-km), which took place on February 16, 2018 (Fig. 2).

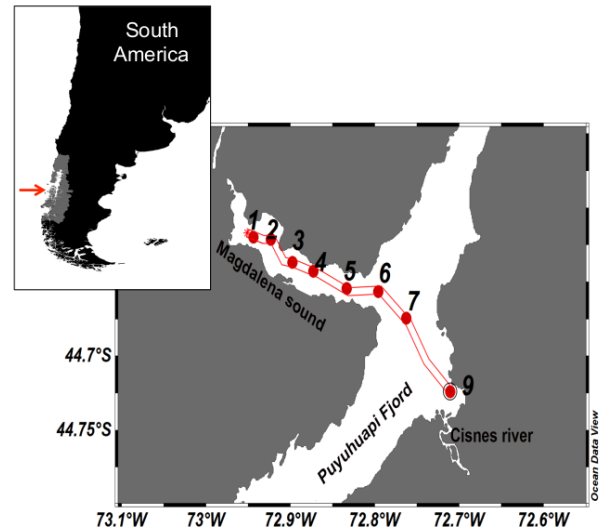


Fig. 2. The study area in Puyuhuapi fjord (Aysén region, Southern Chile) and sampling stations in a 25-km long transect (Magdalena Sound to the mouth of the Cisnes river) visited during the cruise on February 16, 2018.

Vertical profiles of temperature ($^{\circ}\text{C}$), salinity, in vivo fluorescence ($\mu\text{g equiv. chl } a \text{ L}^{-1}$) and dissolved oxygen (ml l^{-1}) (CTD casts) as well as water samples at 2m intervals from surface to 20 m depth (Niskin bottles) for microphytoplankton analyses were collected at each station. Vertical hauls (0-20m) with a 20- μm mesh net were collected for lipophilic toxin analyses.

Results and Discussion

CTD profiles of temperature and salinity obtained along the Magdalena sound and across the Puyuhuapi Fjord showed a fjord characteristic two layer structure: a top layer (0-10 m) of estuarine warm ($12.6^{\circ}\text{C} - 17.9^{\circ}\text{C}$) brackish (11.4 – 29.7 psu) water and a bottom layer (10-50 m) of saltier water (28.0 – 32.7 psu) with a temperature range from 14.2°C at 11 m to 10.5°C at 50 m (Figs. 3a, b). Less saline water was also observed in the first 2-m layer (salinity range, 11.4-18.5), where estuarine water dominated.

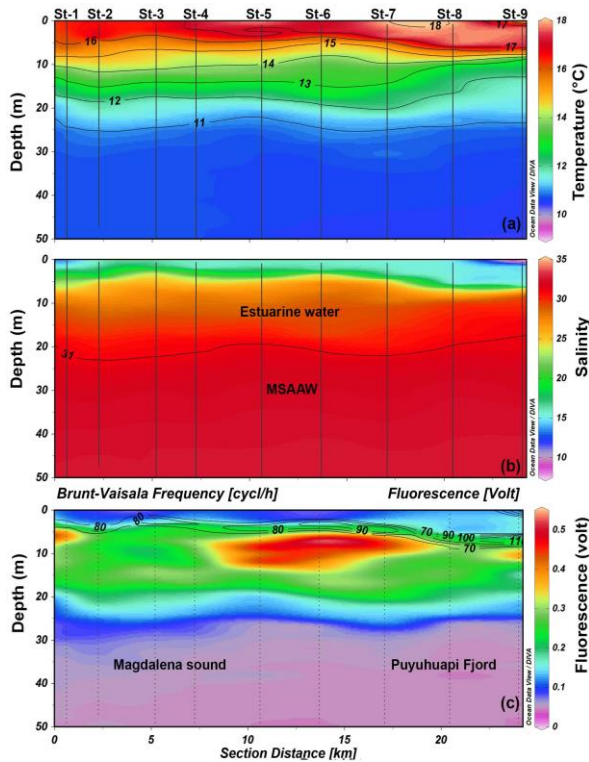


Fig. 3. Vertical distribution of (top) temperature; (middle) salinity and (bottom) fluorescence (counter color) with the Brunt-Vaisala frequency (black lines) along nine sampling stations in a 25-km long transect during the cruise on February 16, 2018.

Minimum values of salinity were registered at station 9 (11.4 psu at 1 m) due to the influence of the Cisnes river discharge (Fig. 3b). Modified Subantarctic Water (MSAAW), according to the description from Schneider et al., (2014) was observed from 20-50 m. This water mass results from the mixing of the estuarine water and the Subantarctic water mass (SAAW) (Sievers and Silva, 2008).

A fluorescence layer, much stronger than those reported by Schneider et al., (2014); extended to the bottom of the pycnocline (> 20m), with an isolated maximum at station 1. An extensive layer with strong fluorescing values was observed in the confluence area of the Magdalena sound and Puyuhuapi Fjord, between station 5 and station 7. This maximum extended 14 km from ~5 to 15 m depth (Fig. 3c).

Maximal *D. acuta* cell densities (118,000 cells L⁻¹) were found at 6m (15.88 °C, 23.36 psu) on station 1 (inner fjord), associated with a vertical thermohaline gradient of 0.2°C m⁻¹ and 1.4 psu m⁻¹ on the top 10 m. Due to the overwhelming dominance of *D. acuta*, the bloom gave a strong fluorescence signal at 6 m coinciding with the

fluorescence maximum located within the layer of maximal water column stability (Fig. 4). This is a rather unusual observation with the more common low biomass blooms of *Dinophysis*. *D. acuta* cells seemed to avoid the low salinity values from Puyuhuapi fjord surface waters, because no cells were detected above the 18 psu isohaline at 2m depth (Fig. 5).

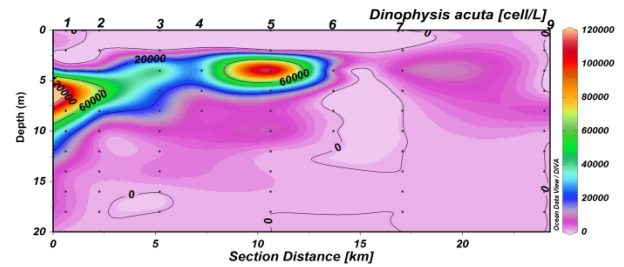


Fig. 4. Vertical distribution of *Dinophysis acuta* (cells L⁻¹) along nine sampling stations in a 25-km transect during the cruise on February 16, 2018.

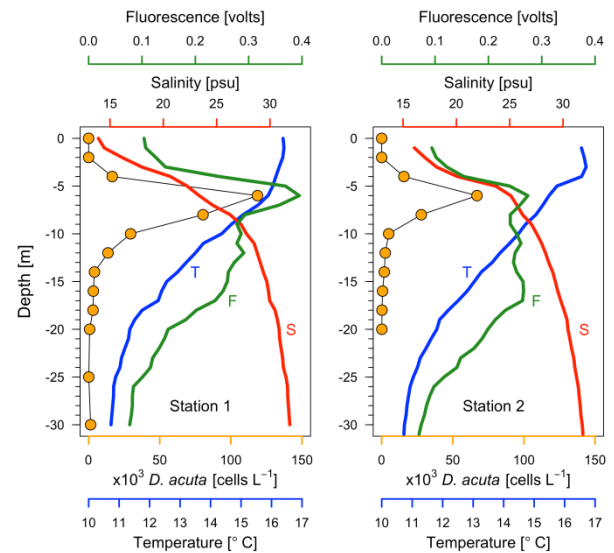


Fig. 5. Vertical profiles of salinity, temperature, chlorophyll-fluorescence and *Dinophysis acuta* cell densities during the cruise on 16 February 2018 at stations 1 and 2.

Toxins analysis of the haul samples showed the presence of OA, dinophysistoxin-1 (DTX1) and PTX2 in addition to yessotoxins (YTX) associated with the co-occurrence of *Protoceratium reticulatum*.

Conclusions

Strong thermohaline stratification during late austral summer (16 February) 2018 in the Patagonian fjord system created the conditions for


an exceptional summer bloom of *Dinophysis acuta*. The bloom formed a sub-surface thin layer (cell maximum of 118,000 cells L⁻¹) located in the layer of maximal static stability. This exceptional summer bloom of *D. acuta* observed in Puyuhuapi fjord, is one of the highest density blooms ever reported worldwide for this species and a record for Chile.

Acknowledgements

We thank Manuel Díaz Vidal for technical assistance during the cruise. This study was funded by project Fondecyt 11170682 “Physical-biological interactions in populations of lipophilic toxic-producers from Southern Chile” from the national research programme of the National Commission for Scientific and Technological Research (CONICYT), Chile, and supported by project REDES170101 from the International Cooperation Programme. Iván Pérez-Santos was funded by COPAS Sur-Austral AFB170006.

References

- Alves de Souza, C., Varela, D., Contreras, C., de la Iglesia, P., Fernández, P., Hipp, B., Hernández, C., Riobó, P., Reguera, B., Franco, J.M., Diogene, J., García, C., Lagos, N., 2014. Deep Sea Res. II 101, 152-162.
- Díaz, P., Molinet, C., Cáceres, M., Valle-Levinson, A., 2011. Harmful Algae 10(2), 155-164.
- Díaz, P.A., Álvarez, A., Varela, D., Pérez-Santos, I., Díaz, M., Molinet, C., Seguel, M., Aguilera-Belmonte, A., Guzmán, L., Uribe, E., Rengel, J., Hernández, C., Segura, C., Figueroa, R.I., 2019. Perspectives in Phycology, DOI: 10.1127/pip/2019/0081.
- Escalera, L., Pazos, Y., Doval, M.D., Reguera, B., 2012. Mar. Pollut. Bull. 64, 106-113.
- GEOHAB, 2010. Global Ecology and Oceanography of Harmful Algal Blooms, GEOHAB Core Research Project: HABs in Fjords and Coastal Embayments. A. Cembella, L. Guzmán, S. Roy, J. Diogene (Eds.), IOC and SCOR, Paris, France and Newark, Delaware USA, 57 pp.
- Hallegraeff, G.M., 2010. J. Phycol. 46(2), 220-235.
- Hallegraeff, G.M., 1993. Phycologia 32, 79-99.
- Reguera B, Velo-Suárez L, Raine R, Park M (2012). Harmful Algae 14:87-106.
- Reguera, B., Riobó, P., Rodríguez, F., Díaz, P.A., Pizarro, G., Paz, B., Franco, J.M., Blanco, J., 2014. Mar. Drugs 12(1), 394-461.
- Sernapesca, 2016. Anuario Estadístico de Pesca. Servicio Nacional de Pesca, Valparaíso.
- Sievers, H., Silva, N., 2008. Water Masses and Circulation in Austral Chilean Channels and Fjords, Progress in the Oceanographic Knowledge of Chilean Interior Waters, from Puerto Montt to Cape Horn, pp. 53-58.
- Schneider, W.; Pérez-Santos, I.; Ross, L.; Bravo, L.; Seguel, R.; Hernández, F., 2014.. *Prog Oceanogr.*, 128, 8-18.



Eco-physiology & cellular biology of harmful algae and cyanobacteria

Diversity and distribution of Harmful Algal Bloom (HAB) species in Coastal Waters of Ghana

Denutsui Dzifa^{1,2}, Marina Cabrini⁴, Adotey K. Dennis^{1,2}, Gyingiri Achel³, Kuranchie-Mensah H^{1,2}, Palm Linda^{1,2}, Beran Alfred⁴, Serfor-Armah Yaw^{*1,2}

¹School of Nuclear and Allied Sciences, University of Ghana, P. O. Box AE 1, Atomic, Ghana

²Nuclear Chemistry and Environmental Research Centre, Ghana Atomic Energy Commission, P. O. Box LG 80, Legon-Accra, Ghana

³Radiological and Medical Science Research Institute, Ghana Atomic Energy Commission, P. O. Box LG 80, Legon-Accra, Ghana

⁴Section of Physical, Chemical and Biological Oceanography, Institute of National Oceanography and Experimental Geophysics, Trieste, Italy

*Corresponding author's email: yawserfor@yahoo.com

Abstract

This study assessed the distribution of harmful phytoplankton along the coast of Ghana. The monitoring study so far has identified eleven potentially harmful species which are mostly toxin-producing thecate dinoflagellates. Some of which are *Lingulodinium polyedra*, *Gonyaulax spinifera*, *Dinophysis caudata*, *Dinophysis ovum* and species of *Alexandrium*. There were seasonal variations observed for both diversity and density of HABs species. A high diversity of species with low cell densities was observed during the rainy season whereas during the dry season, high cell densities with few diverse species were observed. *Lingulodinium polyedra*, with a cell maxima of 5.0×10^4 cells/L, was observed in December 2016 and January 2017 followed by *Gonyaulax spinifera* (3.0×10^4 cells/L) and *Dinophysis caudata* (8.2×10^3 cells/L). This preliminary information indicates that there is a risk for harmful algal bloom events to occur in the coasts of Ghana. The high densities in December may have been caused by high temperatures, salinity, minor upwelling and tidal water accumulation along the shore.

Keywords: Dinoflagellates, harmful algae, Ghana, seafood safety

Introduction

Studies of harmful algae have been ongoing in different parts of the world since the mid-20th century and proved that harmful algal blooms (HABs) are a worldwide phenomenon (Wells et al., 2015). The Ghanaian coastal waters are not exempted from this global challenge, but information on harmful algal blooms in West Africa, particularly Ghana, is very rare. Changes in physical-chemical parameters of the seawater may distress sensitive marine organisms which include microalgae. This phenomenon involves two different aspects, one being the occurrence and the increased frequency of novel phytoplankton blooms and the second being the spreading of toxic species to new geographic areas (García-Portela et al., 2016; Tamale et al., 2019). In the phytoplankton taxonomic knowledge, many toxic species belong to the dinoflagellate group. Toxins from certain dinoflagellate or diatom species accumulate in fish and/or shellfish tissues and become the main source of exposure to seabirds,

sea mammals and humans (Giussani et al., 2016). It is important to note that shellfish exploitations and fisheries are significant components of Ghana's economy (Lazar, 2017) and admittedly, this sector which affords employment to a sizable number of the Ghanaian population has currently seen an increased due to increase demand for seafood products. Shellfish and fish, which are well appreciated and highly priced as a result of their essential sources of protein for the Ghanaian population, have been suspected to accumulate algal toxins, a fact which may subsequently cause poisoning within human consumers. It is therefore significant to study the associated health and economic risks of HABs in Ghana's waters, as well as ascertain natural seafood safety through frequent seafood monitoring and assessment.

This study therefore sought to assess the distribution of harmful phytoplankton species along the coast of Ghana.

Materials and Methods

Study Area



Fig. 1. Map of study area

The area considered in this study is in the Gulf of Guinea (Atlantic sea). Samples were taken from a total of four locations from Tema (5.3088°N, 0.00318° E) to Gomoa Nyanyanor (5.5240°N, 0.2939° W).

Sample Collection

Ghana has two major climatic seasons, the rainy (April-August) and dry (November-February) seasons. During these seasons there is an upwelling in the rainy and a minor or non-upwelling during the dry (Anang, 1979); considering this, water samples were collected monthly with Niskin bottles at a depth of 5m to evaluate the physico-chemical parameters and phytoplankton abundance. Phytoplankton ring nets with mesh size of about 20 μ m were also deployed into the sea and hauled to collect samples at the cod-end and fixed with Ca(HCO₃)²⁻ buffered formaldehyde. Variable volumes of seawater (25-50 mL), depending on cell densities were allowed to settle for at least 48 hours for specie identification. Water and net sample results were reported in this paper. Toxic microalgae species composition was estimated on samples by the Utermöhl's method (1958), using an inverted microscope and a light microscope (Leica DM 1000 LED) equipped with phase contrast at 400 final magnifications. All microscopically identified phytoplankton taxa were recorded and photographed using high quality digital camera (Leica MC 120 HD) and the taxonomic reference list of toxic microalgae (Moestrup et al., 2009).

Results and Discussion

Prevailing conditions during the dry season included high surface temperature (> 25 °C) and salinity < 35 psu. In the rainy season, surface temperature was below 25°C and salinity > 35 psu.

According to the present study, both salinity and temperature showed a stronger influence on temporal variations than spatial.

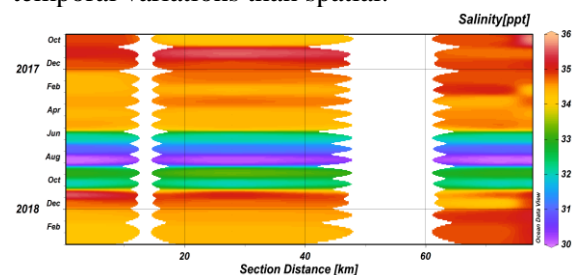


Fig. 2. Salinity (psu) at four sites during the sampling season.

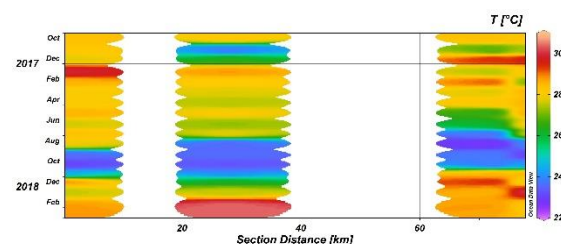


Fig. 3. Temperature (°C) at four sites during the sampling season.

From the results, it was observed in the dry season; a non-upwelling period (November–February) that, when water temperatures are high, the same trend holds for salinity, an observation conforming to Dhib et al., 2013 in the northern part of the Gulf Tunis.

In the monitoring study, eleven potentially harmful species most of which are dinoflagellates were identified from the sampling areas. One of the potentially toxic Dinophysials identified in all sampling areas was *Dinophysis caudata*. *Dinophysis* species are known to be responsible for diarrhetic shellfish poisoning (DSP) and *D. caudata* gave highest density (4510 cells/L) in Gomoa Nyanyanor site, an indication of its abundance in that area.

Species of *Prorocentrum gracile* and *Prorocentrum micans* showed maximum cell densities of 810 cells/L and 700 cells/L respectively in seawater samples. Both do not produce toxins but are examples of high biomass HAB species which may cause fish kills or other harmful events through secondary effects of intensive blooms (Larsen and Nguyen, 2004).

Abundance of HAB species in seawater samples [Cells/L]								
Sampling Site/ HAB Species	Tema		Light-House		Tsokome		Gomoa Nya	
	Min	Max	Min	Max	Min	Max	Min	Max
<i>Alx. spp</i>	0	400	0	0	0	420	0	380
<i>T. Furca</i>	35	480	0	180	35	480	38	480
<i>T.muelleri</i>	0	300	0	80	0	0	0	0
<i>D. caudata</i>	20	720	0	0	0	620	10	560
<i>D. Ovum</i>	0	0	0	0	0	480	0	1100
<i>G.spinefera</i>	120	1400	0	0	100	900	100	1200
<i>L.polyedrum</i>	40	2400	0	230	0	2700	60	6200
<i>N. scintillans</i>	0	300	0	0	0	300	0	160
<i>P.gracile</i>	0	0	0	120	20	620	40	780
<i>P.micans</i>	84	560	0	0	100	700	34	620
<i>S.trochoidea</i>	0	300	0	40	0	420	0	460

Triplos furca and *Triplos muelleri* which recorded maximum densities of 480 cells/L and 280 cells/L respectively in seawater are also planktonic species with the potential to generate very high biomass and to dominate the phytoplankton community for extended periods.

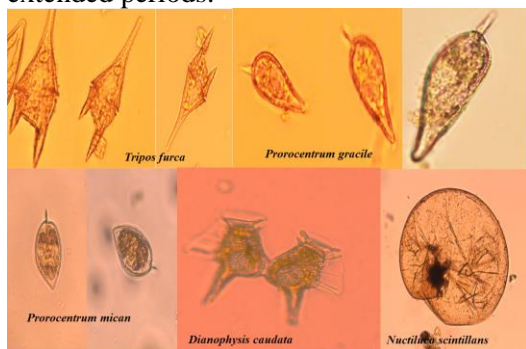


Fig. 4. Images of potentially harmful marine algal species from Ghana.

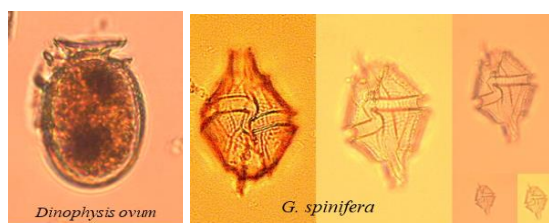


Fig. 5: *Dinophysis* (cf ovum) and *Gonyaulax spinifera*

Gonyaulax spinifera was identified in the Ghanaian coastal waters and found to be abundant. They were estimated to be about 1400 cells/L seawater and 3×10^4 cells L^{-1} in net samples. *Gonyaulax spinifera* is known to produce yessotoxins (YTX) (Rhodes et al. 2006).

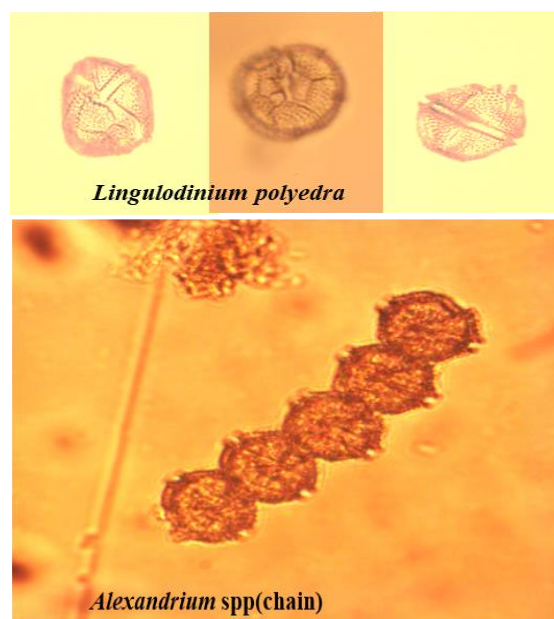


Fig. 6. *Lingulodinium polyedrum* and a chain-forming *Alexandrium* species.

Lingulodinium polyedrum, a potentially toxic dinoflagellate and one of the high biomass bloom forming species, was identified from the coast of Ghana with an abundance a maximum of 6200 cells/L in seawater and 1.6×10^3 cells/L in net samples in December 2016. The high densities in December may have been caused by high temperatures, salinity minor upwelling and tidal water accumulation along the shore. Environmental variables such as salinity and temperature are noted to influence the morphology, cell growth and metabolism of dinoflagellates as has been observed in the North Atlantic coastal waters (Dhib et al., 2013; (Jansson et al., 2014) It is known to produce yessotoxins (YTX) (Lassus et al., 2016) as well as their analogues, the homoyessotoxins (Trainer et al., 2010). Species belonging to the genus *Alexandrium*, which include some of the most toxic HAB species (ROPME, 2012) were also identified with a maximum abundance 425 cells/L seawater in the rainy season but very low densities in the dry season. Several species of *Alexandrium* are known to be responsible for paralytic shellfish poisoning (PSP) events

Conclusion

This study assesses the distribution of harmful phytoplankton along the coast of Ghana. The monitoring study so far has identified eleven harmful species which are mostly thecate dinoflagellates with five of these species (*Lingulodinium polyedrum*, *Gonyaulax spinifera*, *Dinophysis caudata*, *Dinophysis* cf *ovum*,

Alexandrium sp) being toxin producers with the potential to cause diarrhetic shellfish poisoning, paralytic shellfish poisoning, azaspiracid poisoning and yessotoxin-like poisoning symptoms. These species showed a large morphological variability, both in size and shape. Densities and diversity of species also varied with seasons (rainy and dry). Critical densities of *Lingulodinium polyedrum* were recorded in December 2016 and January 2017. Observations also have revealed the presence of species of the genus *Alexandrium*, one of the most toxic genus among the HABs species. This indicates that our shores might be affected by harmful algal blooms.

Acknowledgement

The authors are very grateful to the International Atomic Energy Agency (IAEA) and the Ghana Atomic Energy Commission (GAEC) for sponsoring a member to attend the 18th ICHA, as well other financial and technical supports.

References

Anang, E.R. (1979). *Hydrobiologia*. 62 (1): 33–45.

Dhib, A., Frossard, V., Turki, S., & Aleya, L. (2013). Environmental Monitoring and Assessment, 185, 3369–3382.

García-Portela, M., Riobó, P., Mariano, J., Rosa, M., & Rodríguez, F. (2016). Harmful Algae, 60, 57–69.

Giussani, V., Costa, E., Pecorino, D., Berdalet, E., Giampaulis, G. De, Gentile, M., Fuentes, V., Vila, M., Penna, A., Chiantore, M., Garaventa, F., Lavorano, S., & Faimali, M. (2016). Harmful Algae, 57, 49–58.

Jansson, I., Neil, K., & Head, M. J. (2014). Palaeogeography, Palaeoclimatology, Palaeoecology, 399, 202–213

Larsen, J. and Nguyen, N. L. (2004). Opera Botanica 140: 5–216. Copenhagen. ISBN 87-88702-85-5

Lassus, P., Chomérat, N., Hess, P., Nézan, E. (2016). Toxic and Harmful Microalgae of the World Ocean. Incomplete reference

Lazar, N. (2017). Baseline assessment of demersal fish stocks of the Western Region of Ghana. The USAID/Ghana Sustainable Fisheries Management Project (SFMP). Narragansett, RI: Coastal Resources Center, Graduate School of Oceanography, University of Rhode Island. GH2014_ACT092_CRC. pp 55.

Moestrup, Ø., Akselmann, R., Fraga, S., Hoppenrath, M., Iwataki, M., Komárek, J., Larsen, J., Lundholm, N., Zingone, A. (Eds) (2009 onwards). IOC-UNESCO Taxonomic Reference List of Harmful Micro Algae.

ROPME 2012; Regional Organization for the Protection of the Marine Environment Oceanographic Cruise – Winter 2006. Phytoplankton in the ROPME Sea Area (September 2012) OPME/GC-14/7.

Tamale, J. I., Silva, M., & Vasconcelos, V. (2019). Toxins, 11(58), 1–50.

Trainer, V.L., Pitcher, G.C., Reguera, B., Smayda, T.J. (2010). Progress in Oceanography 85:33–52.

Utermöhl's method (1958). New ways in the quantitative recording of plankton (With special review of the Ultraplanktons). Ratio int. Society. Theor. Angew. Limnol.

Wells, M. L., Trainer, V. L., Smayda, T. J., Karlson, B. S. O., Trick, C. G., Kudela, R. M., Ishikawa, A., Bernard, S., Wulff, A., Anderson, D. M., Cochlan, W. P. (2015). Harmful Algae, 49, 68–93.

Zingone, A., Sarno, D., Siano, R., Marino, D., (2010). The importance Zingone, A., Sarno, D., Siano, R., Marino, D., (2010). Polar Biol., 34:1269–1284.



Taxonomy

Morphological, molecular and toxicological data on *Ostreopsis cf. siamensis* (Dinophyceae) from the Atlantic Iberian Peninsula

Helena David^{1,2*}, Aitor Laza-Martínez³, Mariana Santos^{1,2}, Maria Filomena Caeiro^{2,4}, Luciana Tartaglione^{5,6}, Fabio Varriale^{5,6}, Carmela Dell'Aversano^{5,6}, Antonella Penna^{6,7}, Ana Amorim^{1,2}

¹ MARE-FCUL, University of Lisbon, Campo Grande, 1749-016 Lisbon, Portugal;

² Dept. of Plant Biology, Faculty of Sciences, University of Lisbon, Campo Grande, 1749-016 Lisbon, Portugal;

³ Dept. of Plant Biology and Ecology, Faculty of Science and Technology and Plentziako Itsas Estazioa (PIE), University of the Basque Country (UPV/EHU), Barrio Sarriena S/N, 48940 Leioa, Spain;

⁴ CESAM – University of Lisbon, Campo Grande, 1749-016 Lisbon, Portugal;

⁵ Dept. of Pharmacy, School of Medicine and Surgery, University of Napoli Federico II, via D. Montesano 49, 80131 Napoli, Italy;

⁶ CoNISMa, Piazzale Flaminio 9, 00196 Rome, Italy;

⁷ Dept. of Biomolecular Sciences, University of Urbino, Campus E. Mattei Via Cà le Suore, 61039 Urbino Italy;

* corresponding author's email: hidavid@fc.ul.pt

Abstract

Ostreopsis siamensis, the type species of the genus *Ostreopsis*, was originally described from the Gulf of Thailand based only on morphological characters. Currently, this genus includes 11 accepted nominal species many of which are considered cryptic. Recently, phylogenetic and morphological studies have allowed the identification of well-supported clades, such as the one from temperate waters in Europe and Oceania tentatively named as *O. cf. siamensis*. That designation was based on morphological similarities with *O. siamensis*. However, a recent study on the distribution of *Ostreopsis* spp. in the Gulf of Thailand, where *O. siamensis* was originally described from, did not detect the European/Oceanian ribotype. Its absence suggests that the European/Oceanian ribotype does not include the type of *O. siamensis*. Morphological, molecular and biogeographic differences with other nominal species also preclude the application of any other name, which suggests that a new species should be assigned to this clade. In this study, we clarify the taxonomic status of the European/Oceanian ribotype known as *O. cf. siamensis*, based on morphological, molecular and toxicology data.

Keywords: Benthic Dinoflagellates, *Ostreopsis*, Phylogeny, Taxonomy, Toxicity

Introduction

The benthic dinoflagellate genus *Ostreopsis* Schmidt currently includes 11 species, many of which are known to be toxic, producing palytoxins analogues named ostreocins and ovatoxins (Fernández-Araujo et al., 2013).

This genus was described from the Gulf of Siam (currently Gulf of Thailand), Thailand, with the type species *Ostreopsis siamensis* Schmidt (1901). The original description highlighted the oyster-shaped flat body, the eccentric apex, the presence of a slit-shaped apical pore and porous plates. The original drawings of *O. siamensis* depicted a round-shaped cell in apical view (epitheca), a tear-shaped cell in antapical view (hypotheca), coarse porous

plates and an undulated cell in side view. The reported cell size was large with a dorso-ventral (DV) axis of 90 µm. In 1981, Fukuyo applied this name to specimens from the Ryukyu Islands (Japan) with an undulated body in side view, and gave additional details, such as size range (DV of 60-100 µm; transdiameter of 45-90 µm). In the same work, Fukuyo added two new species to the genus, which were distinguished from *O. siamensis* based on the absence of cell undulation, size (*O. ovata*) and type of thecal pores (*O. lenticularis*). In the following years, six new species were described based on morphology (Norris et al., 1985; Quod, 1994; Faust & Morton, 1995; Faust, 1999).

However, the diagnostic characters limiting the different morphospecies often overlapped or were ambiguous, suggesting the occurrence of cryptic species or morphological plasticity (Parsons et al. 2012). Recently, two additional species (*O. fattorussoi* and *O. rhodesiae*) were described based on both morphological and molecular characterization (Accoroni et al., 2016; Verma et al., 2016a).

The use of molecular taxonomy has shown the existence of distinct ribotypes of *Ostreopsis*, with divergences supporting the description of species. However, establishing the link between the described species and the different clades has been hampered by the lack of biological type material (Pin et al. 2001, Penna et al. 2005, Sato et al., 2011). One such case is the well-defined ribotype *Ostreopsis* cf. *siamensis* first described from the Mediterranean Sea and morphologically similar to *O. siamensis* (Penna et al., 2005). Presently, the *O.* cf. *siamensis* clade includes strains from the Atlantic Iberian Peninsula, the Mediterranean Sea, New Zealand and Australia (David et al., 2013; Verma et al., 2016b), based on ribosomal sequence similarity.

A recent detailed phylogenetic study on the diversity of *Ostreopsis* in the Gulf of Thailand, including sites from the area where *O. siamensis* was originally described, allowed the identification of two major clades in the area, *O.* cf. *ovata* and *Ostreopsis* sp. 6, none of which coincided with the clade known as *O.* cf. *siamensis* (Tawong et al., 2014).

The present work aims at clarifying the taxonomic status of the ribotype known as *O.* cf. *siamensis*, based on previous studies and new morphological, molecular and toxicology data.

Materials and Methods

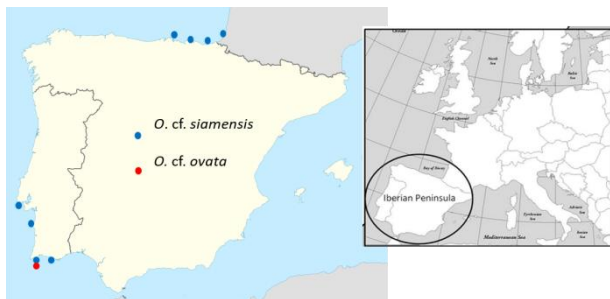


Fig. 1. Study and sampling area (Amorim et al. 2013, David et al. 2013; Laza-Martínez et al. 2011).

Study area and sampling

Epiphytic and planktonic samples were collected from the Atlantic coast of the Iberian Peninsula (Fig. 1). Samples were observed, and cells were

isolated and cultured under controlled laboratory conditions (f/20; 19 °C; 12L:D). Nineteen strains of *O.* cf. *siamensis* were successfully established and are presently kept at the algae culture collection of the University of Lisbon (ALISU).

Morphological analysis

Cultures and Lugol field-fixed samples were observed under the light and scanning electron microscopes, following the methods of David et al. (2013).

Phylogenetic analysis

Approximately 30 ml of exponentially growing cultures were harvested by centrifugation. DNA was extracted and purified using the GRS genomic DNA kit following the manufacturer's instructions (Grisp, Portugal). Amplification was carried out with primers ITSA and ITSB (Adachi et al., 1994) for the ITS-5.8S rDNA region according to Silva et al. (2015). Phylogeny was supported by Maximum Likelihood (ML), Maximum Parsimony (MP) and Neighbour Joining (NJ) methods. Uncorrected genetic pair-wise (p) distances were calculated from the ITS alignment using Mega7 software.

Toxin profile by Liquid Chromatography-High Resolution Mass Spectrometry (LC-HRMS)

Cultures ($10^5 - 10^6$ cells) were centrifuged to separate cell pellets and culture media. Samples were kept frozen at -20°C until analysis. Both pellets and media were extracted following Tartaglione et al. (2016) and all the extracts were analysed by LC-HRMS following Ciminiello et al. (2015).

Toxicity test with a mammalian cell line

Vero E6 cells were cultivated in 96-well culture plates, at 37°C in DMEM medium supplemented with 10% foetal serum. The toxicity assay consisted in exposing cell cultures to dilutions of *Ostreopsis* cell extracts (0, 1/2, 1/4, 1/8) and respective culture medium. The cultures were incubated for 24 hrs at 37°C . A strain of toxic *O.* cf. *ovata* was used as positive control of toxicity and 100% viability correspond to non-treated Vero E6 cultures. The MTT viability assay was carried out and absorbances were recorded. Results reflect the number of viable cells present in each well.

Results and Discussion

Phylogeny

The alignment included 73 sequences, 25 from *O.* cf. *siamensis* of which 14 were from the present study. The sequences assigned to *O.* cf. *siamensis* grouped in a very homogeneous clade (Fig. 2), showing an intra-clade distance of 0.001 (Table 1).

Considering the genetic distance of *O. cf. siamensis* to other species within *Ostreopsis* (Table 1), the minimum genetic distance was 0.113 to *O. rhodesiae*. This value is well above 0.04, the value proposed by Litaker et al. (2007) as the minimum genetic distance allowing delimitation of species in free-living dinoflagellates.

siamensis, namely the presence of cell undulation in lateral view, in conformity with the original description and drawings by Schmidt (1901).

Table 1. Uncorrected genetic p-values (net average genetic distances) between *Ostreopsis* sequences included in the phylogenetic analyses. In diagonal are within-clade distances.

	I	II	III	IV	V	VI	VII
I <i>Ostreopsis cf. ovata</i>	0.023						
II <i>Ostreopsis cf. siamensis</i>	0.226	0.001					
III <i>Ostreopsis rhodesiae</i>	0.231	0.113	0				
IV <i>Ostreopsis fattorussoi</i>	0.321	0.391	0.359	0.004			
V <i>Ostreopsis sp. 7</i>	0.178	0.338	0.302	0.341	0		
VI <i>Ostreopsis lenticularis</i>	0.786	0.547	0.516	0.537	0.694	n/a	
VII <i>Ostreopsis sp. 6</i>	0.467	0.443	0.423	0.441	0.443	0.286	0
VIII <i>Coolia monotis</i>	0.549	0.586	0.647	0.785	0.587	0.735	0.689

The absence of the *O. cf. siamensis* clade from the area where *O. siamensis* was described, and the well-defined ribotype *O. cf. siamensis*, with 0.113 as the minimum value of divergence with its closest clade, means there is support from phylogeography to its consideration as a separate species.

Morphological description

Cells are markedly antero-posterior compressed, tear-shaped to almost round. Cells with no undulation in side view. Dorsoventral diameter in cultures and field: 26-83 μm ($54.3 \pm 13.8 \mu\text{m}$); Width: 13-71 μm ($37.1 \pm 9.8 \mu\text{m}$). Cells in culture show morphological variability even within clonal strains. Figure 3 illustrates the observed variability: elongated vs round hypotheca (Fig. 3a, b), different size of the 7" plate (Fig. 3d, e), diversity in cell size (Fig. 3c) and variable apical pore (Fig. 3f, g). Thecal plates are smooth, covered with randomly distributed pores sometimes with two distinct sizes as previously noticed (David et al., 2013). Plate formula Po, 3', 7'', 5''', 2'''' and 1p.

Distribution

Ostreopsis cf. siamensis is common in the Atlantic coast of Iberia (Amorim et al., 2010, 2013; Laza-Martínez et al., 2011; David et al., 2013). Based on molecular data, this species is also present in the Mediterranean Sea and in the South West Pacific (New Zealand and Australia).

Toxicity

The presence of all the palytoxin analogues so far known (>20) was investigated by LC-HRMS but none of the known congeners was detected. Some potentially new palytoxin congeners, based on their characteristic ionization behaviour, could be present. Further investigation is necessary for their characterization.

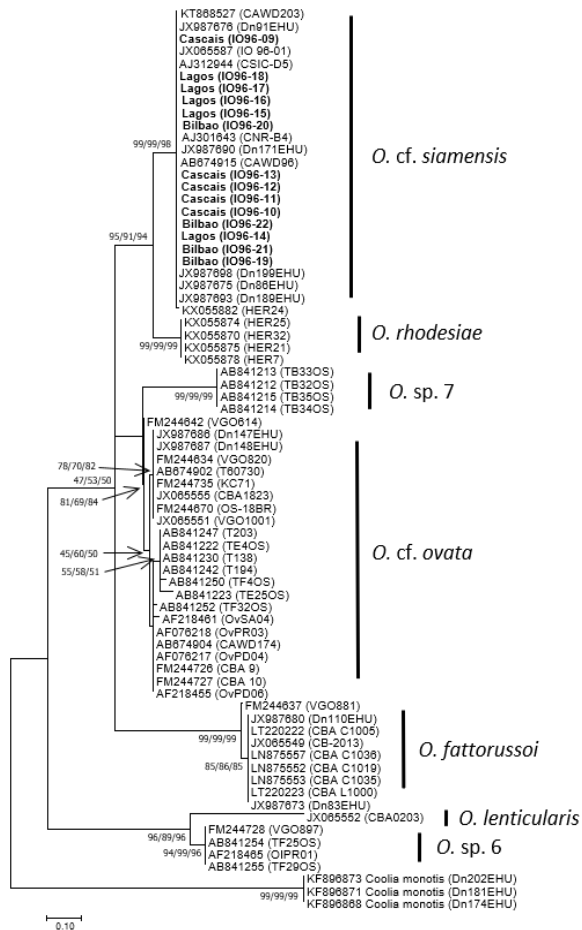


Fig. 2. ML phylogenetic tree of the genus *Ostreopsis* inferred from ITS-5.8S ribosomal gene sequences. The tree is rooted with *Coolia monotis* as outgroup. Numbers on the major nodes represent from the left to right NJ, MP, ML (1,000 pseudoreplicates).

Recent work on the diversity of the genus *Ostreopsis* in Thailand, identified two clades of *O. cf. ovata* and a clade identified as *Ostreopsis sp. 6* in the Gulf of Thailand, where *O. siamensis* was described from, but did not detect strains belonging to the European/Oceanian ribotype of *O. cf. siamensis* (Tawong et al., 2014). In the absence of biological type material of *O. siamensis*, the latter study provides an insight into its possible molecular identity, namely it suggests that the type of *O. siamensis* belongs to one of the clades found by these authors, *Ostreopsis sp. 6* (Fig. 2). This clade included *Ostreopsis* strains from the Gulf of Thailand, and from Japan and Malaysia. Tawong et al. (2014) gave further supporting morphological evidence that this could be considered the true *O.*

The Vero cells assay indicated that all analysed strains of *O. cf. siamensis* had toxicity. Cytotoxicity levels decreased from the undiluted samples to the 1/8, from 83-94% of toxicity to 0-19%. The positive control always showed toxicity over 94%.

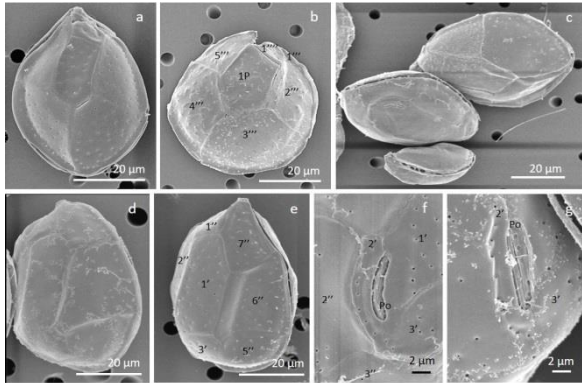


Fig. 3 – SEM micrographs of *O. cf. siamensis* showing variability of cultured strains. a, b - hypotheca, c - group of cells, d, e - epitheca, f, g - Apical pore plate and plate 2'.

Conclusions

Ostreopsis cf. siamensis is a well-defined ribotype that is not present in the area where *O. siamensis* was originally described. It is present along the Atlantic coast of Iberia, the Mediterranean Sea and in a few locations in the south Pacific. Given the genetic distinctiveness and the phylogeographic differences with its morphologically similar species, we propose that the referred ribotype *O. cf. siamensis* should be considered a species different from *O. siamensis* Schmidt and other nominal species. A detailed comparative morphological analysis should show to what extent it is morphologically cryptic in respect to other similar species.

Acknowledgements

Study supported by FCT through strategic projects UID/AMB/50017/2013 and UID/MAR/04292/2019 and postdoc fellowship (SFRH/BPD/121365/2016); Projects Mar2020 Crassoreab Nr16-02-01-FMP-0050, and Portugal2020 AlgaCO₂; The authors would like to thank Dr. Santiago Fraga for stimulating this work.

References

Accoroni, S., Romagnoli, T., Penna, A., et al. (2016). *J. Phycol.* 52, 1064-1084.

Adachi, M., Sako, Y., Ishida, Y. (1994). *J. Phycol.* 30, 857-863.

Amorim, A., Veloso, V., Penna, A. (2010). *Harmful Algae News* 42, 6-7.

Amorim, A., Veloso, V., Battochi, C., et al. (2013). 14th ICHA Proceedings, Greece, 10-12.

Ciminiello, P., Dell'Aversano, C., Dello Iacovo, et al. (2015). *Anal. Bioanal. Chem.* 407, 1463-1473.

David, H., Laza-Martínez, A., Miguel, I., et al. (2013). *Harmful Algae* 30, 44-55.

Faust, M.A., Morton, S.L. (1995). *J. Phycol.* 31, 456-463.

Faust, M.A. (1999). *J. Phycol.* 38, 92-99.

Fernández-Araujo, A., Alfonso, A., Antelo, J.M., et al. (2013). *Oceanography* 1, 104.

Fukuyo, Y. (1981). *Bull. Jpn. Soc. Sci. Fisheries* 47, 967-978.

Laza-Martínez, A., Orive, E., Miguel, I. (2011). *Eur. J. Phycol.* 46, 1-21.

Litaker, R.W., Vandersea, M.W., Kibler, S.R., et al. (2007). *J. Phycol.* 43, 344-355.

Norris, D.R., Bomber, J.W., Balech, E. (1985). Elsevier Publishers, New York, 39-44.

Parsons, M.L., Aligizaki, K., Bottein, M.Y.D., et al. (2012). *Harmful Algae* 14, 107-129.

Penna, A., Vila, M., Fraga, S., et al. (2005). *J. Phycol.* 41, 212-225.

Pin, L., Teen, L., Ahmad, A., Usup, G. (2001). *Mar. Biotechnol.* 3, 246.

Quod, J.P. (1994). *Crypt.-Algol.* 15, 243-252.

Sato, S., Nishimura, T., Uehara, et al. (2011). *PLoS ONE* 6, e27983.

Schmidt, J. (1901). *Botanisk Tidskrift* 24, 212-221.

Silva, T., Caeiro, M.F., Costa, P.R., et al. (2015). *Harmful Algae* 48, 94-104.

Tartaglione, L., Dell'Aversano, C., Mazzeo, A., et al. (2016). *Env. Sci. Technol.* 50, 1023.

Tawong, W., Nishimura, T., Sakanari, H., et al. (2014). *Harmful Algae* 37, 160-171.

Verma, A., Hoppenrath, M., Dorantes-Aranda, J.J., et al. (2016a). *Harmful Algae* 60, 116-130.

Verma, A., Hoppenrath, M., Harwood, T., et al. (2016b). *Phycological Research* 64, 146-159.

Morphological and phylogenetic characterization of *Amphidinium* spp. (Dinophyceae) strains from the Bay of Biscay and the Mediterranean Sea

Louis-Josselin Lavier-Aydat^{1*}, Sergio Seoane¹, Aitor Laza-Martínez¹

¹ University of the Basque Country (UPV/EHU), Department of Plant Biology and Ecology, 48940 Leioa, Spain.

* corresponding author's email: louisj.la76@hotmail.fr

Abstract

Members of *Amphidinium* are among the most diverse benthic dinoflagellates worldwide, as they range from freshwater to marine sandy sediments in tropical, sub-tropical, and temperate ecosystems. Some *Amphidinium* species can still be qualified as cryptic. This issue proves to be of great importance, as diverse reports have demonstrated the potential toxicity of some species, with the dangers it can result from, such as fish mortality. The correct species level identification is therefore critical for a deeper insight into the ecology of the different species, which could help understand the causes and mechanisms of the toxin production. The current study focused on the identification of strains isolated from diverse areas from the Bay of Biscay (Spanish Basque Coast; eleven strains) and the Mediterranean Sea (Spanish, Maltese and Slovenian coasts; nine strains). The semi cryptic nature of some of the species hampered their morphological identification, highlighting the need for the molecular identification of the strains. For this purpose, we proceeded to the amplification of the D1-D3 region of LSU rDNA by PCR, followed by a phylogenetic analysis. Five species were identified from the Bay of Biscay. Most of the strains belonged to the *A. operculatum* complex (four strains), followed in occurrence by *A. carterae* (two strains), *A. thermaeum* (two strains), *A. tomasii* (two strains) and *A. massartii* (one strain). In the Mediterranean Sea the species *A. carterae* (six strains) *A. thermaeum* (one strains), *A. massartii* (one strain) and *A. operculatum* (one strain) were identified. In the case of *A. operculatum* the morphological identification was consistent with the molecular identification. On the other hand, the molecular identification uncovered a cryptic diversity among strains identified as *A. carterae* by morphology.

Keywords: *Amphidinium*, Bay of Biscay, Mediterranean Sea

Introduction

The *Amphidinium* genus is among the most diverse dinoflagellates, as its species range from freshwater (e.g., *Amphidinium achromaticum* and *A. aeschrum*) to marine environments (e.g., *A. carterae*) in tropical, sub-tropical, and temperate ecosystems (Larsen & Patterson, 1990; Flø Jørgensen et al., 2004; Dolapsakis & Economou-Amilli, 2009), making the genus extremely cosmopolitan. *Amphidinium* species grow mainly associated to the benthos (e.g. epiphytic, epipsammic), but other lifestyles were also recorded, such as endosymbiotic. The genus is also highly conserved morphologically. Indeed, several species although possessing almost no structural and/or ultrastructural difference, present clear genetic distinctions between one another, making morphological identification challenging at best. As our understanding of the morphological and genetic diversity of this genus has increased in recent years (Flø Jørgensen et al., 2004; Murray et al., 2004), some original descriptions of species may no longer be adequate to identify them.

Cryptic species diversity has been detected already (Murray et al., 2012), and it is highly likely that further cryptic species will be found. Some *Amphidinium* species have been reported to be toxic (Matsunaga et al., 1999; Rhodes et al., 2010; Karafas et al., 2017) and to be involved in HAB events in various areas worldwide (Baig et al., 2006; Murray et al., 2015). Despite the progress in the study of this genus, some species are still widely considered difficult to identify, which poses a major obstacle when trying to address this genus in environmental samples. As a consequence, most studies only refer to the genus level of these dinoflagellates. Investigations on *Amphidinium* in the Mediterranean Sea, and especially the Bay of Biscay are quite rare. Therefore, a need for a clear identification of *Amphidinium* individuals to the species level is of greater importance, as it is critical for a deepen insight into the ecology and the potential exploitation of the different organisms, as several of its bioactive compounds have potential hemolytic, antimicrobial, and antitumoral

properties (Kobayashi et al., 1991; Matsunaga et al., 1999; Kobayashi & Tsuda, 2004). This will in consequence help further research in both the medical and ecological fields the understanding of the causes and processes of toxin production and their associated action mechanisms.

Materials and Methods

Culture

Twenty *Amphidinium* strains were isolated from macrophyte samples and sediments collected in several areas of the south-east of the Bay of Biscay and the western Mediterranean Sea (Spanish, Maltese, and Slovenian Coasts) (Fig. 1). Macrophytes were put in a bottle with seawater and were shaken to detach the epiphytes.

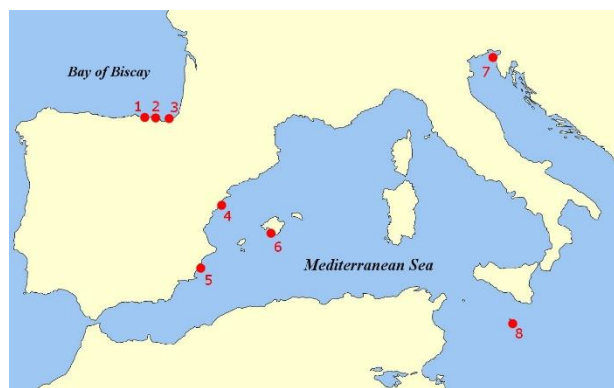


Fig. 1. Locations of the sampling sites from the Bay of Biscay and the Mediterranean Sea. [1] Getxo (1 strain), [2] Mundaka (3 strains), [3] Donostia/San Sebastian (7 strains), [4] Peñíscola (1 strain), [5] Torrevieja (1 strain), [6] Mallorca (1 strain), [7] Piran (5 strains), [8] Malta (1 strain).

The samples with suspended microalgae were observed under an inverted microscope and individual *Amphidinium* cells were picked with a glass capillary and transferred into fresh medium to establish nonaxenic clonal cultures. Successfully established strains were then grown in test tubes, using 10 mL of 35 psu F/2 medium (Guillard, 1975). Cultures were kept in a culture chamber at 18°C, with a 12:12 light:dark cycle.

Light microscopy

Micrographs and morphometric measurements were obtained using a Leica™ DMRB microscope with a Nikon DS-Fi1 digital camera (Nikon, Tokyo, Japan) mounted with a Nikon DS-U2 digital sight (Nikon, Tokyo, Japan). Images and measurements were processed with NIS-elements Imaging software. Length and width of 30 individuals for every strain were measured. Particular features such as metabolic movement were as well noted. A first approach to

morphospecies identity of every strain was performed, from the measurements and the determined features.

DNA extraction, amplification, and sequencing of LSU rDNA domains D1-D3

For DNA extraction of *Amphidinium* strains, a 1.5 mL volume of culture was collected with a plastic Pasteur pipette, then put into Eppendorf tubes. Tubes were centrifuged with a BIOSAN® Microspin FV-2400 in order to obtain a clear pellet of cells. A volume of the pellet varying from 5 to 15 µL was taken and put on a microscope slide. A few cells (between 15 and 30) were collected with a capillary glass taking the least amount of medium possible. The cells were introduced into PCR tubes previously filled with 23 µL of PCR water. PCR tubes were frozen and thawed a couple of times to secure the lysis of cells, to be then safely conserved at -20°C.

LSU rDNA (D1-D3) amplification by PCR proceeded as followed: 2.5 µL of each primer D1R and D3B, as well as 20 µL of BioMix™ mixture (a complete, ready-to-use, 2x reaction mix containing ultra-stable Taq DNA polymerase) were added to the PCR tube containing the water with the cells. The PCR amplification was carried out in a BIOER Technology Co. Thermal Cycler TC-24/H. The cycling conditions consisted of an initial denaturing step of 95°C for 10 min, followed by 35 cycles of 94°C for 1 min, 54°C for 2 min, and 72°C for 3 min, followed by a final extension step of 10 min. Amplification products were sent to the genomic services of SgIker in the UPV/EHU for purification and Sanger sequencing using the same amplification primers.

Phylogenetic analysis

Forty-nine *Amphidinium* sequences belonging to 12 species and three outgroup sequences selected to root the tree were chosen from the GenBank. Sequences were aligned with the ClustalW algorithm, on the BioEdit® software.

The phylogenetic tree construction was performed through a Maximum Likelihood analysis on the MEGA X® software. The substitution model was the Kimura 2-parameter model with a discrete Gamma distribution rate (G) of 4, completed with a 1000 Bootstrap replications test, a complete nucleotide gap deletion, and a Nearest-Neighbor-Interchange (NNI) ML heuristic method.

Results and Discussion

In light of the different observations carried out during light microscopy, some strains exhibited metabolic movement, which was in consequence determining in the species level identification,

leading to the *A. thermaeum* species. Strains assumed to belong to the *A. operculatum* were much easier to identify than the other strains. Molecular results displayed through the phylogenetic tree illustrated a species distribution of seven strains different from our first morphospecies assumption (Table 1), while the *A. operculatum* clade perfectly matched with the microscopic observations.

Table 1. Compiled results of the *Amphidinium* morphospecies assumptions from phylogenetic analysis.

Species	Strains	Site
<i>A. carterae</i>	Mundaka C	Mundaka
	Getxo	Getxo
	Mallorca	Mallorca
	Torrevieja	Torrevieja
	Piran A	Piran
	Piran B	
	Piran C	
	Piran D	
<i>A. thermaeum</i>	Donostia G	Donostia
	Mundaka A	Mundaka
	Peñíscola	Peñíscola
	Donostia B	
<i>A. operculatum</i>	Donostia C	Donostia
	Donostia D	
	Donostia F	
	Piran Grande	Piran
	Donostia E	Donostia
<i>A. massartii</i>	Malta	Malta
<i>A. tomasii</i>	Donostia A	Donostia
	Mundaka B	Mundaka

This supports the idea that identification of specimens belonging to *A. operculatum* can be realized with a relative confidence in the morphologic characterization. This was, on the other hand, not the case for all of the other species, as only a handful of *A. carterae* were correctly identified during our morphospecies assumption: Piran A, B, C & D, Torrevieja, Mallorca, Getxo, and Mundaka C. Seven strains were incorrectly identified based on the morphological features: Donostia A, E & G, Mundaka A & B, Malta & Peñíscola. The genetic results showed that these strains in fact belong to diverse species known to

be highly similar in terms of morphology to *A. carterae*. This information further supports the cryptic nature of the species that has already been mentioned (Murray et al., 2012), as the results showed that highly similar morphologies among several species can completely overlap structural and/or ultrastructural features.

Altogether, five *Amphidinium* species, *A. carterae*, *A. massartii*, *A. operculatum*, *A. thermaeum* and *A. tomasii*, have been identified in the Bay of Biscay and western Mediterranean Sea. All species except *A. tomasii*, that was only found in the Bay of Biscay, were observed in both areas. However, *A. carterae* was represented by four different lineages in the Mediterranean Sea, whereas in the Bay of Biscay only one lineage was found. Overall, our results have successfully characterized the different strains within the Bay of Biscay and the Mediterranean Sea, highlighting the cryptic species and uncovering their hidden biodiversity. Additional studies can be carried out in order to further describe any overlooked morphological features, as well as observing their ecology, and toxicity, which could lead to the inclusion of the described species into current assessment programs.

Acknowledgements

This study is the first author's master thesis project performed in the MER Erasmus Master program. We thank the genomic services of SGIker in the UPV/EHU for their sequencing work.

References

- Baig, H.S., Saifullah, S.M., Dar, A. (2006). Harmful Algae 5, 133–140.
- Dolapsakis, N.P., Economou-Amilli, A. (2009). Acta Protozool. 48, 153–170.
- Flø Jørgensen, M., Murray, S., Daugbjerg, N. (2004). J. Phycol. 40, 351–365.
- Guillard, R.R.L. (1975). pp 26-60. In Smith W.L. and Chanley M.H (Eds.) Culture of Marine Invertebrate Animals. Plenum Press, New York, USA.
- Karafas, S., Teng, S.T., Leaw, C.P., Alves-de-Souza, C. (2017). Harmful Algae 68, 128–151.
- Kobayashi, J., Shigemori, H., Ishibashi, M., Yamasu, T., Hirota, H., Sasaki, T. (1991). J. Org. Chem. 56, 5221–5224.
- Kobayashi, J., Tsuda, M. (2004). Nat. Prod. Rep. 21,77–93

Larsen, J., Patterson, D.J. (1990). *J. Nat. Hist.* 24, 801–937.

Matsunaga, K., Nakatani, K., Ishibashi, M., Kobayashi, J., Ohizumi, Y. (1999). *Biochim. Biophys. Acta* 1427, 24–32.

Murray, S.A., Daugbjerg, N., Flø Jørgensen, M., Rhodes, L. (2004). *J. Phycol.* 40, 366–382.

Murray, S.A., Garby, T., Hoppenrath, M., Neilan, B.A. (2012). *PLoS ONE* 7, e38253.

Murray, S.A., Kohli, G.S., Farrell, H., Spiers, Z., Place, A., Dorantes-Aranda, J.J., Rusczyk, J. (2015). *Harmful Algae* 49, 19-28.

Rhodes, L.L., Smith, K.F., Munday, R., Selwood, A.I., McNabb, P.S., Holland, P.T., Bottein, M.-Y. (2010). *Toxicon* 56, 751–758.

First report of *Alexandrium affine* in Uruguay; molecular, morphological and toxicological study of a bloom during summer 2017

Silvia M. Méndez ^{1*}, Francisco Rodríguez ², Ana Martínez ³, Pilar Riobó ⁴, Maribelle Vargas-Montero ⁵

¹⁻³ DINARA, Laboratorio de Fitoplancton, Constituyente 1497, Montevideo, Uruguay

² Instituto Oceanográfico de Vigo, Subida a Radio Faro 50, 36390, Vigo, Spain

⁴ Instituto de Investigaciones Marinas, C/Eduardo Cabello 6, 36208, Vigo, Spain

⁵ Centro de Investigación en Estructuras Microscópicas CIEMic, Univ. of Costa Rica, San José, Costa Rica

* corresponding author's email: smendez@dinara.gub.uy

Abstract

A bloom of a thecate chain-forming dinoflagellate from the genus *Alexandrium* was reported at the main touristic Uruguayan beach “Punta del Este” in January 2017 (austral summer). This area is under routinely harmful algae monitoring programme since 1980. The bloom reached a density of 1.2×10^6 cells l^{-1} estimated by Utermöhl method. Other two bloom-forming species belonging to *Alexandrium* genus previously reported for this area were the Paralytic Shellfish Toxins (PST) producer *Alexandrium tamarense/catenella* (associated to high toxicity levels in mussels between 1991 and 1996) and *Alexandrium fraterculus*, a non-toxic species. Light microscope and SEM analyses of *Alexandrium* specimens from the bloom were accompanied by molecular identification (LSUrDNA gene sequencing). LSurDNA gene sequence confirmed *Alexandrium affine* as the causative species. This is the first report of this species for the Southwestern Atlantic Ocean. During the bloom, no PST were reported in mussels from the area by the mouse bioassay official method. Moreover, PSTs were neither detected by liquid chromatography with fluorescence detection (LC-FLD), although a very low signal registered in the chromatogram could be attributed to possible traces of GTX3, which should be confirmed in future studies. The report of this cyst-forming species in this intensively monitored area is an example of the global geographic expansion trend for phytoplankton species that could pose the risk of potentially toxic species in this region.

Keywords: *Alexandrium affine*, Uruguay, molecular study

Introduction

The genus *Alexandrium* harbours a large number of species potentially producing paralytic shellfish toxins (PST) worldwide and it has been thoroughly studied because of its ecological, toxicological and economic impacts (Balech 1985). In Uruguay from 1991 to 1996, PST in mussels were detected above regulatory levels every year associated with the presence of *A. tamarense/catenella* at late winter and early spring period (Méndez et al., 1996, Méndez and Ferrari 2002). The toxic profile of this species was determined from cultures initiated from resting cysts (Méndez et al., 2001). The chain forming *Alexandrium fraterculus* had been reported for this area, associated to the austral summer- autumn period, from 1992 to 2016, without any associated toxicity in the local wild mussels (Méndez et al. 1993, Méndez and Brazeiro 1993; Méndez and Ferrari 1995, Martínez et al 2016).

In early January 2017, a bloom of a chain-forming *Alexandrium* species was reported by the monitoring programme. The species developed

high cell density along the Uruguayan coast, reaching 1.2×10^6 cells l^{-1} at Punta del Este and no toxicity was reported during this period in wild mussels from this area.

Materials and Methods

Surface samples for quantitative phytoplankton analysis were taken weekly at Punta del Este station (Fig 1) and fixed with Lugol, from January 1st to March 30th 2017. Temperature and salinity were measured with an YSI probe. Samples were counted in sedimentation chambers, using Utermöhl method (1958) under inverted microscope Leitz Labovert FS. Images were taken at the inverted confocal microscope with a Nikon camera at the IIBCE (Instituto de Investigaciones Biológicas Clemente Estable). During the maximum bloom density, a surface water sample (250 ml) was taken at Punta del Este beach. Two subsamples (50 ml) were fixed with Lugol and 2 subsamples (50 ml) were fixed with Ethanol at 95%

for molecular analysis. A live sample (500 ml) was kept dark at room temperature for 12h. Then, it was concentrated to 40 ml and divided in two aliquots. One aliquot of 10 ml was filtered through Millipore 0.22 μm to collect cells and the filter was introduced into an Eppendorf tube filled with HCl 0.1M for toxin analysis. The other aliquot of 30ml was fixed with Lugol.

Molecular analysis

An environmental sample of the *Alexandrium* bloom (fixed with Lugol's neutral solution) was used to pick cells manually (around 20-50) with a micropipette into 200 μl microtubes. Samples were centrifuged (5,000 rpm, 5 min), rinsed carefully with distilled water and centrifuged again. Supernatants were discarded and kept at -80°C until further molecular analysis.

Partial LSUrDNA gene amplification (D1-D2 domains) was performed by polymerase chain reaction (PCR) in an Eppendorf Mastercycler EP5345 using Horse-Power™ Taq DNA Polymerase MasterMix 2x (Canvax, Spain), using the pair of primers D1R/D2C (5'-ACCCGCTGAATTTAAGCATA-3'/5'-ACGAACGATTTGCACGTCAG-3'; Lenaers et al. 1989). PCR conditions were as follows: initial denaturation at 94°C for 5 min, 35 cycles of denaturation at 94°C for 35 sec, annealing at 52°C for 35 sec, extension at 72°C for 1 min, and a final extension cycle at 72°C for 7 min.

A 8 μL aliquot of each PCR was checked by agarose gel electrophoresis (1% TAE, 80 V) and SYBR™ Safe DNA gel staining (Invitrogen, Carlsbad, CA, USA). The PCR products were purified with ExoSAP-IT (USB, Cleveland, OH, USA), sequenced using the Big Dye Terminator v.3.1 reaction cycle sequencing kit (Applied Biosystems, Foster City, CA, USA), and separated on an AB 3130 sequencer (Applied Biosystems) at the CACTI sequencing facilities (Universidade de Vigo, Spain). The LSUrDNA gene sequence obtained (685 nt) was deposited in GenBank database (Acc. N° **MH973264**, in Fig. 6).

The sequence of the studied *Alexandrium* cells and 41 related *Alexandrium* spp. obtained from GenBank were selected and aligned using BioEdit v.7.2.5. A sequence from *Prorocentrum micans* was used as outgroup. The final alignment for the LSUrDNA phylogeny consisted of 518 positions. The phylogenetic model was selected using MEGA 7 software. Tamura-Nei model (TN93; Tamura and Nei 1993) with a gamma-shaped parameter ($\gamma=0.663$) was selected.

The phylogenetic relationships were determined according to the maximum likelihood (ML) method using MEGA 7 and the Bayesian inference

method (BI) with a general time-reversible model from MrBayes v.3.2 (Huelsenbeck and Ronquist 2001). The two methods rendered very similar topologies. The phylogenetic tree was represented using the ML results, with bootstrap values from the ML method ($n=1,000$ replicates) and posterior probabilities from the BI method. Bootstrap values $<60\%$ and probabilities <0.6 are denoted by hyphens. Branch lengths are measured in the number of substitutions per site.

Toxins

During the bloom were collected 1.5×10^5 cells for analysis of PSTs. Extraction of toxins from microalgae was performed with 1500 μL of HCl 0.1 M and this extract was stored at -20°C until chromatographic analyses. Before toxin analyses, sample was filtered by PTFE syringe filter (0.45 μm , 30 mm diameter) and 10 μL were injected. Determination of PSTs was performed by LC-FLD with post-column oxidation following the method proposed by (Rourke et al. 2008) with slight modifications. A Waters Acquity ultra performance liquid chromatography (UPLC) system (Waters, USA) was used for toxin analysis. Separation of different PSTs was carried out on a Zorbax Bonus RP column (4.6 x 150mm, 3.5 μm particle size). Mobile phase A was 11 mM heptanesulfonate in a 5.5 mM phosphoric acid aqueous solution adjusted to pH 7.1 with ammonium hydroxide. Mobile phase B consisted of 88.5% 11 mM heptanesulfonate in a 16.5 mM phosphoric acid aqueous solution adjusted to pH 7.1 with ammonium hydroxide and 11.5% acetonitrile. Both of the mobile phases were filtered through 0.2 μm membrane filter before use. Gradient was run at a flow rate of 0.8 ml min^{-1} starting at 100% A that was held for 8 min. Then, mobile phase B was linearly increased to 100% in 8 min. This percentage was held for 9 min and then returned to 100% A in 0.1 min. The total run time was 30 min but 5 min of equilibration time was allowed prior to the next injection. Derivatization of the eluate from the column involved mixing continuously with 7 mM periodic acid in 50 mM potassium phosphate buffer (pH 9.0) at a flow rate of 0.4 mL min^{-1} and heating at 65°C by passage through a Teflon coil (0.25 mm i.d., 8 m long). Then, it was mixed with 0.5 M acetic acid at 0.4 ml min^{-1} until neutralization of pH. Fluorescence detector was operated at an excitation wavelength of 330 nm and emission was recorded at 390 nm. PSP standards for GTX4, GTX1, dcGTX3, dcGTX2, GTX3, GTX2, neoSTX, dcSTX and STX were acquired from the NRC Certified Reference Materials program (Halifax, NS, Canada).

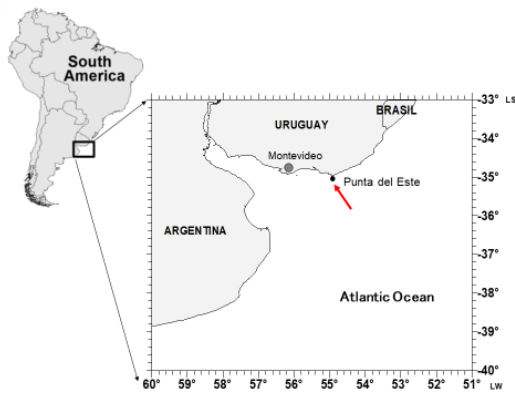


Fig. 1. Study area

Results and discussion

Taxonomic characteristics

Cell is isodiametric (24 μm in diameter), a little longer than wide when is in chain. Length of cells in this bloom ranged between 22.3-28.5 μm (Fig. 2). The Po is long and bullet shaped (Fig. 3A-B), which is one of the most characteristic features of this species. The dorsal is straight and the laterals of this plate are parallel in the dorsal 2/3 of the plate. Plate 1' is connected directly with the Po and has a ventral pore at about half height (Fig.3C-D). The description is coincident with Balech (1995).

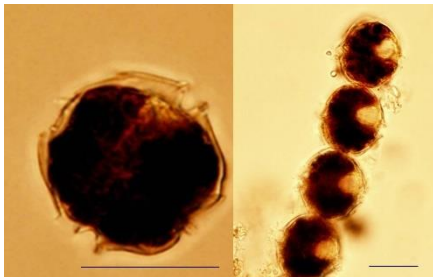


Fig.2. Confocal micrographs of cells fixed with Lugol Solution. A) ventral view of a single cell of *Alexandrium affine* from Uruguay, B) chain forming of 4 cells (IIBCE- Uruguay). Bar=20 μm .

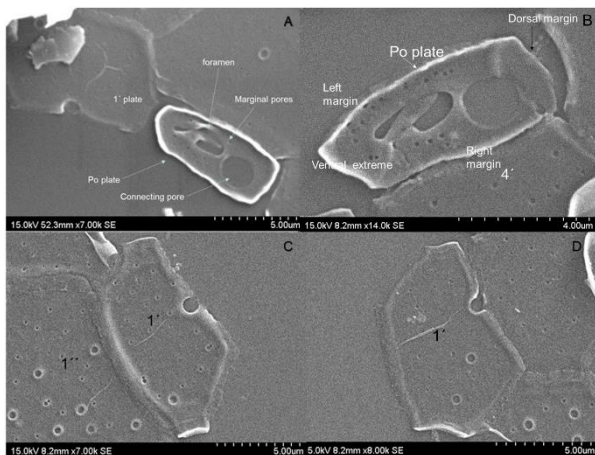


Fig. 3. *Alexandrium affine* from Uruguay. Electronic microscopy A-B Po plate. C-D 1' plate.

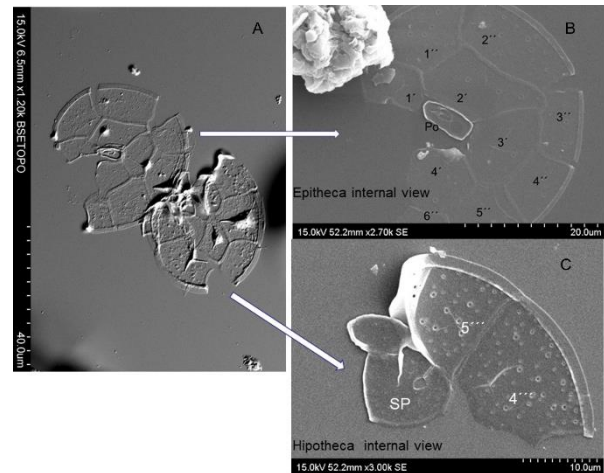


Fig. 4. *Alexandrium affine* from Uruguay. A) Epitheca and Hypotheca, B) Epitheca details of Po, 1' to 4' apical plates and 1'' to 6'' precingular plates; C) Hypotheca plates with sulcal posterior SP, and postcingulars 4''' and 5'''.

The sulcal posterior plate (S.p.) has a round pore that is linked to the right margin by a small channel. (Fig 4C). The taxonomical characteristics seen both at optic and electronic microscopy, coincide with *A. affine*.

Molecular study

The phylogenetic tree shows the clear coincidence of the sample with other sequences of *Alexandrium affine* available in GenBank database (Fig.5).

Toxins

A mixture of 9 PSP toxin standards was prepared and 3 μL were injected on column. Retention times recorded for each one of the toxins were: GTX4 (RT 7.23 min, 0.253 ng/ μL), GTX1 (RT 8.29 min, 0.777 ng/ μL), dcGTX3 (RT 11.96 min, 0.057 ng/ μL), dcGTX2 (RT 12.97 min, 0.255 ng/ μL), GTX3 (RT 14.13 min, 0.107 ng/ μL), GTX2 (RT 15.59 min, 0.282 ng/ μL), neoSTX (RT 21.30 min, 0.320 ng/ μL), dcSTX (RT 23.72 min, 0.191 ng/ μL) and STX (RT 24.52 min, 0.234 ng/ μL). This species was classified by Anderson et al. (2012), as typically low toxic or non-toxic species. Only one report mentions the production of STX, NEO and GTX1-4 (Nguyen-Ngoc (2004).

They were not detected GTX4, GTX1, dcGTX3, dcGTX2, GTX2, neoSTX, dcSTX neither STX in the *A. affine* extract here analyzed. A peak that elutes at the same retention time that GTX3 (RT 14.13 min.) was observed in the sample at trace levels. To confirm the presence of GTX3 in cells of this microalgae species more samples must be collected and analyzed.

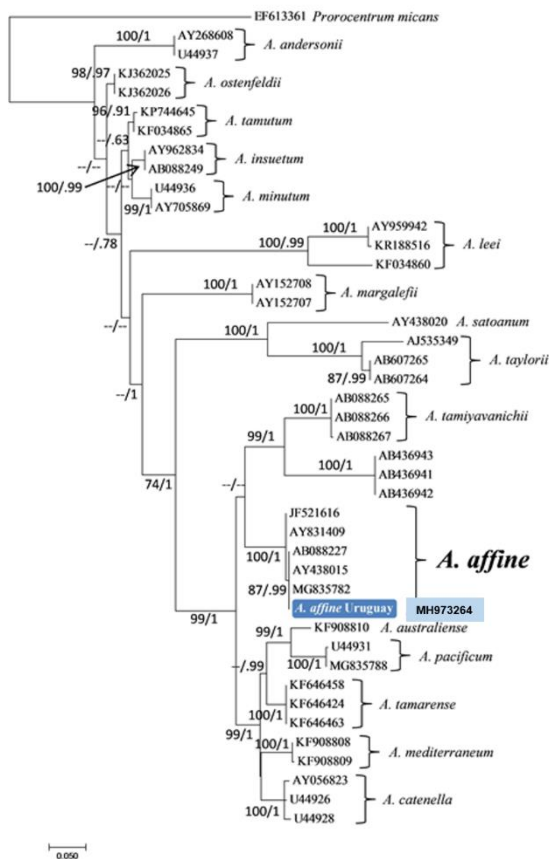


Fig. 5. Phylogenetic tree of the D1-D2 LSU rDNA using 41 *Alexandrium* spp sequences retrieved from GenBank. The Acc. N° for *A. affine* from Uruguay is MH973264.

Environmental conditions

The bloom occurred during a period of strong influence of warm oceanic waters over the Uruguayan coast. The maximum cell density was reported between 22 and 25°C. The bloom finished when the salinity decreased from 28 to 9.2. The Uruguayan coast is showing an increasing trend in seawater temperature, a feature that could favour the occurrence and establishment of new warm water species like *A. affine*.

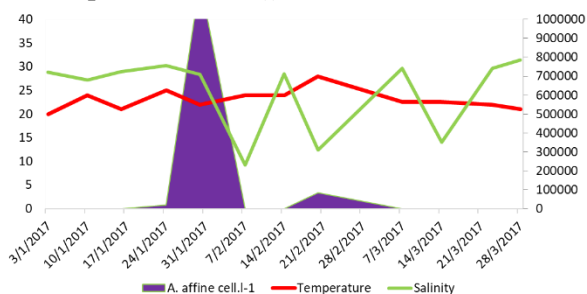


Fig. 6. *Alexandrium affine* density, and fluctuations of temperature and salinity during bloom in Punta del Este.

Acknowledgements

Authors thank specially the International Atomic Energy Agency (IAEA) Project RLA 7022 for its support.

References

- Anderson, D.M., Alpermann, T.J., Cembella, A.D., Collos, Y., Masseret, E., Montresor, M. (2012). Harmful Algae, 14:10-35.
- Balech, E. (1985). The genus *Alexandrium* or *Gonyaulax* of the *tamarense* group. In: D.M. Anderson, A.W. White and D.G. Baden (Eds.) Toxic Dinoflagellates. New York: Elsevier. P. 33-38.
- Huelsenbeck, J.P., Ronquist, F. (2001). Bioinformatics 17, 754e755.
- Lenaers G, Maroteaux L, Michot B, Herzog M, (1989). J. Mol. Evol. 29:40-51.
- Martínez, A., Méndez S., Fabre, A. (2016). Pan-Amer. Jour. of Aq. Sc. (2016), 11(4): 356-360.
- Méndez, S., Ferrari, G. (1995). UNESCO IOC WS Report 101: 37-39.
- Méndez, S., et al. (1993). INAPE, Inf. Téc. 46. 31p.
- Méndez, S., Brazeiro, A. (1993). Toxic Marine Phytoplankton. Conf. Proceedings. Pp 139-140
- Méndez, S.M., Severov, D., Ferrari, G. (1996). Harmful and Toxic Algal Blooms. IOC-UNESCO. Paris. Pp113-119.
- Méndez, S. Kulis, D., D. M. Anderson. (2001). Harmful Algal Blooms 2000. IOC UNESCO. Pp. 352-355.
- Méndez, S.M., Ferrari, G. (2002). Instituto Español de Oceanografía, Madrid. Pp 271-288.
- Nguyen Ngoc L. (2004). Harmful Algae, 3:117-129.
- Rourke, W.A., Murphy, C.J., Pitcher, G., van de Ri et J.M., Burns, B.G., Thomas, K., Quilliam M.A. (2008). J. AOAC Int. 91: 589-597.
- Tamura, K., Nei, M. (1993). Mol. Biol. Evol. 10:512-526.
- Utermöhl, H. (1958). Mitteilung Internationale Vereinigung für Limnologie, 9:1-38.



Toxin analysis – Novel detection methods

Analysis of PSP toxins in Moroccan shellfish by MBA, HPLC and RBA Methods: Monitoring and Research

Rachid Abouabdellah^{1*}, Asmae Bennouna¹, Marie-Yasmine Dechraoui Bottein², Hamza Alkhatib³,
A. Mbarki¹, N. Imzilen¹, M. Alahyane¹

¹National Institute of Fisheries Research, Km 7 route Essaouira, Anza, Agadir, Morocco,

²International Atomic Energy Agency, Environment Laboratories Monaco, France

³Faculté des science Ain Chock, university Hassan II, Casablanca, Morocco

* corresponding author's email: dichar75@yahoo.fr

Abstract

Paralytic shellfish poisoning toxins (PSTs) are secondary metabolites of some toxic species of phytoplankton. The consumption of bivalve shellfish having accumulated these toxins can lead to potentially fatal neurotoxic food poisoning. Cases of toxicity by PSTs occur regularly along the Moroccan coastal waters and have been responsible for severe cases of intoxication in the early 90s. In recent years, the southern Moroccan Atlantic coasts have been particularly affected by strong toxicity episodes and more frequent occurrence of toxic phytoplanktonic species. Within the Moroccan statutory shellfish biotoxin monitoring programme established by the National Institute of Fisheries Research (INRH), a study of PSTs was conducted from 2004 to 2018 in south Moroccan's shellfish. Two shellfish species were studied; the brown mussel (*Perna perna*) sampled from south Agadir region and razor clam (*Solen marginatus*) from Dakhla bay. In parallel, monitoring of toxic phytoplankton in seawater was conducted. The aim of this study was to compare the results of three different methods: high performance liquid chromatography with post column derivatization and fluorescence detection (HPLC-FLD), Receptor Binding Assay (RBA) and mouse bioassay (MBA) for determining PSP toxicity in Moroccan shellfish.

The PST toxicity was associated with *Alexandrium cf. minutum* identified in seawater of south Moroccan coasts. These toxic episodes were widely distributed in time and space and mainly detected during the summer and autumn season. On several occasions toxicity exceeded the sanitary threshold (800 µg eq STX/kg). The PST profile identified by HPLC was dominated by gonyautoxins 2, 3 and a trace of saxitoxin. Comparison between the different methods used in PSTs analysis revealed that MBA data were statistically significantly correlated with RBA (Pearson $r = 0.81$).

Keywords: Paralytic shellfish poisoning, *Alexandrium*, Morocco, HPLC/FLD, RBA, MBA

Introduction

From 1998 to 2016, several episodes of shellfish contamination with PSTs were reported both in the Moroccan Mediterranean and Atlantic coasts, but no case of human intoxication were reported during this period (Abouabdellah et al; 2008; 2011; 2017). In the aim to protect the shellfish consumers, a phycotoxin and toxic phytoplankton monitoring system was established in the early nineties by the National Institute for Fisheries Research (INRH) along the Moroccan coasts.

Materials and Methods

Monitoring of PSTs and lipophilic toxins are carried out by biological method on the mussels from four shellfish areas in the Agadir region. Analysis of two samples from Laayoune and analysis of 12 samples from Dakhla bay (mussels,

razor clam, oyster and cockles) (fig. 1). Regarding samples for ASP toxin analyzes are analyzed weekly by chemical method (HPLC). Other methods were used for analysis of PSP toxins in the aim to determine the spatio-temporal variation during the last decade and for determination of different toxin profiles.

A new method RBA (Receptor Binding Assay) was used in the detection of PSTs and was compared with the MBA.

Analysis of PSP toxins by biological method

PSTs were analysed by MBA according to Association of Official Analytical Chemists (AOAC) method 959.08 (1995). 100 g of homogenized tissues was mixed with 100 ml of chlorhydric acid 0.1 M (pH adjusted to 3) and the

extract boiled for 5 min. After cooling, the pH was adjusted to 3 by HCl 5 M or NaOH 0.1 M. Then the mixture was centrifuged at 3000g for 15 min. One millilitre of the super-natant was injected intraperitoneally into three 18-20 g albinos mice. The values were expressed in μg STX eq/kg meat.

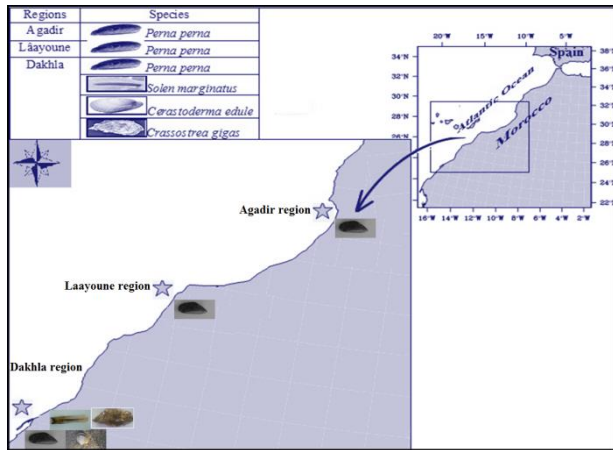


Fig. 1. Shellfish sampling sites in the south of Morocco

Phytoplankton analysis

Phytoplankton identification and especially the potentially harmful species (HABs) were identified and enumerated by inverted microscopy using the Utermohl method (1958).

Analysis of PSTs by chemical method

PSTs profiles were determined by HPLC/FLD according to Thielert et al. (1991), modified by Yu et al. (1998).

Analysis of PSTs by radioactive method

PST detection by RBA was conducted using the AOAC method OMA 2011.27.

Results and Discussion

Detection of PSP

Results of PSP monitoring in south of Agadir showed that several episodes of mussel toxicity were recorded from 2004 to 2018. At the beginning of this study in 2004, the concentrations did not exceed the toxicity threshold, the maximum level value was $715 \mu\text{g}$ of eq STX/kg found in June 2006. During the period 2007-2010, these toxins were not detectable. From 2011 until 2018, these toxins were detected in November 2011, May 2012, May 2014, August and September 2015 and in July of 2017 and 2018 with concentrations exceeding eight times the threshold. When PSTs exceeded the regulatory limit ($800 \text{ eq. } \mu\text{g STX/kg}$), the collection and commercialization of shellfish was prohibited until the toxin levels decreased below the

regulatory limit (fig 2). At Dakhla bay, PSTs were detected in the end of December 2006 and beginning of January 2007 in different shellfish (mussels, oysters, cockles and razor clams).

In Dakhla Bay, in the exception of razor clam where PSTs concentrations exceeded $1215 \mu\text{g eq. Stx / kg}$, the concentrations in other bivalves did not exceed the thresholds ($800 \mu\text{g eq. STX/kg}$), the maximum recorded was that recorded in the Boutalha in December 2006. At Laayoune region, the PSTs were detected from June to August 2005 with a maximum of $450 \mu\text{g eq. Stx / kg}$.

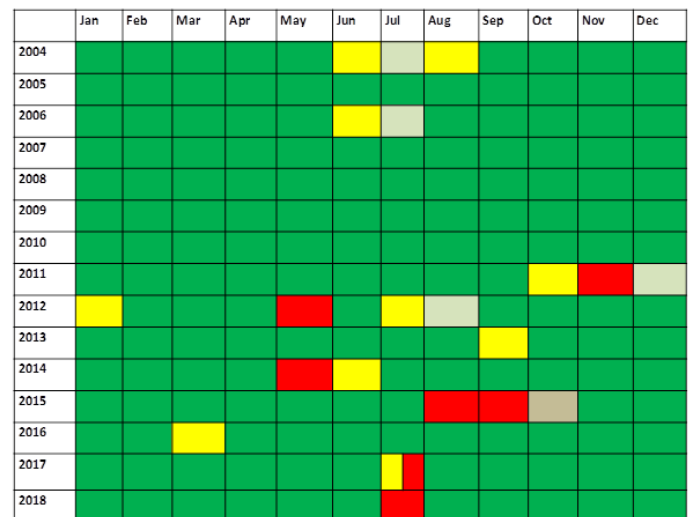
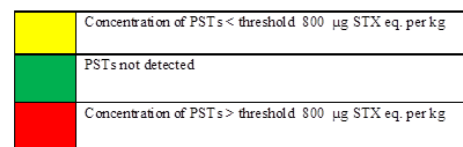


Fig 2. Detection of PSTs in mussels of South of Agadir (Morocco)

HABs monitoring

Monitoring of *Alexandrium* spp in the south of Agadir area starts from 2004. Thus, the *Alexandrium* concentrations show significant spatial and temporal variability (fig. 3). Indeed, the taxa has been irregularly present, at low concentrations in winter. The maximum concentrations reached $1.5 \times 10^3 \text{ cell L}^{-1}$ in spring 2014. Then, the species mark a major efflorescence in August 2015 with $6.12 \times 10^3 \text{ cell L}^{-1}$. In 2017 and 2018 *Alexandrium* recorded higher concentrations in spring and summer respectively ($\sim 10^3 \text{ cell L}^{-1}$).

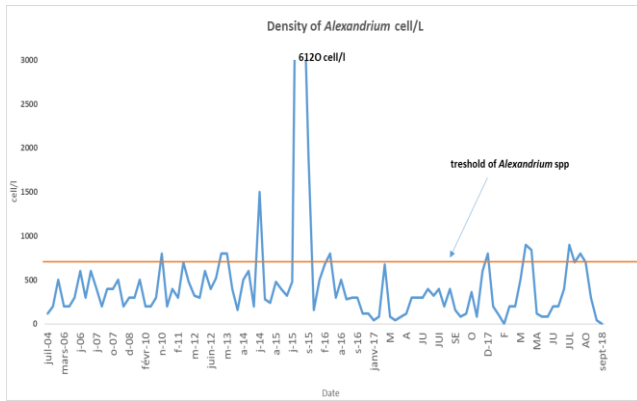


Fig 3: Variation of *Alexandrium* spp in seawater of South of Agadir (Morocco).

Toxic potential of *Alexandrium* species from Agadir will be studied in culture for determination of toxin profile and overall toxicity.

The agitated areas they will not be breeding grounds for the proliferation of this dinoflagellates, often inhibited by agitation, this will explain the low concentrations of this species it should be noted that concentrations along the water column may be higher than in the surface

PSTs profile

At Dakhla Bay and Agadir region: analyzes of PSTs profiles by HPLC/FLD in razor clams and mussels showed a presence of carbamate toxins, especially gonyautoxines (GTX1,2,3,4) and saxitoxins. GTX2 and 3 were the most dominant with minority of saxitoxin (fig. 4)

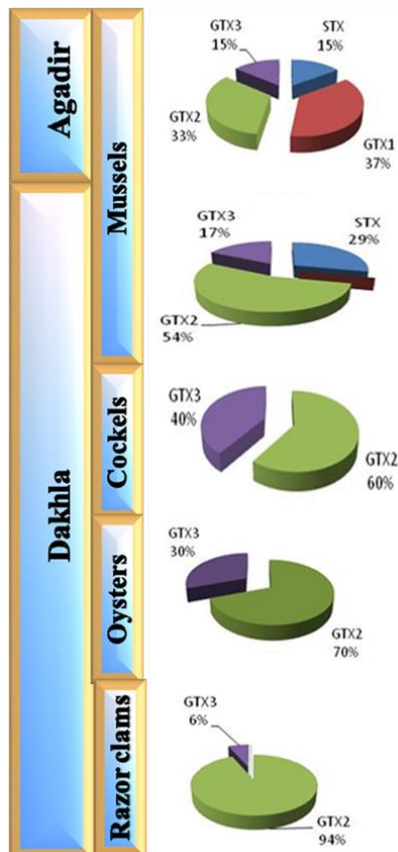


Fig. 4. PSTs profile in Shellfish from Agadir region and Dakhla bay.

Detection of PSPTs by MBA, RBA and HPLC

All samples with toxicity superior to sanitary threshold were detected by RBA, this method allowed detection of very small amount of PSTs (fig. 5). LOD of RBA and MBA were 35.24 ± 5.99 and $325 \mu\text{g STX eq. per kg}$, respectively.

Despite the effectiveness of the mouse test in the PSTs monitoring it remains semi quantitative and over estimates the real toxicity of the samples, beside the use of animals and the large amount of standards needed. Concerning the RBA method, it

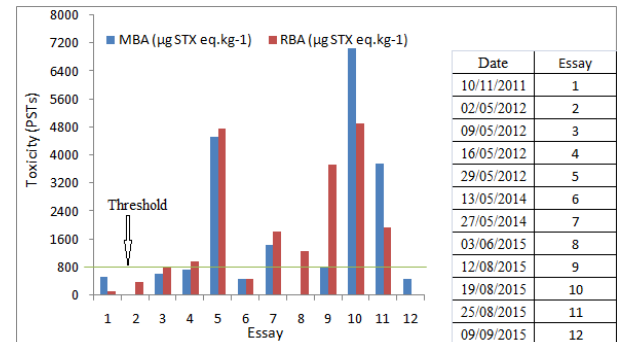


Fig. 5. Detection of PSTs by RBA and MBA in Agadir's mussels

is very sensitive and faster but the use of radioactivity requires special conditions of use. However, the comparison between the different methods used in PSTs analysis revealed that MBA data were statistically significantly correlated with RBA (Pearson $r = 0.81$). The RBA method limit of quantification was found to be 10-fold lower than that of the MBA method ($35.24 \pm 5.99 \mu\text{g STX eq. per kg}$ and $325 \mu\text{g STX eq. per kg}$, respectively).

Acknowledgements

Our acknowledgements to IAEA Staff of RAF 7012/7014 TC project; to INRH scientific staff in INRH-Dakhla for their collaboration in this work, and to INRH General and Regional Direction specially Dr S. El Ayoubi.

References

- Abouabdellah R, Taleb R, Bennouna A, Erler K, Chafik A, Moukrim K, 2008. *Toxicon* 51(4): 780-786.
- Abouabdellah R., A.Bennouna, J. El Attar , Katrin Erler , Abdelghani Chafikc 2011. The detection of PSP and LSP toxins in bivalves from the southern Moroccan coasts by HPLC and mouse bioassay. *Marine and Freshwater Toxins Analysis. Second Joint Symposium and AOAC Task Meeting Baiona, Spain May 1-5, 2011.*

Abouabdellah R., Bennouna A., Dechraoui-Bottein M-Y., El Attar J., Dellal M., Mbarki A., Imzilen N., Alahyane M. and BenbrahimS., 2018. IJBCRR, 21 (2) 1-12, 2018; Article no.IJBCRR.40032.

AOAC (Paralytic Shellfish Poison, Biological method, Final Action, Method 959.08, in Official Methods of Analysis (1995) of the Association of Official Analytical Chemists (AOAC), Natural Toxins, Chapter 49, page 46

Thielert G., Kaiser I. and Luckas B., 1991. HPLC determination of PSP toxins. In: J.M. Frey

(eds.) Proceedings of symposium on marine biotoxins. Editions CNEVA, Maisons-Alfort. pp. 121-125.

Uthermol, H. 1958. Mitt. Int. Ver. Theor. Angrevo. Limnol 9: 1-38.

Van Dolah, F,M, Fire,S,M, Leighfield, T, A., Mikulski, C, M, Doucette, G, J, 2012. JAOAC Intl. Vol. 95, No. 3, 2012.

Yu R.C, Hummert C, Luckas B, Qian P.Y, Yhou M.J, 1998. Chromatographia, 48:671- 675

Bioassays for detection and identification of cyclic imine toxins

Rómulo Aráoz^{1,2*}, Jordi Molgó^{1,2}, Denis Servent²

¹ CNRS, Institut de Neurosciences – Paris Saclay, UMR9197, Université Paris-Saclay. 91198 Gif sur Yvette,

² CEA/ DRF/ Institut des Sciences du Vivant Frédéric Joliot, Service d'Ingénierie Moléculaire des Protéines (SIMOPRO), Université Paris-Saclay, 91191, Gif-sur-Yvette, France.

* corresponding author's email: araoz@inaf.cnrs-gif.fr; romulo.araoz@cea.fr

Abstract

Marine neurotoxins rapidly move up the food chain through shellfish that filter-feed on toxic dinoflagellate species constituting a serious hazard for Public Health. Monitoring of regulated marine toxins is performed by physicochemical analyses. It is essential however to develop functional bioassays as an alternative to mouse bioassay for high-throughput detection of novel and emergent marine toxins. Cyclic imine toxins are very-fast acting neurotoxins highly lethal to mice acting as potent antagonists of nicotinic acetylcholine receptors. Although not regulated, chronic exposition to cyclic imine toxins is of concern given their high affinity for neuronal and muscle nicotinic receptors and their capacity to cross the intestinal and the brain blood barriers. A series of bioassays based on the mode of action of cyclic imine toxins are here reviewed.

Keywords: Cyclic imine toxins, gymnodimines, spirolides, pinnatoxin, receptor-binding assay, toxin fishing

Introduction

Cyclic imines toxins (CiTXs) constitute a large family of emergent marine phycotoxins associated with harmful algal blooms and shellfish toxicity (Gueret and Brimble 2010; Stivala et al., 2015). The growing family of CiTXs purified from toxic dinoflagellates and/or contaminated shellfish includes 43 toxic members: **7 gymnodimines** (A-E and 12-methylgymnodimine), **16 spirolides** (SPX) (A-D, G-I, 13-desmethyl SPX-C, 27-hydroxy-13-desmethyl SPX-C, 13,19-didesmethyl SPX-C, 20-hydroxy-13,19-didesmethyl-SPX-C, 27-hydroxy-13,19-SPX-C, 27-oxo-13,19-dides-methyl SPX-C, 13-desmethyl SPX-D, 20-hydroxy-13,19-didesmethyl-SPX-D and 20-methyl-SPX-G), **8 pinnatoxins** (A-H), **3 pteriatoxins** (A-C), **1 spiroporocentrime**, **6 prorocentrolides** and **2 portimines** (A and B). *Karenia selliformis* synthesises gymnodimines. *Alexandrium ostenfeldii* strains produce spirolides and 12-methylgymnodimine. *Prorocentrum* sp. produces prorocentrolides. *Vulcanodinium rugosum* produces pinnatoxins and portimines. (For references see : Fribley et al., 2018; Zurhelle et al., 2018; Molgó et al., 2017; Stivala et al., 2015; Gueret and Brimble 2010; Torigoe et al., 1988). Early reports on CiTXs go back to the eighties (Torigoe et al., 1988) and their physicochemical characterization back to the nineties (Hu et al., 1995; Seki et al., 1995; Uemura et al., 1995). CiTXs exhibit strong neurotoxicity to mice by oral

or intraperitoneal administration at lethal doses provoking transient hyperactivity, followed by a decrease of the respiratory rate with prominent abdominal breathing leading to death by respiratory arrest within 3-5 minutes following i.p. administration (Kharrat et al., 2008; Selwood et al., 2010; Takada et al., 2001). In fact, cyclic imine toxins were long-time considered as false positives for lipophilic toxin monitoring by mouse bioassay forcing in the past the prophylactic closure of conchylicultural activities in Foveaux Strait, New Zealand (Seki et al., 1995) and Arcachon, France (Amzil et al., 2007). CiTXs display potent antagonism and broad selectivity towards muscle and neuronal nicotinic acetylcholine receptors (nAChRs) (Aráoz et al., 2011; Molgó et al., 2017; Stivala et al., 2015). Although not regulated in Europe, chronic exposition to CiTXs is of concern given their high affinity for neuronal and muscle nAChRs and their capacity to cross the intestinal and the brain blood barriers (Alonso et al., 2013; Munday et al., 2012).

In the European Union, liquid chromatography coupled to mass spectrometry (LC-MS/MS) has replaced mouse bioassay by for the simultaneous monitoring of internationally regulated marine biotoxins. Nevertheless, novel functional assays are needed to replace mouse bioassay for rapid detection of unknown marine neurotoxins directed against key receptors targets of the nervous system

(Campbell et al., 2011; Davidson et al., 2015). Herein is presented a short overview of receptor-based assays for the detection of CiTXs.

The receptor target of CiTXs

nAChR are ligand-gated cation-selective transmembrane pentameric proteins activated by acetylcholine. Muscle ($\alpha 1$) $2\beta 1\gamma\epsilon/\delta$ nAChR that mediate fast transmission at the skeletal neuromuscular junction necessary for muscle contraction, respiration and escape from predation, are a primary target for a wide array of neurotoxins including CiTXs (Albuquerque et al., 2009; Araújo et al., 2015; Changeux 2010). Neuronal nAChRs display a higher structural and functional diversity and broad brain occupancy. Neuronal nAChRs are homopentameric or heteropentameric and result from the assembly of $\alpha 2$ - $\alpha 7$, $\alpha 9$ and $\alpha 10$ subunits with $\beta 2$ - $\beta 4$ subunits. Neuronal nAChRs modulate neurotransmitters release participating in fundamental aspects of synaptic plasticity involved in attention, learning, memory, and development (Bertrand et al., 2015; Changeux and Christopoulos

2016). $\alpha 4\beta 2$ and $\alpha 7$ nAChR subtypes are major pharmacological targets for the treatment of Alzheimer disease, Parkinson disease, schizophrenia, epilepsy, and addiction.

Receptor-based methods for detection of CiTX

The development of ligand binding assays for nAChRs was headed by two important discoveries: *i*) the finding of biological tissues extremely rich in nAChRs, namely the electric organ of *Torpedo californica* and *T. marmorata*: nAChRs represent ~40% of the total protein content of *Torpedo*-electrocyte membranes, and are surrounded by their natural lipids and clustering proteins. Thereby, the receptors are stable and functional. *ii*) The characterization of α -bungarotoxin from the venom of the snake *Bungarus multicinctus*. (Changeux 2010). This peptide toxin is a highly potent competitive antagonist of nAChR and is used as toxin tracer even after functionalization with radioactive elements, biotin or fluorescent compounds. Since CiTXs are potent antagonists of nAChRs, several receptor assays were developed.

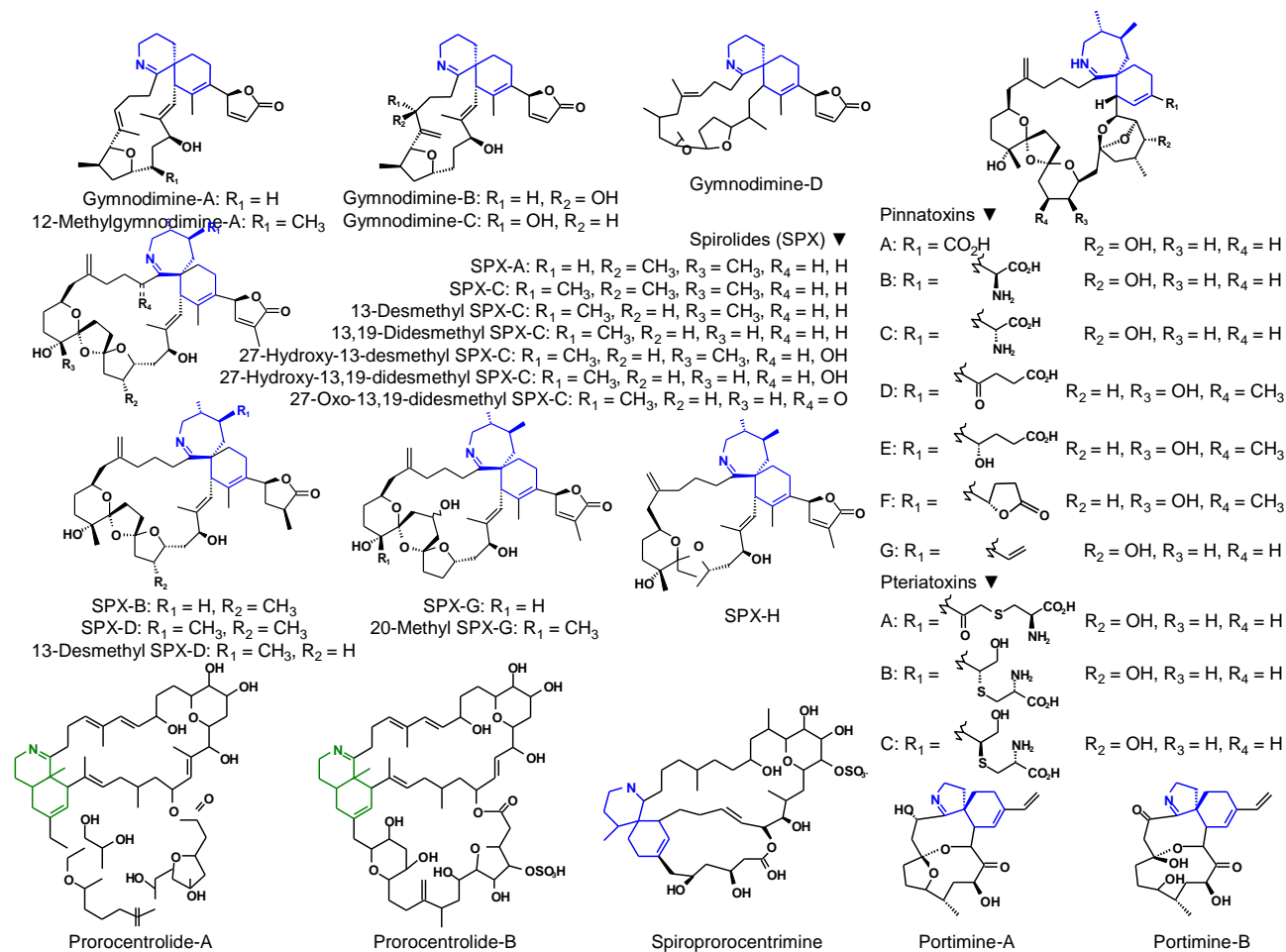


Fig. 1. Chemical structure of CiTXs.

Filtration radioactive ligand-binding assay.

This is the reference method for screening nAChR ligands. CiTXs are incubated to equilibrium with *Torpedo*-nAChR⁴. CiTXs inhibit the binding of ¹²⁵I-bungarotoxin to the ACh binding site of the receptor. Following radio ligand displacement, the complex receptor-radio ligand is retained on a filter membrane. Successive washing steps remove unbound radio ligand prior to scintillation counting from dried filters. Radioactive binding assay was essential to show the affinity and selectivity of CiTXs for muscle and neuronal nAChRs subtypes using eukaryotic cellular lines expressing neuronal nAChRs (Couesnon et al., 2016; Kharrat et al., 2008; Stivala et al., 2015).

Fluorescence polarization binding assay

Upon excitation by plane polarized light, a given fluorophore will emit fluorescence in the same plane as the exciting light: *i.e.*, α -bungarotoxin Alexa Fluor 488 conjugate tumbles rapidly in solution (4.1 ns fluorescent lifetime) and when excited by plane polarized light, the resulting emission fluorescence is low. The binding of α -bungarotoxin Alexa Fluor 488 to *Torpedo*-nAChR strongly decreases the rotation of the fluorophore tracer, and when excited by plane polarized light, the resultant emitted fluorescence will be high. The presence of gymnodimine-A, 13-desmethyl SPX-C or 13,19-didesmethyl SPX-C in the reaction mixture inhibited the binding of the fluorescent tracer to *Torpedo*-nAChR in a concentration-dependent manner. (Vilariño et al., 2009; Fonfria et al., 2010a). The use of fluorescein fluorophores to label *Torpedo*-nAChRs also enabled the detection of 13-desmethyl SPX-C and 13,19-didesmethyl SPX-C by Fluorescence polarization (Otero et al., 2011). The matrix effect of mussels, clams, cockles and scallops on the performance of the competitive fluorescence polarization assay was negative (Fonfria et al., 2010b).

Solid-phase receptor-based assay

The method consists on the immobilization of biotin- α -bungarotoxin on 96-well microplates coated with streptavidin. In the absence of CiTXs, *Torpedo*-nAChRs bind the toxin tracer to form the complex streptavidin-[biotin- α -bungarotoxin-*Torpedo*-nAChR]. The receptors are detected with primary antibodies anti-nAChR from *T. marmorata*. A conjugated secondary antibody allows the visualization of the captured receptors by chemiluminescence, fluorescence, or

colorimetry (Rodriguez et al., 2011). The presence of CiTXs in the reaction mixture inhibits the binding of biotin- α -bungarotoxin to *Torpedo*-nAChR reducing the secondary antibody-evoked signal. The method is suited for high-throughput survey of CiTXs using 384-well microplates on shellfish samples (Rodriguez et al., 2013a).

Flow cytometry receptor-based assay

Carboxylated microspheres are conjugated with *Torpedo*-nAChR or acetylcholine binding protein from the freshwater snail *Lymnaea stagnalis*. The conjugated microspheres are incubated with shellfish samples and later with biotin- α -bungarotoxin. After filtration, the fluorophore streptavidin-R-Phycoerythrin is added. The competitive binding is recorded by flow cytometry. The presence of CiTXs in the samples reduces the fluorescence yield in a concentration dependent manner. Further, it is possible to use microspheres beads owing different intrinsic fluorescence emission, consequently, different receptors or channel subtypes could be simultaneously analysed in the same sample (Rodriguez et al., 2013b).

Torpedo-microplate receptor binding-assay

Torpedo-nAChR are immobilized on the wells of plastic microplates. Biotinylated α -bungarotoxin is used as toxin tracer and streptavidin-horseradish peroxidase enables the detection and quantitation of anatoxin-a in surface waters, and of CiTXs in shellfish extracts (Aráoz et al., 2012; Rubio et al., 2014). CiTXs competitively inhibit biotinylated- α -bungarotoxin binding to *Torpedo*-nAChR in a concentration-dependent manner. The method compares favourably in terms of sensitivity to LC-MS/MS and provides accurate results for CiTXs monitoring (Aráoz et al., 2012). This functional assay is a high throughput method for rapid detection of known and emerging neurotoxins from marine and freshwater organisms that target nAChR directly in environmental samples with minimal sample handling, high sensitivity, reduced matrix effect and low cross-reactivity.

Neurotoxin fishing

A methodology for capturing novel ligands directed against nAChRs from complex mixtures containing small size alkaloids or large peptides was developed by using *Torpedo*-nAChR immobilized on the wells of plastic microplates (Aráoz et al., 2012) or *in-solution* (Echterbille et al., 2017). This methodology allows the direct

⁴ *Torpedo*-nAChR refers to *Torpedo marmorata*-electrocyte membranes rich in nAChR of muscle type.

capture of a toxin by the nAChR target. After washing under stringent conditions, the captured toxins are eluted by using solvents or by changing the pH. Afterwards, the eluates could be analysed for activity using electrophysiological techniques or by mass spectrometry to determine the chemical nature of the captured toxins.

Concluding remarks

The European Food Safety Agency that prompted the use of LC-MS/MS for monitoring internationally regulated marine biotoxins also encourages the development of novel functional assays. The bioassays presented here are rapid, cost-effective, high-throughput and user-friendly for the detection of cyclic imine toxins in complex matrices that could be used in routine monitoring of CiTXs and later confirmed by LC-MS/MS.

Acknowledgements

The authors acknowledge the LABEX LERMIT for funding DETECTNEUROTOX project and to Interreg/ Atlantic Area for funding the ALERTOX-NET EAPA_317/2016 project.

References

- Albuquerque, E.X., Pereira, E.F.R., Alkondon, M. et al. (2009). *Physiol. Rev.* 89, 73-120.
- Alonso, E., Otero, P., Vale, C. et al. (2013). *Curr. Alzheimer Res.* 10, 279-289.
- Amzil, Z., Sibat, M., Royer, F. et al. (2007). *Mar. Drugs* 5:168-179.
- Aráoz, R., Servent, D., Molgó, J. et al. (2011). *J. Am. Chem. Soc.* 133, 10499-10511.
- Aráoz, R., Ramos, S., Pelissier, F. et al. (2012). *Anal. Chem.* 84, 10445-10453.
- Aráoz, R., Ouanounou, G., Iorga, B.I. et al. (2015). *Toxicol. Sci.* 147, 156-167.
- Bertrand, D., Lee, C.H., Flood, D. et al. (2015). *Pharmacol. Rev.* 67:1025-1073.
- Campbell, K., Vilariño, N., Botana, L.M. et al. (2011). *Trac-Trends Anal. Chem.* 30, 239-253.
- Changeux, J.-P. (2010). *Annu. Rev. Pharmacol. Toxicol.* 50, 1-38.
- Changeux, J.-P., Christopoulos, A. (2016). *Cell* 166:1084-1102.
- Couesnon, A., Aráoz, R., Iorga, B.I. et al. (2016). *Toxins* 8, 249-263.
- Davidson, K., Baker, C., Higgins, C. et al. (2015). *Marine Drugs* 13, 7087-7112.
- Echterbille, J., Gilles, N., Araoz, R., et al. (2017). *Toxicon* 130, 1-10.
- Fonfria, E.S., Vilariño, N., Molgó, J. et al. (2010a). *Anal. Biochem.* 403, 102-107.
- Fonfria, E.S., Vilariño, N., Espiña, B. et al. (2010b). *Anal. Chim. Acta* 657, 75-82.
- Fribley, A.M., Xi, Y., Makris, C. et al. (2018). *ACS Med. Chem. Lett.* (*in-press*)
- Gueret, S.M., Brimble, M.A. (2010). *Nat. Prod. Rep.* 27, 1350-1366.
- Hu, T.M., Curtis, J.M., Oshima, Y. et al. (1995). *J. Chem. Soc., Chem. Commun.* 20, 2159-2161.
- Kharrat, R., Servent, D., Girard, E. et al. (2008). *J. Neurochem.* 107, 952-963.
- Molgó, J., Marchot, P., Aráoz, R. et al. (2017). *J. Neurochem.* 142 Suppl 2, 41-51.
- Munday, R., Selwood, A.I., Rhodes, L. (2012). *Toxicon* 60, 995-999.
- Otero, P., Alfonso, A., Alfonso, C. et al. (2011). *Anal. Chim. Acta* 701, 200-208.
- Rodriguez, L.P., Vilariño, N., Molgó, J. et al. (2011). *Anal. Chem.* 83, 5857-5863.
- Rodriguez, L.P., Vilariño, N., Molgó, J. et al. (2013a). *Toxicon* 25, 35-43.
- Rodriguez, L.P., Vilariño, N., Molgó, J. et al. (2013b). *Anal. Chem.* 85, 2340-2347.
- Rubio, F., Kamp, L., Carpino, J. et al. (2014). *Toxicon* 91, 45-56.
- Seki, T., Satake, M., Mackenzie, L. et al. (1995). *Tetrahedron Lett.* 36, 7093-7096.
- Selwood, A.I., Miles, C.O., Wilkins, A.L. et al. (2010). *J. Agric. Food Chem.* 58, 6532-6542.
- Stivala, C.E., Benoit, E., Aráoz, R. et al. (2015). *Nat. Prod. Rep.* 32, 411-435.
- Takada, N., Umemura, N., Suenaga, K. et al. (2001). *Tetrahedron Lett.* 42, 3495-3497.
- Torigoe, K., Murata, M., Yasumoto, T. et al. (1988). *J. Am. Chem. Soc.* 110, 7876-7877.
- Umemura, D., Chou, T., Haino, T. et al. (1995). *J. Am. Chem. Soc.* 117, 1155-1156.
- Vilariño, N., Fonfria, E.S., Molgó, J. et al. (2009). *Anal. Chem.* 81, 2708-2714.
- Zurhelle, C., Nieva, J., Tillmann, U. et al. (2018). *Mar. Drugs* 16, 446.

Sea turtle mortality in El Salvador: Analysis by receptor binding assay confirms saxitoxin findings

Oscar A. Amaya^{1*}, Marie-Yasmine Dechraoui Bottein², Rebeca Quintanilla¹, Gerardo Ruíz¹

¹ Laboratorio de Toxinas Marinas de la Universidad de El Salvador (LABTOX-UES). Facultad de Ciencias Naturales y Matemática, Final Av. Mártires y Héroes del 30 de julio, San Salvador, El Salvador;

² Environmental Laboratories, Department of Nuclear Science and Application, International Atomic Energy Agency, 98000 Monaco.

* Corresponding author's email: oscar.amaya@ues.edu.sv

Abstract

With the measured values of saxitoxin concentration of 3000 µg STX eq/kg of sample, it is likely that the turtles analyzed have died from toxins associated with microalgae. However, the level of saxitoxins in marine turtles is not well described in the scientific literature. By measuring concentration of paralytic type toxins, the fast operation of the receptor binding assay has allowed environmental authorities to rapidly respond to mass mortality of sea turtles in El Salvador. Analysis of microalgae in gastric and stomach contents of dead sea turtles revealed the presence of debris of diatoms and dinoflagellates. The highest cell concentrations correspond to diatoms *Dactyliosolen fragilissimus* with 110,235 cells/L and *Pseudo-nitzschia* spp. with 4,033 cells/L. The presence of potentially toxic or harmful species, such as *Alexandrium* sp. and *Gonyaulax* sp., was also detected but at low cell concentrations. It is presumed that the turtles acquired saxitoxins from a harmful algae bloom located far from the coastal area where they were stranded.

Keywords: RBA, receptor binding assay, sea turtle, marine biotoxins, saxitoxins

Introduction

At the end of October 2017, once again the coasts of El Salvador in Central America were affected by hundreds of dead sea turtles (Figure 1). In order to provide a rapid response to the phenomenon, the receptor binding assay (RBA; AOAC method 2011.27) was carried out to assess the presence of saxitoxins in turtle tissues. More than 25 dead green turtles (*Chelonia mydas*) samples, including organs, tissues and stomach contents were analysed. In parallel, the Ministry of the Environment of El Salvador sent to NOAA in USA a set of samples of dead sea turtles who confirmed the presence of saxitoxins, using ELISA and HPLC methods [Amaya et al, 2018]. Sea turtle mortalities are recurring in El Salvador, with events reported in 2005, 2006, 2009, 2010 and 2013, and each time saxitoxins were detectable in turtle organs [Amaya et al, 2014]. In the sea turtle mortality that occurred in 2013, the receptor binding assay (RBA) was run, determining high concentrations of paralyzing toxins and corroborating the results with the Marine Environment Laboratory of the IAEA (International Atomic Energy Agency) located in Monaco. This study provided information on toxins tissue distribution in marine turtles,

particularly for green turtle which is a globally endangered species.

Materials and Methods

Saxitoxins analyses

In the Marine Toxin Laboratory of the University of El Salvador (LABTOX-UES), 25 samples of green turtles (*Chelonia mydas*) from the Bay of Jiquilisco and Los Cóbano beach were received (2 blood samples, 2 liver samples, 1 intestine sample y 20 flipper samples). The samples were delivered by technical staff of the Wildlife Management Unit of the Ministry of Environment and Natural Resources (MARN) on November 6 and 7, 2017. All samples were taken from different dead sea turtles, with the exception of blood samples that were collected on a live sea turtle and one dying sea turtle; unfortunately, samples of sea turtle flesh were not available for analyses. Five grams of each sample were weighed and analysed using the RBA; except for the flipper samples that were pooled due to the reduced amount of tissue available.

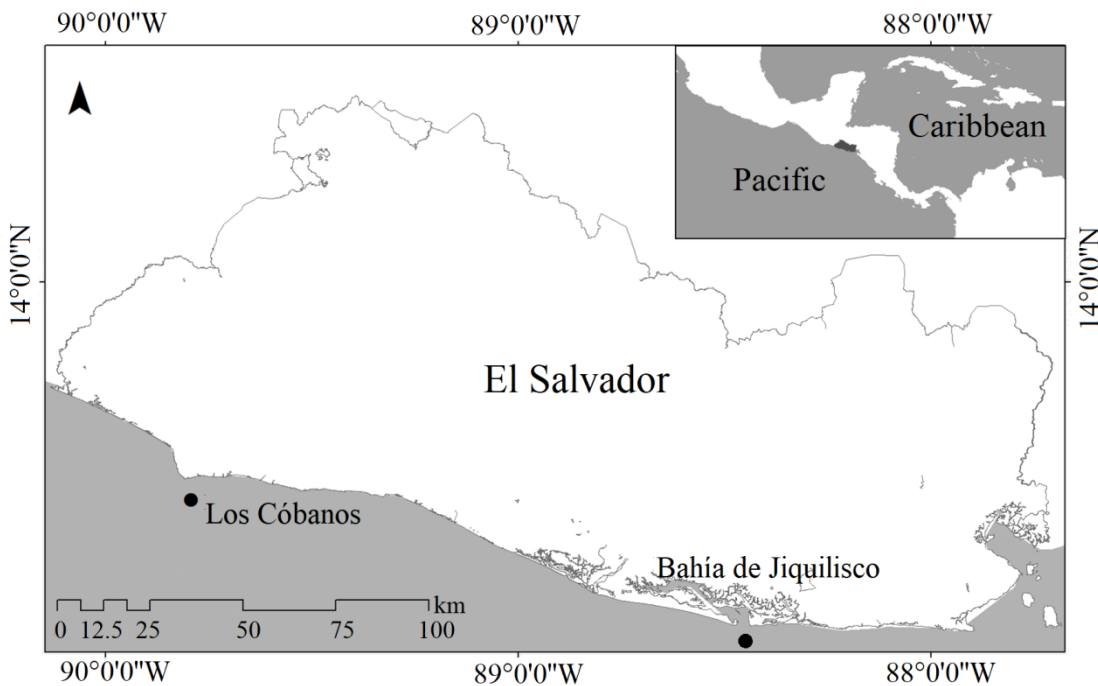


Fig. 1. Location of sites where *Chelonia mydas* individuals were found dead in October-November 2017.

The RBA is based on the interaction between saxitoxins and voltage-gated sodium channels (receptors) [Van Dolah et al, 2019]. Tritiated saxitoxins compete with unlabeled saxitoxins in the extracts for a finite number of available receptor sites in a brain membrane homogenate.

Unbound saxitoxins are removed by filtration and the remaining tritiated saxitoxin is measured with a scintillation counter (Figure 2A). The amount of radioactivity present is indirectly related to the amount of saxitoxin-like activity in the sample. The essential equipment and materials needed to conduct this assay are: a microplate scintillation counter 1450 LSC MicroBeta TriLux and a Multiscreen vacuum manifold. The reagents used are: [3H] STX, STX di-HCl standard solution, 0.003M HCl, a MOPS/choline chloride buffer, brain membrane homogenates and Optiphase liquid scintillation cocktail. Data analysis was conducted using Graphpad Prism software using non-linear regression with variable slope, which is based on the Hill equation for competitive binding assays.

Phytoplankton monitoring

A field sampling was carried out on the coast of Los C6banos, in the western coast of El Salvador, to monitor harmful microalgae, in cooperation with technicians from the Ministry of the Environment

(November 7, 2017, between 8:30 AM and 12:00 AM, Figure 1). Water samples were collected at two depths, along a 15 nautical mile transect perpendicular to the coastline. In addition, qualitative samples of seawater were taken using a phytoplankton net of 20 micrometers mesh. The samples were analyzed using a Carl Zeiss inverted microscope applying the Uterm6hl method.

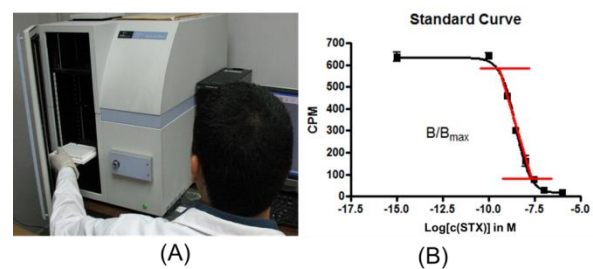


Fig. 2. (A) Equipment required includes basic labware and a microplate scintillation counter (MicroBeta TriLux 1450 LSC). (B) Saxitoxin receptor binding assay standard curve. Quality Control points include: Estimated reference, B_{max} . Slope 1.0 ± 0.2 . $EC_{50} \sim 2$ nM. Unknown sample are quantified only using data points that fall on the linear part of the curve ($B/B_{max} = 0.2-0.7$), where: $B = CPM$ in the sample $B_{max} = \max CPM$. RSD of replicates is <30 .

Results and Discussion

Saxitoxins analyses

Paralytic toxin activity (saxitoxin group) was detected in all sample types, with higher values in liver and blood (Figure 3). Maximum concentrations of 3652 μg STX eq/kg were found in blood sample from dying sea turtle. Data reported here are those that have an expanded uncertainty less than $k=2$, and flipper showed values below the limit of quantification ($70 \mu\text{g}$ STX eq/kg).

Some of the results presented here have been published elsewhere [Amaya et al. 2018] making a broader description of the problem related to the death of the turtles in 2013 and 2017; the samples of dead sea turtles were collected in similar circumstances with the difference that in El Salvador the RBA method was used and in the former the HPLC and ELISA methods were used.

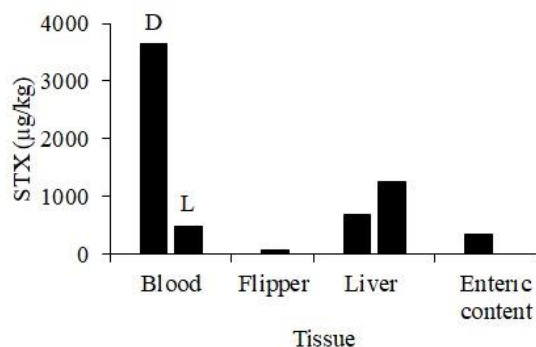


Fig. 3. Concentrations of saxitoxins found in green turtles (*Chelonia mydas*) using the Receptor Binding Assay. D: dying turtle, L: living turtle.

Phytoplankton analyses

The analysis of microalgae in gastric and stomach contents of dead sea turtles revealed the presence of debris of diatoms and dinoflagellates (whole cells of *Planktoniella sol*, *Scrippsiella trochoidea*, *Prorocentrum* c.f. *compressum* and *Prorocentrum* sp.; Figure 4). The highest cell concentrations correspond to diatoms *Dactyliosolen fragilissimus* with 110,235 cells/L and *Pseudo-nitzschia* spp. with 4,033 cells/L; it was not possible to identify *Pseudo-nitzschia* cells to species level, as well as we could not distinguish toxic from non-toxic species. Potentially toxic or harmful species, such as *Alexandrium* sp. and *Gonyaulax* sp. were identified however at low cell concentrations, both with 672 cell/L.

Though cell concentration of potentially toxic species was low, it is suspected that sea turtles were exposed to the toxin through a vector that

accumulated STX from an offshore toxic algae bloom that might have occurred several days before the mass mortality event, as it happened in 2013.

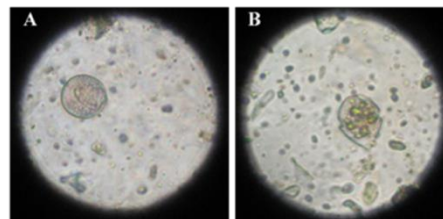


Fig. 4. Photographs taken under the microscope of microalgae found in intestinal and stomach contents of sea turtles. A) *Prorocentrum* sp. B) *Scrippsiella trochoidea*.

It has been suggested that zooplankton species such as jellyfish and tunicates, act as vectors of saxitoxins transferring the toxins from the primary producer dinoflagellates to sea turtles [Herrera-Galindo et al. 2015].

Further efforts are needed to monitor and understand the impact of HABs on endangered sea turtle species in order to aid in management and conservation.

Acknowledgements

This work was supported by the International Atomic Energy Agency (IAEA) Technical Cooperation regional project RLA/7022 “Strengthening Regional Monitoring and Response for Sustainable Marine and Coastal Environments”

The authors thank the staff of the Wildlife Management of the Ministry of Environment and Natural Resources (MARN), El Salvador.

References

- Amaya O, Quintanilla R, Stacy BA, Dechraoui Bottein M-Y, Flewelling L, Hardy R, Dueñas C and Ruiz G (2018). *Front. Mar. Sci.* 5:411. doi: 10.3389/fmars.2018.00411
- Amaya, Ruiz, Espinoza, Rivera (2014) *Harmful Algae News* 48: 6-7
- Espinoza, Amaya, Quintanilla, (2014). *Atlas of Marine Phytoplankton*. San Salvador. ELS. LABTOX
- Van Dolah, Fire, Leighfield, Mikulski, Doucette, (2012) *J. AOAC International* 95(3): 795-812
- Fux, E., Biré, R., Hess, P. (2009). *Harmful Algae* 8, 523-537.
- Herrera-Galindo JE et al. 2015. *Ciencia y Mar* 14(56) : 41-49.

Boronate techniques for clean-up and concentration of the *vic*-diol-containing tetrodotoxins from shellfish

Daniel G. Beach¹, Elliott S. Kerrin¹, Pearse McCarron¹, Jane Kilcoyne², Sabrina D. Giddings¹, Thor Waaler³, Thomas Rundberget^{3,4}, Ingunn A. Samdal³, Kjersti E. Løvberg³, Christopher O. Miles^{1,3,*}

¹ Biotoxin Metrology, National Research Council of Canada, Halifax, Nova Scotia, Canada

² Marine Institute, Rinville, Oranmore, Co. Galway, H91 R673, Ireland

³ Toxinology Research Group, Norwegian Veterinary Institute, Oslo, Norway

⁴ Norwegian Institute for Water Research, Oslo, Norway

* corresponding author's email: chris.miles@nrc.ca

Abstract

Boronates bind reversibly to *vic*-diols, a common structural feature of algal toxins. This boronate–diol interaction can be exploited for selective toxin clean-up and concentration. Boric acid gel (BAG) solid phase extraction (SPE) was recently shown to eliminate interferences and matrix effects in LC-MS analyses of azaspiracids (AZAs) in mussel extracts. Here, we report a modified approach for cleanup of tetrodotoxin (TTX) and many of its congeners, which also contain *vic*-diols. The reaction between TTX and boronic acids was first investigated in solution to optimize conditions for TTX binding. Then, TTX-contaminated mussel extracts were applied to BAG SPE columns. TTXs were selectively bound and released from the BAG to yield very clean extracts containing TTX analogues and very little else. Potential interferences in LC-MS analyses, such as arginine and other amino acids, were completely eliminated, making this a promising approach for analytical sample preparation.

Keywords: azaspiracid, tetrodotoxin, boronate, marine biotoxin, LC-MS, matrix effect, sample preparation

Introduction

vic-Diols react reversibly with borate and boronic acids (Espina-Benitez et al., 2017). Many marine algal toxins contain *vic*-diols, but only very recently has this been exploited for extraction and clean-up of such toxins from the complex matrices in which they are often found. Miles et al. (2018) showed that AZAs react reversibly with a polymeric boronic acid (Fig. 1), and this reaction was used in a 1-step SPE clean-up to greatly reduce the complexity of the resulting LC-MS chromatograms (Fig. 2). This procedure also greatly reduced signal suppression from the sample matrix during LC-MS analysis.

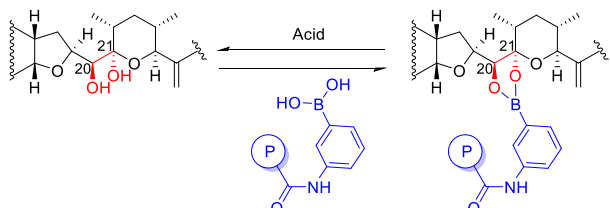


Fig. 1. Reversible reaction of the *vic*-diol (red) in AZA1 with BAG, a polymeric phenylboronic acid (blue).

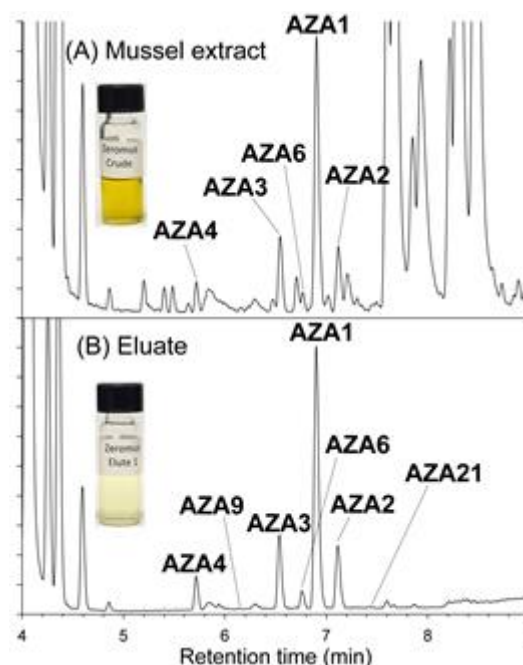


Fig. 2. Effect of BAG SPE on the colour of mussel extracts (insets) and on full scan LC-MS chromatograms of an AZA-contaminated mussel extract (modified from Miles et al. (2018)).

Tetrodotoxin (TTX) is a neurotoxin most commonly associated with puffer fish poisoning, but that has been detected in a wide range of marine and terrestrial organisms (Bane et al., 2014). TTX has recently been detected in European shellfish (Turner et al., 2017a) and an LC-MS method has been validated for routine analysis of TTX in shellfish (Turner et al., 2017b). The presence of arginine (Arg) in extracts was identified as the primary contributor to matrix suppression in LC-MS, and method development focused on optimizing the chromatographic separation between Arg and TTX to mitigate this. Given the success achieved with AZAs and because TTX also contains a *vic*-diol, we set out to investigate the feasibility of selective extraction of TTX with boronate-containing materials, and whether this could be used to remove Arg and other potential interferences.

Materials and Methods

Samples and reagents

BAG, phenylboronic acid, 2-naphthylboronic acid and pyrene-1-boronic acid ($\geq 95.0\%$) were from Sigma–Aldrich (Oakville, ON, Canada). A certified reference material calibration solution for TTX (CRM-TTX) was from the National Research Council of Canada (Halifax, Canada). Buffers were 0.1 M acetate (pH 5), phosphate (pH 6, 7 or 8), or borate (pH 9). Mussel tissue positive for TTX was simulated by blending $\sim 10\%$ of highly toxic sea slug (*Pleurobranchaea maculata*) tissue with control blue mussel (*Mytilus edulis*) tissue, as reported by Turner et al. (2017b). Mussel tissue homogenates were extracted with an equal volume of 0.1 M HCl, mixed with an OmniPrep tissue homogenizer and centrifuged at $6700 \times g$ for 10 min.

Boronate extractions and reactions

Solution-phase reaction kinetics were performed in 2:1 MeCN–phosphate buffer (pH 7) with 2 mM arylboronic acid at 20 °C unless otherwise specified. TTX was dissolved in borate buffer to test for reaction with borate, and in phosphate buffers in the absence of added boronic acids to test stability. SPE cartridges were prepared by packing BAG (0.5 g) in H₂O into 3-mL SPE tubes with frits, activated according to the manufacturer's instructions, and conditioned with phosphate buffer (10 mL, pH 7). Extracts (100 μ L) were diluted with pH 7 phosphate buffer (900 μ L), loaded onto the cartridges, washed with 50% MeCN (1 mL), and eluted with 0.1 M HCl (1 mL).

LC-HRMS analyses

LC-HRMS analyses were carried out using 1 μ L injections on an Agilent 1200 series HPLC (Palo Alto, CA, USA) coupled to a Thermo Scientific Q Exactive HF. A combined full scan and MS/MS method using the 60000 resolution setting, a full scan range of m/z 50 to 560 and a spray voltage of 3 kV were used. HILIC separations were performed with a Waters ACQUITY UPLC BEH Amide Column (1.7 μ m, 2.1 \times 100 mm) at 40 °C, with mobile phases of 50 mM ammonium formate in H₂O (pH 7) (A) and 95% MeCN–H₂O (B). Elution (0.3 mL/min) was with a linear gradient from 0 to 60% A in 10 min, 60% A for 4 min, and post-run equilibration at 0% A for 10 min. Reverse-phase (RP) separations used a Waters Symmetry Shield RP18 Column (3.5 μ m, 2.1 \times 150 mm) at 40 °C. Elution (0.4 mL/min) was with a linear gradient from 10 to 90% MeCN in H₂O over 20 min, 90% MeCN for 2 min, and post-run equilibration at 10% MeCN for 7 min.

Results and Discussion

Initial studies showed that TTX reacted rapidly with the borate in borate buffer, forming a stable complex that survived neutral (but not acidic) HILIC chromatography, and gave a prominent peak with m/z 346.1052 with a characteristic boron isotope pattern, corresponding to a 1:1 TTX–borate complex (Fig. 3). To aid MS/MS interpretation, a precursor ion selection window of 1.5 Da with a -0.5 Da offset was used to select both the base peak and the $M-1$ isotope peak in order to preserve the boron isotope pattern in boron-containing product ions. The MS/MS spectrum of the complex (Fig. 3C) showed a characteristic product ion at m/z 206.0730 with a boron isotope pattern, corresponding to an additional BO₂H compared with the main product ion of TTX at m/z 162.0661 (Fig. 3B). This indicated that complexation occurred at the vicinal 6,11-diol on TTX, as shown in Fig. 3.

The BAG used in the SPE clean-up has a phenylboronic acid functionality. To optimize conditions for TTX retention on BAG, the reaction kinetics of TTX with monomeric arylboronic acids was assessed in solution by LC-HRMS at a range of pH values and temperatures (Figs 4 and 5). While the TTX–borate complex was polar and could be readily analysed by HILIC, TTX complexes with naphthyl- and pyrenylboronic acids were relatively non-polar and were analysed by RPLC. However, the TTX–phenylboronic acid complex, which was the closest model for the interaction of BGA with TTX, was of intermediate polarity and could not be readily separated from the

phosphate buffer by either HILIC or RPLC. The kinetics of reactions between TTX and phenylboronic acid could therefore only be investigated by measuring the disappearance of TTX by HILIC–HRMS.

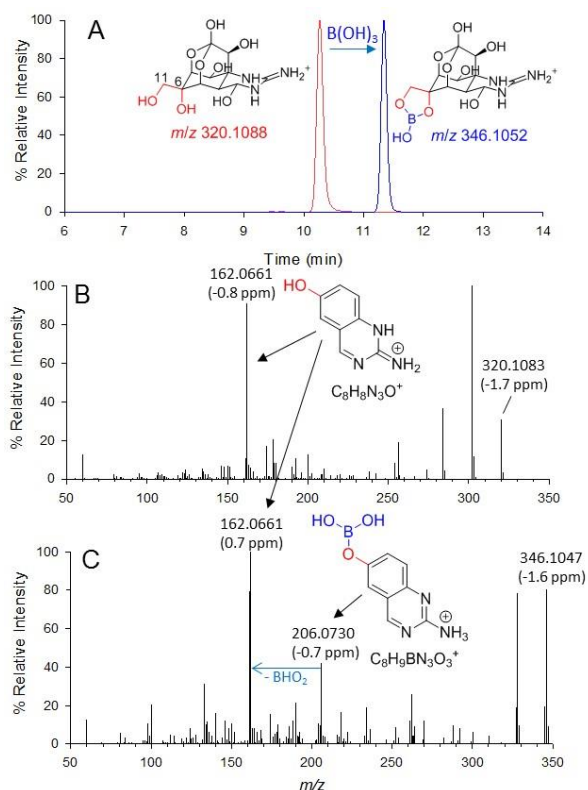


Fig. 3. HILIC–HRMS/MS analysis of TTX in borate showing overlaid extracted-ion full scan chromatograms of TTX before (red) and after (blue) reaction (A), and product ion spectra (CE 40 eV) of TTX (B) and its borate complex (C).

In all cases the data gave an excellent fit to pseudo-first-order kinetics. The rate and yield of the reaction with naphthylboronic acid increased with pH up to pH 7, but at pH 8 the yield was lower than at pH 7 despite the reaction rate being slightly faster (Fig. 4). This suggests partial decomposition of the TTX at pH 8. Clean-up experiments were therefore conducted at pH 7, and an investigation of TTX stability in the absence of boronic acid showed that TTX was sufficiently stable over the timescale required for sample clean-up at this pH.

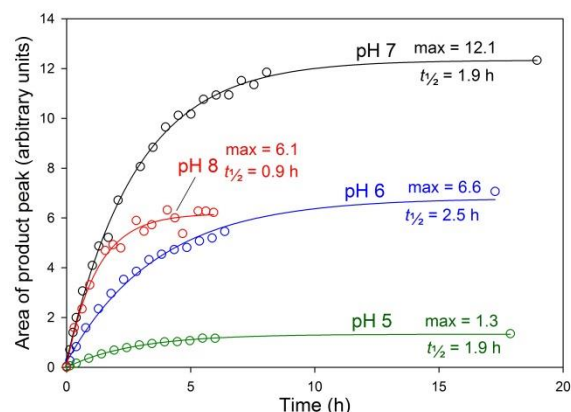


Fig. 4. Effect of pH on the concentration of the TTX–naphthylboronate complex with time.

As expected, LC–HRMS showed the rate of reaction of TTX with pyrenylboronic acid increased with temperature (Fig. 5). But even at 10 °C the half-life of the reaction was less than 1 hour. Thus, all the kinetic data indicated a normal equilibrium reaction between TTX and boronic acids that heavily favours complexation at pH 7, even at low concentrations of boronic acid.

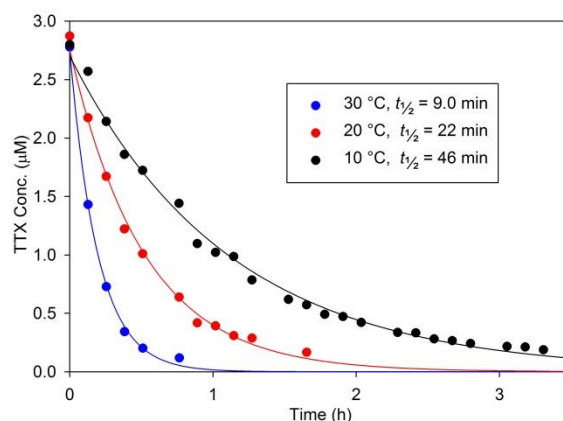


Fig. 5. Effect of temperature on the disappearance of TTX during reaction with pyrenylboronic acid.

The promising results obtained with borate buffer and arylboronic acids prompted trials of SPE clean-up of TTXs with BAG. Initial experiments showed complete retention of TTX and that elution with strong acid was required for acceptable recoveries, so 0.1 M HCl was used for elution of TTXs in extracts of mussels. These experiments showed excellent clean-up of TTX from the sample, and complete removal of Arg (Fig. 6) and other amino acids from extracts. However, recoveries were variable and low (30–80%), and TTX analogues without the *vic*-diol, such as the 11-deoxy- and 11-nor-TTXs, were not retained on the BAG SPE. Since amino acids such as Arg have been reported as the main contributors to signal suppression in

LC–MS analysis of TTX in shellfish (Turner et al., 2017b), removal of amino acids should reduce matrix suppression. Studies are underway to improve recoveries and optimize the BAG SPE for analysis of TTXs in shellfish and fish.

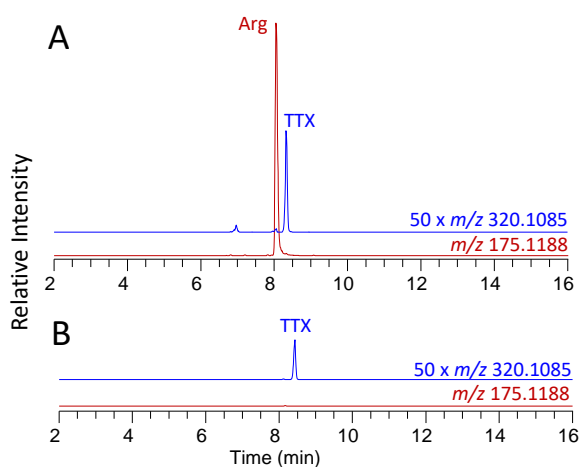


Fig. 6. Extracted-ion full scan HILIC–HRMS chromatograms of TTX and Arg before (A), and after (B), clean-up of the TTX-contaminated mussel tissue on a BAG SPE cartridge.

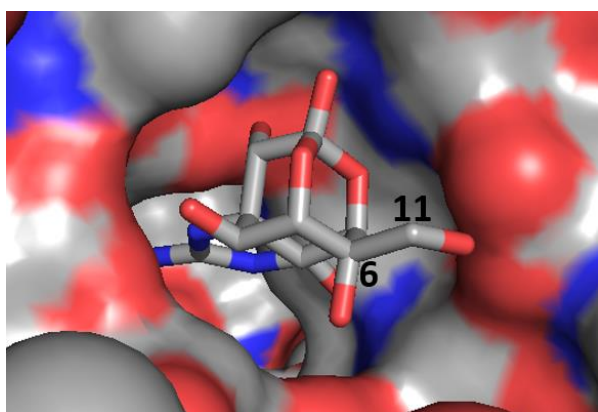


Fig. 7. Cryo-electron microscopy structure of TTX bound to the Na⁺ channel (Shen et al., 2018). The vicinal 6,11-diol of TTX, which is able to bind to borate (Fig. 3), is labelled.


Interestingly, Kobayashi et al. (2004) showed reduced toxicity to mice of TTX in seawater, and demonstrated that this was attributable to the presence of borate, an important buffer component present naturally in seawater. Our results showing that TTX readily complexes with borate (Fig. 3) help shed some light on the mechanism of this detoxification. Shen et al. (2018) showed that the *vic*-diol of TTX is involved in binding of TTX to voltage-gated sodium channels (Fig. 7), and complexation of the 6,11-diol to borate may account for the reduced toxicity. Borate complexation of other *vic*-diol-containing algal toxins in seawater can also be expected, and could profoundly affect their biological activities.

Acknowledgements

This work was supported by the First Call for Transnational Research Projects within the Marine Biotechnology ERA-NET, Project No. 604814 (“Enhanced Biorefining Methods for the Production of Marine Biotoxins and Microalgae Fish Feed”). The authors thank Michael J. Boundy (Cawthron Institute, Nelson, New Zealand) for the sea slug tissue.

References

- Bane, V., Lehane, M., Dikshit, M., Riordan, A., Furey, A., 2014. *Toxins* 6, 693-755.
- Espina-Benitez, M.B., Randon, J., Demesmay, C., Dugas, V., 2017. *Sep. Purif. Rev.*, 1-15.
- Kobayashi, T., Nagashima, Y., Kimura, B., Fujii, T., 2004. *Shokuhin Eiseigaku Zasshi* 45, 76-80.
- Miles, C.O., Kilcoyne, J., McCarron, P., Giddings, S.D., Waaler, T., Rundberget, T., Samdal, I.A., Løvberg, K.E., 2018. *J. Agric. Food Chem.* 66, 2962–2969.
- Shen, H., Li, Z., Jiang, Y., Pan, X., Wu, J., Cristofori-Armstrong, B., Smith, J.J., Chin, Y.K.Y., Lei, J., Zhou, Q., King, G.F., Yan, N., 2018. *Science* 362, eaau2596.
- Turner, A., Dhanji-Rapkova, M., Coates, L., Bickerstaff, L., Milligan, S., O’Neill, A., Faulkner, D., McEneny, H., Baker-Austin, C., Lees, D.N., Algoet, M., 2017a. *Mar. Drugs* 15, 277.
- Turner, A.D., Boundy, M.J., Rapkova, M.D., 2017b. *J. AOAC Int.* 100, 1469-1482.



Risk assessment for algal and cyanobacterial toxins

Monitoring the invasive cyanobacterium *Cylindrospermopsis raciborskii* – a case of dispersion into northern Portuguese freshwater systems

Cristiana Moreira¹, Cidália Gomes¹, Vitor Vasconcelos^{1,2}, Agostinho Antunes^{1,2*}

¹ CIIMAR/CIMAR, Interdisciplinary Centre of Marine and Environmental Research, University of Porto, Terminal de Cruzeiros do Porto de Leixões, Av. General Norton de Matos s/n, 4050-208 Matosinhos, Portugal;

²Department of Biology, Faculty of Sciences, University of Porto, Rua do Campo Alegre, 4169-007 Porto, Portugal.

*corresponding author's email: aantunes@ciimar.up.pt

Abstract

Cylindrospermopsis raciborskii is a freshwater cyanobacterium species known for its invasion from tropical to temperate environments. Some strains of this species are able to produce cyanotoxins. In Portugal (Southern Europe) its occurrence was firstly recorded in the South Region (Alqueva Reservoir, 2000) in where it is known to form blooms and where the water temperatures are usually higher than the rest of the country. In 2008, it was recorded in a lagoon (Vela Lagoon) in the Centre Region of Portugal. An ongoing project (CYANOTOX) aims to survey cyanobacteria in freshwater systems of North and Centre Portugal with a focus on *C. raciborskii*. Molecular methods (PCR), microscopic observation, strain isolation and collection of bloom samples has allowed the evaluation of the presence and invasive nature of *C. raciborskii* in Portuguese freshwater systems and these were applied between May to September of 2017. Molecular identification of *C. raciborskii* was achieved through PCR amplification of the RNA polymerase *rpoC1* gene in all water samples. Molecular data showed the appearance of *C. raciborskii* in northern ecosystems while microscopic observation failed in identifying this cyanobacterium species in the same samples. Microscopic isolation found again *C. raciborskii* in Vela Lagoon. In conclusion, this study found some evidence of the dispersion of *C. raciborskii* into northern ecosystems, reflecting adaptation mechanisms and supports its biogeographical invasion in Portuguese freshwater systems. Also genomic tools proved to be valuable in determining the invasion of *C. raciborskii*.

Keywords: *Cylindrospermopsis raciborskii*, PCR, Portugal.

Introduction

Cylindrospermopsis raciborskii is a filamentous bloom forming cyanobacterium globally associated with the production of two cyanotoxins: cylindrospermopsins (Asia, Oceania) and saxitoxins (South America) (Hawkins et al. 1985; Lagos et al. 1999). On a biogeographical perspective its invasion to temperate environments is its main characteristic since it was first recorded in tropical ecosystems (Padisak, 1997). In Europe its first records were in Greece in 1937 (Antunes et al., 2015) being since then continuously detected throughout the continent where some blooms have been known to occur such as in Germany and Portugal among others. In Portugal (Southern Europe) its first record was in the South Region (Alqueva Reservoir, 2000) where it is known to form blooms and where trace amounts of CYN (Cylindrospermopsin) have been detected in water but not attributed to *C. raciborskii* though tests

were conducted on isolated strains and showed negative for CYN presence (Caetano et al., 2015). Later in 2008 this cyanobacterium species was found to occur in a lagoon in the Centre Region of Portugal (Vela Lagoon) also without forming blooms and with higher CYN values however, still not attributed to *C. raciborskii* (Freitas, 2009; Moreira et al., 2017). In cyanobacteria surveillance molecular and analytical methods can be used as well as microscopic manipulation techniques and field observation. Despite having so far no associated toxicity in Portuguese freshwater systems being a well-known invasive cyanobacterium its surveillance in North ecosystems of Portugal is therefore demanded. Recently a national funded project (CYANOTOX 2016-2019) has allowed the monitoring of *C. raciborskii* in Portugal including the North Region. Therefore with the purpose of monitoring *C.*

raciborskii in Portuguese freshwater systems samples from seven highly impacted ecosystems (water provision, drinking, recreation) were analysed in order to determine the potential dispersion of *C. raciborskii* with special emphasis to the North and Central Regions.

Materials and Methods

Sampling

A total of seven freshwater systems located in the North (River Tâmega, Torrão Reservoir, Porto City Park separate Lakes 1, 2 and 3) and Centre (Mira Lagoon, Vela Lagoon) Regions of Portugal were sampled between the months of Spring and Summer (May to September of 2017) (Fig. 1).

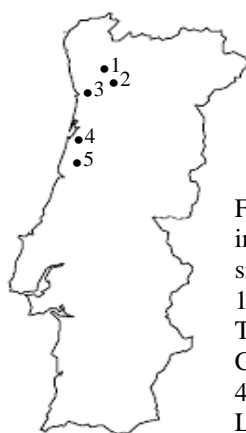


Fig. 1. Map of Portugal indicating all the sampling sites included in this study: 1 - River Tâmega; 2 - Torrão Reservoir; 3 - Porto City Park Lakes 1, 2 and 3; 4 - Mira Lagoon; 5 - Vela Lagoon.

Up to 6 L of superficial water was collected once a month from the near shore of each ecosystem. All have distinct impact on human use such as water provision, drinking and recreation. Plankton was additionally collected with a plankton net. All samples were transported to the laboratory under appropriated conditions such as low light and low temperature. In total, 35 water and plankton net samples were collected during May to September of 2017.

Sample processing

Water samples were filtered with Munktell® MGC (Falun, Sweden) micro-glass fiber paper filters. The filtered biomass was kept at -20°C before proceeding to DNA extraction. Filtered water volumes were inferior to 1 L in each sampled location. Plankton samples were visualized under a light microscope to observe the presence of *C. raciborskii* and other cyanobacteria. When present the isolates were transferred and subcultured in Z8 culture medium (Kotai, 1972). Culturing conditions occurred under a $25 \pm 1^{\circ}\text{C}$ and illuminated under a 14h:10h light-dark cycle with an average photon flux density of $10 \mu\text{mol m}^{-2} \text{s}^{-1}$.

DNA extraction

Filters were defrosted and scraped with a sterile scalpel to remove the filtered biomass and placed in a sterile eppendorf. DNA was extracted with the PureLink™ Genomic DNA Mini Kit (Invitrogen, Carlsbad, California, USA) following the protocol for Gram-negative bacteria in accordance with the manufacturer recommendations. A 50 μL of eluted DNA was stored at -20°C before PCR amplification.

PCR amplification

All PCR reactions were performed in a volume of 20 μL containing 1 x PCR buffer, 2.5 mM MgCl_2 , 250 μM of each deoxynucleotide triphosphate, 10 pmol of each primer and 0.5 U of *Taq* DNA polymerase (Bioline, Luckenwalde, Germany). Presence of total cyanobacteria were detected initially through PCR amplification of the 16S rRNA gene marker followed by the specific amplification of *C. raciborskii* through the gene marker RNA polymerase *rpoC1*. PCR conditions of the 16S rRNA were as follows: initial denaturation at 95°C for 2 min and 35 cycles at 92°C for 20 s, 50°C for 30 s and 72°C for 60 s (Jungblut et al., 2005; Neilan et al., 1997). PCR conditions of the RNA polymerase *rpoC1* were the following: initial denaturation at 95°C for 2 min and 35 cycles at 95°C for 90 s, 45°C for 30 s and 72°C for 50 s (Wilson et al., 2000). In the RNA polymerase *rpoC1* amplification of a positive sample was added and that was DNA of a *C. raciborskii* obtained from the Blue Biotechnology and Ecotoxicology Culture Collection (LEGE-CC) (LEGE strain 97047) (Ramos et al., 2018). Its specificity has already been established by Wilson et al., (2000). Water was used as a negative control in all PCR reactions.

Results and Discussion

During the period of May to September of 2017 a total of seven freshwater systems with distinct impacts on human use (water provision, drinking, recreation) were screened. In these water and plankton net samples were collected to determine the presence of *C. raciborskii* in each ecosystem. Previous surveillance has showed that this cyanobacterium species is commonly found in the South Region of Portugal and also in a lagoon of the Centre Region (Vela Lagoon) (Freitas 2009; Saker et al., 2003; Valério et al., 2005). Prior surveillance in the North Region of Portugal and conducted sporadically has failed in identifying this cyanobacterium species (personal communication). Between May and September of

2017 blooms were found to occur in 24% of the samples in distinct sampling sites and in none of them *C. raciborskii* was a bloom forming species. Bloom composition either belonged to the genera *Microcystis* spp., *Dolichospermum* spp., and/or *Chrysochloris* spp.. A cause of concern is if temperatures rise as it seems to be common lately in Portugal with low precipitation in the colder months and hot events in the warmer months the probable appearance of *C. raciborskii* in the North Region of Portugal may probably become a common phenomenon. Also supporting these data is the molecular evaluation of the presence of total cyanobacteria and *C. raciborskii* in both regions. The results showed that all 35 water samples were positive for the 16S rRNA marker, while the *C. raciborskii* RNA polymerase *rpoC1* gene was detected in all the ecosystems analysed (Table 1). Frequency of detection was higher in the Porto City Park Lake 1 and Vela Lagoon with three sampling months testing positive and in the Porto City Park Lake 3 with two sampling months showing positive results (Table 1). In the remaining ecosystems the frequency of detection was of only one month. In terms of seasonal variation, the earliest detection was in Mira and Vela Lagoon in May (late spring) both located in the Centre Region. In all sampling sites *C. raciborskii* was detected both in the early and mid-summer and Porto City Park Lakes 1 and 3 and Vela Lagoon had its late detection (September) spite the normal climate conditions in the positive months. Previous data shows that in Vela Lagoon (Centre Region) *C. raciborskii* appears in the end of summer (September - October) in higher densities (10^6 and 10^7 cells/mL) (Moreira et al., 2011).

In our study plankton net samples were simultaneously collected and observed under light microscopy for the presence of *C. raciborskii*. The results showed that in all samples the presence of this cyanobacterium species was not observed except in Vela Lagoon where one isolate was obtained in August and subsequently cultured in Z8 culture medium under appropriated culture conditions. The sample gave also a positive PCR amplification of the gene associated with *C. raciborskii* presence (Table 1).

In summary *C. raciborskii* was not observed in the North Region through microscopic observation. However several positives for *C. raciborskii* presence were obtained with molecular method in all sampling sites at least in one of the sampled months.

Table 1. Description of *C. raciborskii* PCR positive months in all water samples.

Geographic Origin	Sampling Site	PCR Positive Months
North	River Tâmega	Jun
	Torrão Reservoir	Sep
	Porto City Park Lake 1	Jun, Jul, Sep
	Porto City Park Lake 2	Jun
	Porto City Park Lake 3	Aug, Sep
Centre	Mira Lagoon	May
	Vela Lagoon	May, Aug, Sep


This new data suggests to include the screening of this cyanobacterium species in the north freshwater systems of Portugal in future monitoring campaigns. The molecular methods employed in our study showed to be valuable in determining *C. raciborskii*. Also with this study it is highlighted the importance of the dispersion of *C. raciborskii* in the Centre Region, where Mira Lagoon had one positive amplification (month of May) and where previous surveillance has failed in its detection (Table 1). In this sense with this study it is suggested some evidence of dispersion of *C. raciborskii* in Portuguese freshwater systems where it was initially a cyanobacterium species associated with warmer water conditions being particularly found in the South Region where it is well-known to form blooms (Caetano et al., 2015). However the warmer weather conditions observed in the North Region, particularly in the sampled year (2017) may have favoured the spread of this cyanobacterium species to the North Region. Biogeographically several vectors are described being associated with the dispersion of cyanobacteria such as winds, water courses, birds or even humans (Kristensen, 1996). Strain isolation and toxicity analysis are necessary to determine if *C. raciborskii* is a toxic cyanobacterium species in northern Portuguese freshwater systems.

Acknowledgements

This research was funded by the PTDC/AAG-GLO/2317/2014 (POCI-01-0145-FEDER-016799) project, partially supported by the Strategic Funding UID/Multi/04423/2013 through national funds provided by FCT – Foundation for Science and Technology and European Regional Development Fund (ERDF), in the framework of the programme PT2020, and by the Postdoctoral fellowship to Cristiana Moreira (Ref. SFRH/BPD/122909/2016) from FCT.

References

- Antunes, J.T., Leão, P.N., Vasconcelos, V.M. (2015). *Front Microbiol.* 18(6): 473.
- Caetano, S. (2015). Dissertation, University of Algarve, Portugal.
- Freitas, M. (2009). Dissertation, University of Porto, Portugal.
- Hawkins, P.R., Runnegar, M.T.C., Jackson, A.R.B., Falconer, I.R. (1985). *Appl. Environ. Microbiol.* 50, 1292–1295.
- Lagos, N., Onodera, H., Zagatto, P.A., Andrinolo, D., Azevedo, S.M., Oshima, Y. (1999). *Toxicon* 37(10),1359-1373.
- Jungblut, A.- D., Hawes, I., Mountfort, D., Hitzfeld, B., Dietrich, D.R., Burns, B. P. and Neilan, B. A. (2005). *Environ. Microbiol.* 7(4), 519–529.
- Kristiansen, J. (1996). *Hydrobiologia* 336 (1-3), 151-157.
- Kotai, J. (1972). Norwegian Institute for Water Research, Oslo.
- Moreira, C., Martins, A., Azevedo, J., Freitas, M., Regueiras, A., Vale, M., Antunes, A., Vasconcelos, V. (2011). *Appl. Microbiol. Biotechnol.* 92(1), 189-197.
- Moreira, C., Mendes, R., Azevedo, J., Vasconcelos, V., Antunes, A. (2017) *Toxicon* 130, 87-90.
- Neilan, B.A., Jacobs, D., Del Dot, T., Blackall, L.L., Hawkins, P.R., Cox, P.T., Goodman, A.E. (1997). *Int. J. Syst. Bacteriol.* 47(3), 693-697.
- Padisak, J. (1997). *Archiv für Hydrobiologie/Suppl* 107, 563-593.
- Ramos, V., Morais, J., Castelo-Branco, R., Pinheiro, Â., Martins, J., Regueiras, A., Pereira, A.L., Lopes, V., Frazão, B. Gomes, D., Moreira, C., Costa, M.S., Brûle, S., Faustino, S. Martins, R., Saker, M., Osswald, J., Leão, P.N., Vasconcelos, V.M. (2018). *J Appl Phycol.* 30(3),1437-1451.
- Saker, M.L., Nogueira, I.C.G., Vasconcelos, V.M., Neilan, B.A., Eaglesham, G.K., Pereira, P. (2003). *Ecotox. Environ. Safe.* 55, 243–250.
- Valério, E., Pereira, P., Saker, M.L., Franca, S., Tenreiro, R. (2005). *Harmful Algae* 4, 1044–1052.
- Wilson, K.M., Schembri, M.A., Baker, P.D., Saint, C.P. (2000). *Appl. Environ. Microbiol.* 66(1), 332–338.



Ciguatera and related benthic HAB organisms and toxins

Application of a Receptor Binding Assay to the Analyses of Ciguatera toxin in Reef fish, Thailand

Wutthikrai Kulsawat^{1*}, Boonsom Porntepkasemsan¹, Phatchada Nochit¹

¹Thailand Institute of Nuclear Technology (Public Organization), Nakhon-Nayok 26120, Thailand

* corresponding author's email: wutthikrai@tint.or.th

Abstract

Ciguatoxins are marine toxins which accumulate in many types of tropical reef fish and cause ciguatera fish poisoning (CFP) in humans. However, CFP has been largely neglected in many countries due to lack of standard testing protocol. This study examined 72 carnivorous reef fish belonging to 4 distinct species i.e. grouper, snapper, streak spinefoot, and trevally. Fish samples were wild caught from the coastal waters of Thailand. Extracts from 20 gram fish flesh of 27 grouper, 15 snapper, 15 streak spinefoot and 15 trevally were purified and analyzed for the presence of ciguatera toxins (CTXs). A receptor binding assay in microplate format was used in this study. Results showed that CTXs could not be detected in the seventy-two fish samples analyzed. The negative control test was conducted by analyzing random samples under a different method. Those samples were subjected to chemical analysis via liquid chromatography tandem-mass spectrometry (LC/MS/MS) which revealed negative results as the previous tests. This study confirmed the receptor binding assay technique be an effective tool for CTX monitoring programme.

Keywords: Receptor binding assay, Reef fish, Thailand

Introduction

Ciguatera fish poisoning (CFP) is an illness caused by consumption of tropical and subtropical fish that have accumulated lipophilic polyester ciguatera toxins named ciguatoxins (CTXs). CTXs bind voltage gated sodium channels causing an influx of Na⁺ into the cell, disrupting cellular functions including signal transmission in nerves (Lewis, R.J., 2000). Typical CFP cause gastrointestinal, cardiovascular (bradycardia with hypotension), and neurological (paraesthesia) symptoms that can last from weeks to months, including the diagnostic hot cold temperature reversal (dysesthesia) (Bagnis et al., 1979). Treatment of CTX poisoning is mainly supportive and symptomatic.

It was estimated that at least 25,000 CFP cases occur each year worldwide. CTX comes from a benthic microalgae (dinoflagellate) in the genus *Gambierdiscus* and *Fukuyoa*. These dinoflagellates grow epiphytically on macroalgae in coral reef environments of tropical and subtropical areas. This microbial biomass is digested by herbivorous fish, which passes up to carnivorous fish and ultimately to humans. The destruction of coral reefs from fishery activities and tourism allows for greater growth of the algae carrying dinoflagellates (David et al., 2009). Many types of reef fish are susceptible to accumulate CTXs which have been reported in 207 fish species

worldwide. This includes Spotted sicklefish (*Drepane punctate*), Streak spinefoot (*Siganus javus*), trevally (*Caranx atropus*), Brown stripe snapper (*Lethrinus vitta*), Russell's snapper (*Lutjanus russellii*), Sixbar grouper (*Epinephelus sexfasciatus*), Coral hind grouper (*Cephalopholis miniata*), Orange spotted grouper (*Epinephelus coioides*), Greasy grouper (*Epinephelus tauvina*), and Longfin grouper (*Epinephelus quoyanus*).

There is no regulatory limit for CTXs in fish, but a guidance level of 0.01 ppb P-CTX-1B equivalents, based on a 10-fold reduction of the lowest concentration of CTXs in meal remnants found to cause human illness has been recommended by the United States Food and drug Administration (Dickey, R.W., Plakas, S.M., 2010). The endemic areas of ciguatera are oceans in the latitudes between 35⁰ north and south of the equator. Thailand is located in the range of latitude 5⁰ to 20⁰ north of equator and longitudes 97⁰ to 105⁰ east, a ciguatera endemic area.

In the present study, 72 carnivorous reef fish wild-caught from the upper Gulf of Thailand belonging to 4 distinct species i.e. grouper, snapper, streak spinefoot, and trevally were investigated. The radioligand-receptor binding assay (RBA) technique was used in this study since it has been proved to be an effective screening tool and

provides a timely and sensitive alternative method to the mouse bioassay.

Materials and Methods

Study area

The upper gulf of Thailand (Fig.1) is bounded by geographic coordinates of longitude 100° 00' to 101° 00' and latitude 12° 30' to 13° 30' N. It covers an area of 10,000 km² and is surrounded by land to the North, East, and West. It opens into the South China Sea to the south and southeast. It has an average depth of about 20 m and average tidal heights of about 1 to 3 meters (Suwanlertcharoen, T and Prukpitikul, S. 2018).

The climate in the Gulf of Thailand is influenced by the northeast and southwest monsoons. The southwest monsoon originates from the Indian Ocean and brings moisture and rain to Thailand from May to August. Southwest monsoon winds can circulate either clockwise or counter clockwise depending on various prevailing atmospheric conditions. The northeast monsoon, which lasts from November to January, brings high-pressure, counter-clockwise rotating winds that cover the entire upper gulf of Thailand. High frequency radar measurements obtained in 2013 show that surface current patterns in the upper gulf of Thailand were consistent with the seasons of Thailand. The average current velocities were higher for the northeast monsoon than for the southwest monsoon (Kongprom et al., 2015).

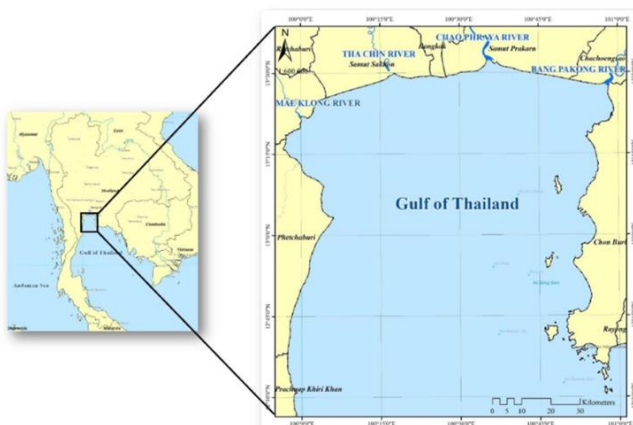


Fig. 1. Maps showing the location of the Upper Gulf of Thailand

Fish sampling in the upper Gulf of Thailand

A total of 72 wild caught fish samples included 4 species of fish (27 of grouper, 15 of snapper, 15 of streak spinefoot and 15 of trevally) were collected from the upper Gulf of Thailand in 2016. Specimens were identified according to the collector, and the date and location of collection

was recorded. Upon collection, samples were placed in Ziploc bags, and transported to the laboratory on ice where they were weighed, measured and frozen at -80°C prior to analyses for CTXs. Information was logged into a database in our system,

Fish extraction for RBA

Tissue samples were extracted and analysed using an RBA microplate format according to the IAEA TecDoc 1729 (2013) protocol, Fig. 2.

The RBA technique involves isolated brain membrane containing abundant Na⁺ channels and a fixed amount of tritiated PbTx-3 ([³H]-PbTx-3). Unlabeled CTXs present in the samples compete quantitatively with the radiolabelled [³H]-PbTx-3 for site 5 on the sodium channel receptor. Therefore, the binding of radiolabelled PbTx-3 is inversely related to the concentration of unlabelled CTXs in the sample. This method is adapted from the PbTxs RBA because CTXs and PbTxs bind to the same sodium channel receptor site (Van Dolah and Ramsdell 2001).

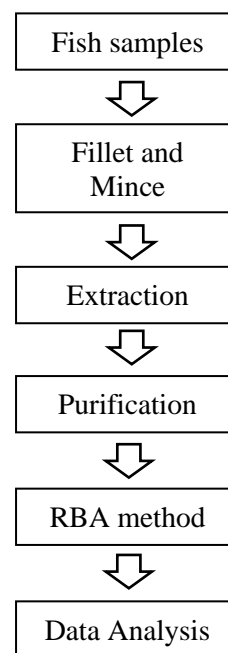


Fig. 2 Schematics of fish processing procedures used to produce fish extracts for the various toxicity evaluations performed.

The negative control test was performed by analysing the randomized negative samples using liquid chromatography tandem-mass spectrometry (LC/MS/MS) (personal communication: Supanoi Subsinghserm).

Data analysis

The software GraphPad Prism (GraphPad Software, Inc., La Jolla, California, USA) was used to generate curves and to perform data analysis by

using non-linear regression with a variable slope, which is based on the Hill equation for competitive binding assays.

Results and Discussion

Of seventy-two fish samples examined, no sample tested positive for CTXs using the RBA method. To rule out that the lipid matrix or extraction solvents might affect the RBA results, the same extraction procedures were followed for a pelagic fish collected from a Hazard Analysis Critical Control Point (HACCP) aquaculture farm that was not expected to be contaminated with CTXs. Results were scored as follows: negative, borderline and positive. The specimens with borderline or positive results were repeatedly tested in triplicate. If the repeated result turns to negative, it was considered as negative. If all repeated results remained borderline or positive, it was considered as borderline or positive.

The negative control test was conducted by analyzing random samples under differing method. Those samples were subjected to chemical analysis via liquid chromatography tandem-mass spectrometry (LC-MS/MS) which revealed negative results as the previous tests. Due to matrix effect potentially masking the activity of CTXs, further investigation of the matrix effects on LC-MS/MS method will be conducted when sufficient amounts of CTXs analogues are available. Nonetheless matrix effect on RBA method was verified in this study using the lean fresh waterfish. Note that rather small seasonal variation of seawater in terms of temperature, salinity and major ion elements were observed.

The RBA method represents an alternative technique for estimating CTX concentrations and has been used successfully in recent years (Diaz-Asencio et al., 2018; Darius, et al., 2007). In conclusion, the RBA can be used to rapidly screen fish for the presence of ciguatoxins.

Acknowledgements

This study was carried out under the IAEA RAS7026-project. The authors would like to thank Ms. Marie-Yasmine Dechraoui Bottein and Mr. Abdul Ghani Shakhshiro for their invaluable assistance and advice during this study. The authors would like to thank S. Subsinghserm of FIQD for LC-MS/MS analysis (to be published separately). Special thanks are also extended to the editor and two anonymous reviewers for their insightful critiques and constructive comments to substantially improve the quality of the earlier version of the manuscript.

References

- Lewis, R.L. (2000). *The Drug Monit* 22, 61-64
Doi: 10.1097/00007691-200002000-00013
- Bagnis, R., Kuberski, T., Laugier, S., (1979). *Am. J. Trop. Med. Hyd.* 28, 1067-1073.
- David, R.M., Winter, M.J., Chipman, J.K., (2009). *Environ Toxicol. Chem.* 28, 1893-1900.
- Dickey, R.W. and Plakas, S.M., (2010). *Toxicol* 56, 123-136.
- Suwanlertcharoen, T. and Prukpitikul, S. (2018). *J. Environ Nat. Resources.* 16(1), 9-20.
- Kongprom A, Prukpitikul S, Buakaew V, Kesdech W, Suwanlertcharoen T. (2015). *Proceeding of the 35th Asian conference on Remote Sensing; 2015 Oct 19-22, Manila: Philippines.*
- IAEA-TECDOC-1729 (2013) International Atomic Energy Agency, Vienna Austria.
- Díaz-Asencio, L., Clausing, R.J., Ranada, Ma. L., Alonso-Hernandez, C.M., Dechraoui Bottein M.Y. (2018). *J. Environ Radioact.* 192, 289-294.
Doi: 10.1016/j.jenvrad.2018.06.019
- Darius, H., Ponton, D., Revel, T., Cruchet, P., Ung, A., Fouc, M.T., (2007). *Toxicol.* 50, 612–626.
- VanDolah, F, and Ramsdell, J. S., (2001). *J. AOAC Int.* 84, 1617–1625.

Global distribution of the genera *Gambierdiscus* and *Fukuyoa*

Patricia Tester^{1*}, Lisa Wickliffe², Jonathan Jossart², Lesley Rhodes³, Henrik Enevoldsen⁴, Masao Adachi⁵, Tomohiro Nishimura³, Francisco Rodriguez⁶, Mireille Chinain⁷, Wayne Litaker⁸

¹ Ocean Tester, LLC, 295 Dills Point Road, Beaufort, North Carolina 28516, USA;

² CSS, Inc., Beaufort, North Carolina 28516, USA;

³ Cawthron Institute, 98 Halifax Street East, The Wood, Nelson 7010, New Zealand;

⁴ IOC, UNESCO, University of Copenhagen, Universitetsparken 4, 2100, Copenhagen, Denmark;

⁵ Kochi University, Laboratory of Aquatic Environmental Science, Monobe, Otsu-200, Nankoku, Kochi 783- 8502, Japan;

⁶ Centro Oceanografico de Vigo, Instituto Espanol de Oceanografia, Subida a Radio Faro 50, 36390 Vigo, Spain;

⁷ Laboratoire des Micro-algues Toxiques, Institut Louis Malarde, BP 30 - 98713 Papeete-Tahiti, French Polynesia;

⁸ NOAA, National Ocean Service, 101 Pivers Island Road, Beaufort, North Carolina 28516, USA.

* corresponding author's email: Ocean.Tester@gmail.com

Abstract

Historically, species in the genus *Gambierdiscus* Adachi & Fukuyo were viewed as pantropical organisms distributed between 35°N and 34°S and ubiquitous throughout the Caribbean, the Hawaiian Islands, French Polynesia, Australia and the Indian Ocean. Between 2016 and 2017 four new species were added to the genus *Gambierdiscus* from the South Pacific Ocean. In addition, four new species have been described in areas where *Gambierdiscus* was previously unknown, including two from the Canary Islands, one from Japan and another from Korea. In total, there are now sixteen described *Gambierdiscus* species and three species of *Fukuyoa*, a closely related genus, previously included in the genus *Gambierdiscus*. Among these nineteen species, and several, as yet, unsubscribed species (ribotypes), toxicity varies significantly. To better understand the distribution of these species, occurrence data from recently published literature (ca. 2009 – 2018) and two culture collections, where species identification was confirmed molecularly, were collated and archived in the biogeography of harmful algal species (HABMAP) subsection of the IOC-UNESCO Ocean Biogeographic Information System (OBIS). This manuscript represents a demonstration project illustrating how the spatially distributed HABMAP data can be employed to visualize the global distribution of *Gambierdiscus* and *Fukuyoa* species. These data will also inform the ISSHA-IOC contribution to the first Global HAB Status Report describing the global distribution of all toxin-producing microalgae in OBIS.

Keywords: HABMAP, OBIS, harmful microalgae

Introduction

The HABMAP project is developing a comprehensive biogeographical database on the distribution of harmful algal species in collaboration with the International Society for the Study of Harmful Algae. All data will be hosted by the Ocean Biogeographic Information System (OBIS) within the International Oceanographic Data and Information Exchange (IOOE) of the Intergovernmental Oceanographic Commission (IOC) of UNESCO (<http://haedat.iooe.org/>). When fully established, HABMAP will provide information on harmful algal species occurrences and blooms (<http://www.marine-species.org/hab/index.php>). This manuscript represents a demon-

stration product detailing how HABMAP can be used to document the global and regional distributions of two genera, *Gambierdiscus* and *Fukuyoa*, responsible for ciguatera poisoning (Darius et al., 2017; 2018). Toxicity varies greatly among the nineteen described and assorted undescribed species (ribotypes) belonging to these two genera, making site-specific species maps useful to resource managers and public health officials (Table 1).

Materials and Methods

Data for these maps were from published literature, predominantly from 2009 through 2018, The

Cawthron Institute Culture Collection, Nelson, New Zealand and the Culture Collation of the Institut Louis Malardé, Tahiti. All species identifications were verified by molecular analysis (Table 1). For demonstration purposes only one record per species is mapped for each location (N = 320) using ArcGIS. Quality control was performed on the

entire data set and then converted into a point shapefile for visualization. Because an initial review indicated a high degree of geographical overlap of observations, a relative presence symbology was used to show species present at each location, either globally or regionally to resolve spatially overlapping observations (Figs. 1-5).

Table 1. Described *Gambierdiscus* and *Fukuyoa* species with type locations, representative toxicity and selected references. Negative toxicity assays are not reported. MBA, mouse bio-assay, Neuro-2A assay (N2), Liquid chromatography mass spectrometry (LCMS). *Previously *Gambierdiscus* species type 6. **Previously *Gambierdiscus* species type 2. ***Previously *Gambierdiscus* species type 1. ****Previously *Gambierdiscus* ribotype 1.

Species	Type Location	Toxicity Cell ¹	Species Description & Toxicity References
<i>G. australes</i>	Australes Archipelago, French Polynesia, South Pacific Ocean	MBA+; N2a+; 22.25 fg PCTX3C eq. RBA; 0.6-1.4 fg CTX3C eq. N2a; 0- 697 fg CTX1B eq. N2a	(Chinain et al. 1999) Chinain et al. 2010 Pisapia et al. 2017 Reverte et al. 2018
<i>G. balechii</i> *	Celebes Sea, Pacific Ocean	MBA+; 1.1-19.9 fg PCTX1 eq. N2a	(Fraga et al. 2016) Dai et al. 2017
<i>G. belizeanus</i>	Belize, Central America, Caribbean Sea	0.85 fg CTX3C eq. N2a	(Litaker et al. 2009) Litaker et al. 2017
<i>G. caribaeus</i>	Belize, Central America, Caribbean Sea	0.66 fg CTX3C eq. N2a	(Litaker et al. 2009) Litaker et al. 2017
<i>G. carolinianus</i>	North Carolina, western Atlantic	0.27 fg CTX3C eq. N2a	(Litaker et al. 2009) Litaker et al. 2017
<i>G. carperntri</i>	Belize, Central America, Caribbean Sea	0.89 fg CTX3C eq. N2a	(Litaker et al. 2009) Litaker et al. 2017
<i>G. cheloniae</i>	Cook Islands, Pacific Ocean	MBA+; No CTX	(Smith et al. 2016) Munday et al. 2017
<i>G. excentricus</i>	Canary Islands, Eastern Atlantic Ocean	1,426 fg CTX1B eq. N2a; 469 fg CTX3C eq. N2a	(Fraga et al. 2011) Litaker et al. 2017
<i>G. honu</i>	Cook & Kermadec Islands, Pacific Ocean	MBA+ ; no CTX LC-MS	(Rhodes et al. 2017) Munday et al. 2017
<i>G. jejuensis</i> **	Jeju Island, Korea, East China Sea	Unknown	(Jang et al. 2018)
<i>G. lapillus</i>	Great Barrier Reef, Australia, Pacific Ocean	MBA+, CTXs? by LC-MS; CTX positive in FLIPR bioassay	(Kretzschmar et al. 2017) Larsson et al. 2018
<i>G. pacificus</i>	Tuamot Archipelago, French Polynesia, Pacific Ocean	MBA+, N2a+; 0.54-1.1 fg CTX3C eq. N2a; 31.7-75.8 fg CTX1B eq. N2a	(Chinain et al. 1999) Darius et al. 2018 Caillaud et al. 2011
<i>G. polynesiensis</i>	Australes & Tuamotu Archipelagos, French Polynesia, Pacific Ocean	MBA+, N2a+ 2,800-4,400 fg CTX3C eq. RBA; 1,610 – 2,130 CTC3C eq. N2a; 18,200 fg CTX eq. LC-MS	(Chinain et al. 1999) Chinain, 2010 Darius et al. 2018 Rhodes et al. 2014
<i>G. scabrosus</i> ***	Kashiwa-jima Island off southern Honshu, Japan; Pacific Ocean	MBA+, CTX+ by mouse bioassay; CTX+ by N2a+	(Nishimura et al., 2013, 2014) Pisapia et al. 2017
<i>G. sylvae</i> ****	Canary Islands, eastern Atlantic Ocean	19.6 fg CTX3C eq. N2a	(Fraga & Rodríguez 2014) Litaker et al 2017
<i>G. toxicus</i>	Gambier Islands, French Polynesia, eastern Pacific Ocean	2.5 fg PCTX3C eq. RBA	(Adachi & Fukuyo 1979) Chinain et al. 2010
<i>Gambierdiscus ribotype 2</i>	Belize, Central America, Caribbean Sea	6.6 fg CTX3C eq. N2A	(Litaker et al. 2009) Litaker et al. 2017
<i>Fukuyoa paulensis</i>	Ubatuba, São Paulo, Brazil	MTX+, CTX- N2a; 54-deoxy CTX1B+ LC-MS	(Gómez et al. 2015) Laza-Martínez et al. 2016)
<i>F. ruetzleri</i>	Belize, Central America, Caribbean Sea	10.6 fg CTX3C eq. N2a	(Litaker et al. 2009; Gomez et al. 2015) Litaker et al 2017
<i>F. yasumotoi</i>	Singapore Island, Pacific Ocean	Unknown	(Holmes 1998, Gomez et al. 2015)

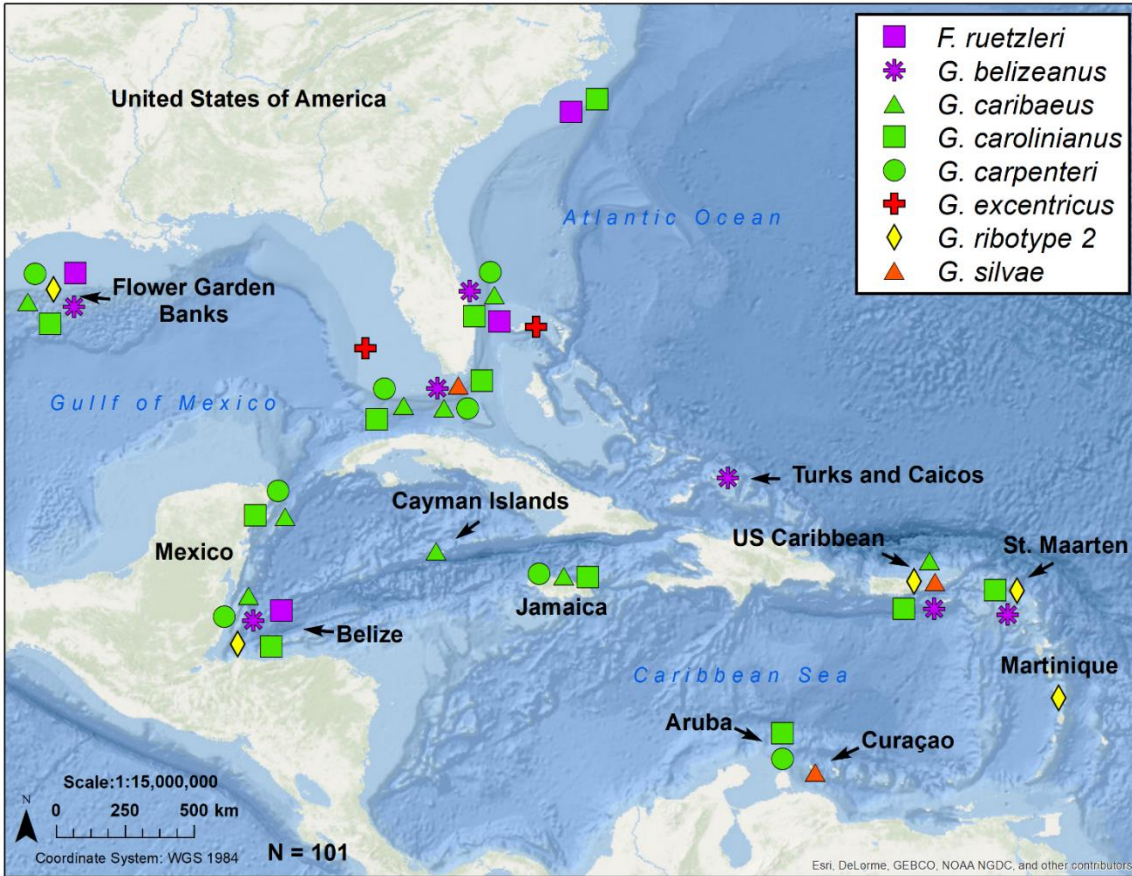


Fig. 1. *Gambierdiscus* and *Fukuyoa* occurrence in the Caribbean and adjacent seas, N=101. US Caribbean includes Puerto Rico and the United States Virgin Islands.

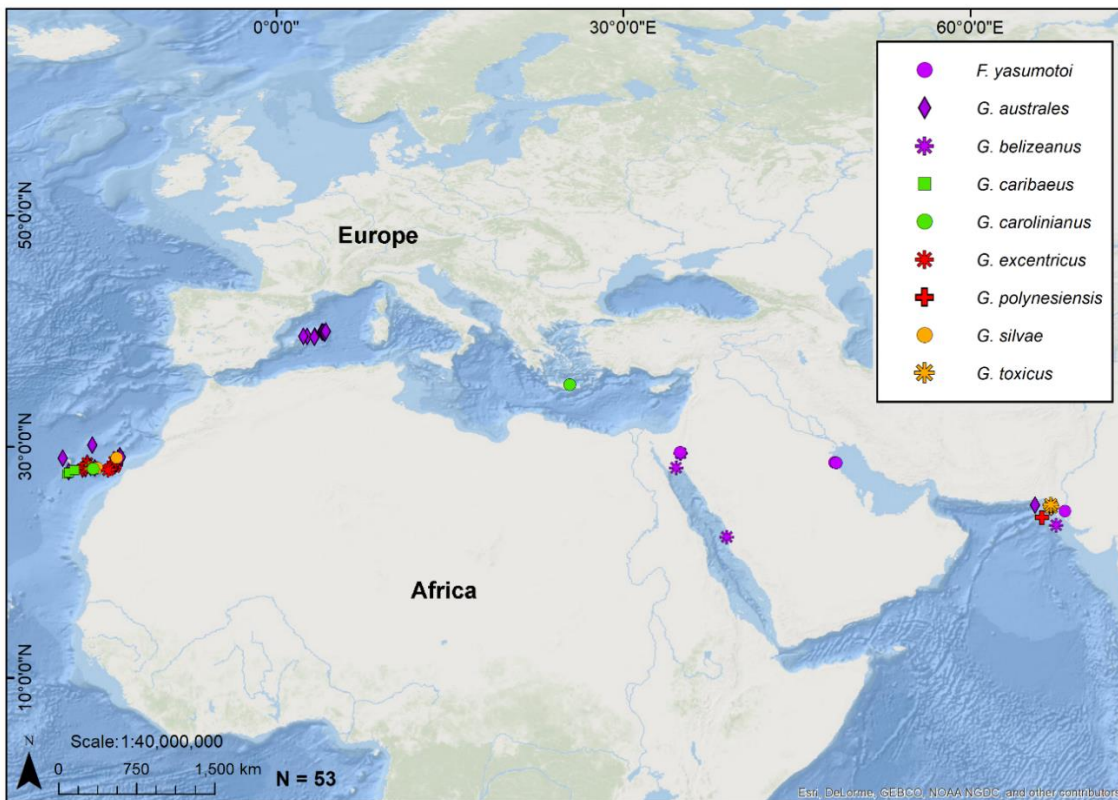


Fig. 2. *Gambierdiscus* and *Fukuyoa* occurrence in Macronesia, Europe and the Middle East, N=53.

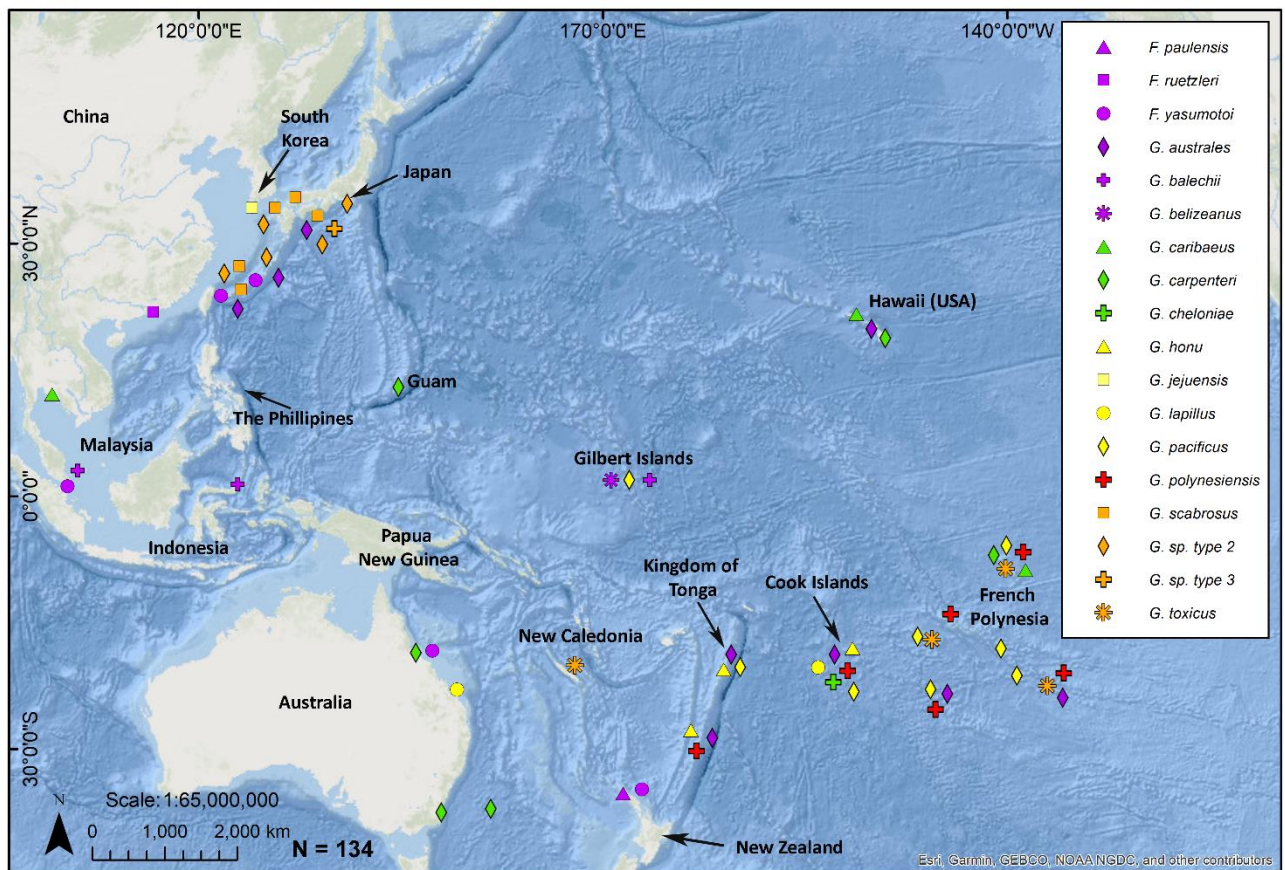


Fig. 3. *Gambierdiscus* and *Fukuyoa* occurrence in the Pacific Ocean, N=134.

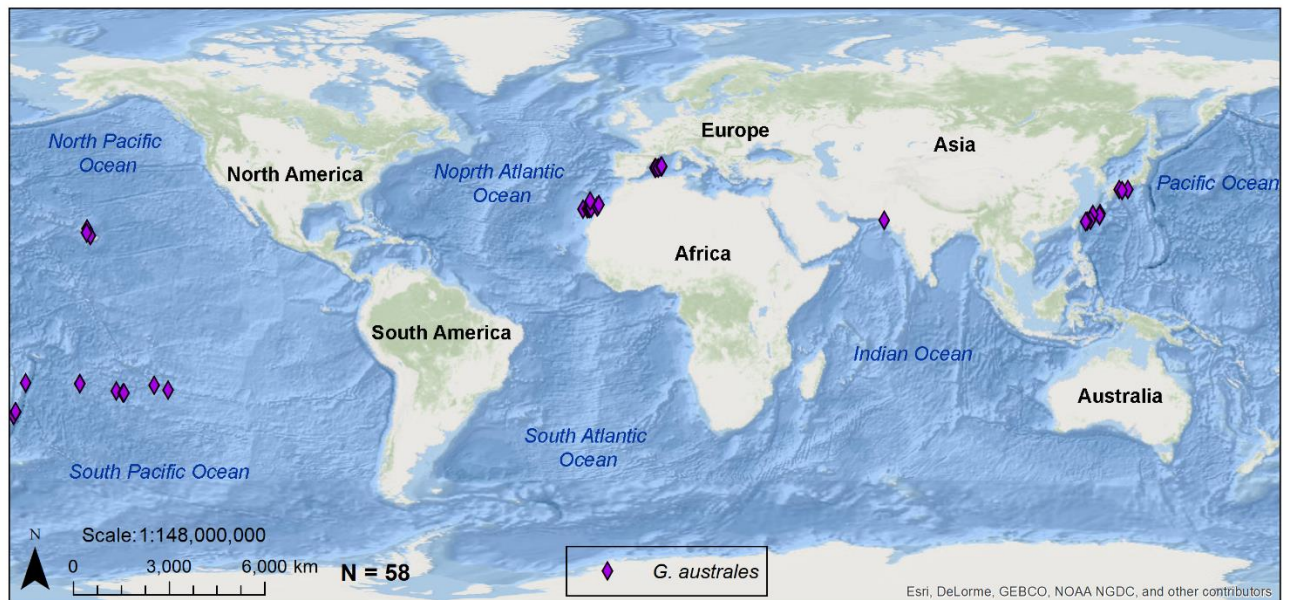


Fig. 4. Global occurrence of *Gambierdiscus australes*, N=58.

Results and Discussion

It is frequently of interest and utility to see species data displayed spatially. This allows comparisons or contrasts of environmental variables (Kibler et al. 2015, Xu et al. 2014) or habitat suitability (Tan et al. 2013, Yong et al. 2018). Examples of regional displays of *Gambierdiscus* and *Fukuyoa* species are shown in Figures 1-3, while observations of a single species, *G. australes* is mapped in Figure 4. Figure 5 displays the global *Gambierdiscus* and *Fukuyoa* distribution and includes all 320 records archived in the HABMAP database. The next

phase in the HABMAP project will add replicate published observations and collect unpublished occurrences of *Gambierdiscus* and *Fukuyoa* for inclusion in the database. This combined dataset can be used to better understand the distribution of species and identify areas where additional sampling is needed, particularly with respect to the high toxicity species, which may contribute disproportionately in causing ciguatera fish and shellfish poisoning.

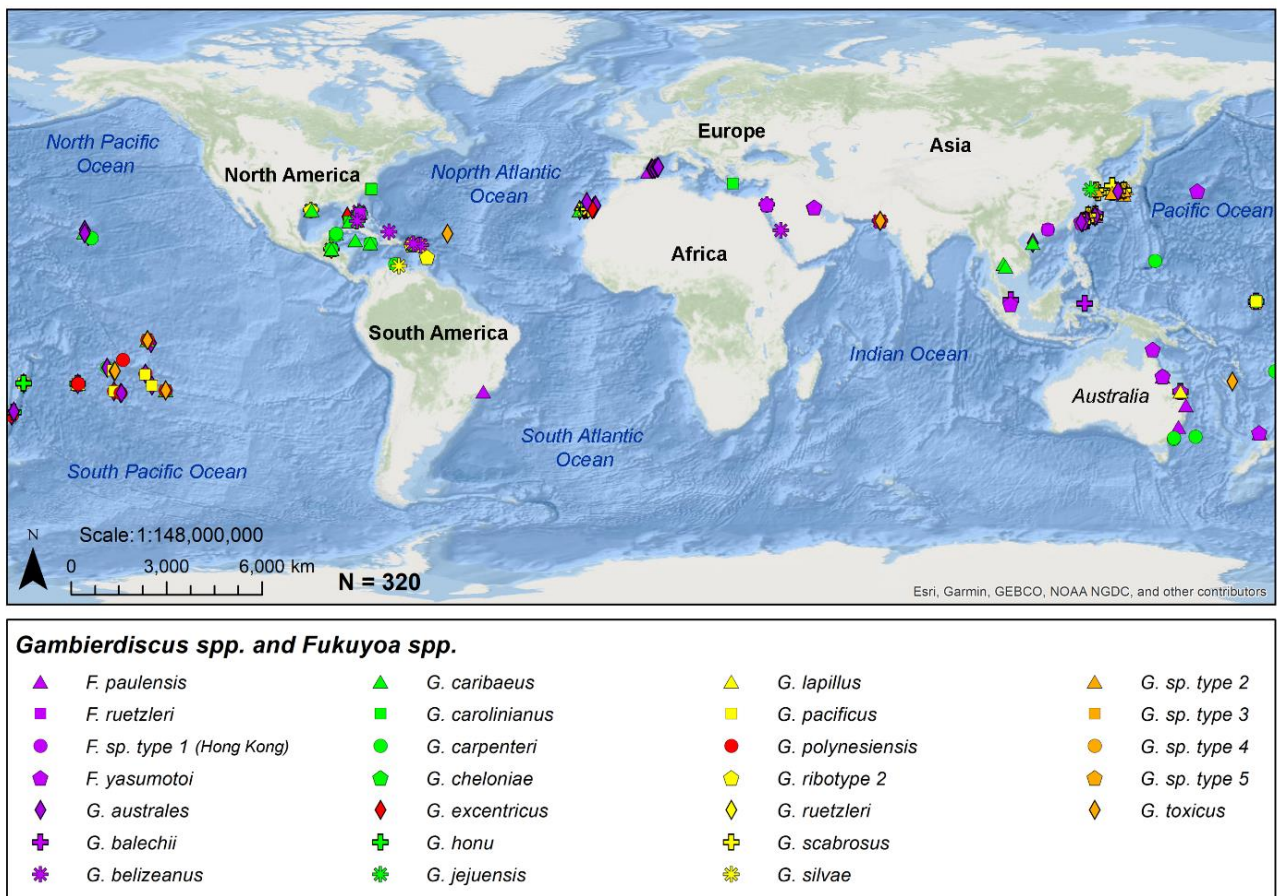



Fig. 5. Global *Gambierdiscus* and *Fukuyoa* occurrence from published records from 2009-2018, N=320.

References

- Adachi, R., Fukuyo, Y. (1979). *Nippon Suisan Gakkaishi* 45, 67–72.
- Caillaud, A., de la Iglesia, P., Barber, E., Eixarch, H., Mohammad-Noor, N., Yasumoto, T., Diogène, J. (2011). *Harmful Algae* 10, 433-446.
- Chinain, M., Faust, M.A., Pauillac, S. (1999). *J. Phycol.* 35, 1282–1296.
- Chinain, M., Darius, H.T., Ung, A., Cruchet, P., Wang, Z., Ponton, D., Laurent, D., Pauillac, S. (2010). *Toxicon* 56, 739-750.
- Dai, X., Mak, Y.L., Lu, C.-K., Mei, H.-H., Wu, J.J., Lee, W.H., Chan, L.L., Lim, P.T., Mustapa, N.I., Lim, H.C., Wolf, M., Li, D., Lou, Z., Gu, H., Leaw, C.P. (2017). *Harmful Algae* 67, 107-18.
- Darius, H.T., Roué, M., Sibat, M., Viallon, J., Gatti, C.M.I., Vandersea, M.W., Tester, P.A., Litaker, R.W., Amzil, Z., Hess, P. Chinain, M. (2017). *Toxins* 10.3390/toxins10030102.
- Darius, H.T., Roue, M., Sibat, M., Viallon, J., Gatti, C.M.I., Vandersea, M.W., Tester, P.A., Litaker, R.W., Amzil, Z., Hess., Chinain. (2018) *Mar. Drugs* 16, 122-144.
- Fraga, S., Rodriguez, F. (2014). *Protist* 165, 839-853.
- Fraga, S., Rodriguez, F., Caillaud, A., Diogene, J., Raho, N., Zapata, M. (2011). *Harmful Algae* 11, 10–22.
- Fraga, S., Rodriguez, F., Riobo, P, Barvo, I. (2016). *Harmful Algae* 58, 93-105.
- Gómez, F., Qiu, D., Lopes, R.M., Lin, S. (2015). *PLOS ONE* 10(4):e0119676.
- Holmes, M.J. (1998). *J. Phycol.* 34, 661-668.
- Jang, S.H., Jeong, H.J. Yoo, Y.D. (2018). *Harmful Algae* 80, 149-157.
- Kibler, S.R., Tester, P.A., Kunkel, K.E., Moore, S.K., Litaker, R.W. (2015). *Ecol. Model.* 316, 194-210.
- Kretschmar, A.L., Verma, A., Harwood, T., Hoppenrath, M., Murray, S. (2017). *J. Phycol.* 53, 283-297.
- Larsson, M.E., Laczka, O.F., Harwood, D.T., Lewis, R.J., Himaya, S.W.A., Murray, S.A., Doblin, M.A. (2018). *Mar. Drugs* 16(1):7, DOI: 10.3390/md16010007
- Laza-Martinez, A., David, H., Riobó, P., Miguel, I., Orive, E. (2016). *J. Eukaryotic Microbiol.* 63, 481-497.
- Litaker, R.W., Vandersea, M.W., Faust, M.A., Kibler, S.R., Chinain, M., Holmes, M.J., Holland, W.C., Tester, P.A. (2009). *Phycologia* 48, 344-390.
- Litaker, R.W., Holland, W.C., Hardison, D.R., Pisapia, F., Hess, P., Kibler, S.R., Tester, P.A. (2017). *PLoS One* doi.org/10.1371/journal.pone.0185776
- Munday, R, Murray, S, Rhodes, L.L, Larsson, M.E; Harwood, D.T. (2017). *Marine Drugs* 15(7): 208, DOI:10.3390/md15070208
- Nishimura, T., Sato, S., Tawong, W., Sakanari, H., Uehara, K., Shah, M.M.R., Suda, S., Yasumoto, T., Taira, Y., Yamaguchi, H. & Adachi, M. (2013). *PLoS ONE*, 8(4):e60882
- Nishimura, T., Sato, S., Tawong, W., Sakanari, H., Yamaguchi, H., Adachi, M. (2014). *J. Phycol.* 50, 506-514.
- Pisapia, F., Holland, W.C., Hardison, D.R., Litaker, R.W., Fraga, S., Nishimura, T., Adachi, M., Nguye-Ngoc, Sechet, V., Amzil, Z., Herrenknect, C., Hess, P. (2017) *Harmful Algae* 63, 173-183.
- Reverte, L, Toldra, A., Andree, K.B. Fraga, S., de Falco, G., Campas, M., Diogene, J. (2018). *J. Appl. Phycol.* 30, 2447-2461.
- Rhodes, L., Harwood, T., Smith, K., Argyle, P., Munday, R. (2014). *Harmful Algae.* 39:185–190.
- Rhodes, L., Smith, K.F., Verma, A., Curley, B.G., Harwood, D.T., Murray, S., Kohli, G.S., Solomona, D., Rongo, T., Munday, R., Murray, S.A. (2017). *Harmful Algae* 65, 61-70.
- Smith, K.F., Rhodes, L., Verma, A., Curley, B.G., Harwood, D.T., Kohli, G.S., Solomona, D., Rongo, T., Munday, R, Murray, S.A. (2016). *Harmful Algae* 60, 45-56.
- Tan, T.-H., Lim, P.-T., Mujahid, A., Usup, G., Leaw, C.-P. (2013) *Marine Research in Indonesia* 38 (2), DOI: https://doi.org/10.14203/mri.v38i2.59
- Xu, Y., Richlen, M.L., Morton, S.L., Mak, Y.L., Chan, L.L., Tekiau, A., Anderson, D.M. (2014). *Harmful Algae* 34, 56-68.
- Yong, H.L., Mustapa, N.I., Lee, L.K., Lim, Z.F., Tan, T.-H., Usup, G., Gu, H., Litaker R.W., Tester, P.A., Lim, P.-T., Leaw, C.P. (2018) *Harmful Algae* 78, 56-68.



Medical applications of algae, cyanobacteria and their toxins

Gambierol enhances evoked quantal transmitter release and blocks a potassium current in motor nerve terminals of the mouse neuromuscular junction

Jordi Molgó^{1,2*}, Sébastien Schlumberger², Makoto Sasaki³, Haruhiko Fuwa³, M. Carmen Louzao⁴, Luis M. Botana⁴, Denis Servent¹, Evelyne Benoit^{1,2}

¹ CEA, Institut des sciences du vivant Frédéric Joliot, Service d'Ingénierie Moléculaire des Protéines, Université Paris-Saclay, bâtiment 152, 91191 Gif sur Yvette, France;

² Institut des Neurosciences Paris-Saclay, UMR 9197 CNRS / Université Paris-Sud, CNRS, Gif sur Yvette, France;

³ Graduate School of Life Sciences, Tohoku University, Sendai, Japan;

⁴ Departamento de Farmacología, Facultad de Veterinaria, Universidad de Santiago de Compostela, Lugo, Spain.

* corresponding author's email: jordi.molgo@cea.fr

Abstract

In recent years, a great interest was developed to synthesize biologically-active natural products of marine origin. This is due to both their complex molecular structures and chemical diversity, and also to their unique biological activities. Among ladder-shaped toxins, gambierol, originally isolated from cultured *Gambierdiscus toxicus* dinoflagellate cells, together with ciguatoxins, has been successfully synthesized permitting detailed analyses of its mode and mechanism of action. Gambierol and analogs are known to inhibit some voltage-gated K⁺ (Kv) channel subtypes in various cell types. The aim of the present study was (i) to investigate whether gambierol has an action on quantal transmitter release evoked by nerve impulses and (ii) to determine whether Kv channels in motor nerve terminals of the mammalian neuromuscular junction are sensitive to the toxin action. Using electrophysiological techniques, the results obtained show that gambierol (2-20 nM) had no significant action on the resting membrane potential of mouse hemidiaphragm muscle fibers. In addition, spontaneous quantal transmitter release, measured by recording spontaneous miniature endplate potential frequency, remained unaffected by gambierol in resting neuromuscular junction. Gambierol (2 nM) increased about eight-fold the mean quantal content of evoked endplate potentials, as determined at individual junctions of the phrenic-hemidiaphragm preparation equilibrated in a low-Ca²⁺ and high-Mg²⁺ medium. The ability of gambierol to enhance quantal transmitter release was related to the reduction of a fast K⁺ current in nerve terminals. Overall, the present results show for the first time that gambierol enhances evoked quantal transmitter release in response to nerve stimuli, suggesting that it can be used to reverse pre- or post-synaptic neuromuscular blockade.

Keywords: Gambierol, marine biotoxin, nerve terminal, quantal transmitter release, potassium current

Introduction

Gambierol is a marine polycyclic ether toxin, first isolated and chemically characterized from cultured *Gambierdiscus toxicus*, dinoflagellates isolated in French Polynesia (Satake et al., 1993). The genus *Gambierdiscus* is known to produce the ladder cyclic compounds known as ciguatoxins responsible for ciguatera or ciguatera-like poisoning. The successful chemical synthesis of gambierol and analogues by independent groups (Alonso et al., 2012; Furuta et al., 2009; Fuwa et al., 2002; Johnson et al., 2005) allowed the detailed analyses of its mode of action. Gambierol is

characterized by a transfused octacyclic polyether core containing 18 stereogenic centers and a partially skipped triene side chain including a conjugated (Z,Z)-diene system, as shown in Fig. 1.

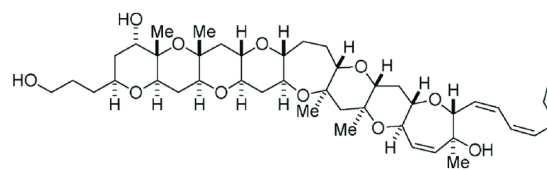


Fig. 1. Chemical structure of gambierol.

Gambierol and analogs have been reported to inhibit native or expressed voltage-gated K⁺ (Kv) channels in various cell types including mouse taste cells (Ghiaroni et al., 2005), mammalian Kv1.1-Kv1.5 channels expressed in *Xenopus* oocytes or Chinese hamster ovary (CHO) cells (Cuypers et al., 2008; Konoki et al., 2015), Kv3.1 channels expressed in mouse fibroblasts (Kopljár et al., 2009), *Xenopus* skeletal myocytes (Schlumberger et al., 2010), murine cerebellar neurons (Pérez et al., 2012), and human Kv1.3 channels from T lymphocytes (Rubiolo et al., 2015). In contrast, gambierol does not block or affect voltage-gated Na⁺ channels at nanomolar concentrations in the cell types investigated. At the skeletal neuromuscular junction of vertebrates, acetylcholine (ACh) is released in multimolecular packets. Each transmitter packet, stored in a synaptic vesicle, is called a “quantum” that contains ~6,000 ACh molecules and provides the unit that makes-up synaptic events (Katz, 1966). The quantal release of transmitter from motor nerve terminals occurs either spontaneously, when a single transmitter packet (quantum) is released from a single vesicle at a given time, or when hundreds of transmitter packets (quanta) are released simultaneously in response to nerve stimulation and Ca²⁺ ions entry into the terminals. Kv channels, by regulating the duration of the presynaptic action potential, play an important role in controlling both the amount of Ca²⁺ entry into the terminal and the number of quanta released (quantal content) (reviewed in Molgó and Tabti, 1989; Van der Kloot and Molgó, 1994). In this work, the effects of synthetic gambierol was investigated on quantal transmitter release and presynaptic currents at single mammalian neuromuscular junctions, using intracellular recordings that allowed evaluating the amount of transmitter released upon nerve stimulation and high resolution external focal current recordings from nerve terminals.

Materials and Methods

Gambierol with purity of ~97% was produced by chemical synthesis, as reported previously (Fuwa et al., 2002). Synthetic gambierol, identical to natural gambierol, was dissolved in dimethyl sulfoxide (DMSO) and then diluted in the physiological solution. The total DMSO concentration in solutions did not exceed 0.1%. D-tubocurarine chloride was purchased from Tocris Bioscience (Bristol, UK).

Adult male and female Swiss mice (20-30 g) were

obtained from the CNRS animal house in Gif sur Yvette (France). Experiments were performed in accordance with European Community guidelines for laboratory animal handling and with the official edict presented by the French Ministry of Agriculture and the recommendations of the Helsinki Declaration. Mice were anesthetized with isoflurane inhalation (Aerrane, Baxter S.A., Lessines, Belgium) before being euthanized by dislocation of cervical vertebrae.

Isolated nerve-muscle preparations were mounted in silicone-lined organ baths superfused with an oxygenated standard Krebs-Ringer solution of the following composition (in mM): NaCl 140, KCl 5, CaCl₂ 2, MgCl₂ 1, D-glucose 11, and HEPES 5 (pH 7.4) In some experiments, the CaCl₂ was reduced to 0.4 mM and MgCl₂ was increased to 7.0 mM, the osmolarity being kept constant.

Presynaptic currents were recorded with fire-polished glass microelectrodes (filled with standard saline and having resistance of 1-2.10⁶ ohms) and an Axoclamp-2A system (Axon Instruments, Union City, CA, USA) from motor nerve terminals of the *levator auris longus* nerve-muscle preparation (Angaut-Petit et al., 1987). An Ag-AgCl pellet located in the bath served as the reference electrode.

Intracellular recordings of the resting membrane potential, end-plate potential (EPP) and miniature end-plate potential (MEPP) were made with standard techniques, using an Axoclamp-2A system and glass microelectrodes filled with 3 M KCl and with resistances of 5-8.10⁶ ohms. The phrenic nerve was stimulated through a suction electrode by supramaximal square wave pulses of 0.05 ms duration at a frequency of 0.25 Hz. The quantal content (*m*) of the EPP was assessed directly as the ratio of the average EPP amplitude and the average MEPP amplitude (at least 25 MEPPs and 75 EPPs were averaged). EPPs with amplitude exceeding 3 mV were corrected for nonlinear summation of quanta. The equilibrium potential for ACh used in the calculations was -7 mV (the maximal correction rarely exceeded 7%). When the quantal content of EPPs was low, the following equation based on Poisson statistics was used: $m = \ln(N/No)$, where *m* is the average number of transmitter quanta released per impulse, *N* is the total number of stimulations, and *No* is the corresponding number of failures of release (*i.e.*, the number of stimuli not followed by an EPP).

Signals were collected, amplified and digitized with the aid of a computer equipped with a Digidata-1322A A/D interface board (Axon

Instruments). Data acquisition and analysis were performed with the WinWCP V3.9.6 software program, kindly provided by Dr. John Dempster (University of Strathclyde, Scotland). All experiments were carried out at constant room temperature (22°C).

The results are expressed as the mean \pm S.E. Statistical differences were calculated using either paired or unpaired Student's *t*-test. *P* values $<$ 0.05 were considered statistically significant.

Results and Discussion

To determine if gambierol had an effect on the resting membrane potential and MEPP frequency, experiments were performed on isolated phrenic nerve-hemidiaphragm muscle preparations. Under control conditions the mean resting potential of muscle fibers in the mouse hemidiaphragm was -69.2 ± 2.8 mV. After 2, 10 and 20 nM gambierol treatment for 30 min, it was -67.9 ± 2.7 , -68.2 ± 1.9 and -69.6 ± 2.2 mV, respectively ($n = 28$ to 36 fibers sampled from hemidiaphragms of 3 different mice for each condition). These results indicate that gambierol, in the range of concentrations studied had no significant action on the resting membrane potential of muscle fibers ($P > 0.05$).

Spontaneous quantal transmitter release, measured by recording MEPP frequency in resting junctions, was not significantly modified by 10 nM gambierol applied for 30 min (1.70 ± 0.33 vs 1.58 ± 0.29 s⁻¹; $n = 20$ junctions sampled from 3 different hemidiaphragms; $P > 0.05$). This is in marked contrast to the action of both Pacific ciguatoxin-1B and Caribbean ciguatoxin-1 which greatly increase MEPP frequency, the increase being sensitive to the sodium channel blocker tetrodotoxin (Mattei et al., 2010; Molgó et al., 1991, 1990). Those results strongly suggested that such an action was related to the activation of voltage-gated Na channels (Molgó et al., 1992).

The mean quantal content of evoked EPPs was determined at individual junctions of the phrenic-hemidiaphragm preparations equilibrated for 30 min with a low-Ca²⁺ (0.4 mM) and high-Mg²⁺ (7.0 mM) physiological medium. Under control conditions, the mean quantal content of EPPs (mean number of transmitter quanta that enters in the composition of a synaptic response during a series of nerve stimulations) was 0.70 ± 0.07 ($n = 26$ junctions from 5 hemidiaphragms; m values ranged between 0.3 and 1.5, with a coefficient of variation = 0.53), indicating that a high proportion of nerve impulses failed to release the transmitter and to evoke an EPP. Interesting, after 20 min

equilibration with 2 nM gambierol, most of the junctions examined had no failure of release upon nerve stimulation, and mean m values were increased to 5.9 ± 0.4 ($n = 26$ junctions from 5 hemidiaphragms; m values ranged between 2.8 and 9.6, with a coefficient of variation = 0.35). Thus, there was an about eight-fold increase in m values.

The action of gambierol was investigated to clarify if its ability to enhance evoked quantal ACh release was related to an action on presynaptic currents. Typical focal current recordings, performed in a standard Krebs-Ringer solution containing d-tubocurarine (2.5 μ M) to block neuromuscular transmission and muscle contraction, are shown in Fig. 2.

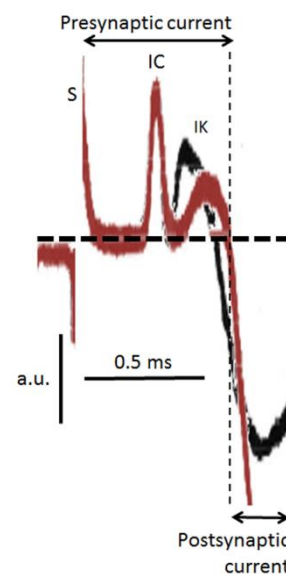


Fig. 2. Superimposed traces of focally recorded pre- and post-synaptic currents (truncated) at a single neuromuscular junction, before (black trace) and after the addition of 2 nM gambierol (coloured trace) to the standard Krebs-Ringer solution. S designates the nerve stimulus artefact; IC is the transient capacity current; IK shows the fast K⁺ current that is partially blocked by gambierol. Each trace is the average of 16 focal current recordings. Vertical calibration is in arbitrary units (a.u.) due to the unknown resistance between the recording microelectrode and the nerve terminal membrane.

When the current microelectrode was gently placed on the nerve terminal of a single neuromuscular junction, two positive signals were detected. The first peak relates to the capacity current (IC) leaving the terminal, due to the Na⁺ influx into the nodes of Ranvier of the parent axon. The second peak corresponds to a fast K⁺ current (IK) generated in the nerve terminals (see Fig. 2). The addition of gambierol (2-10 nM) to the medium

caused, within 10-15 min, a reduction of the IK signal of presynaptic currents without affecting the IC component.

Altogether, the results here presented show for the first time that gambierol enhances evoked quantal transmitter release in response to 0.25-Hz nerve stimulation, without affecting spontaneous quantal release recorded as MEPP frequency. On equimolar basis, gambierol, is more potent than 3,4-diaminopyridine, a well-known Kv-channel blocker of motor nerve terminals that has been previously studied in mammalian neuromuscular junctions (Molgó et al., 1980). Thus, blockade of the fast IK current in motor nerve terminals by gambierol lengthens the action potential duration and increases evoked quantal transmitter release. Experiments are in progress to determine whether gambierol influences the phasic entry of Ca²⁺ into the terminals.

Our results strongly suggest that gambierol and analogues can have potential medical application in neuromuscular transmission, under conditions in which it is necessary to antagonize pre- or post-synaptic neuromuscular blockade, or both.

Acknowledgements

This study was supported in part by the project ALERTOX-NET (EAPA_317/2016) funded by the Interreg Atlantic program, and in part by the CNRS. We thank Mrs Patricia Villeneuve for technical assistance.

References

Alonso, E., Fuwa, H., Vale, C., Suga, Y., Goto, T., Konno, Y., Sasaki, M., LaFerla, F.M., Vieytes, M.R., Giménez-Llort, L., Botana, L.M. (2012). *J. Am. Chem. Soc.* 134, 7467-7479.

Angaut-Petit, D., Molgó, J., Connold, A.L., Faille, L. (1987). *Neurosci. Lett.* 82, 83-88.

Cuypers, E., Abdel-Mottaleb, Y., Kopljar, I., Rainier, J.D., Raes, A.L., Snyders, D.J., Tytgat, J. (2008). *Toxicol.* 51, 974-983.

Furuta, H., Hasegawa, Y., Mori, Y. (2009). *Org. Lett.* 11, 4382-4385.

Fuwa, H., Kainuma, N., Tachibana, K., Sasaki, M. (2002). *J. Am. Chem. Soc.* 124, 14983-14992.

Ghiaroni, V., Sasaki, M., Fuwa, H., Rossini, G.P., Scalera, G., Yasumoto, T., Pietra, P., Bigiani, A. (2005). *Toxicol. Sci.* 85, 657-665.

Johnson, H.W., Majumder, U., Rainier, J.D. (2005). *J. Am. Chem. Soc.* 127, 848-849.

Katz, B. (1969). *The release of neural transmitter substances.* University Press, Liverpool, pp. ix-60.

Konoki, K., Suga, Y., Fuwa, H., Yotsu-Yamashita, M., Sasaki, M. (2015). *Bioorg. Med. Chem. Lett.* 25, 514-518.

Kopljar, I., Labro, A.J., Cuypers, E., Johnson, H.W., Rainier, J.D., Tytgat, J., Snyders, D.J. (2009). *Proc. Natl. Acad. Sci. USA* 106, 9896-9901.

Mattei, C., Marquais, M., Schlumberger, S., Molgó, J., Vernoux, J.P., Lewis, R.J., Benoit, E. (2010). *Toxicol.* 56, 759-767.

Molgó, J., Lundh, H., Thesleff, S. (1980). *Eur. J. Pharmacol.* 61, 25-34.

Molgó, J., Benoit, E., Comella, J.X., Legrand, A.M. (1992). *Meth. in Neurosci.* 8, 149-164

Molgó, J., Comella, J.X., Legrand, A.M. (1990). *Br. J. Pharmacol.* 99, 695-700.

Molgó, J., Comella, J.X., Shimahara, T., Legrand, A.M. (1991). *Ann. New York Acad. Sci.* 635, 485-489.

Molgó, J., Tabti, N. (1989). *Acta Physiol. Pharmacol. Latinoam.* 39, 333-342.


Pérez, S., Vale, C., Alonso, E., Fuwa, H., Sasaki, M., Konno, Y., Goto, T., Suga, Y., Vieytes, M.R., Botana, L.M. (2012). *Chem. Res. Toxicol.* 25, 1929-1937.

Rubiolo, J.A., Vale, C., Martín, V., Fuwa, H., Sasaki, M., Botana, L.M. (2015). *Arch. Toxicol.* 89, 1119-1134.

Satake, M., Murata, M., Yasumoto, T. (1993). *J. Am. Chem. Soc.* 115, 361-362.

Schlumberger, S., Ouanounou, G., Girard, E., Sasaki, M., Fuwa, H., Louzao, M.C., Botana, L.M., Benoit, E., Molgó, J. (2010). *Toxicol.* 56, 785-791.

Van der Kloot, W., Molgó, J. (1994). *Physiol. Rev.* 74, 899-991.



**Impact of
microalgae/cyanobacteria
on aquatic organisms
(incl. fish kills and
shellfish mortalities)**

Contribution of the HAB_f INDEX for fish farm's risk analysis

Alejandro Clément^{1*}, Thomas Husak², Sofia Clément¹, Francisca Muñoz¹, Marcela Saldivia³, Carmen G. Brito⁴, Roberta Crescini³, Nicole Correa¹, Karenina Teiguel¹, César Fernández¹, Gustavo Contreras¹, Stephanie Saez¹

¹ Plancton Andino SpA Terraplen 869, Puerto Varas, Chile;

² OXZO, Puerto Montt, Chile;

³ Plancton Andino SpA, Bordemar, Castro, Chiloé, Chile;

⁴ Plancton Andino SpA, Coyhaique, Patagonia, Chile.

* corresponding author's email : alexcle@plancton.cl

Abstract

In recent years in Chile, numerous HAB events have been observed, particularly photo-autotrophic flagellate species, which have caused problems in fisheries and aquaculture. The Chilean fjord ecosystem has been intensely monitored and studied for key phytoplankton species, including characterization of cells using FlowCam analysis, photosynthesis and ocean color remote sensing.

The results provide valuable information as they contribute to understanding the oceanographic and ecological significance of such HABs. Here, we developed an *on-line* biological indicator such as a HAB_f INDEX (=HABFIX) that provides fish farmers, authorities and general users an integrated and comparable variable for a risk information system.

HABFIX is based on an algorithm that considers different weighting factors and risk coefficients of various parameters. Specifically, the structure of the algorithm is based on the sum of the water-column-weighted average of each harmful algal abundance and their ratios. With this novel algorithm we attempt to include the synergies of harmful algal effects on fish farms.

In hindsight we are able to run HABFIX, checking a large dataset from phytoplankton monitoring through e-cloud computing using business intelligence software. While the results of HABFIX show a direct relation with harmful algae bloom effects on fish farms there are, however, a few challenges to overcome.

Keywords: HAB_f INDEX, monitoring, phytoplankton, algorithm

Introduction

Southern Chile is a marine ecosystem providing numerous benefits for society, most importantly sustainable economic development, including aquaculture and fisheries, maritime activities, tourism, fjord bio-diversity and conservation.

Most scientists believe HABs are increasing in frequency, magnitude, and duration worldwide (Wells et al., 2015). Locally, we have observed an increase in duration and intensity of HABs depending on the species. These outbreaks have significant economic and social impacts, and climatic anomalies are playing important role triggering extreme events (Clément et al., 2017; Trainer et al., 2019). Our major focus of interest is to apply several techniques, such as, bio-optics, cell imaging, harmful algal algorithms for monitoring and forecasting HABs.

Phytoplankton monitoring has been carried out in Southern Chile for more than 29 years (Clément &

Guzmán 1989; Montes et al., 2018) but since the 2000s more air-sea complexities have been observed (León-Muñoz et al., 2018). Until now, the main species of concern are photosynthetic flagellates; *A. catenella*, *Pseudochattonella* spp., and *Karenia* spp. From a practical point of view, the risk of occurrence of HABs can be estimated as a function, influenced by harmful algae ratios and weight factors. Under this complex biological environment, we have developed and tested a novel HAB_f INDEX = (HABFIX) to ease, and improve decision making process for official authorities and fish farmers. In Europe the Plankton Community Index is a quantitative method for evaluating changes in the community structure of phytoplankton using a state-space perspective (Tett et al., 2008). Several phytoplankton indices have been used, but very few focus on HABs. Anderson et al., 2014 developed the HAB INDEX, for

shellfish poisoning toxicity in the Gulf of Maine. There also exists the *K. brevis* Bloom Index (KBBI) that is based on remote sensing optical techniques for detecting and classifying the toxic dinoflagellate *Karenia* spp., (Amin et al., 2009). The main objective of this study was to develop an algorithm that measures the risk of several harmful algal species in the marine coastal ecosystem, with emphasis on fish farms areas.

Materials and Methods

The phytoplankton dataset comes from the monitoring program of the Chilean salmon farming industry, called POAS ([Programa Oceanografico Ambiental en Salmonidos](#); Clément, 2016). This program runs since 1998 and has over 40 sites, and provides weekly samples with no chemical fixatives, and at 4 depth levels (0, 5, 10 and 15 m). The program covers a large area of 80,000 km² (Fig. 1). For water and cells analysis we use several phytoplankton techniques, including inverted microscopy of fresh cells, imaging flow cytometer (FlowCam), FRRf3 measuring active and variable chlorophyll fluorescence (Fo, Fm & Fv) to obtain an eco-physiological approach of the cells (Oxborough et al., 2012). The phytoplankton data is archived in a local database (<http://sispal.plancton.cl/clientes/>) and we apply business intelligence software [for data visualization for fish farmers and other users](#).

HABFIX is an algorithm using a series of variables and coefficients, which include: water column weighted average concentration of total phytoplankton, ratio of specific harmful algae concentration divided by the critical or threshold value to damage fish tissue (Mardones & Clément 2016; Montes et al., 2018).

The synergistic effects, i.e., presence of 2 or more harmful algae are calculated using different ratios, applying specific empirical constants and coefficients factors. The HABFIX is dimensionless, and its numerical range varies from 0 to practically 560, though it could be larger. The maximum value of 560 was observed for the *Pseudochattonella* cf. *verruculosa* 2016 bloom.



Fig. 1. [Study area and POAS phytoplankton monitoring stations at fish farm and weekly average of HABFIX.](#)

Mathematical formulations

The first term, [Harmful], is the sum of several ratios of harmful algae species that produce damage and/or mortality to farmed-fish. The second term, [Phyto], represents the ratio of total phytoplankton averaged concentration (C_T), divided by the Critical Total Concentration (C_{XT}) defined as 25,000 cell/mL (See Eq. 3). Waters at high phytoplankton concentration are very turbid (Secchi Disk < 2 m) and produce organic exopolymeric substances (EPS) generated mainly from phytoplankton (Jenkinson & Arzul 1998).

$$\text{Eq. (1)} \quad \text{HAB}_f = [\text{Harmful}] + [\text{Phyto}]$$

The main formula of the algorithm is Eq. 2 which include a series of summation of harmful algae ratios, averaged in the water column, multiplied by the amplification factor $(2 + 0.5 \cdot \lambda_i)$, by α_i , and d . In addition, both variables \bar{C}_i and C_{X_i} are raised to exponents < 1, to modulate the resulting values of the HABFIX, as high phytoplankton abundance (e.g. > 5000 cell/mL) can lead to significant differences.

$$\text{Eq. (2)} \quad [\text{Harmful}] = \sum_i^M \left((2 + 0.5 \cdot \lambda_i) \cdot \frac{\bar{C}_i^{-0.75}}{C_{X_i}^{0.6}} \cdot \alpha_i \cdot d \right)$$

Description of main parameter, coefficients and terms of the algorithm

\overline{C}_i	Enhanced Mean is an integrated water column average concentration of each harmful algae (<i>i</i>) species (cell/mL).
Cx_i	Critical Concentration of harmful algae(<i>i</i>). Tabulated values [1-50000 cell/mL], which are captured directly from database. Empirical value obtained from POAS, historical HABs, & Montes et al., 2018.
λ_i	Amplification Factor: Amplifies the effect of each harmful species <i>i</i> in case: $\overline{C}_i \geq Cx_i \rightarrow \lambda_i = 1$; $\overline{C}_i < Cx_i \rightarrow \lambda_i = 0$
α_i	Harmful species (<i>i</i>) risk coefficient. Weights the noxious effect of each harmful algae, according to the degree of damage in fish aquaculture. Tabulated values [0 - 1].
d	Type of damage. Discriminates the contribution of each harmful species in order to differentiate mathematically the effect of ichthyotoxic species ($d = 2$) and those that cause physical damage ($d = 1,1$).
M	Summation that depends on the number and concentration of harmful algae species in water samples.
N	Number of layers or depths sampled in water column.
$C_{i,z}$	Concentration of species <i>i</i> at depth <i>z</i> .

Eq. 3 represent averaged water column phytoplankton ratio, but risk coefficients and type of damage are not included. The associate multiplicative amplification factor and exponent have less weight that those from the [Harmful] term. Therefore, [Phyto] term have low impact in total value of **HABFIX**, particularly with phytoplankton concentration lower than 25,000 cells/mL.

Eq. (3)

$$[\text{Phyto}] = (0.4 + 0.5 \cdot \lambda) \cdot \left(\frac{\overline{C}_T}{Cx_T} \right)^{0.6}$$

HABFIX is an integrate value in the water column:
Enhanced Mean, \overline{C}_i , is slightly > than simple arithmetic average, especially when number of layers analyzed in water column is > 1 ($N > 1$). This factor is applied to avoid bias values resulting

from highly heterogeneous cells distributions, such as those found in thin layers and bloom situations (Clément et al., 2017).

$$\text{Eq. (4)} \quad \overline{C}_i = \frac{\sum_z C_{i,z}}{N^{0,9}}$$

Results and Discussion

We checked and hindcast the algorithm on the SQL database to evaluate different harmful algae concentrations, species risk coefficients (α), and compared the damage to a fish farm. We present **HABFIX** spatial and temporal data on a daily basis, to follow the risk of HABs for the fish aquaculture industry. Different harmful algae species and abundance apparently produce distinct a mechanism of mortality to fish (Mardones et al., 2015). Therefore, we weight the risk in the algorithm at several harmful algal concentrations (Fig. 2). **HABFIX** is based upon an algorithm that takes into account different weighting factors and risk coefficients. Basically, the weighted average ratio of each harmful algae and abundance determines the **HABFIX** magnitude (Eq. 2). The algorithm includes the sum of different harmful algae and concentrations in the same mathematical term, and in doing so, intrinsically takes into account synergist effects, e.g., we have observed several HABs of *L. danicus* and *Pseudochattonella* cf. *verruculosa* practically co-existing in time and space.

Results of **HABFIX** show a close relation with harmful algal distribution and its impacts on salmon farms, particularly with fish mortality rates.

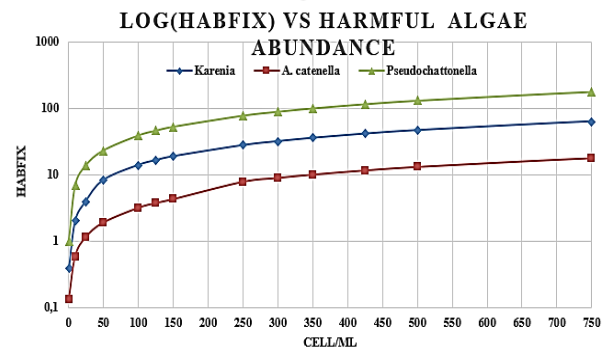


Fig. 2. The log of [HABFIX] in function of abundance of 3 different harmful algae. *Karenia* spp., *Pseudochattonella* spp., and *A. catenella*

New published data of critical concentration of weighting factors and coefficients are essential (Montes et al., 2018). After phytoplankton dataset is entered and saved to the server database, **HABFIX** is automatically calculated and shared [on](#)

[line](#) for users; fish farmer, or official authorities, among others. Therefore, within a large fish farms network, is available through *e-cloud* as useful indicator of HAB risk, because describes spatial-temporal dynamics and synergistic effects of several harmful algae in the monitoring area, alerting the potential damage for marine fish culture zones.

The *P. cf. verruculosa* summer 2019 bloom in Chiloé Archipelago reached a **HABFIX** maximum of 59.5, increasing exponentially over a few days. During summer of 2018 a bloom of *Karenia* spp. in Chile's Patagonian Fjords showed an increased rate lower than *P. cf. verruculosa*. Within a week **HABFIX** can increase from 1 to 9 indicating an early warning situation for fish farmers, managers and authorities.

HABFIX is a novel algorithm as it provides a summary of several parameters in one integrated and comparable variable estimating the risk of several harmful phytoplankton species and concentration in fish farm area. Fish farmers, official authorities and others users can use **HABFIX** > 2, as early warning limit, regardless the species of harmful algae in the water. Fish farmers can decrease feeding rates and set up HABs mitigations techniques under the scope of an empirical algorithm. The next step and challenge will be to forecast the **HABFIX** index.

Acknowledgements

This study was carried out under the POAS program led by Plancton Andino and funded by the fish farmers producers. We appreciate the collaboration of H. Nelson from Fluid Imaging Technologies very much. We thank to rest of our team for the support.

References

Amin, R., Zhou, J., .. , B., Moshary, F., & Ahmed, S. (2009). Opt. Express 17, (11), 9126–9144.

Anderson, D.M., Couture, D.A., Kleindinst, J.L., Keafer, B.A.,..., Hickey J.M., Solow, A.R. (2014). Deep-Sea Research Part II: 103, 264–276.

Clément, A. (2016). POAS Versión 2016. Plancton Andino. 1-18.

Clément, A., Guzmán, L. (1989). IN: Okaichi, T. Anderson, D.M., Nemoto, T. (Eds.) Red tides: Biology, environmental science, and toxicology. 121–124.

Clément A., Muñoz F., Brito C.G., Correa N., ..., Contreras, G., Egenau. O. (2017). pp. 34–37. IN: Proença, L. A. O. & Hallegraeff, G.M. (eds). Proc. of the 17th Int. Conference on Harmful Algae. ISSHA.

Jenkinson, I. R., Arzul, G. (1998). IN: Harmful Algae. Reguera, B., Blanco, J., Ferndandez M. L., & Wyatt, T. Xunta Galicia & IOC UNESCO 1998. 425–428.

León-Muñoz, J., Urbina, M.A., Garreaud, R., Iriarte, J.L. (2018). Scientific Reports, 8:1, 1330.

Mardones, J., Clément, A. (2016). Manual de Microalgas del Sur de Chile. Ewos.

Mardones, J.I., Dorantes-Aranda, J.J., Nichols, P.D., Hallegraeff, G.M., 2015. Harmful Algae 49, 40–49.

Montes, R.M., Rojas, X., Artacho, P., Tello, A., & Quiñones, R.A. (2018). Harmful Algae, 77, 55–65.

Oxborough, K., Moore, C. M., Suggett, D. J., Lawson, T., Chan, H. G., & Geider, R. J. (2012). Limno. & Ocean: Methods, 10, 142–154. <https://doi.org/10.4319/lom.2012.10.142>

Tett, P., Carreira, C., Mills, D.K., van Leeuwen, S., .., E., Gowen, R. J. (2008). ICES Journal of Marine Science, 65: 1475–1482.

Trainer, V. L., Moore, S. K., Hallegraeff, G., Kudela, R. M., Clément, A., Mardones, J. I., & Cochlan, W. P. (2019). In press. Harmful Algae. <https://doi.org/10.1016/J.HAL.2019.03.009>

Wells, M.L., Trainer, V.L., Smayda, T. J., Karlson, B. S. O.,... Cochlan, W. P. (2015). Harmful Algae, 49, 68–93.

Harmful Algal bloom species associated with massive Atlantic salmon mortalities while transported through the Gulf of Penas, southern Chile

Carolina Toro¹, Cesar Alarcón¹, Hernán Pacheco¹, Pablo Salgado¹, Máximo Frangopulos², Francisco Rodríguez³, Gonzalo Fuenzalida⁴, Roberto Raimapo¹, Gemita Pizarro¹ and Leonardo Guzmán^{4*}

¹ Centro de Estudios de Algas Nocivas (CREAN), Instituto de Fomento Pesquero (IFOP), Enrique Abello 0552, Punta Arenas, Chile.

² Centro de Investigación GAIA-Antártica (CIGA), Universidad de Magallanes, Av. Bulnes 01855, Punta Arenas, Chile; Centro FONDAP-IDEAL, Av. El Bosque 01789, Punta Arenas, Chile.

³ Instituto Español de Oceanografía (IEO), Subida a Radio Faro 50, 36390 Vigo, España.

⁴ Centro de Estudios de Algas Nocivas (CREAN), Instituto de Fomento Pesquero (IFOP), Padre Harter 574, Puerto Montt, Chile.

* corresponding author's email: leonardo.guzman@ifop.cl

Abstract

During January (Austral Summer) 2017, in the Gulf of Penas (47° S), a mortality of around 130 tons of farmed smolts of Atlantic salmon occurred while they were transported by three wellboats from the Aysén region (45° S) to the western area of the Strait of Magellan (54° S). The ichthyotoxic *Karenia* cf. *mikimotoi* was identified as the likely causative agent of mortality. Therefore, four field researches were conducted between February 2017 and March 2018 to assess the abundance and distribution of *Karenia* in the Gulf and surrounding areas. In addition, data from this period provided by the Red Tide Monitoring Programme were considered. The results showed the presence of different species of *Karenia* (*K.* cf. *mikimotoi*, *K.* cf. *brevis*, *K.* cf. *bicuneiformis*). The highest abundances occurred in the Gulf of Penas (700 and 4,500 cells L⁻¹, in February 2017 and 2018, respectively). The distribution of these species ranged from Paso Tamar (52°S), Magellan region (100 cells L⁻¹) to Inchemo island (45° S), Aysén region (200 cells L⁻¹), both in March 2017. Interestingly, *Azadinium* spp. for the first time were also identified at the Magellan region during 2017, between Puerto Eden (49° S) and Mariotti Islets (55° S), reaching up to 2,800 cells L⁻¹ at Estero Wickham (53° S) in February 2018. The abundances and distributions of *Karenia* spp. and *Azadinium* spp suggest that their densities increased initially in the open Pacific Ocean, followed by a passive hydrodynamical transport to the Gulf of Penas, and later on to the Magellan region fjords.

Keywords: Gulf of Penas, Aysén-Magellan regions, Fjords, Red Tide-Monitoring Programme, ichthyotoxins, *Karenia* spp, *Azadinium* spp.

Introduction

The presence of *Karenia* and *Azadinium* in Chilean fjords is not well documented, although for *Karenia* spp. there is more information. Blooms of *Karenia* spp. have always been linked to fish and invertebrate mortalities, in coastal areas of the Pacific Ocean, including channels directly connected to it. In January 2017, a mortality of about 130 tons of farmed smolts of Atlantic salmon (*Salmo salar*) occurred in the Gulf of Penas (47° S) while they were transported by wellboats from the Aysén region (45° S) to the western area of the Strait of Magellan (54° S). *Karenia* cf. *mikimotoi* was identified as the most probable agent causing death of salmon; however, there is scarce

information on the abundance and spatio-temporal distribution of *Karenia* in the Gulf of Penas and the surrounding areas of southern Chile, as well as the species that make it up, all known to be harmful to aquaculture (Clément, 1999).

Materials and Methods

Study area

The study area encompasses the Reloncaví Sound (41° S) in the northern area of the fjords to the western area of the Strait of Magellan (54° S), southern Chile (Fig. 1).

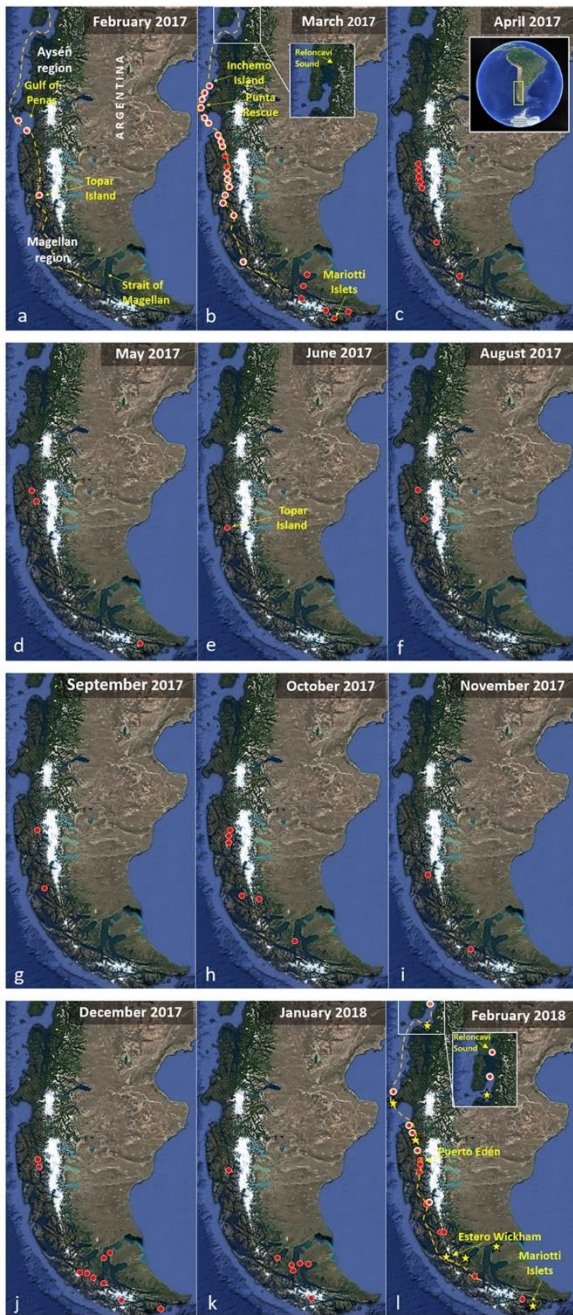


Fig. 1. Study area and spatial-temporal variation of *Karenia* spp., from February 2017 to February 2018, considering the results from samples taken from wellboats and samples collected at the Magellan region by the Red Tide-Monitoring Programme. The dashed line (---) symbolizes the track made by wellboats and the red circles with thick white line (●) symbolizes the sites with *Karenia* presence along the same track. The red dots with white thin line (◉) symbolize presence of *Karenia* in the stations monitored at the Magellan Region by the Red Tide-Monitoring Programme. Yellow stars (★) indicate the presence of *Azadinium* during February 2018 considering both sources of information (Source of the maps: Google Earth).

Abundance and distribution

Water samples from wellboats tanks were obtained during February and March 2017 and February 2018, and analyzed by microscopy using a Sedgwick-rafter chamber. Data from the Magellan region between March 2017 and February 2018 provided by the fjord system Red Tide-Monitoring Programme, were also considered.

Algal identification

For the identification of *Karenia*, light microscopy and PCR analysis were utilized. DNA extraction was performed with the CTAB method. DNA integrity was corroborated by Agarose gel, while for the concentration, a QUBIT V4.0 equipment was used. Primers described by Kamikawa et al. (2006) for *K. mikimotoi* and primers designed by Tillman et al. (2017) for *Azadinium* spp., were used.

Results and Discussion

Karenia spp. were detected from the Reloncaví Sound (41° S) to the Mariotti Islets (55°) in sampling sites located in the Pacific Ocean or sites with oceanic influence (Fig. 1). During March 2017 and February 2018 *Karenia* spp. appeared in a greater number of sampling sites, in months with more favorable climatic conditions for phytoplankton growth (Garreaud, 2018). The highest abundances were observed in the Gulf of Penas, during February in 2017 and 2018 (700 and 4,500 cells L⁻¹, respectively).

A total of seven morphotypes of *Karenia* were identified (Fig. 2a-g): *K. mikimotoi*, *K. selliformis* (both confirmed with PCR), *K. bicuneiformis*, *K. cf. papilionacea*, *K. cf. brevis*, *K. cf. brevisulcata* and *Karenia* sp.

Historically, *Gymnodinium* spp. has already been described for a sector of great geographic coverage, from the Chiloé archipelago to the Magellan Strait (42° - 54° S) in 1999 (Clément et al., 2000; Uribe and Ruiz, 2001). Later, in samples collected from Costa Channel, zone within the mentioned geographical area, collected in 1999 during the flowering of *Gymnodinium* spp, *Karenia* cf. *mikimotoi* were identified by PCR (GenBank number U92250) (Guillou et al., 2002), species that was later identified as *K. selliformis* (Haywood et al. 2004). If the *Gymnodinium* bloom observed on 1999 was monospecific, it is difficult to establish. Old bloom probably was composed by other

morphospecies, as it is reported by Uribe and Ruiz (2001) in agreements with our results.

Three different morphotypes belonging to the *Amphidomataceae* family were observed, one of them like *Azadinium spinosum* (Fig. 2h), one unidentified (*Azadinium* sp. 1, Fig. 2j) and one belonging to the genus *Amphidoma* (*Amphidoma* cf. *parvula*) (Fig. 2i). These morphotypes were identified in Punta Rescue (Pacific Ocean, Aysén region) on March 2017, and on February 2018 it was also identified at the Magellan region, between Puerto Edén (49° S) and Mariotti Islets Conference), about the presence within the fjords and channel system of south pacific Patagonia of these (55° S), reaching 2,800 cells L⁻¹ at Estero Wickham (53° S). It is important to pointed out that

this is the first formal report, together with the poster presented by Frangópulos et al., (2018, this lipophilic toxin producing dinoflagellates, with different morphotypes. Previously, Tillmann et al., (2017) reported the first record from Chile of the genus *Azadinium* detected in the Pacific north Chilean coastal. Nevertheless, already in 1973 Campodónico and Guzmán (1974) had described a red tide produced by *Amphidoma* sp. in the Strait of Magellan.

In conclusion, 7 morphospecies of *Karenia* and 3 species of *Amphidomataceae* group were identified in the fjord area of Chile, some or all of them could have been associated the massive salmon mortalities registered during the summer of 2017.

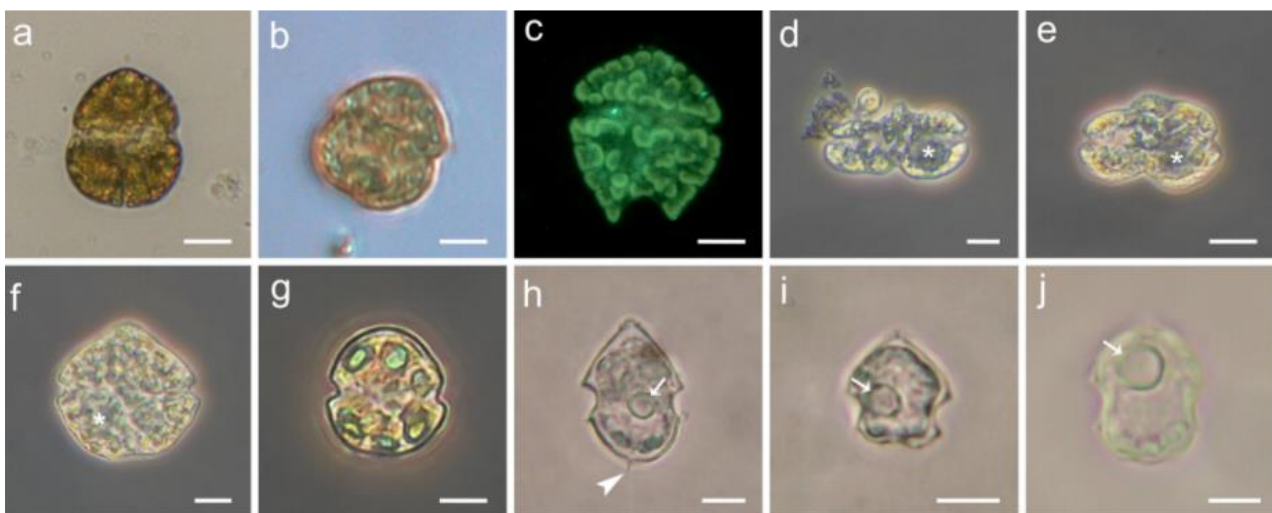


Fig. 2. Species of the genus *Karenia* and *Azadinium* identified in the Southern zone of Chile using light microscopy. a) *Karenia mikimotoi*, b) *Karenia selliformis*, c) *Karenia bicuneiformis*, d) *Karenia* cf. *papilionacea*, e) *Karenia* cf. *brevis*, f) *Karenia* cf. *brevisulcata*, g) *Karenia* sp., h) *Azadinium* cf. *spinosum*, i) *Amphidoma* cf. *parvula*, j) *Azadinium* sp. 1. White arrows: Pyrenoids. White arrowhead: Antapical spine. White asterisk: nucleus. Scale bars: a-g, 10 mm; h-j, 5 mm.

Acknowledgements

This study was carried out under the Red Tide Monitoring Program in the regions of Los Lagos, Aysén and Magallanes, XI Stage, led by IFOP and financially supported by Subpesca-MINECON of the State of Chile.

References

Campodónico, I., Guzmán, L. (1974). Anales del Instituto de la Patagonia 1-2: 209-213.

Clément A. (1999). Informe Técnico. Programa Monitoreo Fitoplancton INTESAL. 29 pp.

Clément, A., Seguel, M., Arzul, G., Guzmán, L., Alarcón, C. (2001). In: Harmful Algal Blooms 2000, Hallegraeff *et al.* (ed). Intergovernmental Oceanographic Commission of UNESCO 2001, pp. 66-69.

Haywood, A.J., Steidinger, K.A., Truby, E.W., Bergquist, P.R., Bergquist, P.L., Adamson, J.

MacKenzie, L. (2004). Journal of Phycology 40, 165-179.

Frangopulos, M., Iriarte, J.L., Gonzalez, H., Pacheco, H., Menschel, E., Pinto, M., Alarcon, C., Toro, C. (2018). The 18th International

Conference on Harmful Algae, ICHA 2018,
Abstract book, p. 293.

Garreaud, R.D. (2018). *Clim Res* 74:217-229.

Guillou, L., Nézan, E., Cueff, V., Erard-Le Denn,
E., Cambon-Bonavita M.A., Gentien, P., Barbier
G. (2002). *Protist* 153: 223-238.

Tillmann, U., Elbrächter, M., Krock, B., John, U.,
Cembella, A.D. (2009). *Eur. J. Phycol.* 44, 63–79.

Uribe, J., Ruiz, M. (2001). *Revista de Biología
Marina y Oceanografía* 36 (2): 155– 164



**New major events &
exploitation of longtime
series (monitoring & case
studies)**

Occurrence of Yessotoxins in Canadian Shellfish from 2012-2018

Wade Rourke^{1*}, Nicola Haigh²

¹ Canadian Food Inspection Agency, Dartmouth Laboratory, 1992 Agency Drive, Dartmouth, NS, B3B 1Y9, Canada;

² Microthalassia Consultants Inc, 3174 Rock City Road, Nanaimo, BC, V9T 1T4, Canada.

* corresponding author's email: Wade.Rourke@canada.ca

Abstract

Yessotoxins (YTXs) are a group of lipophilic shellfish toxins produced by the dinoflagellate *Protoceratium reticulatum* and other species of phytoplankton. The European Union has regulated a maximum limit (ML) of 3.75 mg YTX eq/kg, but there is no ML in Canada. The Canadian Food Inspection Agency (CFIA) has monitored YTX in Canadian shellfish since 2003 in support of export activities and to generate data for a Canadian risk assessment. A seven-year dataset (2012-2018) is presented, with accompanying phytoplankton data when available. Mussels (*Mytilus spp.*) were sampled most frequently. *P. reticulatum* was detected on both the Atlantic and Pacific coasts of Canada, but YTX levels in shellfish were higher and more prevalent on the Pacific coast. YTXs were detected in 65% of Pacific samples, but only 2% of Atlantic samples. Just 3.8% of monitoring samples exceeded the EU ML; only one of these samples was from the Atlantic coast. The highest total YTX concentration detected was 12 mg YTX eq/kg, which is one of the highest shellfish contamination levels reported in the literature. YTX and 45-hydroxy YTX (45-OH YTX) were detected in shellfish samples. YTX was the dominant analogue, but samples were more likely to exceed the EU ML when 45-OH YTX concentrations were equal to or greater than YTX concentrations. *P. reticulatum* cell counts peaked slightly before shellfish YTX concentrations in nearby areas. In general, shellfish YTX concentrations increased rapidly and then decreased slowly, although some variability was observed in rate of decrease. No known human illnesses were linked to high YTX concentrations in shellfish harvested legally under the conditions of Canada's federal food safety program during this time.

Keywords: Yessotoxins, marine biotoxins, *Protoceratium reticulatum*

Introduction

Yessotoxin (YTX) is a polyether compound that was first discovered in Japan (Murata *et al.*, 1987), and is produced by the dinoflagellates *Protoceratium reticulatum* (Satake *et al.*, 1997), *Gonyaulax spinifera* (Rhodes *et al.*, 2006), and *Lingulodinium polyedrum* (Paz *et al.*, 2004). Over 100 analogues have been identified in shellfish, but many have not been well-characterized.

This family of compounds has been shown to have potential for cardiac cell damage, but gaps remain in the research (Tubaro *et al.*, 2010). Recent studies (Bagryantseva *et al.*, 2018) have attempted to address these gaps, but the mechanism of action is still unknown. Other research has suggested potential therapeutic uses of YTX to treat cancer or Alzheimer's disease (Alonso *et al.*, 2013; Tobio *et al.*, 2016).

These compounds have been regulated in the European Union since 2002 (European Union,

2002) with a maximum level (ML) of 1 mg YTX eq/kg shellfish. A 2008 risk assessment (Anonymous, 2008) led to an increase in the ML, to 3.75 mg YTX eq/kg shellfish (European Union, 2013). This regulation includes 4 compounds: YTX, 45-hydroxy YTX (45-OH YTX), homoYTX, and 45-OH homoYTX. There are no ML regulations in Canada, but the Canadian Food Inspection Agency (CFIA) has monitored YTX concentrations in shellfish since 2003.

The most commonly observed regulated analogues are YTX and 45-OH YTX; 45-OH YTX is a shellfish metabolite of YTX (Aasen *et al.*, 2005; Röder *et al.*, 2011). Both YTX and 45-OH YTX have been reported previously in Canadian samples (Finch *et al.*, 2005), and *P. reticulatum* has been identified as a YTX-producer in Canada (Stobo *et al.*, 2003).

Materials and Methods

Significant sampling sites are shown in Figure 1.

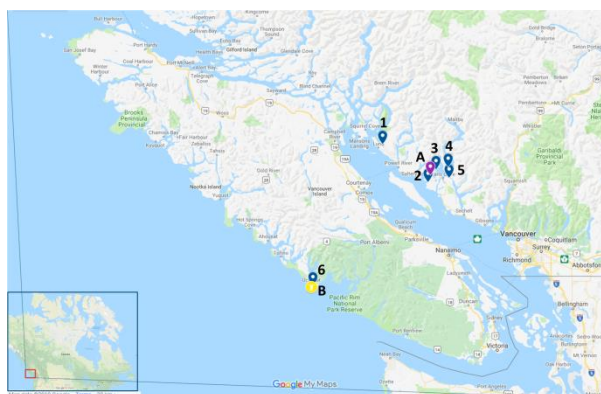


Fig. 1. BC sampling sites for shellfish: 1) Okeover Inlet, 2) Ballet Bay, 3) Sykes Island, 4) Goliath Bay, 5) Egmont, and 6) Spring Cove. BC sampling site for phytoplankton: A) Ahlstrom. BC sampling location for sea surface temperature (SST): B) Amphitrite Point Lighthouse.

Shellfish sampling and analysis

Live molluscan shellfish samples were collected from harvest sites between April 2012 and September 2018 as part of the Canadian Shellfish Sanitation Program (CSSP) (Table 1). Samples were sent to a CFIA laboratory, where they were cleaned, shucked, and homogenized. Sample homogenates were either analysed immediately or stored frozen prior to analysis.

Table 1. Distribution of shellfish species sampled from Atlantic and Pacific Canada (April, 2012-August, 2018)

Species	Pacific (%)	Atlantic (%)
Mussels	94.1	57.8
Clams	2.7	27.5
Geoducks	2.9	--
Scallops	0.1	8.4
Oysters	0.2	5.4
Whelks	--	1.0

Shellfish sample homogenates were analysed for YTXs as part of a multi-toxin lipophilic shellfish toxin method; 2.0 g subsamples of tissue homogenate were extracted following the EU harmonized SOP (EURLMB, 2015) with no SPE cleanup and separation on a Waters Acquity UPLC BEH Shield RP18, 1.7 μm , 2.1 x 100 mm column with acidic mobile phase (Villar Gonzalez *et al.*,

2011). Analyses were carried out with either an Agilent 1290 UHPLC system (Agilent Technologies, Kirkland, QC, Canada) coupled to an AB Sciex 5500 QTrap MS/MS (AB Sciex, Concord, ON, Canada) or a Waters I-Class UPLC coupled to a Waters Xevo TQ-S Micro MS/MS (Waters Limited, Millford, MA, USA). YTX analogues were detected using negative electrospray mode multiple-reaction monitoring (MRM) and details are shown in Table 2. HomoYTX was quantified against a homoYTX certified reference material (CRM) from the National Research Council Canada (NRCC) (Halifax, NS, CA), and the other YTX compounds were quantified against a YTX CRM from NRCC, assuming equimolar response factors as YTX.

Table 2. MRM transitions for YTX compounds

Compound	Precursor Ion	Product Ion
YTX	1141.5	1061.5
homoYTX	1155.5	1075.5
45-OH YTX	1157.5	1077.5
45-OH homo YTX	1171.5	1091.5

Phytoplankton sampling and analysis

Phytoplankton samples were collected for the Harmful Algae Monitoring Program (HAMP), a monitoring program in BC funded by the salmon aquaculture industry. Sites near or at fish farms around Vancouver Island and the BC Central Coast were monitored; 120 mL discrete water samples were taken weekly from 1 m, 5 m, and 10 m depths, preserved with Lugol's iodine solution (Thronsdon, 1978), and sent to the HAMP lab in Nanaimo, BC for taxonomic analysis. Sampling was done from March/April to October/November. Sampling sites varied in number (10 to 16 sites from 2012 – 2018) and placement from year to year.

Preserved HAMP samples were analysed within 1–2 days of arrival. Identification and enumeration of phytoplankton was done with a compound microscope using a Sedgewick-Rafter slide (LeGresley and McDermott, 2010). Identification was based on morphology to the lowest taxonomic level possible (Hasle, 1978). Enumeration (as cells mL^{-1}) was done only for species that are known or suspected to be fish-killers, and the species or group that is dominant in the sample. Phytoplankton species that are of concern due to shellfish toxicity (e.g. *P. reticulatum* or other toxic

dinoflagellates and diatoms) were noted if present, and were counted if very numerous or if time permitted.

Results and Discussion

Yessotoxins were detected in shellfish samples from both the Atlantic and Pacific coasts of Canada, but were significantly higher and more prevalent on the Pacific Coast (Table 3).

Table 3. Prevalence and maximum concentrations of YTX in shellfish flesh sampled in Pacific and Atlantic Canada (April 2012 - August 2018)

Year	Prevalence (% Detected)		Maximum Total YTX eq (mg/kg)	
	Pacific	Atlantic	Pacific	Atlantic
2012	85	3	12	0.09
2013	74	1	7.0	1.5
2014	71	2	11	1.6
2015	58	3	3.5	1.0
2016	55	1	5.2	0.19
2017	43	0	3.4	0.26
2018	54	3	11	0.35

Shellfish sampling was conducted to determine the highest food safety risk - not to compare toxin levels between species. Mussels are often used as the sentinel species in toxin monitoring, and were sampled more than other species (Table 1). This was a retrospective data-analysis study and cannot be used to support conclusions about YTX risk or accumulation rates between shellfish species.

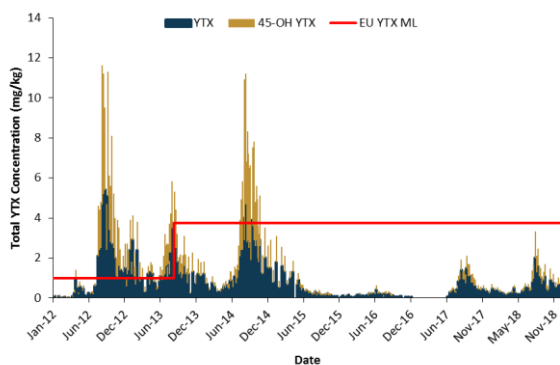


Fig. 2. YTX analogues detected in shellfish samples collected at Okeover Inlet, BC.

The most commonly detected analogues in Canadian shellfish were YTX and 45-OH YTX, but 45-OH YTX was never observed without YTX (Fig. 2). This is consistent with information that significant 45-OH YTX concentrations are a result of YTX metabolism in shellfish (Aasen *et al.*, 2005; Röder *et al.*, 2011).

The primary dataset was the shellfish YTX concentrations, and other datasets were overlaid to find trends. It should be noted that these comparisons are not perfect, with separation of up to 16 km and 4 days between shellfish and phytoplankton sampling (Fig.3, Fig. 4).

HAMP phytoplankton data were compared with toxin data from nearby CSSP monitoring sites on the Pacific coast. Results showed *P. reticulatum* increased just before total YTX levels (Fig. 3).

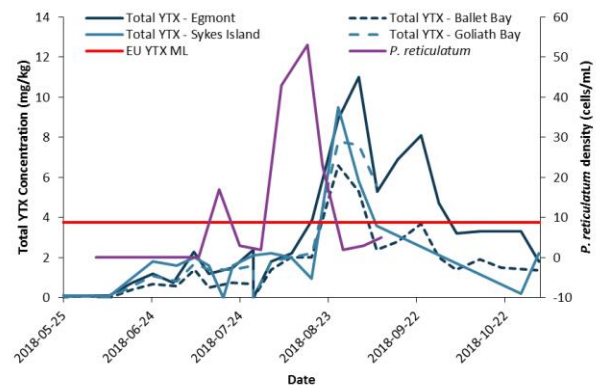


Fig. 3. *P. reticulatum* cell counts and total YTX concentrations in shellfish from Jervis Inlet, BC.

YTX data were compared with SST data. Fig. 4 reveals that peak total YTX concentrations occur near peak temperatures. SST often peaked slightly earlier than total YTX concentrations, but this lag could be expected as increased SST allowed *P. reticulatum* to bloom, and produce YTX, which then contaminated shellfish.

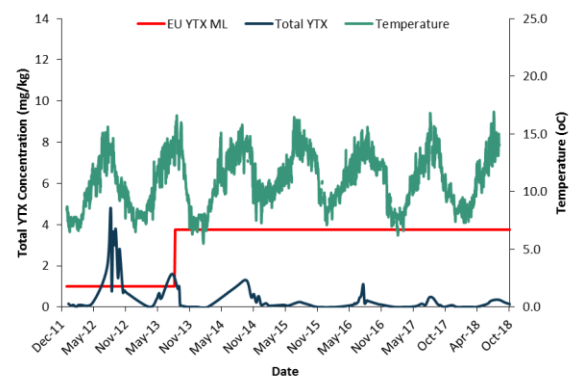


Fig. 4. Total YTX concentrations in shellfish from Spring Cove, BC and SST data from lighthouse at Amphitrite Point, BC.

This dataset shows continued YTX detections in Canadian shellfish, with significantly higher and more prevalent YTX concentrations on the Pacific coast. YTX and 45-OH YTX were detected with a maximum of 12 mg YTXeq/kg. Most of these data (73%) were based on mussel samples, with insufficient data to draw conclusions about YTX uptake for other species. High YTX concentrations have not been detected every year, but in years when high concentrations are detected, the peak concentration in shellfish seems to happen when the SST is highest. It is significant to note that no reported human illnesses have been associated with these high YTX concentrations in shellfish.

Acknowledgements

YTX concentrations were from CSSP monitoring samples analysed by the CFIA Dartmouth Laboratory. *P. reticulatum* counts were from HAMP, funded by BC salmon aquaculture companies: Grieg Seafood BC, Cermaq Canada, Creative Salmon, and Marine Harvest Canada. SST data was obtained from Fisheries and Oceans Canada BC lightstations: <http://www.pac.dfo-mpo.gc.ca/science/oceans/data-donnees/lightstations-phares/index-eng.html>.

References

- Aasen, J., Samdal, I.A., Miles, C.O., Dahl, E., Briggs, L.R., Aune, T., 2005. *Toxicon* 45, 265-272.
- Alonso, E., Vale, C., Vieytes, M.R., Botana, L.M., 2013. *ACS Chem Neurosci* 4, 1062-1070.
- Anonymous, 2008. *EFSA Journal* 907, 1-62.
- Bagryantseva, O.V., Gmoshinskii, I.V., Evstratova, A.D., Trushina, E.N., Mustafina, O.K., Soto, K.S., Shipelin, V.A., Shumakova, A.A., Panova, A.D., Khotimchenko, S.A., 2018. *Health Risk Analysis*, 112-119.
- EURLMB, 2015. EU-Harmonized Standard Operating Procedure for Determination of Lipophilic Marine Biotoxins in Molluscs by LC-MS/MS Version 5, Vigo, Spain.
- EuropeanUnion, 2002. *Off J Eur Union* 75, 62-64.
- EuropeanUnion, 2013. *Off J Eur Union* 220, 14.
- Finch, S.C., Wilkins, A.L., Hawkes, A.D., Jensen, D.J., MacKenzie, A.L., Beuzenberg, V., Quilliam, M.A., Olseng, C.D., Samdal, I.A., Aasen, J., Selwood, A.I., Cooney, J.M., Sandvik, M., Miles, C.O., 2005. *Toxicon* 46, 160-170.
- Hasle, G.R., 1978. Identification Problems, in: Sournia, A. (Ed.), *Phytoplankton Manual*. UNESCO, Paris, pp. 125-128.
- LeGresley, M.M., McDermott, G., 2010. Counting chamber methods for quantitative phytoplankton analysis - haemocytometer, Palmer-Maloney cell and Sedgewick-Rafter cell, in: Karlson, B., Cusack, C.K., Bresnan, E. (Eds.), *Microscopic and Molecular Methods for Quantitative Phytoplankton Analysis*. UNESCO, Paris, pp. 25-30.
- Murata, M., Kumagai, M., Lee, J.S., Yasumoto, T., 1987. *Tetrahedron Letters* 28, 5869-5872.
- Paz, B., Riobo, P., Fernandez, M.L., Fraga, S., Franco, J.M., 2004. *Toxicon* 44, 251-258.
- Rhodes, L., McNabb, P., de Salas, M., Briggs, L., Beuzenberg, V., Gladstone, M., 2006. *Harmful Algae* 5, 148-155.
- Röder, K., Fritz, N., Gerdt, G., Luckas, B., 2011. *Journal of Shellfish Research* 30, 167-175.
- Satake, M., Mackenzie, L., Yasumoto, T., 1997. *Natural Toxins* 5, 164-167.
- Stobo, L., Lewis, J., Quilliam, M., Hardstaff, W., Gallacher, S., Webster, L., Smith, E., McKenzie, M., 2003. *Canadian Technical Report of Fisheries and Aquatic Sciences* 2498, 8-14.
- Thronsen, J., 1978. Preservation and Storage, in: Sournia, A. (Ed.), *Phytoplankton Manual*. UNESCO, Paris, pp. 69-74.
- Tobio, A., Alfonso, A., Madera-Salcedo, I., Botana, L.M., Blank, U., 2016. *PLoS One* 11, e0167572.
- Tubaro, A., Dell'ovo, V., Sosa, S., Florio, C., 2010. *Toxicon* 56, 163-172.
- Villar Gonzalez, A., Rodriguez-Velasco, M.L., Gago Martinez, A., 2011. *Journal of AOAC International* 94, 909-922.

Comprehensive study of the occurrence and distribution of lipophilic marine toxins in shellfish from production areas in Chile

Benjamín A. Suárez-Isla^{1*}, Fernanda Barrera¹, Daniel Carrasco¹, Leonardo Cigarra¹, Américo M. López-Rivera¹, Ignacio Rubilar¹, Carmen Alcayaga¹, Víctor Contreras¹ and Miriam Seguel²

¹Laboratory of Marine Toxins, Institute of Biomedical Sciences, Faculty of Medicine, University of Chile. Santiago and Castro.

²Centro Regional de Análisis de Recursos y Medioambiente (CERAM) Universidad Austral de Chile, Puerto Montt, Chile.

*corresponding author's email: bsuarez@u.uchile.cl

Abstract

Lipophilic marine biotoxins accumulate in shellfish and can produce negative impacts in human health and local economies. In the southernmost regions of Aysén and Magallanes (44°S-54°S) the persistent presence of *Dinophysis acuta* and accumulation of okadaic acid and dinophysistoxins in benthic shellfish have been reported since 1994. Application of an UHPLC-MS/MS method in Los Lagos Region for the determination of lipophilic toxins (EURLMB SOP, 2015) as part of a National Shellfish Sanitation Programme, generated for the first time a detailed survey of their occurrence and distribution in 67 sampling stations located in the Chiloé Inner Sea (41.5°S-45.5°S). In samples obtained from October 2015 to September 2018, yessotoxin accounted for 80.1% of total detected samples and this showed correspondence with the density distribution of *Protoceratium reticulatum* in some locations. Pectenotoxin-2 was detected in 17.0% of detected samples and its presence could be explained by the concurrent detection of *Dinophysis cf. acuminata*. In contrast, okadaic acid, dinophysistoxin-1 and -2, and azaspiracids-1 and -2 were detected in only 3.0% of detected samples. Interestingly, all samples above LOD had toxin concentrations below the maximum permitted levels and no precautionary closures needed to be enforced. Distribution analyses of phytoplankton abundance vs. % of detections of lipophilic toxins per sampling station, showed a clear North-South latitudinal distribution gradient for *P. reticulatum* abundance and YTX levels.

These results indicate that Los Lagos Region is characterized by: a) a latitudinal asymmetric distribution of *P. reticulatum* and *Dinophysis cf. acuminata*, b) a very low prevalence of diarrheagenic lipophilic toxins and their causative species and, c) low accumulation levels of these toxins in mussels and clams.

Keywords: lipophilic marine biotoxins, yessotoxins, *Protoceratium reticulatum*, mussels

Introduction

Since 1994 the persistent presence of lipophilic and paralytic marine toxins has caused serious damage to local industries in the southernmost regions of Aysén and Magallanes (44°-54°S) (Uribe et al., 2001). More infrequent events have affected the Los Lagos Region (41°S-43.5°S) one of the most important mussel aquaculture areas in the world (Seguel and Sfeir, 2010). Mussel aquaculture has grown steadily since 2002 at an annual rate of 12%. More than 380.000 tons were landed in 2017 and over 90% of this production was destined for exports totalling over US\$250 million. Other species are harvested for export and domestic consumption (Rivera et al., 2017).

The presence of dinoflagellates of the *Dinophysis* genus, such as *D. acuta*, *D. acuminata* (see note) and *D. rotundata*, was confirmed previously in several southern coastal areas (Guzmán and Campodónico, 1975). The first human DSP shellfish intoxications were reported in Los Lagos Region in 1970 and 1971. They were associated with extensive blooms of *Dinophysis* species. A high proportion of dinophysistoxin-1 and lower concentrations of okadaic acid were reported in mussels and cholgas (*Aulacomya atra*) collected from the affected areas together with the first detections of pectenotoxins and yessotoxin in the region (Zhao y cols., 1993).

In recent years, mussels and ribbed mussel (*Aulacomya atra*) from aquaculture sites in the Chiloe Archipelago showed accumulation of DTX-1, DTX-3, YTX and PTXs (García et al., 2012). A comprehensive study on endemic bivalve and carnivorous species from the Aysén Region identified highly variable concentrations of AO, DTX-1, AZA-1, PTX-2 and YTX (Zamorano et al., 2013).

LC-MS analysis of phytoplankton concentrates containing *D. acuminata* from Arica Bay (18.30°S) yielded yessotoxin, PTX-2, PTX-11 and PTX-2 seco acid (Krock et al., 2009). Pectenotoxin-2 was detected in isolated cells from *D. acuminata* and bivalve species collected from Atacama and Coquimbo regions (Blanco et al., 2007). During a bloom of *Dinophysis* species in Reloncaví fjord (42°S) high concentrations of PTX-2 in phytoplankton concentrates that contained *D. acuminata*, *D. tripos* and *D. subcircularis*, were reported (Alves de Souza et al., 2013) (Note: The original denominations in previous publications as *D. acuminata* have been kept).

The National Shellfish Sanitation Program (NSSP, 2018) was implemented in 1996. This includes routine weekly sampling from over 100 stations. Frequencies are increased during periods where toxin levels exceed pre-established concentrations and/or after detection of toxic phytoplankton species. The NSSP also includes concurrent phytoplankton monitoring that complements toxicity determinations and provides an early warning system to stakeholders. A comprehensive monitoring programme was initiated in 2006 in the southern regions of Los Lagos, Aysén and Magallanes (41.5°S-54°S) by the Institute for Fisheries Research that provided time series of phytoplankton distribution and toxin levels together with environmental and oceanographic parameters (Guzmán et al., 2018).

Materials and Methods

Shellfish samples and analysis

After replacement of the mouse bioassay by LC-MS/MS methods in 2014 (SOP Version 5, 2015), a previously unknown detailed picture of lipophilic toxin levels and their distribution in shellfish was obtained for Los Lagos Region.

Statutory analyses were performed at the Laboratory of Marine Toxins on samples provided by the NSSP, by liquid chromatography coupled to tandem mass spectrometry (UHPLC-MS/MS) (EURLMB, 2015; and Braña-Magdalena et al., 2014) with modifications. Targeted analyses were

performed on a HPLC-system (Agilent 1200) coupled to a triple-quadrupole mass spectrometer (Agilent 6430) with ESI interface. Acidic conditions (pH range 3.25-3.45) were used. Analytes were detected by negative or positive ion mode using multiple reaction monitoring (MRM). Positive MRM was used for AO, DTX-1, DTX-2, PTX-1, PTX-2, AZA-1, AZA-2 and AZA-3 and negative MRM for YTX, 45-OH-YTX, 45-OH-homo-YTX and homo-YTX. Certified reference materials were provided by NRCC, Canada. The method was in-house validated and ISO 17025:2005 accredited. Its performance was periodically assessed by QUASIMEME proficiency testing rounds.

Data sets

This study covered a 36 months period (October 2015 to September 2018). Shellfish samples (mussels) were obtained from sampling stations of the NSSP. A subset of 67 sampling stations from a total of 100 sites was selected. They corresponded to shellfish aquaculture zones and wild-shellfish beds located in the Chiloé Inner Sea (41.5°S-43.5°S) (Fig. 1). The subset corresponded to stations that were monitored for at least 18 months and that provided a minimum of 72 samples during the reporting period. Thus, observed trends did not depend on sampling frequency or distribution through the reporting period. Phytoplankton cell densities were retrieved from data sets from 42 stations included in the IFOP regional monitoring programme reports that include 10 monthly surveys per year (Guzmán et al, 2018).

Results and Discussion

Application of an UHPLC-MS/MS method in Los Lagos Region for the determination of lipophilic toxins generated for the first time a detailed survey of their occurrence and distribution in sampling stations corresponding to aquaculture centres and shellfish beds located in the Chiloé Inner Sea (41.5°S-43.5°S) (Fig 1).

Regulated lipophilic toxins were detected above LOD in 8.7% of all samples (N=965/11,100). Yessotoxin accounted for 80.1% of all samples above LOD (773/965) and this correlated well with the density of *Protoceratium reticulatum* in some locations.

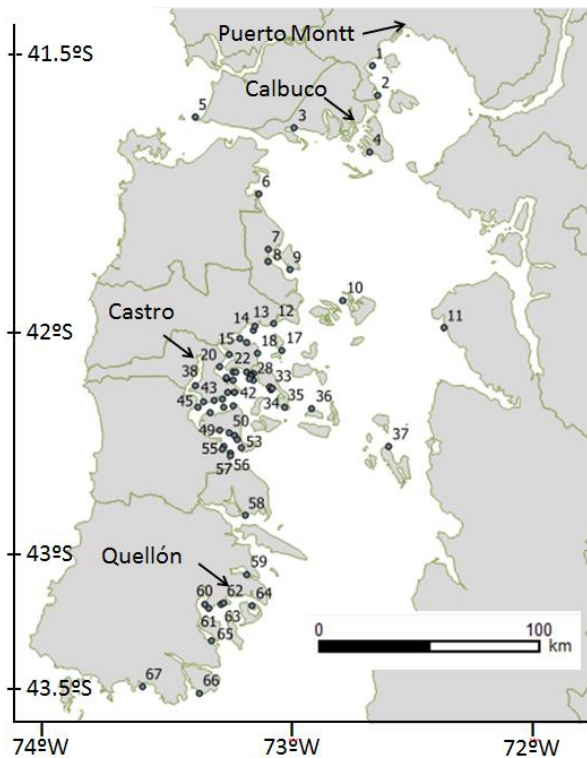


Fig. 1. Distribution of NSSP sampling stations for lipophilic toxins.

Pectenotoxin-2 was detected in 17.0% of samples (174/965) and could be explained by the presence of *Dinophysis* cf. *acuminata* (Fux et al. 2011). Much fewer samples containing okadaic acid, dinophysistoxin-1 and -2 (1.5%; 14/965) and azaspiracid-1 and 2 (1.5%; 14/965) could be observed. Interestingly, all samples above LOD had toxin levels below the maximum permitted levels and no precautionary closures needed to be enforced.

Distribution analyses of phytoplankton abundance vs. % of detections of lipophilic toxins per sampling station and toxicity levels, showed a clear North-South latitudinal gradient for *P. reticulatum* abundance and YTX levels. (Fig. 2). Maximum abundances of *P. reticulatum*, number of YTX detections and toxicity levels were consistently found in sampling stations to the north of the Los Lagos Region, in areas of significant shellfish production located near the town of Calbuco (41.5°S) (Fig. 1). A similar latitudinal trend was observed for PTX-2 and *D. cf. acuminata* (not shown). In aquaculture areas located in the central part of the Island of Chiloé (42°) that provide over 65% of landed tons of mussels per year, all detection parameters were much lower as compared to northern areas.

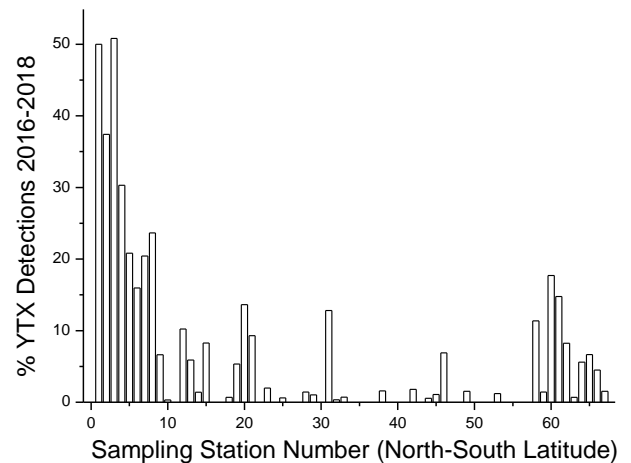


Fig. 2. Latitudinal distribution of % detections of YTX in mussels obtained from 67 sampling stations distributed between 41° and 43.5°S in the Chiloé Island. Percent detections per sampling station were obtained as N° of detections*100/ N° of monthly samples.

These results confirm that during the reporting period, the Los Lagos Region was characterized by a low risk of human intoxications due to the scarce presence of diarrheagenic toxins, in contrast to the severe and extensive PSP outbreak that impacted the same area during March-May 2016 (Strub et al., 2019) with record levels of saxitoxins accumulation. Interestingly, the occurrence and distribution of these toxin groups in shellfish produced by *D. cf. acuminata* and *P. reticulatum*, may be explained in part by oceanographic forcings and environmental cues on the causative species as recently reported (Alves de Souza et al., 2019; Strub et al., 2019).

Acknowledgements

This study was carried out as part of statutory work for the National Shellfish Sanitation Programme. The support by the National Fisheries and Aquaculture Service (Sernapesca) is gratefully acknowledged. Useful comments by two anonymous reviewers are gratefully acknowledged

References

- Alves-de-Souza, C., Varela, D., Contreras, C., de La Iglesia, P., Fernández, P., Hipp, B., Hernández, C., Riobó P., Reguera B., Franco, J.M. (2014). Deep Sea Res. II Top. Stud. Oceanogr. 101, 152–162.

- Alves-de Souza, C., Iriarte, J.L., Mardones, J. (2019) *Toxins*, 11(1), 19; doi:10.3390/toxins11010019
- Blanco J., Álvarez G., Uribe E. (2007). *Toxicon* 49: 710–716.
- Braña-Magdalena, A., Leao-Martins, J.M., Clauner, T., Gago-Martinez, A. (2014). *J. AOAC International*, 97, 285-292.
- EURLMB, 2015. EU-Harmonised SOP for determination of lipophilic marine biotoxins in molluscs by LC-MS/MS Version 5 (2015). European Union Reference Laboratory for Marine Biotoxins.
- Fux, E., Smith, J. L., Tong, M. M., Guzman, L., Anderson, D. M. (2011). *Toxicon* 57: 275-287.
- García C., Rodríguez-Unda N., Contreras C., Barriga A., Lagos N. (2012). *Food Addit. Contam.* 29: 1011–1020
- Guzmán L, Campodónico I. (1975). *Publ. Instituto de la Patagonia. Ser. Mon.* 1975; 9: 44.
- Guzmán, L. et al. (2018). INFORME FINAL Programa Manejo y Monitoreo de las mareas rojas en las regiones de Los Lagos, Aysén y Magallanes. XI etapa, 2017-2018. Tomos I y II. 77 pp. Subsecretaría de Pesca y Acuicultura (<https://www.ifop.cl/busqueda-de-informes/>)
- Krock B., Seguel C.G., Valderrama K., Tillmann U. (2009). *Toxicon* 54: 364–367.
- Lembeye, G. (1991). *Red Tide Newsletter*, 4 (2–3), 24.
- NSSP 2018. National Shellfish Sanitation Program (Sernapesca) (last access 25 Jan 2019). (http://www.sernapesca.cl/sites/default/files/part_ii_section_i_control_at_origin_version_31.01.18.pdf)
- Rivera A., Unibazo J., León P., Vásquez-Lavín F, Ponce R., Mansura, L., Gelcicha, S. (2017). *Aquaculture*, 479, 423–431.
- Seguel M. and Sfeir A. (2010). *Cienc.Tecnol.*33: 43–55.
- Strub, P.T., James, C., Montecino, V., Rutllant, J.A., Blanco, J.L. (2019). *Progr. Oceanography* <https://doi.org/10.1016/j.pocean.2019.01.004>
- Uribe J.C., García C., Rivas M., Lagos N. (2001). *J. Shellfish Res.* 20: 69–74.
- Zamorano R., Marín M., Cabrera F., Figueroa D., Contreras C., Barriga A., Lagos N., García C. (2013). *Food Addit Contam: Part A.* 30:1660–1677.
- Zhao J., Lembeye G., Cenci G., Wall B., Yasumoto T. (1993). In: *Toxic Phytoplankton Blooms in the Sea*. Editors Samyda T.J. and Shimizu Y. Elsevier Science Publishers. 587-92.

Ichthyotoxic skeleton-forming silicoflagellates in British Columbia, Canada; Results from the Harmful Algae Monitoring Program, 1999 – 2017

Nicola Haigh¹, Tamara Brown¹, and Devan Johnson¹

¹ Microthalassia Consultants Inc, 3174 Rock City Road, Nanaimo, BC, V9T 1T4, Canada.

* corresponding author's email: nicky@microthalassia.ca

Abstract

The silicoflagellates *Octactis speculum* and *Dictyocha fibula* are regular components of the phytoplankton community in British Columbia (BC) waters (48-76% of monitored weeks), with *O. speculum* being particularly prevalent throughout the year. Data from the BC salmon aquaculture industry's Harmful Algae Monitoring Program indicate blooms of both *O. speculum* and *D. fibula* cause mortalities of farmed salmon, including Atlantic (*Salmo salar*) and Chinook (*Oncorhynchus tshawytscha*). Fish-kills occurred with cell counts of 300 – 500 cells mL⁻¹ of either species of algae. Blooms of *O. speculum* were more limited in duration and extent than those of *D. fibula*. *O. speculum* blooms were most often observed in the spring (April to June), whereas *D. fibula* blooms occurred in summer to early autumn (July to September). *O. speculum* was generally observed in the skeletal form, but *D. fibula* cells observed were predominantly the non-skeletal form, with intermediate and skeletal forms more common later in the blooms. Not all thick blooms were associated with fish kills; mortalities were more often observed when significant concentrations of the algae were seen throughout the water column (surface to 15m depth) than with surface blooms only. In all reported fish kill events dissolved oxygen levels were not limiting, and pathological signs in salmon mortalities were consistent with a toxic mechanism.

Keywords: silicoflagellates, *Octactis*, *Dictyocha*, Harmful Algae Monitoring Program, fish kills, salmon

Introduction

Farmed salmon is the largest agricultural export in British Columbia (BC), with ca. 85.6 thousand tonnes, with a market value of ~CAD\$730 million, produced in 2017 (Statistics Canada 2017). There are approximately 130 salmon farm tenures in western Canada, sited around Vancouver Island and in the Central Coast area of BC, with 75 – 80 of these sites in active production at any given time (Government of Canada 2019).

Salmon aquaculture in BC has been impacted by harmful algal species since its beginning in the late 1970s (Black 1990; Whyte et al. 1999; Taylor & Harrison 2002). In 1999, the salmon farmers in BC started the Harmful Algae Monitoring Program (HAMP) with the support of Fisheries and Oceans Canada (DFO) to monitor, manage, and mitigate harmful algal blooms (HABs). Early research identified *Heterosigma akashiwo* and two mechanically harmful *Chaetoceros* species as the most common causative species of fish kills. Since 1999, HAMP monitoring has also provided data on farmed salmon kills caused by *Dictyocha*, *Chrysochromulina*, *Chattonella*, and *Pseudo-*

chattonella species (Haigh et al. 2014, N. Haigh, unpubl. data).

The silicoflagellates are little studied. For this reason, as well as their complex life histories with multimorphic life stages, the taxonomy of the Dictyochales has been poorly understood. Recently, Chang et al. (2017) undertook a revision of this group based on multiple characteristics, including molecular phylogeny, and recommended that *Dictyocha speculum* be moved to the *Octactis* genus.

Dictyocha and *Octactis* species frequently reach bloom concentrations in BC waters (Wailes 1939, Fagerness 1984, Haigh et al. 1992) and their fossils are found in sediments formed over the last 10,000 years (McQuoid and Hobson 2001).

Dictyocha / *Octactis* species have been reported to cause mortalities of Atlantic salmon and rainbow trout in Scotland, Denmark, France and Spain (reviewed in Landsberg 2002 and Smayda 2006).

Here we report the spatial and temporal distribution of *Octactis speculum* and *Dictyocha fibula*, and fish kills due to these species, at HAMP monitoring

sites on the southwest coast of BC between 1999 and 2017.

Materials and Methods

HAMP phytoplankton sampling sites were selected by the participant salmon aquaculture companies based on historical presence of harmful algae and logistical concerns. Sampling was usually done from March or April to October or November. Sampling sites varied in number (10 to 28 sites from 1999 – 2017) and placement from year to year. Data from the HAMP monitoring sites are grouped by area (Fig. 1).

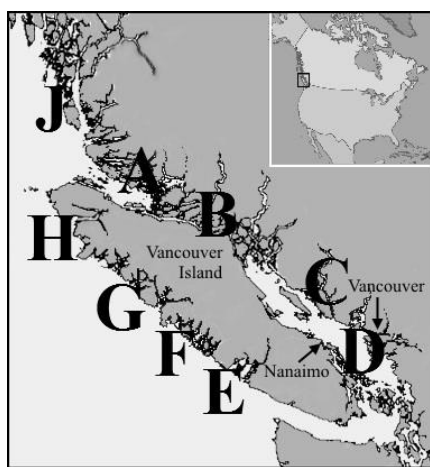


Fig. 1. Map of sampling region and HAMP sampling areas.

Water samples (120 ml discrete samples at 1, 5 and 10 m depths) were collected weekly at HAMP sites by farm personnel using a Niskin, LaMotte or homemade sampling bottle. After preservation with Lugol's iodine solution (Thronsen, 1978) the samples were sent to the HAMP lab in Nanaimo for taxonomic analysis.

Additionally, farm staff collect water samples for routine on-site plankton analysis, and environmental data (temperature, salinity, dissolved oxygen) twice daily during plankton season. Samples collected using a 20 µm net tow or discrete sampler are examined live or preserved on Sedgewick Rafter slides on a compound microscope with 40X to 400X magnification. Identification of harmful algal species in routine samples triggers more frequent sampling at the site or nearby "sentinel sites" that are known to see harmful algae earlier or at higher concentrations. Preserved HAMP samples were typically analysed within 1 – 2 days of receipt. Identification and enumeration of phytoplankton were done with a compound microscope using a Sedgewick-Rafter slide (LeGresley and McDermott, 2010).

Identification was done to the lowest taxonomic level possible, based on morphology (Hasle, 1978). Enumeration was usually only done of species known or suspected to be fish-killers, and the species or group that was dominant in the sample.

Results and Discussion

O. speculum and *D. fibula* are the most frequently observed species of the Dictyochaales in HAMP samples. Skeletal and non-skeletal forms are regularly seen; identification of non-skeletal forms to species solely based on morphology is difficult. Blooms of non-skeletal *Dictyocha* seen during the summer months appear to be *D. fibula*; this assumption is made due to their larger size (35 – 60 µm) and the frequent observation of intermediate form cells containing partial skeletons, followed by *D. fibula* skeletal cells, in the latter stages of these blooms. Figure 2 shows typical cells of these species from HAMP samples.

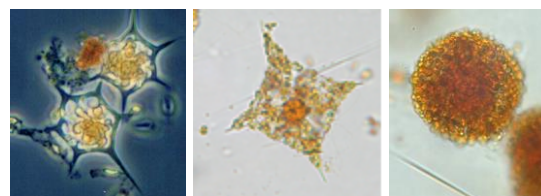


Fig. 2. Silicoflagellates from Lugol's iodine preserved HAMP samples. a) *Octactis speculum* b) *Dictyocha fibula* c) non-skeletal *D. fibula*.

O. speculum and *D. fibula* are both common in the marine phytoplankton community in BC. *O. speculum* is often seen at low levels throughout the sampling season, and in combination with *D. fibula* was present in the different HAMP areas from 48 – 76% of sampled weeks (Table 1).

The Dictyochaales display a definite seasonality in BC. Significant blooms of *O. speculum* occur in late spring (April – June), whereas blooms of non-skeletal *D. fibula* are seen in summer (late June to early September), followed by skeletal *D. fibula*. Figure 3 shows this typical seasonality in cell count data from four sites in 2016.

Both *O. speculum* and non-skeletal *Dictyocha* have been reported to be fish-killers in Denmark, France, Spain and Scotland (Smayda 2006). Blooms of skeletal *D. fibula* are less common, and mortalities due to this form have not been reported in the literature. In BC, HAMP has recorded mortalities due to all three forms; from 2003 to 2012 eight fish kills associated with *Dictyocha* / *Octactis* species blooms were observed (Table 2). Table 1. Mean prevalence (as presence in percentage of weeks monitored annually 1999 – 2017) of skeletal and non-skeletal *Dictyocha* and

Octactis species (grouped as “*Dictyocha*”) at high concentrations (>300 cells mL⁻¹) or any concentration (“total”) in HAMP sampling areas, and mean number of weeks monitored in each area.

HAMP Area	<i>Dictyocha</i>		Mean weeks mon
	prev % total	prev % high	
A	70.4	0.3	27
B	75.3	1.2	27
C	53.2	1.1	28
D	52.0	0.4	25
F	76.4	0.3	28
G	48.2	0.0	20
H	61.8	0.6	26
J	55.8	0.0	22

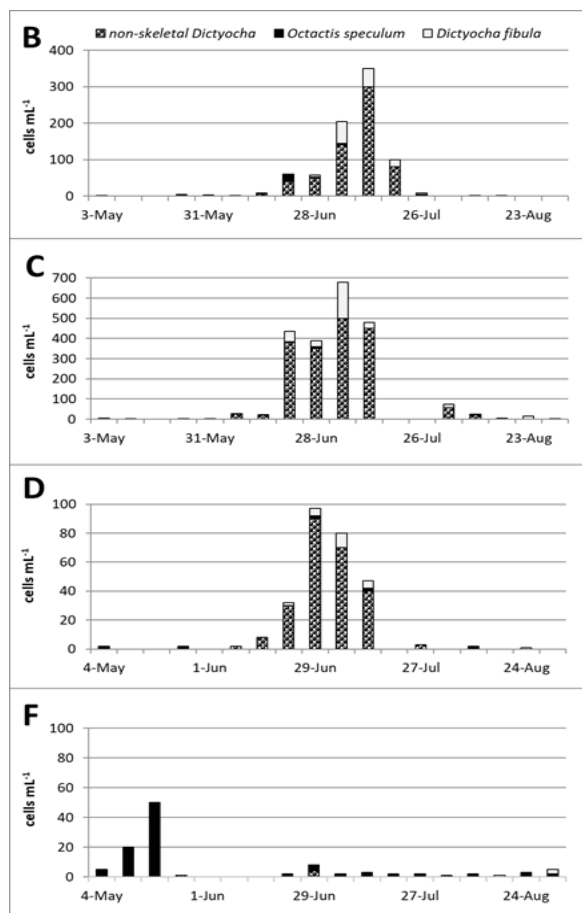


Fig. 3. Data from four HAMP sites in areas B, C, D, and F in 2016 showing typical seasonality of *D. fibula*, *O. speculum*, and non-skeletal *Dictyocha* / *Octactis*. Cell counts are maximum concentrations from 1m, 5m, and 10m depth samples.

Mortality events occurred in areas east of Vancouver Island in 2003, 2004, and 2007. In 2003 low level fish-killing blooms were reported in Area B in mid-July, and in Area C in August; *D. fibula*, *O. speculum* and non-skeletal *Dictyocha* were present in Area B, and *D. fibula* and non-skeletal

Dictyocha in Area C. During the latter event fish died when cell counts reached 600 cells mL⁻¹. *D. fibula* combined with 200 cells mL⁻¹ non-skeletal *Dictyocha*. In Area A in 2004 a bloom of 1000 cells mL⁻¹ motile flagellated *O. speculum* caused a small fish kill. In June 2007 moderate mortalities associated with a bloom of *O. speculum* and non-skeletal *Dictyocha* was seen at a site in Area C.

Table 2. Fish kills associated with *D. fibula* and *O. speculum* blooms 2003 – 2012. Mortality level is ranked from 1 (low, 100s of fish) to 3 (high, tonnes of fish). Species are coded O.s.: *O. speculum*; D.f.: *D. fibula*; n-s: non-skeletal form. (+) indicates presence of other harmful algae species.

Year-month	Area	Mort level	O.s.	D.f.	n-s
03-07	B	1	+	+	+
03-08	C	1		+	+
03-09	F	3		+	+
04-06	A	1	+		
06-05	H	3	+	(+)	
07-05	H	3	+	(+)	
07-06	C	2	+		+
12-04	H	n.d.	+		

Sites on the west coast of Vancouver Island have also been affected by fish kills due to these species. In September 2003 a site in Area F had a high level mortality event with *D. fibula* and non-skeletal *Dictyocha*. The maximum cell density of 1500 cells mL⁻¹, primarily *D. fibula*, was observed at 3 – 5 m sampling depths, and cell counts up to 300 cells mL⁻¹ were seen to depths of 15 m. Sites in Area H in May of 2006 and 2007 saw large fish kills from blooms of *O. speculum* and an unidentified *Chrysochromulina* species.

Farmed Atlantic salmon killed during these blooms did not exhibit the gross pathological signs (high mucus, bloody gills) typical of mechanical irritation. In the *O. speculum* and non-skeletal *D. fibula* bloom in Area B in July 2003, salmon gills were reported to be “gummy”, and *Dictyocha* cells were observed in the mucus. However, in the large mortality of farmed Chinook salmon in Area F due to *D. fibula* in September 2003, killed fish were reported to have very little in the way of mucus, with “pale gills with red patches” and no other notable pathological signs.

During *D. fibula* and *O. speculum* fish kill events, good quality environmental data were not always provided to HAMP, although in all these cases dissolved oxygen (DO) levels were reported to be adequate. Figure 4 shows data for the 2003 Area B

bloom when mortalities of Atlantic salmon occurred in mid-late July, with maximum cell counts of 320 cells mL⁻¹ non-skeletal *Dictyocha* and 80 cells mL⁻¹ *D. fibula*, temperature 16.8 C and salinity 25 at 1m, and DO 8.7 – 9.5 mg L⁻¹ at all sampling depths.

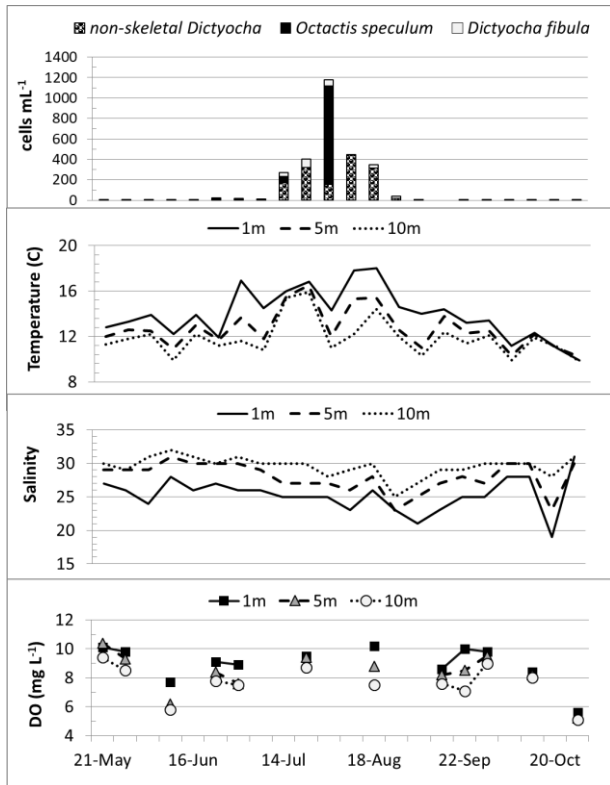


Fig. 4. Area B site *O. speculum*, *D. fibula*, and non-skeletal *Dictyocha* maximum cell concentrations (1m, 5m and 10m sampling depths), temperature, salinity, and DO in 2003. From HAMP data.

As shown by the HAMP seasonality, prevalence, and mortality data, the *Dictyocha* are common in BC and are significant fish-killers. While *O. speculum* and non-skeletal *Dictyocha* have previously been reported to cause mortality to fish (Smayda 2006), this is, to our knowledge, the first time that the skeletal form of *D. fibula* has been shown to be ichthyotoxic to farmed salmon.

Acknowledgements

HAMP is funded by BC salmon aquaculture companies: Grieg Seafood BC, Cermaq Canada, Creative Salmon, and Marine Harvest Canada. Thanks to Norma Ginther for support and editing.

References

Black, E.A. (1990). Red Tide Newsletter 3: 11-12.
 Chang, F.H., Sutherland, J., Bradford-Grieve, J. (2017). Phycol. Res. 65. 235–247.

Fagerness, V.L.(1984) M.Sc. thesis. Oregon State Univ.https://ir.library.oregonstate.edu/concern/graduate_thesis_or_dissertations/zg64tp62c

Government of Canada (2019). <https://open.canada.ca/data/en/dataset/522d1b67-30d8-4a34-9b62-5da99b1035e6>

Haigh, N., Esenkulova, S., Pudota, J. et al. (2015). In: Proceedings 16th ICHA, pp. 270 – 273.

Haigh R., Taylor, F.J.R., Sutherland, T.E. (1992). Mar. Ecol. Prog. Ser. 89:117-134.

Hasle, G.R. 1978. Monographs on Oceanographic Methodology, vol. 6. UNESCO Publishing, pp. 125-128.

Landsberg, J.H.(2002). Reviews in Fisheries Science, 10:2, 113-390.

LeGresley, M., McDermott, G. (2010). IOC Manuals and Guides, 55. UNESCO Publishing, pp. 25-30.

McQuoid, M. R., Hobson,L.A.(2001). Mar. Geol. 174, 111–123.

Smayda, T.J. (2006) Paper 2006/3. <https://www.gov.scot/Publications/2006/02/03095327>. ISBN 0 7559 131.

Statistics Canada. (2017). Table 32-10-0107-01.

Taylor, F.J.R., & Harrison, P.J. (2002). In: PICES Rep. 23, pp. 77-88.

Thronsen, J. (1978). Monographs on Oceanographic Methodology, vol. 6. UNESCO Publishing, pp. 69-74.

Wailes, G. H. (1939). Canadian Pacific Fauna: Protozoa, Mastigophora. Fish. Res. Board Can. 45p.

Whyte, J.N.C., Ginther, N.G., Keddy, L.J. (1999). In J. L. Martin and K. Haya [eds.]. Can. Tech. Rep. Fish. Aqua. Sci. 2261.



New tools (omics, lab-on-a-chip, ecotron...)

Characterisation of azaspiracid producers in New Zealand waters using molecular tools

Julie Steynen^{*1,2}, Kirsty Smith¹, Lesley Rhodes¹

¹ Cawthron Institute, Nelson, New Zealand

² Liège University, Liège, Belgium

* corresponding author's email: julie.steynen@gmail.com

Abstract

Azaspiracids (AZAs) are lipophilic polyether marine toxins produced by *Azadinium* and *Amphidoma* species. They can accumulate in shellfish species and cause azaspiracid shellfish poisoning (AZP) in humans when contaminated seafood is consumed. The distribution of azaspiracids is worldwide but the producer of these toxins cannot always be identified. In New Zealand AZAs have been detected at low concentrations in shellfish but the responsible organism remains unknown. The identification of the producer(s) is however crucial to significantly improve the monitoring efficiency of seafood safety programs and to ensure the protection of consumers. In this study, seawater samples collected as part of the New Zealand Marine Phytoplankton Monitoring Program were screened for *Azadinium* and *Amphidoma* using real-time PCR assays. Several sites were positive using the Amphidomataceae assay and the specific *A. poporum* and *A. spinosum* assays. Sediment samples were also screened for *Azadinium* cells and were identified in samples collected in narrow embayments. This result highlights the benefit of including sediment analyses in monitoring programs for early warning purposes. Toxin production of cultures that were morphologically similar to *Azadinium* and of a positive control, Chinese *A. poporum* strain CAWD219, were analysed by liquid chromatography with tandem mass spectrometry (LC-MS/MS) to detect currently regulated azaspiracids, i.e. AZA-1, -2, -3. Cryopreservation trials on *Azadinium* cultures from China (CAWD219, 220) were also performed in order to ensure the long-term viability of the cultures but were unfortunately unsuccessful. Further trials will be carried out in order to develop optimized protocols for *Azadinium* species.

Keywords: *Azadinium*, New Zealand, real-time PCR

Introduction

New Zealand's seafood industry is expanding rapidly and can be considered as a major economic and nutritional asset (Wood et al. 2013). However, harmful microalgae are an issue in New Zealand's marine and freshwater environment as they can produce toxins which are a major risk faced by this primary production sector (Rhodes et al., 2001). Toxins are most commonly produced by dinoflagellates and are transferred through the food web to higher trophic levels, particularly bivalves (Delia et al., 2015). Bivalves, filter-feed on microscopic algae, accumulate toxins in their tissues and act as vectors to humans, causing acute intoxications (Whittle and Gallacher 2000). During the last few decades, toxic harmful algal blooms have severely increased in frequency and international accredited monitoring programs have been instigated to tackle issues linked to these blooms (Lassus et al., 2016; Rhodes et al., 2013).

The Cawthron Institute leads the Safe New Zealand Seafood platform, which is a government funded research program enabling seafood production to meet market safety requirements. This program includes the characterization of unknown producers of marine biotoxins present in New Zealand waters, for example azaspiracids (AZAs). Azaspiracids are lipophilic polyether marine toxins produced by *Azadinium* and *Amphidoma* species (Tillman et al. 2017). They can accumulate in shellfish species and cause AZA shellfish poisoning (AZP) in humans consuming contaminated seafood (Twiner et al., 2008). The distribution of AZAs is worldwide and they have been detected in many countries including: Ireland, UK, Norway, Morocco, Portugal, North Africa, Japan, Chile, Canada, United States, Argentina and New Zealand (Kim et al. 2017; Salas et al. 2011; Smith et al. 2016; Tillmann et al. 2016). However,

the culprit producer of these toxins has not been identified in each of these regions. In New Zealand for instance, AZAs have been detected at low concentration in shellfish ($<0.04 \text{ mg kg}^{-1}$) but the responsible organism remains unknown. *Azadinium poporum* has been detected previously in New Zealand but did not produce AZA-1, -2 or -3. In order to protect human consumers and enable cost savings for the seafood industry, increased knowledge about the aetiology of AZP as well as an improved risk assessment for AZAs in shellfish is of utmost importance (Furey et al. 2010). In particular, the identification of the culprit producer of AZAs in New Zealand waters is a crucial requirement to significantly improve the efficiency of monitoring systems. To that end, molecular tools, i.e. real-time polymerase chain reaction (PCR), can provide information on bloom development, potential toxin production, and transfer of microalgae in the marine food web (Plumley, 1997). These tools can provide a better understanding of toxin production in the marine environment and will enable surveillance studies to become more efficient (Wood et al., 2013).

Materials and Methods

Environmental sampling

Seawater samples (100 mL) were collected from various depths at several stations as part of the New Zealand Marine Phytoplankton Monitoring Program. Samples containing cells morphologically similar to *Azadinium* spp. cells were split and 50 mL was filtered. The remaining sample was stored to perform cell isolations. Sediment samples were collected from several stations in the Marlborough Sounds aboard a fishing boat using a Van Veen grab. Sediments from the upper 0-1 cm of the grab samples were collected in duplicate and stored in the dark at 4°C.

DNA extraction

Genomic DNA from filters and 0.25 g of sediment was extracted using a Qiagen PowerSoil™ DNA isolation kit following the manufacturer's instructions.

Real-time PCR assay targeting Amphidomataceae species

Extracted DNA was analysed using a SYBR green real-time PCR targeting Amphidomataceae species (Smith et al., 2016). Positive samples were then analysed using species specific assays for *Azadinium poporum* and *Azadinium spinosum*.

Unialgal culturing and characterisation

Positive samples for the Amphidomataceae assay were examined through an Olympus CKX41 inverted microscope and *Azadinium*-like cells were isolated using micropipettes and transferred to 12-well tissue culture plates. F/2 medium (Guillard and Ryther 1962) was added to the wells, and the cells were incubated at 18 °C, $90 \mu\text{mol photons m}^{-2} \text{ s}^{-1}$ under a 12:12 L/D cycle. DNA extractions and sequencing from the *Azadinium*-like cell cultures was performed as previously described (Smith et al. 2016).

LC-MS/MS for detection and quantification of azaspiracids

Toxin analysis for AZA-1, -2 and -3 was performed on different cultures, isolated *Azadinium*-like cell cultures and a culture of a Chinese *A. poporum* strain CAWD219 as previously described (Smith et al. 2016).

Cryopreservation

Chinese *Azadinium* cultures (CAWD219 and CAWD220) from the CICC were grown to stationary phase in standard growth media and under standard growth conditions of 18 °C \pm 2°C, $90 \mu\text{mol photons m}^{-2} \text{ s}^{-1}$ under a 12:12 L/D cycle. Micro-algae were trialled with three different cryoprotective agent solutions (DMSO, ethylene glycol, propylene glycol) and loaded into cryopreservation straws. The straws were then plunged into liquid nitrogen. Two control straws from each treatment was processed as above but not cryopreserved to test the effect of the cryoprotective agent solutions survival independently of the freezing process. After one week, straws were thawed, and viability was assessed.

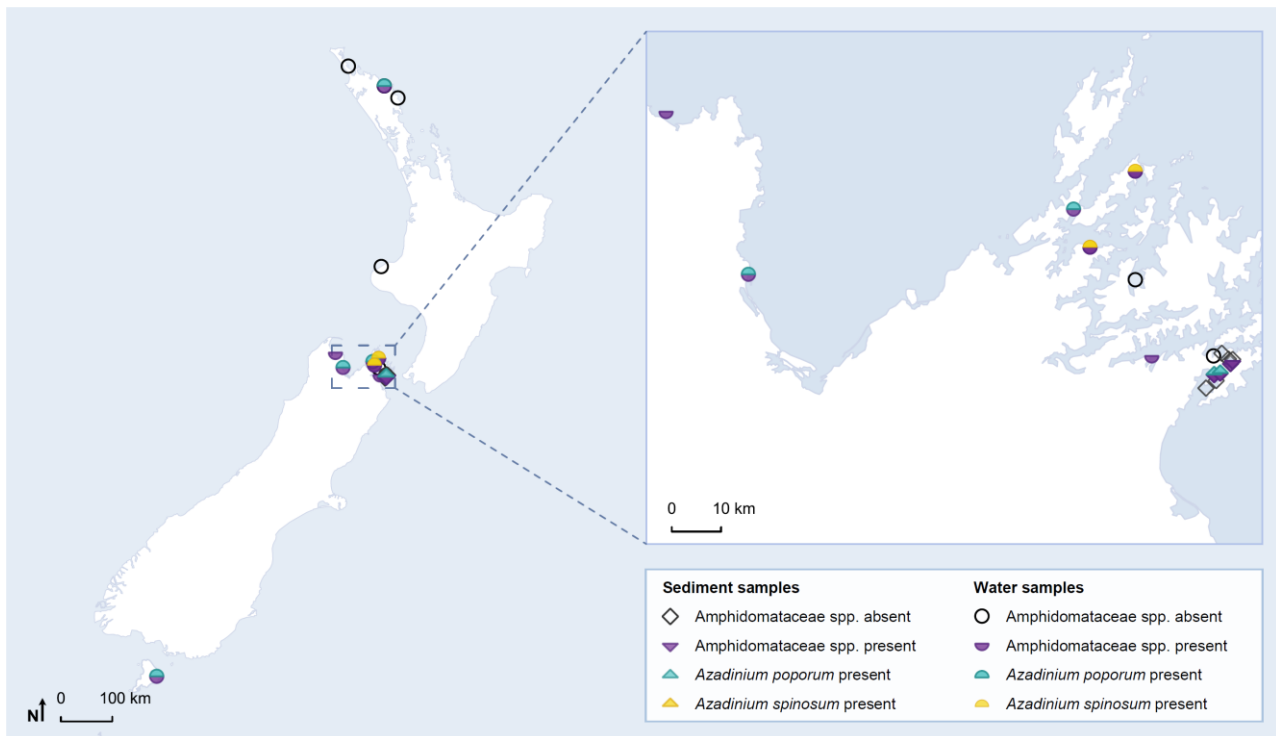


Fig. 1. Sampling sites (water and sediment samples) that were analysed using the real-time PCR assays for Amphidomataceae spp., *Azadinium poporum* and *Azadinium spinosum*.

Results & Discussion

This study has increased our knowledge of the distribution of *Azadinium* and *Amphidoma* species in New Zealand waters. Nineteen seawater samples were screened for Amphidomataceae species as well as *A. poporum* and *A. spinosum*. Thirteen samples were positive using the Amphidomataceae assay, five of them were positive using the *A. poporum* assay and five of them were positive using the *A. spinosum* assay (Figure 1).

Positive results were also obtained for several sediment samples from embayment areas. This result highlights the benefits of including sediment analyses in monitoring programs for harmful algal bloom early warnings.

Unialgal cell cultures were established but DNA sequencing revealed these cultures were *Heterocapsa* sp. and *Biecheleria* sp. Hence, current regulated AZAs were not detected in these unialgal cultures through the the toxin analysis by LC-MS/MS.

In order to ensure the long-term viability of microalgal cultures, alternative methods to serial subculturing should be developed. Therefore, this study also investigated the potential of cryopreservation to achieve that ambition. In the control samples (non-cryopreserved), living cells were only found in the 15% DMSO treatment while no living cells were found in the cryopreserved

samples (Table 1). Further trials will be carried out in order to develop optimized protocols for *Azadinium* species. The type of cryoprotective agent that is used, the cryoprotective agent concentration, and the employed cooling rate will be investigated. As a starting point, this study demonstrated that 15% DMSO should be further examined as a cryoprotective agent.

Table 1. Strains of *Azadinium poporum* used for the cryopreservation trials, cryoprotective agent treatments applied and corresponding morphological observations. NA, no relevant observation; DMSO, dimethyl sulfoxide; EG, ethylene glycol; PG, propylene glycol; C, cryopreserved samples; NC, non-cryopreserved samples (control samples).

Cryoprotective agent	C / NC	CAWD2 19	CAWD 220
10% DMSO	C	NA	NA
	NC	NA	NA
10% EG	C	NA	NA
	NC	Non motile cells	NA
10% PG	C	Murky	Murky
	NC	Murky	Murky

15% DMSO	C	Disintegrated cytoplasm	NA
	NC	Live cells	NA
15% EG	C	Murky	NA
	NC	Murky	NA
15% PG	C	Murky	Murky
	NC	Murky	Murky

Conclusion

Currently, AZAs are reported additively in New Zealand (addition of AZA-1, -2 and -3), and AZA-1 and -2 have been detected at low concentrations in New Zealand shellfish. *Azadinium* spp. are reported regularly in New Zealand's coastal waters by the Cawthron Institute micro-algae monitoring laboratory, but, due to the difficulty of differentiating *Azadinium* from other morphologically similar species by light microscopy, it is reported as cf. *Azadinium* sp. Due to these difficulties, a real-time PCR assay was designed for the detection of *Azadinium* spp. and *Amphidoma languida* to determine if field samples reported as having cf. *Azadinium* sp. are in fact positive for that genus and to aid in the isolation of potential AZA producers from New Zealand. In this study we detected *Azadinium* spp. (including *A. poporum* and *A. spinosum*) from several environmental samples from several sites around New Zealand. The real-time PCR assays allowed rapid determination of positive environmental samples and enabled those with Amphidomataceae species present to also be targeted for cell isolations. The assay is a useful tool for monitoring programmes and taxonomic surveys worldwide.

Acknowledgements

This research has been funded through the "Seafood Safety Platform" (MBIE contact # CAWX1801). We would like to thank Tim Harwood, Janet Adamson, Laura Biessy, Jacqui Stuart, and Lincoln MacKenzie (Cawthron) for technical help with this study, the Cawthron Institute Biotxin and Microalgae Laboratories for azaspiracid analyses and *Azadinium* notifications,

respectively, and Dr. Haifeng Gu (Third Institute of Oceanography, China) for kindly providing the *Azadinium poporum* cultures. Thanks also to MSQP for allowing the use of commercial samples for research purposes.

References

- Delia, A.S., Caruso, G., Melcarne, L., Caruso, G., Parisi, S. and Laganà, P. (2015). *In* Microbial toxins and related contamination in the food industry. Pp. 13-55. Springer, Cham.
- Furey, A., O'Doherty, S., ... and James, K.J. (2010). *Toxicon* 56, 173-190.
- Guillard, R. R. L., and Ryther, J. H. (1962). *Can. J. Microbiol.* 8, 229-239.
- Kim, J. H., Tillmann, U.,... and Trainer, V. L. (2017). *Harmful Algae* 68, 152-167.
- Massart, S., Brostaux, Y.,... and Steyer, S. (2008). *Eur. J. Plant Pathol.* 122, 539-547.
- Plumley, F. G. (1997). *Limnol. Oceanogr.* 42, 1252-1264.
- Rhodes, L., Smith, K. and Moisan, C. (2013). *Environ. Sci. Pollut. Res.* 20: 6872-6877.
- Salas, R., Tillmann, U., Cantwell, C., ... and Silke, J. (2011). *Harmful Algae* 10, 774-783.
- Smith, K. F., Rhodes, L., Harwood, D. T., ... and Tillmann, U. (2016). *J. Appl. Phycol.* 28, 1125-1132.
- Tillmann, U., Elbrächter, M., Krock, B., John, U., and Cembella, A. (2009). *Eur. J. Phycol.* 44, 63-79.
- Tillmann, U., Borel, C.M., Barrera, F, ... and Trefault, N. (2016). *Harmful Algae* 51, 40-55.
- Tillmann, U., Jaén, D., Fernández, L., ... and Krock, B. (2017). *Harmful Algae* 62, 113-126.
- Toebe, K., Joshi, A.R., Messtorff, P., Tillmann, U., Cembella, A., and John, U. (2013). *J. Plankton Res.* 35, 225-230.
- Twiner, M.J., Rehmann, N., Hess, P. and Doucette, G.J. (2008). *Mar. Drugs* 6: 39-72.
- Whittle, K. and Gallacher, S. (2000). *Brit. Med. Bull.* 56: 236-253.
- Wood, S.A., Smith, K.F., Banks, J.C., Tremblay, L.A., Rhodes, L., ... and Pochon, X. (2013). *New Zeal. J. Mar. Fresh.* 47, 90-119.

The Phosphopantetheinyl Transferases in Dinoflagellates

Ernest P Williams*, Tsvetan R Bachvaroff, and Allen R Place*

Institute of Marine and Environmental Technology, University of Maryland Center for Environmental Science, 701 East Pratt Street, Baltimore MD. 21202

*corresponding author's email: williamse@umces.edu & place@umces.edu

Abstract

The attachment of the phosphopantetheine arm of CoA to provide a substrate upon which polyketides and fatty acids are synthesized is performed by a phosphopantetheinyl transferase (PPTase) that is usually specific for either an acyl carrier protein used in lipid synthesis or a protein complex that synthesizes polyketides. We exploited the specificity of this rate-limiting reaction to begin to differentiate PPTases in dinoflagellates. Phylogenetically speaking the dinoflagellate species surveyed possessed one to three PPTases that grouped into three clades distinct from bacterial, fungal, and human sequences as well as algae in the genus *Chalmydomonas* and apicomplexans in the genus *Cryptosporidium*. Although dinoflagellates that are not known to produce a toxin were suspiciously absent from one of the clades (Clade 1), co-expression of each of the three PPTases from *Amphidinium carterae* with a reporter gene indicating PPTase activation of non-lipid synthesis showed minimal activation by the Clade 1 PPTase while the other two PPTases showed moderate to high activation of the reporter. These results demonstrate the utility of phylogenetics in candidate gene assignment but also the need for biochemical verification of the assignment.

Keywords: PPTase, fatty acids, polyketides, phylogenetics, dinoflagellates

Introduction

4'-Phosphopantetheinyl transferases (PPTase) are responsible for the post-translational modification of carrier proteins (CPs) in many primary and secondary metabolic pathways. The CPs can be stand-alone proteins such as the bacterial acyl carrier proteins (ACP) in fatty acid synthesis, or domains within multifunctional proteins such as the ACP or peptidyl carrier protein (PCP) domains in polyketide synthases (PKS) and non-ribosomal peptide synthetase (NRPS) (Beld *et al.*, 2014). PPTases transfer the phosphopantetheinyl group of co-substrate CoA to a conserved serine residue in CPs. The modification of CPs with the flexible phosphopantetheinyl group allows them to shuttle acyl intermediates between proteins or domains through reversible formation of a thioester linkage. From available transcriptomes of the dinoflagellates we collated gene sequences that appeared to be PPTases based on annotations. We find three clades for the dinoflagellates with members from Clade 2 and 3 being able to activate an indigoidine-synthesizing non-ribosomal peptide synthetase BpsA as a reporter.

Materials and Methods

Data collection and construct generation

Transcriptomes of dinoflagellates species used in this study were assembled using Trinity v2.3.2 from sequences deposited in the Community Cyberinfrastructure for Advanced Marine Microbial Ecology Research and Analysis (CAMERA) database as described in (Janouškovec *et al.*, 2017). *Amphidinium carterae* (Hulbert 1957) was used as the representative species among “core” dinoflagellates because it is the most basal toxin producing species and has a small genome. Candidate phosphopantetheinyl transferases (PPTases) were retrieved from the *A. carterae* transcriptome using annotations from the BLASTX results against the non-redundant protein database at the National Center for Biotechnology Information (NCBI). These three sequences were then modeled against available crystal structures for PPTases using the protein homology/analogy recognition engine (Phyre v2.0) to confirm the annotation based on conserved structure and residues from Beld *et al.* 2014. PPTases from other dinoflagellates species were retrieved using reciprocal TBLASTX against the assembled transcriptomes with each of the *A. carterae* sequences as query. A reciprocal approach was used to minimize spurious sequences whereby the subject sequence of each search was used as a

query and was kept only if it produced the original query sequence as the top BLAST hit in its own search. Outgroup sequences were obtained from NCBI's Genbank from *Homo sapiens* and several other fungi and bacteria known to produce secondary metabolites via polyketide synthases. All sequences from selected species that were annotated as phosphopantetheinyl transferases were used as candidate sequences in initial alignments. Trees were constructed from the resultant alignment using RAxML v8.2.12 (Stamatakis, 2014) with a gamma distribution and invariant site estimations using the WAG substitution model. Rapid bootstrapping was employed with 100 replicates and random seed 1111. Long branches from the resultant tree were assessed in the alignment and removed if it was determined that the sequence was truncated or likely to be a spurious annotation based on conserved residues. This was done iteratively until an increase in bootstrap scores was no longer attainable. To validate function, sequences for the three PPTases from *A. carterae*, as well as the PcpS gene from *Pseudomonas aeruginosa* (positive control with documented activation of the reporter (Finking *et al.*, 2002) were codon optimized for expression in bacteria and ligated into pET 20b (Novagen, Madison WI.) with a T7 promoter and a 6X histidine tag by Genscript (Piscataway NJ.). Inserts were verified by Sanger sequencing. The BpsA construct was kindly provided by the Ackerley lab in Wellington New Zealand (Owen *et al.*, 2011).

Transformation and gene expression

All constructs were independently transformed into 250 μ l of JM109 cells for plasmid maintenance by incubating 250 ng of plasmid with competent cells on ice, heat shocking the cells at 42° C for 30 seconds, cooling on ice, expression of antibiotic resistance in SOC medium for 1 hour at 37° C, and plating on LB agar with appropriate antibiotics. Constructs were then transformed into BL21(DE3) competent cells with the pLysS plasmid for protein expression (Thermo Scientific). Resultant colonies were picked and grown overnight in LB media with appropriate antibiotics and subsequently diluted 1:1 with 30% glycerol and frozen at -80° C. Proteins were expressed by inoculating 10 ml of LB media with antibiotics from a small scraping of the frozen stock followed by overnight incubation at 37° C with shaking at 250 rpm. This culture was then diluted 1:50 with fresh media and grown for 2 hours to an OD 600 of approximately 0.4. The temperature was lowered during this growth phase to 30° C and then lowered again to 25° C prior to induction to maximize soluble protein expression.

Induction of expression was accomplished with the addition of 500 μ l of 0.1M IPTG and a final incubation for 3 hours.

Recombinant expression and reporter assay

BL21(DE3) cells with the pLysS plasmid were co-transformed with the BpsA reporter construct and either one of the PPTase constructs or the PcpS construct as a positive control. Cells with the BpsA reporter alone were used as a negative control. These were grown and protein was expressed as described under transformation and gene expression. For endpoint quantification the cells were removed from the supernatant after 3 hours by centrifugation at 12,000 x g for 25 minutes at 4° C and the supernatant absorbance at 590 nm was measured for each culture.

Transcript and Protein abundance

Amphidinium carterae strain NCMA 1314 was grown axenically in L1 medium without silicate and with 100 μ g/ml carbenicillin, 50 μ g/ml kanamycin, and 50 μ g/ml spectinomycin at 20° C and 14 hours of light at approximately 50 μ mol of photons $\text{cm}^{-2} \text{s}^{-1}$. The culture was split into thirteen duplicate 25 cm^2 vented flasks and a whole flask was taken at each timepoint over a 12-hour period. Starting at 6 hours before lights out a sample was taken every two hours until 2 hours before lights out, after which a sample was taken every 30 minutes until two hours after lights out returning to a sample every two hours. Each sample was split into two 50 ml tubes and centrifuged at 1000 x g for 10 minutes to collect the cells. One half of each sample was suspended in 2x SDS PAGE loading buffer (80mM Tris pH 6.7, 2% sodium-dodecyl sulfate, 10% glycerol, 1mM dithiothreitol, and 6 ppm bromophenol blue) while the other half was suspended in Tri-Reagent (Sigma T9424). RNA was extracted from the Tri-Reagent fraction according to the manufacturer and cDNA was generated from 1 μ g of total RNA using random primers (Invitrogen 48190011) and Superscript II (Invitrogen 18064-022) according to the manufacturer's directions. Relative quantification of transcripts was determined using the primers in Table 1 and primers for rpl7 (Jones *et al.*, 2015) as a normalizing control at 500 nmol and the iTaq Supermix with ROX (Bio-Rad 1725121) according to the manufacturer's directions with the following thermal cycling parameters in an Applied Biosystems 7500 Fast Real Time PCR machine: Initial denaturation at 95° C for 2 minutes followed by forty cycles of denaturation at 95° C for 15 seconds and annealing and extension at 60° C for 30 seconds. Data was acquired during the annealing and extension stage and the reaction was

followed by a melt curve to test for spurious products. The resultant cycle thresholds (Cts) were subtracted from a common zero template value of 35 cycles to give inverse Cts for visualization. Protein abundance was determined by western blotting using antibodies generated by Genscript made from the epitopes listed in Table 1. For each Clade of PPTase, 15 μ l of each timepoint in 2x SDS PAGE sample buffer were loaded onto a 4-12% Bis-Tris gel (Novex NP-0323) and run in MOPS buffer at a constant voltage of 165 for 50 minutes. Peptides used to generate the antibodies for each other PPTase were also loaded as a negative control. The gel was transferred onto a PVDF membrane using a Bio-Rad Trans-Blot Turbo using the high molecular weight transfer protocol according to the manufacturer's directions. The blot was probed using the Novex iBind Western system with a 1:400 dilution of the 1^o antibody and a 1:400 dilution of the goat-anti rabbit HRP conjugated 2^o antibody according to the manufacturer's protocol. The probed blot was exposed to the Bio-Rad Clarity Western ECL substrates for 5 minutes and imaged using a Bio-Rad ChemiDoc Touch imaging system with optimal exposure. Band density was determined using Image Lab software (Bio-Rad v5.2.1) and transformed into a relative abundance within the timecourse of each PPTase Clade.

Table 1. Forward and Reverse primer sequences given as "F Primer" and "R Primer", respectively used to amplify PPTase cDNA. Also shown is the epitope used to generate rabbit antibodies specific to each of the PPTases from *A. carterae*.

PPTase	F Primer	R Primer	Epitope
Clade 1	TTGCCAGAAGCAGACAGAGA	AAGTTGGGCATACGATCTGG	CAAPQLERGEEDLS
Clade 2	GTGATTGGGTCGTTCTTGCT	TGGAAGGCCTCATAGAGCAT	CVRQEGSLPARYEGA
Clade 3	TCGGCATTGATGTAGCAGAG	CATCCCCTTAGCTTTCACG	KGDRLHYKLSKSGSSC

Results and Discussion

A final alignment was made of phosphopantetheinyl transferases from 38 species of dinoflagellates among 45 transcriptomes including three transcriptomes from co-infections of a core dinoflagellate and a dinoflagellate parasite of the genus *Amoebophyra*, and the non-photosynthetic species *Oxhyrris marina*, *Noctiluca scintillans*, and *Cryptocodinium cohnii*. Dinoflagellate sequences coded for a predicted helical and sheet secondary structure described as a hallmark of PPTase amino acid sequences (Beld *et al.*, 2014). Non-dinoflagellate sequences annotated as PPTases included *Chlamydomonas*

eustigma (2 sequences), *Chlamydomonas reinhardtii* (1 sequence), *Homo sapiens* (1 sequence), *Phellinus noxius* (3 sequences), *Sterium hirsutum* (4 sequences), *Punctularia strigosozonata* (2 sequences), *Streptomyces venezuelae* (11 sequences), *Streptomyces lividans* (7 sequences), *Streptomyces laurentii* (1 sequence), and the species from which the BpsA gene used in the reporter construct was isolated *Streptomyces lavendulae* (12 sequences). The total alignment length was 976 characters including gaps. The resultant tree (Fig. 1) placed all dinoflagellate sequences (excluding *Oxhyrris marina* placed in its own clade) outside of all other clades with 68% bootstrap support.

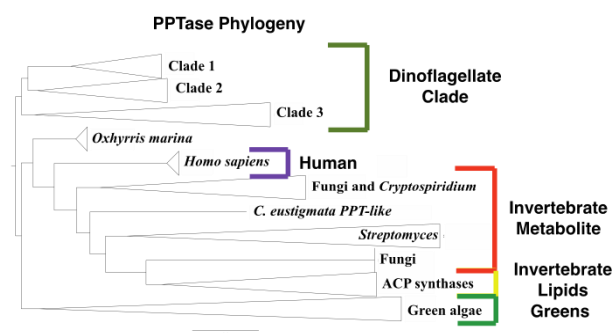


Fig. 1. Phylogeny of phosphopantetheinyl transferases using the WAG substitution model, an estimation of invariant sites, and a gamma distribution of substitution rates. Clades are collapsed with the length of the triangle indicating the number of sequences (including duplicates from multiple repository depositions) within a clade. The scale bar shows the branch length for two substitutions. Other collapsed clades are labeled with the most common source group.

Within the dinoflagellates there were three clades with poor bootstrap support. These were named Clade 1 (*Amphidinium carterae* sequence comp10839_c0_seq1, 24% bootstrap support), Clade 2 (*Amphidinium carterae* sequence comp29939_c0_seq1, 52% bootstrap support), and Clade 3 (*Amphidinium carterae* sequence comp25404_c0_seq1, 32% bootstrap support). Using each of the representative sequences from *A. carterae* as a query in a BLAST search of dinoflagellate transcriptomes resulted in the retrieval of most if not all of each species' PPTase sequences, indicating that the low bootstrap support is due to high sequence similarity among the PPTase clades. Removal of the dinoflagellates lowered the bootstrap support for most outgroup clades except for the three *Chlamydomonas* sequences that approximately doubled their bootstrap support (tree not shown). Dinoflagellate Clade 3 PPTases contained all species examined while Clade 2 and 1 contained 30 and 27,

respectively. All species contained at least two PPTase isoforms with the exception of *Protoceratium reticulatum* that only contained a Clade 3 sequence despite a robust transcriptome. *O. marina* also only appears to have one PPTase that was placed outside of all dinoflagellate clades. For *A. carterae* PPTases, sequence comparison found 85 conserved residues with pairwise similarities of 39.1%, 37.7% and 45.4% for Clade 1 versus 2, Clade 1 versus 3 and Clade 2 versus 3, respectively.

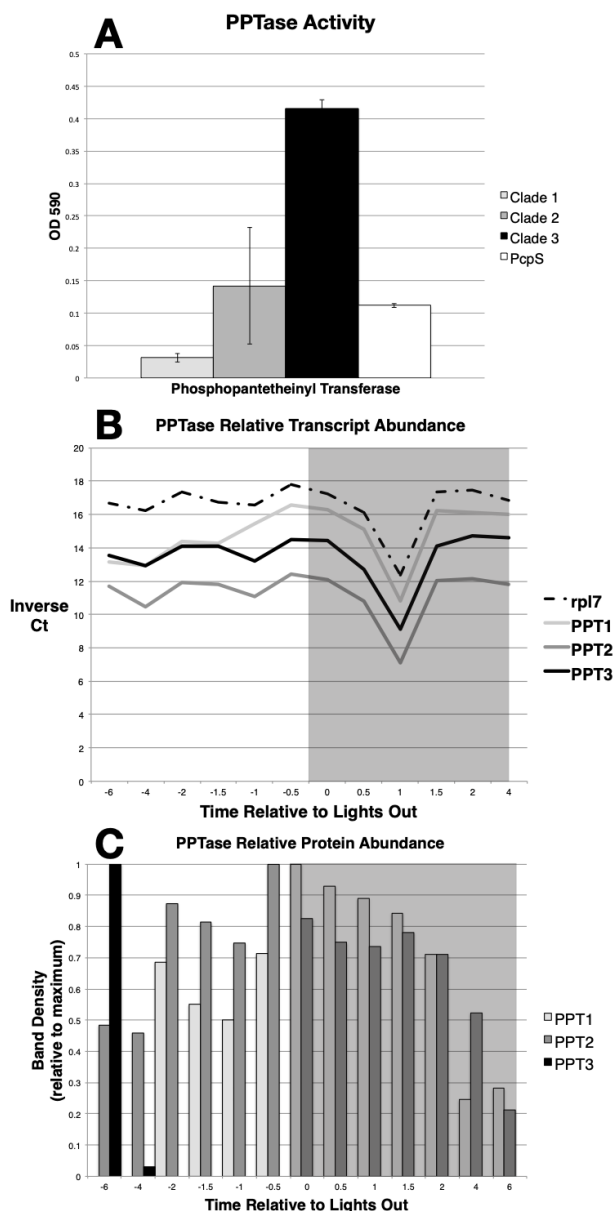


Fig. 2: (A) Activity of the three PPTases and the control PPTase from *Streptomyces aeruginosa* based on indigoidine production with standard deviation based on three biological replicates (Finking et al., 2002). Box B shows the relative transcript abundance for each of the three PPTases, as well as the control gene *rpl7*, over a diel time course. Box C shows protein abundance from the same time points by western blot.

Chemiluminescence values have been normalized to the relative abundance within the time course for each of the three PPTases. PPT1 and 2 appear to have similar expression patterns across all timepoints while PPT 3 is absent during the day. Also, the protein abundance does not correlate with transcript abundance for any PPTase.

To test the ability of each PPTase to perform secondary metabolite synthesis, we co-expressed each *A. carterae* PPTase with the indigoidine-synthesizing non-ribosomal peptide synthetase BpsA as a reporter for PPTase activity (Owen *et al.*, 2011). BpsA catalyses the conversion of two molecules of L-glutamine into indigoidine, a pigment that can be readily detected either *in vivo* or *in vitro* owing to its strong absorbance at 590 nm (Takahashi et al., 2007). As evident in Figure 2A, the *A. carterae* PPTase from Clade 2 and 3 can phosphopantetheinate the reporter BpsA and produce indigoidine. Clade 1 PPTase appears to not activate the BpsA reporter despite having the highest transcript abundance (Fig. 2B). Also, the variance in Clade 2 reporter activation is quite high. This may be linked to the empirical observation of inclusion bodies during expression relative to the other Clades indicating a possibly undescribed interacting partner or stabilizing element *in-situ*. Protein expression (Fig. 2C) varies throughout the timecourse with Clade 1 and 2 PPTases showing similar expression patterns relative to the Clade 3 PPTase that is absent during the dark phase. It is unclear based on the expression data which of the three PPTases in *A. carterae* is responsible for lipid synthesis via the phosphopantetheination of the acyl carrier protein, but at least one PPTase is required for lipid synthesis. *Protoceratium reticulatum* only has the Clade 3 copy giving rise to the possibility that this PPTase could be involved in lipid and toxin synthesis if the functionality is conserved across species.

Acknowledgements

This is contribution #5633 from UMCES, and #19-013 for IMET. This research was funded in part by NOAA-NOS-NCCOS-2012-2002987 to ARP.

References

- Beld, J., Sonnenschein, E. C., Vickery, C. R., Noel, J. P., & Burkart, M. D. (2014). *Nat Prod Rep*, 31(1), 61-108.
- Finking, R., Solsbacher, J., Konz, D., Schobert, M., Schafer, A., Jahn, D. et al. (2002). *J Biol Chem*, 277(52), 50293-50302.

Janouškovec, J., Gavelis, G. S., Burki, F., Dinh, D., Bachvaroff, T. R., Gornik, S. G. et al. (2017). *Proc Natl Acad Sci U S A*, 114(2), E171-E180.

Jones, G. D., Williams, E. P., Place, A. R., Jagus, R., & Bachvaroff, T. R. (2015). *BMC Evol Biol*, 15, 14.

Owen, J. G., Copp, J. N., & Ackerley, D. F. (2011). *Biochem J*, 436(3), 709-717.

Stamatakis, A. (2014). *Bioinformatics*, 30(9), 1312-1313.

Takahashi, H., Kumagai, T., Kitani, K., Mori, M., Matoba, Y., & Sugiyama, M. (2007). *J Biol Chem*, 282(12), 9073-9081.

Life without Chargaffs Rules: Mapping 5-hydroxymethyluracil in genomic DNA

Allen R Place^{1*}, Ernest P Williams¹, Tsvetan R Bachvaroff¹ and Robert Sabatini²

¹Institute of Marine and Environmental Technology, University of Maryland Center for Environmental Science, 701 East Pratt Street, Baltimore MD. 21202

²University of Georgia, Athens, GA 30602-7229

* corresponding author's email: place@umces.edu

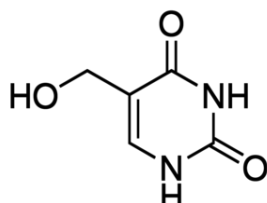
Abstract

One of the tenets for life on earth is that it obeys Chargaff's rules which states that DNA from any cell of all organisms should have a 1:1 ratio (base Pair Rule) of pyrimidine and purine bases and, more specifically, that the amount of guanine should be equal to cytosine and the amount of adenine should be equal to thymine. A major group of primitive eukaryotes, the dinoflagellates, uniformly break this rule. On average for all core dinoflagellate genera, 40.4±13.1 % (Williams and Place, 2012) of thymine bases are modified to 5-hydroxymethyluracil (5-hmU) in genomic DNA. We present data here showing the modified base exists in the nucleotide pools, both ribose and deoxyribose pools. During DNA replication 5-hmU appears to be randomly inserted in genomic DNA. In addition, another modified base, Base J, which is β-D-glucopyranosyloxymethyluracil, is found in most of the dinoflagellates we examined, except for two species of *Pyrocystitis*.

Keywords: PPTase, fatty acids, polyketides, phylogenetics, dinoflagellates

Introduction

When Peter Rae (Rae, 1973) set out to describe the ribosomal gene arrangement in the dinoflagellate *Cryptothecidium cohnii* he noticed a large discrepancy between the GC content as determined by buoyant density versus the T_m of the melting curve for the isolated DNA. He was able to explain this discrepancy when he found the thymidines were being extensively replaced by the modified base 5-hydroxymethyluracil (hmdU). This base has the effect of raising the density and lowering the thermal stability (~4° lower than T) of the DNA. Recent work has shown it does not interfere with the activity of restriction endonucleases, ligases and DNA methylases. An NMR spectroscopy-based study demonstrated that 5-hmU:A base pair is intrahelical, paired in accordance with Watson-Crick geometry, does not alter overall conformation of DNA but enhances

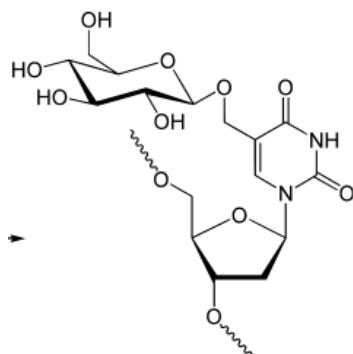


DNA flexibility and can enhance or inhibit promoter function with bacterial RNA polymerase. He went on to show this replacement was a natural

feature of all dinoflagellates he examined (Rae, 1976). Rae further proposed four possibilities for this replacement: (a) hmdU is involved in chromosome structure; (b) hmdU is involved in a modification-restriction system; (c) hmdU in DNA is required for nuclear metabolism in dinoflagellates; and (d) hmdU in DNA is a vestige, and it performs no contemporary role. Based largely on the ability of *Tetrahymena pyriformis* to incorporate large quantities of hmdU with no apparent effects he concluded that “*We believe that we are thus left with the consideration that hmdU in dinoflagellate DNA represents a neutral vestige of a mechanism that operated in earlier times*”. We extended these pioneering studies by examining the hmdU content of DNA from sister taxa believed to be basal to the dinoflagellates. The replacement of thymidine by hmdU appears to be restricted to the species with a nuclear organization lacking nucleosomes e.g. a dinokaryon.

Accordingly, we re-examined the genomic DNA from members of various dinoflagellate genera and found that between 10 and 60% of the thymine bases were substituted by 5-hydroxymethyluracil (Williams and Place, 2012). We also observed elevated levels of 5 methyl cytosine. When we examined sister taxa to the dinoflagellates we did

not find this modified base. This included DNA from *Perkinsus marinus*, *Oxyrrhis marina*, *Hematodinium atlanticus*, and three species of *Amoebophrya* (*Amoebophrya ex sanguinem*, *Amoebophrya ex instriatum*, *Amoebophrya ex K. veneficum*). The replacement of the normal thymine base by 5-hydroxy-methyluracil appears to be a prerequisite for the dinokaryon character to



be manifested.

Another modified base, Base J (shown above), is found in trypanosomes, which are closely related to dinoflagellates. As opposed to most eukaryotes, transcription in trypanosomes (and all kinetoplastids) is primarily polycistronic, with long arrays of genes assembled into a PTU (polycistronic transcriptional unit). Genes within one PTU are transcribed from the same strand. Adjacent PTUs can be either transcribed from opposing DNA strands (divergent or convergent), or from the same strand and organized in a head-to-tail fashion. All mRNAs corresponding to a PTU are processed post-transcriptionally by a splicing reaction, which adds a 39-nt leader to the 5'-end of every mRNA, and polyadenylation of the 3'-end of the mRNA. This is very reminiscent of transcription in dinoflagellates. The poly-cistronic nature of Pol II transcription indicates the importance of post-transcriptional regulatory mechanisms of gene expression, including RNA processing and protein translation. In fact, most, if not all, gene expression in these two groups of organisms is thought to occur at the level of RNA processing, stability and degradation. This finding may have direct implications for a strictly post-transcriptional model of regulated gene expression in kinetoplastids and dinoflagellates.

In our current work, we determined whether hmU is found in the ribonucleotide and/or deoxyribonucleotide pools. We also examine the relationship between hmdU and Base J in a variety of protists.

Materials and Methods

To prepare nucleotides from genomic DNA, approximately 10^6 cells was resuspended in DNA extraction buffer (500 μ l of 0.1M EDTA pH 8.0, 0.5% SDS) which was supplemented with proteinase K to 200 μ g/ml to extract bulk DNA. Samples were incubated overnight at 55°C in a hybridization oven. 82.5 μ l each of 5M NaCl and pre-warmed 10% CTAB, 0.7M NaCl was added and the samples were further incubated at 55°C for 10 minutes to remove polysaccharides. Samples were extracted with one volume of chloroform for 15 minutes to remove excess detergents and spun at 10,000 x g for 10 minutes. The supernatant was transferred to a fresh tube and two volumes of Zymo DNA binding buffer was added and mixed by inversion. Samples were bound to a Zymo clean and concentrate-5 column for one minute at 10,000 x g and the effluent was discarded. The column was washed twice with ethanol combined washing buffer for one minute at 10,000 x g discarding the effluent at each wash. Ten μ l of DEPC treated water was added to the column and incubated at room temperature for five minutes. The unbound DNA was washed from the column at 10,000 x g for two minutes and quantified using a Nanodrop ND-1000 spectrophotometer. Samples with an OD 260/280 of less than 1.6 were further treated with 2 volumes of 4M urea, 3M guanidine thiocyanate, 1% Tween 20, 50mM tris pH 8.0, 20mM EDTA at 60°C for 3 hours and repurified on a Zymo column to remove contaminating proteins and other non-nucleic acid organic molecules. Samples were diluted to 100ng/ μ l and 10 μ l were heat denatured at 95°C for five minutes and snap cooled on ice. 10 μ l of 40mM MgCl₂, 2mM ZnSO₄, 1mg/ml nuclease P1 (>200U) pH adjusted to 6.6 was added and mixed by inversion. Nucleic acids were digested for one hour at 55°C in an MJ thermal cycler with heated lid. Ten μ l of 2.4U/ml *E. coli* alkaline phosphatase was added and mixed by inversion. Nucleotides were dephosphorylated for one hour at 37°C.

For quantification of nucleoside pools, approximately 10^6 cells of *A. carterae* (CCMP 1314) were suspended in 10mM Tris pH 8.0 and 10mM magnesium sulfate. Cells were lysed using a Barocycler (Pressure Biosciences, Easton MA.) with 25 cycles of high pressure at 34,000 PSI for 20 seconds, pressure release for 15 seconds, and a lag period of 10 seconds. The lysed suspension was centrifuged at 12,000 x g for 60 minutes at 4°C. The supernatant was transferred to a new tube and 10U of shrimp alkaline phosphatase was added. Nucleotides were dephosphorylated at 37°C for one hour. High molecular weight nucleic acids and

proteins were removed by centrifugation at 190,000 x g for 44 hours at 4° C. The supernatant was passed through a 3 kDa Amicon Ultracel centrifugal filter at 10,000 x g for 10 minutes. This was repeated until all the supernatant had passed through the filter. Free nucleosides were separated into deoxyribonucleotides and ribonucleotides fractions on Affi-Gel boronate (1 x 4 cm column) equilibrate with 0.1M ammonium bicarbonate (pH 9.5). The deoxyribonucleotides were not retained. The buffer was switched to 0.1 M ammonium acetate pH 5.0 to elute the ribonucleotides. After lyophilization, the samples were analyzed by the HPLC method described below.

HPLC Separation of nucleosides

Nucleoside compositions were determined by LC-UV and LC-MS. Fifteen microliters of the digested DNAs were injected onto an Agilent Prep C18 column (LiChrosphere 125 mm x 4 mm, 5 mm bead size RP-18, Agilent; Santa Clara, CA) at 45°C and subjected to a 0.9 mL/ min isocratic elution with 0.1 M triethanolamine acetate pH 6.5 using an Agilent 1100 HPLC (Agilent 1100 LC/MS system; Agilent, Santa Clara, CA). UV peaks were detected based on their UV absorbance at 254 and 270 nm. For the MS analysis, the flow from the HPLC (0.9mL/ min) was pumped into the MS electrospray chamber with the addition of 0.1 mL min of 1 % formic acid in methanol. The MS was set up for optimal nucleotide/nucleoside ionization by using a fragmentor voltage of 350 V and a capillary voltage of 4000 V. At these settings, doubly charged ions were minimized and the total ion abundance of the singly charged parent was at a maximum. Nucleosides standards (adenosine, cytidine, 2'-deoxyadenosine, 2'-deoxycytidine, 2'-deoxyguanosine, 2'-deoxythymidine, guanosine, uridine, 5-methyl deoxycytidine, and 5-hydroxymethyldeoxyuracil) purchased from Sigma (Sigma; St Louis, MO) were run under the same condition for each sample analysis.

Determination of the genomic level of J

To quantify the genomic J levels, we used the anti-J DNA immunoblot assay as described (Van Leeuwen et al. 1997) on total genomic DNA as described above. Briefly, serially diluted genomic DNA was blotted to nitrocellulose and incubated with anti-J antisera. Bound antibodies were detected by a secondary goat anti-rabbit antibody conjugated to HRP and visualized by ECL.

Results and Discussion

As clear from the data presented in Figure 1, 5-hydroxymethyluracil is found in both ribose and deoxyribose pools of *A. carterae*. This indicates

DNA polymerase can incorporate hydroxyl-methyluracil in genomic DNA. However, we never found it in any RNA species (data not shown).

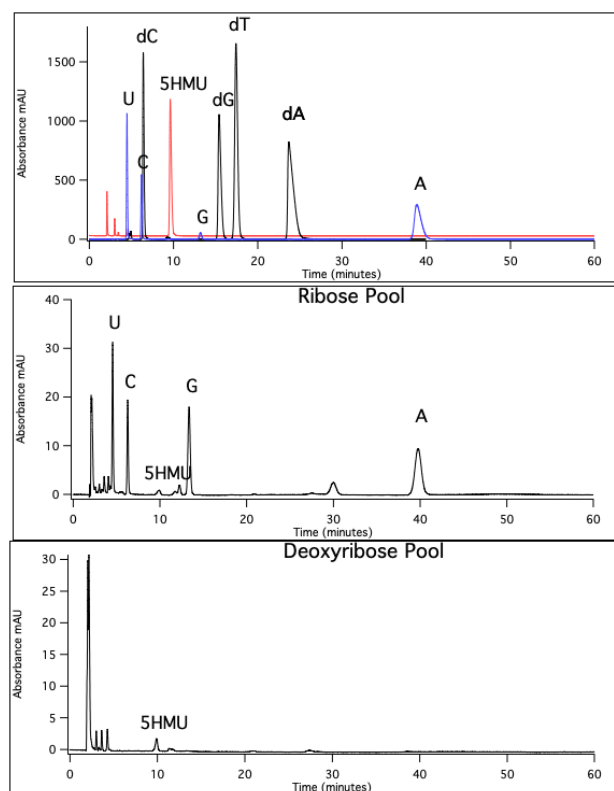


Fig. 1. Ribonucleoside and deoxyribonucleosides pools in *A. carterae*.

The most basal members of the dino-flagellates that have high levels of thymidine replacement with hmdU are *Hematodinium perezii* and *Noctiluca scintillans*, which are the earliest branching dinoflagellates shown to have definitive dinokaryons in at least some life stages (Williams and Place, 2012). One of the most striking features of the dinokaryon is the lack of histones as the dominant nucleoprotein. This highly basic protein binds to the electronegative phosphate backbone of the DNA strand that wraps around the protein providing tertiary structure. The orientation of the phosphate of hmdU is altered, however, and may be sterically incompatible with histones (Vu et al. 1999; Sobell et al. 1976). Also, a recent study has shown that histones, as the major nucleoprotein, have been replaced in dinokaryon containing species by a virally derived nucleoprotein called dinoflagellate / viral nucleoprotein (DVNP) (Gornik et al. 2012). Thus, it is proposed here that the dinokaryon is a result of the acquisition of a DVNP which allowed for the proliferation of hmdU in the chromosomes and a rejection of histone binding, thereby altering the three-dimensional conformation of the chromosome to a liquid crystal state. However, it cannot be

overstated that dinoflagellates still possess and express histones and that Rae found 10% of DNA in *Cryptocodinium cohnii* to be without hmdU. Therefore, some regions of the chromosomes of dinokaryon containing dinoflagellates probably still retain some traditional chromatin structure. Concerning Base J (Figure 2) we find it at different levels in the genomic DNA from single cell organisms with and without a dinokaryon. Surprisingly, *Oxyrrhis marina* exhibited the highest levels. Hence, Base J is not correlated with the dinokaryon. Base J had been previously described in *Euglena gracilis* (Doijes et al. 2000).

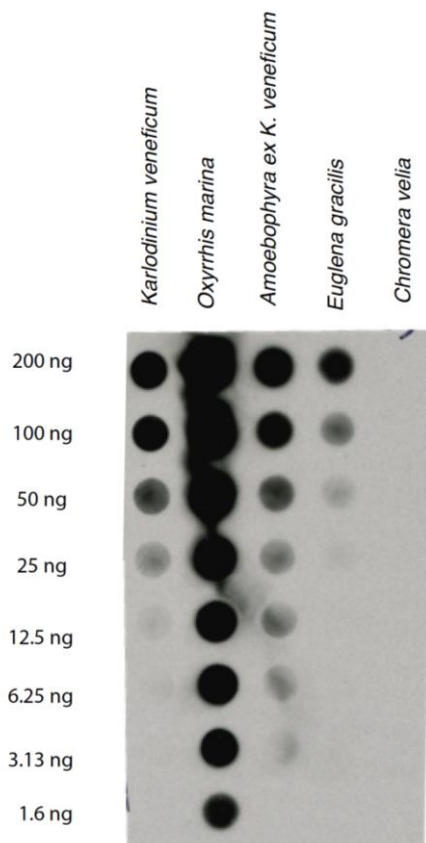


Fig. 2. Dot blot of serial diluted genomic DNA incubated with anti-J serum. Bound antibodies were detected with a second antibody conjugated to horseradish peroxidase and were visualized by enhanced chemiluminescence.

Most of the dinoflagellates we examined (See below) exhibited both hmdU and Base J in their genomes, except for two species of *Pyrocystis*. We do not have explanation for this finding at this time.

Expanding the base J world


	hmdU	Base J
<i>Karlodinium veneficum</i>	+	+
<i>Amphidinium carterae</i>	++	+
<i>Protoceratium reticulatum</i>	++	+
<i>Polarella glacialis</i>	++	++
<i>Lingulodinium polyhedra</i>	+	+
<i>Pyrocystis fusiformis</i>	+	-
<i>Pyrocystis lunola</i>	+	-
<i>Chromera velia</i>	-	-
<i>Oxyrrhis marina</i>	-	++
<i>Amoebophrya K. veneficum</i>	-	+
<i>Perkinus marinum</i>	-	-
<i>Euglena gracilis</i>	+	+

Acknowledgements

This is contribution #5632 from UMCES and #19-012 for IMET. This research was funded in part by grants from OHH NIH R01ES021949-01/NSFOCE1313888 and NOAA-NOS-NCCOS-2012-2002987 to ARP.

References

- Dooijes, D., Chave, I., Kieft, R. et al. *Nucleic Acids Res* 2000: 3017-3021.
- Gommers-Ampt, J., Lutgerink, J. & Borst, P. (1991). *Nucleic Acids Res.* 19: 1745-1751.
- Gornik, S.G., Ford, K.L., Mulhern, T.D. et al. (2012). *Curr. Biol.* printed online
- Rae, P.M.M. (1973). *Proclamations of the National Academy of Science* 70: 1141-1145.
- Sobell, H.M., Tsai, C., Gilbert, S. G. et al. (1976) *Proclamations of the National Academy of Science* 73: 3068-3072.
- Van Leeuwen, F., Wijsman, E.R., Kuyl-Yeheskiely, E., et al. (1997). *Gene Dev.* 11: 3232-3241.
- Vu, H. M., Pepe, A., Mayo, L. et al. (1999). *Nucleic Acids Res.* 27: 4143-4150.
- Yu, Z., Genest, P.A., ter Riet, B. et al. (2007). *Nucleic Acids Res.* 35: 2107-2115.
- Williams E.W., Place A.R. In: Kim H.G., Reguera B., Hallengraeff G.M., Lee C.K., Han M.S., Choi J.K., editors. *Harmful Algae, Proceedings of the 15th International Conference on Harmful Algae, Changwon, Korea, 29/10–2/11/2012; Busan, Korea: 2014.* pp. 153–156.



Mitigation of HABs and water treatment technologies

Development of an information sharing system for broad harmful algal bloom distributions

Sou Nagasoe^{1*}, Akiko Maeda², Takahisa Tokunaga¹, Yukihiro Matsuyama¹, Kazumaro Okamura¹, Kazuko Ichihashi², Katsunori Kimoto¹

¹ Seikai National Fisheries Research Institute, Japan Fisheries Research and Education Agency, 1551-8, Taira-machi, Nagasaki-shi, Nagasaki 851-2213, Japan;

² System and Development Department, ICOC Co., Ltd., 6-41, Tsukuba-machi, Isahaya-shi, Nagasaki 854-0065, Japan.

* corresponding author's email: nagasoe@affrc.go.jp

Abstract

Mass mortalities of fish caused by harmful algal blooms (HABs) remains a serious problem affecting Japanese fish farming. To avoid fish kills caused by red tides, finfish farmers relocate aquaculture rafts to lower HAB sites and stop feeds. Finfish farmers are thus eager to obtain real-time spatial information on red tide occurrence so that they can plan the relocation of rafts and the exact times for stopping feeds.

Considering farmers' requests, municipalities in each prefecture and local fish farming organizations investigate the fluctuations in HAB species and release the results to finfish farmers. In general, field surveys of areas with red tide occurrence are conducted in the morning, and finfish farmers are alerted in the early evening or at night. Moreover, there is a further time lag in obtaining information from other water surveys conducted by different organizations. To eliminate this information delay, we develop a quasi-real-time HAB alert system that allows fish farmers to use information published in various places. In particular, we develop a geographic information system (GIS) where users can input data such as sampling points (latitude and longitude), species name, and cell density of phytoplankton; spatial species-specific distributions of HABs are generated by the system and automatically displayed on a website in real time. In this report, we introduce this information sharing system and provide some case examples.

Keywords: HAB, red tide, GIS, ICT, information sharing, Ariake Bay, Yatsushiro Bay

Introduction

Harmful algal blooms (HABs) frequently occurred in Japan during the 1970s due to eutrophication accompanying high economic growth. The resulting damages to fish farms in the Seto Inland Sea resulted in serious social problems. Under such circumstances, the Interim Law for the Conservation of the Environment of the Seto Inland Sea was enacted in 1973. The number of red tides occurring in this area decreased to one-third of its maximum annual frequency (Honjo, 2015; Tada et al., 2014). However, serious fishery damages caused by HABs are still frequent in other coastal areas such as in the coast of the Bungo Channel and the western waters of Kyushu Island (Furukawa and Ura, 2017; Honjo, 2015). In particular, the number and duration of red tides have increased in the last two decades in the Ariake and Yatsushiro Bays, which are located in the

western coast of Kyushu, Japan (Hashimoto et al., 2005; Sonoda et al., 2008).

Thus far, various techniques have been developed to minimize damage caused by HABs; for example, relocation of aquaculture rafts to lower HAB sites, stopping feeds, and dispersion of cray (Honjo, 2015; Shirota, 1989). However, these countermeasures and associated preparations interfere with normal aquaculture work and fattening of cultured fish. Therefore, finfish farmers do not want to take these measures until an HAB crisis approaches; they require spatial information on red tide occurrence on a day-to-day basis, to judge the necessity of these measures.

In Japan, municipalities in each prefecture and local fish-farming organizations investigate fluctuations in HAB species and release the results to finfish farmers via fax and through each institutions' website; information for a small area

is often unclear, and information that summarizes a wide range of HAB distribution is lacking. Field surveys of areas with red tide occurrences are held in the morning, and finfish farmers are alerted early evening or at night. Moreover, because each prefecture and local organization prioritize information provision to fishermen within their prefectural and/or local boundaries, there is a further time lag in obtaining information from other water surveys. Therefore, many finfish farmers strongly request the development of an information-sharing framework across prefectural and/or local boundaries. Considering this situation, we developed a quasi-real-time HAB alert system that utilizes current information and communication technologies to allow fish farmers access to information published in various places. In this paper, we introduce an information sharing system and report its actual use in the Ariake and Yatsushiro Bays.

On the one hand, the Ariake Bay is the main area for laver seaweed farming in Japan, and fish farming is not conducted here. On the other hand, fish farming (e.g. red sea bream and yellowtail) is actively carried out in Yatsushiro Bay. Therefore, fish farms in Yatsushiro Bay are damaged by HABs in summer (*Chattonella* spp., *Karenia mikimotoi*, and *Cochlodinium polykrikoides*). In 2000, *C. polykrikoides* bloom caused damages of about 4.0 billion yen (Kim et al., 2004); *Chattonella antiqua* bloom caused damages of 2.9 and 5.3 billion yen in 2009 and 2010, respectively (Onitsuka et al., 2011).

Materials and Methods

Study site

The developed information-sharing system can be applied to all global water bodies. However, to demonstrate how the system works, we report on the use of this system in the Ariake and Yatsushiro Bays (Fig. 1). The Ariake and Yatsushiro Bays are surrounded by four (Nagasaki, Saga, Fukuoka, and Kumamoto) and two (Kumamoto and Kagoshima) prefectures, respectively. Further, they are connected by the Misumi and Ōto Straits.

Input method of investigation data

The information-sharing system was first developed in 2012 and has been improved every year. This system does not require special software, and it can be operated using a commercial web browser and Microsoft Excel. To input data, the user has to first access the system website (refer to the URL shown at the end of the text) and

download the provided template. Then, the user enters the investigation location (longitude and latitude), sampling date, time, and depth, and parameters such as water temperature, salinity, turbidity, and phytoplankton information (species and density) as per the investigation. Finally, the user can upload the completed template on the data server.

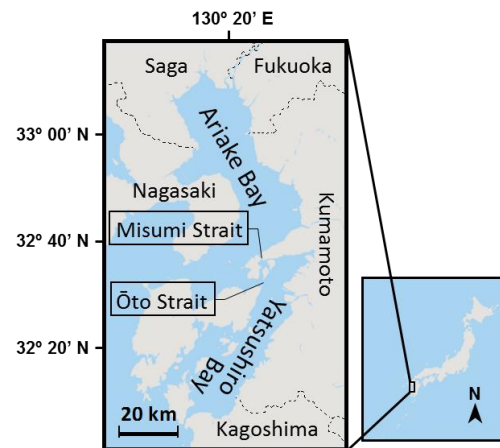


Fig. 1. Location of the study site.

Display of registration data

Using GIS techniques, data collected in the server can be displayed spatially on the website. The distribution of HAB species is presented as shown in Fig. 2. The user can view a specific distribution by selecting the species of phytoplankton and the investigation date or period.

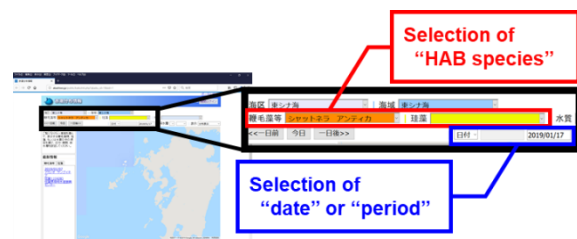


Fig. 2. Website interface of our information sharing system.

Results and Discussion

The red tide outbreak pattern in Ariake and Yatsushiro Bays is as follows: (i) a massive red tide occurs in the inner part of Ariake Bay; (ii) it spreads throughout the bay; (iii) a small part of the red tide flows into Yatsushiro Bay through the Misumi and/or Ōto Straits; (iv) the red tide seawater flowing from Ariake Bay introduces a seed population of harmful algae that begins to grow in the northern part of Yatsushiro Bay; and

(v) finally, Yatsushiro Bay encounters an outbreak of massive red tide.

Based on this outbreak pattern, it is important to predict the timing of red tide occurrence in Yatsushiro Bay. Two pieces of information are important to make an accurate prediction: (i) the time when a small part of the red tide of Ariake Bay starts flowing into Yatsushiro Bay and (ii) confirmation that the seed population is growing in the northern part of Yatsushiro Bay. Based on these two points, finfish farmers can browse HAB distribution information from our system. They can then predict the timing of the occurrence of red tide near their own rafts based on their own experience combined with other factors such as tidal currents and weather information. They can then plan measures to reduce red tide damages. Actual distribution information data from our system are shown in Figs. 3 and 4. On July 23, 2018, high-cell density (over 1,000 cells/mL) of *Chattonella* spp. was confirmed in the western part of Ariake Bay (Fig. 3). A massive red tide of this species was observed throughout Ariake Bay by July 31; however, it was hardly observed in Yatsushiro Bay in July (Fig. 3). In Yatsushiro Bay, *Chattonella* spp. could only be detected from concentrated seawater samples (< 1 cell/mL); however, this species was observed in non-concentrated seawater (≥ 1 cell/mL) at many investigation points on August 7; this implied the seed population was growing (Fig. 4). After August 16, the red tide of *Chattonella* spp. occurred extensively in Yatsushiro Bay, even when there were few investigation points which observed algal density ≥ 100 cells/mL (Fig. 4). Our information sharing system makes it possible to visually grasp a wide range of information (e.g. information that exceeds prefectural boundaries). Finfish farmers can browse the information-sharing system several times in a day during the unsafe period of red tide occurrence as the information automatically update when someone registers new data. Furthermore, a more detailed and large-scale information sharing system can be achieved with an increase in the number of users who contribute data into the database. To date, registrations to the database are conducted not only by public organizations (local governmental institutions and universities) but also by finfish farmers (Furukawa and Ura, 2017). The drop in the fishery damages caused by red tides in Ariake and Yatsushiro Bays in 2018 can be attributed to the use of our sharing system combined with better awareness and active participation of farmers.

Our immediate goal is to make this sharing system more versatile for predicting red tide occurrence by including modelling parameters such as tidal currents and weather information.

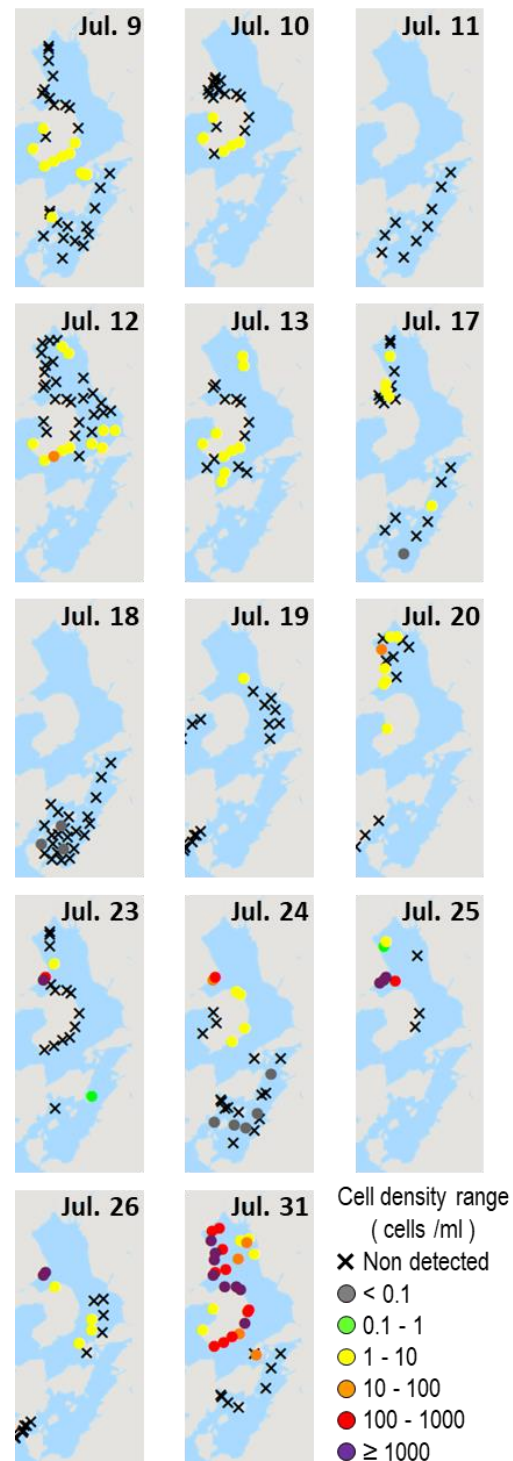


Fig. 3. Transition of *Chattonella* spp. distribution in Ariake and Yatsushiro Bays, Japan in July 2018.

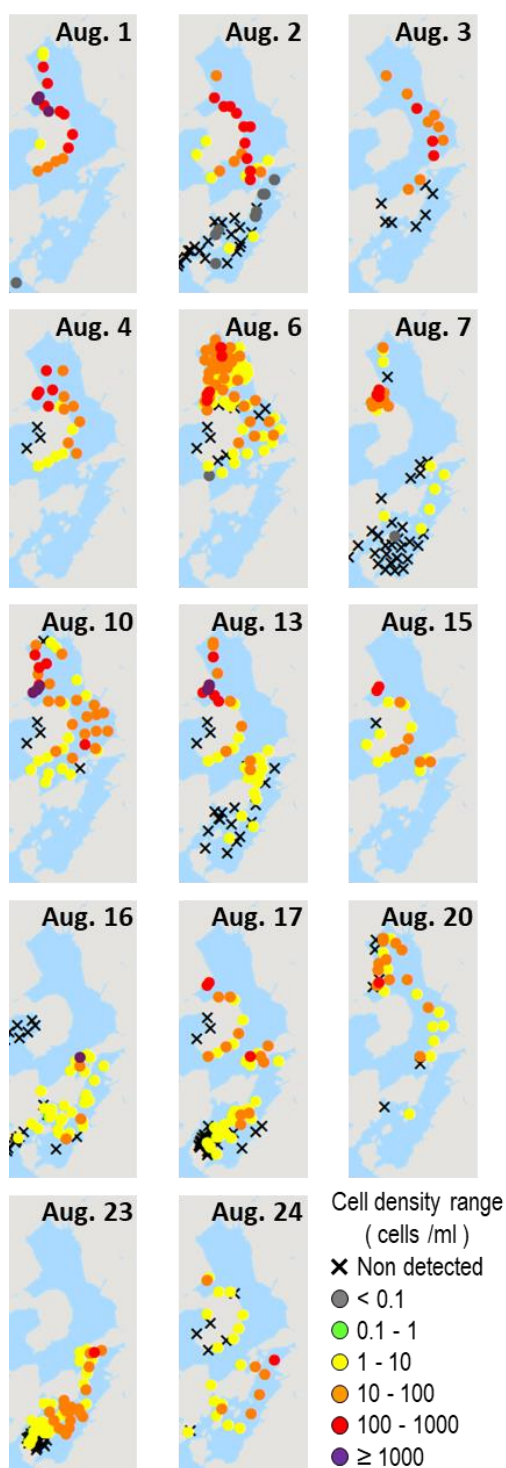


Fig. 4. Transition of *Chattonella* spp. distribution in Ariake and Yatsushiro Bays, Japan in August 2018.

Acknowledgements

This work was supported by a Japan Fisheries Agency-commissioned project for addressing red tides and oxygen-depleted water masses. The authors would like to appreciate everyone who cooperated in HAB investigations and data registration to our system.

References

- Furukawa, S., Ura, K. (2017). Nippon Suisan Gakkaishi 83, 703-706.
- Hashimoto, A., Sekine, A., Arita, M. (2005). Proceedings of Coastal Engineering, JSCE 52, 931-935.
- Honjo, T. (2015). Environmental evaluation 44, 4-15.
- Kim, D.I., Nagasoe, S., Oshima, Y., Yoon, Y.H., Imada, N., Honjo, T. (2004). Proceedings of the Xth International Conference on Harmful Algae, October 2002, 83-85.
- Onitsuka, G., Aoki, K., Shimizu, M., Matsuyama, Y., Kimoto, K., Matsuo, H., Kitadai, Y., Nishi, H., Tahara, Y., Sakurada, K. (2011). Bull. Jpn. Soc. Fish. Oceanogr. 75, 143-153.
- Shirota, A. (1989). Int. J. Aq. Fish. Technol. 1, 195-223.
- Sonoda, Y., Takikawa, K., Saitho, T. (2008). Proceedings of Civil Engineering in the Ocean 24, 615-620.
- Tada, K., Nishikawa, T., Tarutani, K., Yamamoto, K., Ichimi, K., Yamaguchi, H., Honjo, T. (2014). Bulletin on Coastal Oceanography 52, 39-47.

URL for accessing the information-sharing system :

http://akashiwo.jp/public/kaikuInIt.php?qkaiku_id=1&sid=1



Socio-economic impacts of HABs

Saxitoxin and the Cold War

Patricia A. Tester^{1*}, Julie Matweyou², Brian Himelbloom², Bruce Wright³, Steven R. Kibler⁴,
R. Wayne Litaker⁴

¹ Ocean Tester, LLC, 295 Dills Point Road, Beaufort, North Carolina 28516, USA;

² Kodiak Seafood and Marine Science Center, 118 Trident Way, Kodiak, Alaska 99615, USA;

³ Aleutian Pribilof Island Association, 1131 E. International Airport Road, Anchorage, Alaska 99518, USA;

⁴ National Oceanic and Atmospheric Administration, National Ocean Service, Beaufort Laboratory,
101 Pivers Island Road, Beaufort, North Carolina 28516, USA.

* corresponding author's email: Ocean.Tester@gmail.com

Abstract

A contract for clams and a shipping receipt to the US Army's Biological Warfare Laboratories at Ft. Detrick, Maryland were found during a data rescue mission of hundreds of mouse bioassay records related to paralytic shellfish poisoning projects conducted near Ketchikan Alaska (1947-1958). These records raised a question about whether Alaskan clams were the source of saxitoxin used by the United States Central Intelligence Agency in their search to find a replacement for the standard cyanide L-pill issued to agents in hazardous situations? Yes, saxitoxin from these clams appears to have been used, at least, on one occasion. Francis Gary Powers, a U-2 pilot, carried a saxitoxin-filled, grooved needle inside a silver dollar when he departed on an ill-fated surveillance flight across Russia, 1 May 1960.

Keywords: Select Agent List, Patriot Act, poison pin, cyanide L-pill, U-2, Church Senate Committee Hearings

Introduction

In November 1940, the Fishery Products Laboratory was established in Ketchikan Alaska and by 1943, staff members were tasked with investigating marine species as emergency food sources in the event of protein shortages brought about by World War II. The vast shellfish resources on the Alaskan coast were recognized and significant efforts were directed toward shellfish utilization starting with a clam canning industry in 1943 in southeast Alaska. In the peak year 1946, 15,000 cases of clams worth more than \$2 million USD (converted to 2018 value) were shipped (Fig. 1). Unfortunately, saxitoxin was found in shipments of butter clams that year by the US Food and Drug Administration and clam processing in southeast Alaska was discontinued. Saxitoxin is the cause of paralytic shellfish poisoning in humans and marine mammals and can be fatal (Berdalet et al., 2015).

Extensive surveys of clam beaches and other studies were undertaken from 1947 through the late 1950s by the Fisheries Products Laboratory in Ketchikan Alaska (renamed Ketchikan Technolo-

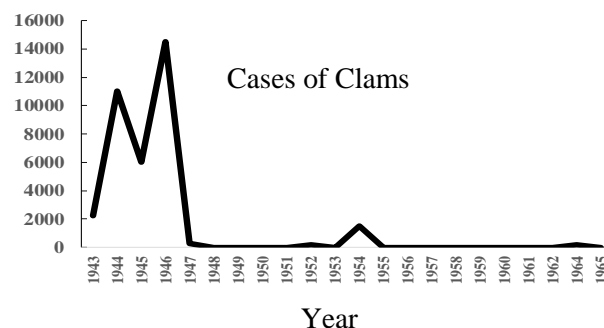


Fig. 1. Cases of hard-shelled clams canned in Alaska from 1943-1964. Data from Pacific Fisherman Yearbook (1965) and Neal (1967).

gical Laboratory). After a number of efforts, it was concluded clams of moderate toxicity were widely distributed, and beach closures would not be a reasonable management option (Magnusson and Carlson, 1951, Neal 1967). In 1971 the Ketchikan Laboratory was closed, and personnel and equipment were relocated to a newly constructed facility at Kodiak Alaska. Nearly 3,500 records of mouse bioassays and associated data from work completed at the Ketchikan Laboratory were archived and forgotten until 2013-2014 when

rumours about “lost Paralytic Shellfish Poisoning” (PSP) data began to circulate. In the summer of 2014 multiple lab notebooks were scanned along with PSP data from studies conducted from 1947-1958 to preserve these records. Among the data were a 1952 contract for clams and a shipping receipt to the US Army’s Biological Warfare Laboratories at Camp Detrick (later renamed Ft. Detrick) Maryland. This finding triggered a detective journey through Cold War history to determine if saxitoxin from Alaskan clams had been used in a poison pill for espionage agents.

“A major early requirement of the Agency [Central Intelligence Agency] was to find a replacement for the standard cyanide L-pill issued to agents in hazardous situations during WW II. This was the basis on which eventually we discovered the shellfish toxin.”

Intelligence Activities Senate Resolution 21, 1975

Results and Discussion

Much of the evidence for this inquiry came from the lengthy hearings of the Senate Select Committee to Study Governmental Operations with Respect to Intelligence Activities chaired by Senator Frank Church. These hearing were called in 1975, in part, to determine if direct orders of the President of the United States were disobeyed by employees of the Central Intelligence Agency (CIA).

On 25 November 1969, President Nixon renounced the use of biological weapons and ordered disposal of existing stocks of bacteriological weapons. The Ft. Detrick program would remain, but only for research into biowarfare defences. Further, Nixon requested ratification of the 1925 Geneva Protocol prohibiting the use of chemical and biological weapons by the US Senate. Information from the Church Committee Hearings on the Unauthorized Storage of Toxic Agents from September 16-18, 1975, revealed activities of the CIA and the US Army’s Biological Laboratories at Ft. Detrick regarding retention of a “*small*” amount (11 grams) of shellfish toxin retained in violation of President Nixon’s order (Intelligence Activities Senate Resolution 21, 1975).

After the discovery by the Committee that saxitoxin from the Ft. Detrick program had not been destroyed and the CIA’s admission of a secret stockpile of saxitoxin, saxitoxin was placed on the Federal Select Agents’ List administered by the US Centers for Disease Control and Prevention. Remaining amounts of saxitoxin were distributed to researchers. The Patriot Act of 2011 has since modified the amounts of saxitoxin that can be held or shipped.

“No definitive quantities or amounts are listed in the law, and the standard will likely be what a reasonable person with knowledge in the affected scientific field would consider to be justified.”

The Congressional Hearings not only confirmed that the US supply of saxitoxin had not destroyed, they also confirmed how saxitoxin was used.

“A tiny saxitoxin-impregnated needle hidden inside a fake silver dollar was issued to Francis Gary Powers, an American U-2 pilot, who was shot down while flying over the USSR in May 1960.”

Powers did not use the needle and warned his Russian captors about it (Fig. 2). There was major international fallout over the downing of the U-2. Not knowing Gary Powers had been captured alive and that large parts of the wreckage of the plane were found intact, the US attempted to cover up the flight, claiming it was a failed weather observation mission. This caused the cancellation of a scheduled Paris Summit planned to lessen tensions between the US and the USSR (The New York Times 1960).

In Russia, Gary Powers was tried, convicted of espionage and sentenced to 10 years in a Soviet prison. In a spy exchange on 10 February 1962, Powers was released on the Glienicke Bridge in Berlin and a spy, known in the US as Rudolph Able, was returned to the USSR (CIA 2015). The exchange was the subject of a film “Bridge of Spies” starring Tom Hanks (Touchstone Pictures 2015). After returning to the US, Powers was vindicated by the US Armed Services Committee but never worked for the US government again. He worked as pilot in California until a fatal crash in 1977.



Fig. 2. Sheath and pin found wrapped in a newspaper article from the estate of Milton Frank's of Fredrick, Maryland (PBS History Detectives, 2005). Photo courtesy of PBS History Detectives.

It was not until ca 1985, when a small plastic box filled with tiny drill bits, taps and springs, along with a newspaper clipping about a pin provided to Gary Powers, was discovered at the auction of Milton Frank's estate in Fredrick Maryland that the full story of the source of the delivery mechanism for saxitoxin was clarified. Frank was a machinist in Special Operations at Ft. Detrick and the discovery of his grooved pin as a delivery mechanism for saxitoxin was verified by the Public Broadcasting Station's History Detectives (Episode 1, 2005). Examination of the National Security Archive at Georgetown University provided the History Detectives staff with the link between the CIA and Ft. Detrick's Special Operations Department where Milton Frank worked. The pin Gary Powers carried on 1 May 1960 is reported to be in a Moscow museum (Powers and Gentry, 1970).

Soviet records report the toxin on the needle confiscated from Powers upon his arrest was tipped with curare. However, this is not correct. There was confusion in early studies on the pharmacology of shellfish poison and it was likened to curare (Kellaway 1935). The pharmacology of saxitoxin was not clarified until the mid-1960s (Evans 1964; Kao and Nishiyama. 1965).

Francis Gary Powers is the only person known to have carried a saxitoxin poison pin (Fig. 2). There is no public record of saxitoxin ever being used to intentionally harm anyone. As of September 2018, 182 State Parties, including the US, are signatories to the United Nations Convention on the Prohibition of the Development, Production and Stockpiling of Bacteriological (Biological) and

toxin Weapons (Referred to as the Biological Weapons Convention, BWC).

As an update on the progress in Alaska, there are still no State approved shellfish beaches in Alaska. Since 1973 over 150 outbreaks of PSP have been reported there but monitoring costs for the extensive Alaskan coastline still precludes using beach monitoring and closures as an effective management strategy for safe shellfish harvesting. All Alaskan commercial shellfish products are, of course, tested in accordance with the Interstate Shellfish Sanitation Conference (<http://www.issc.org/2017-nssp-guide->) but no state-run program routinely tests subsistence and recreationally harvested shellfish. Community efforts, grant-funded projects and combined State-Community efforts have been initiated to test non-commercially harvested shellfish on a seasonal basis to address this need. Shellfish testing in Southwestern Alaska has been conducted since 2006 through support by the Aleutian Pribilof Islands Association and regional partners; a State-Community pilot program was conducted from 2012-2015 in four regions and efforts in Southeast Alaska to conduct regional testing began in 2017. These combined efforts and collaborations through the newly formed Alaska Harmful Algal Bloom Network (<https://aous.org/alaska-hab-network/>) are promising steps toward addressing safe shellfish harvesting in Alaska. However, much work is needed to fully understand harmful algal bloom ecology in Alaska and provide residents with responsive and cost-effective tools to monitor their harvests (Vandersea et al., 2018).

Acknowledgements

A hearty thanks is given to Rose Ann Cattolico for help in scanning the toxicity records. This project was completed in collaboration with North Pacific Research Board's Projects #1215 and #1616. The National Oceanic and Atmospheric Administration is acknowledged for maintaining the mouse bioassay and clam toxicity records.

References

- Berdalet, E., Fleming, L.E., Gowen, R., Davidson, K., Hess, P., Backer, L.C., Moore, S.K., Hoagland, P., Enevoldsen, H. 2015. *J. Mar. Biol. Assoc. U.K.* doi:10.1017/S0025315415001733
- Church Committee Hearings. (1975). Intelligence Activities Senate Resolution 21, Hearings before the Select Committee to Study Governmental Operations with Respect to Intelligence Activities of the United States Senate, 94th Congress, First Session, (Vol 1) – Unauthorized Storage of Toxic Agents September 16-18, 1975. https://archive.org/stream/Church-CommitteeHearings-Volume1-Toxic-Agents/Vol1ToxicAgents_djvu.txt
- CIA. (2015). <https://www.cia.gov/news-information/featured-story-archive/2015-featured-story-archive/francis-gary-powers.html>
- Evans, M.H. (1964). *Brit. J. Pharmacol.* 2, 478-485
- Evans, M.H. (1964). *Brit. J. Pharmacol.* 2, 478-485.
- Kao, C.Y., Nishiyama, A. (1965). *J. Physiol.* 180, 50-66.
- Kellaway, C.H. (1935). *Aust. J. exp. Biol. Med. Sci.* 13, 79-94.
- Magnusson, H.W., Carlson, C.J. (1951). *Alaskan Fish. Exptl. Comm., Fish. Products Lab., Tech Rept.* 2, 1-10.
- Neal, R.A. (1967). Fluctuations in the levels of paralytic shellfish toxin in four species of lamellibranch mollusks near Ketchikan, Alaska, 1963-1965. Ph.D. dissertation, University of Washington, Seattle. 179 pp.
- Pacific Fishermen Yearbook. (1965). Miller Freeman, San Francisco.
- Patriot Act. (2011). <https://www.govinfo.gov/content/pkg/PLAW-107publ56/pdf/PLAW-107publ56.pdf>
- Powers, F.G., Gentry, C. (1970). *Operation Overflight*. Holt, Rinehart and Winston, NY. 375 pp.
- Public Broadcasting Station, History Detectives. (2005). Episode 1, Season 5. <http://www.pbs.org/opb/historydetectives/>
- The New York Times. (1965). May 4.
- Touchstone Pictures. (2105). 20th Century Fox. https://en.wikipedia.org/wiki/Bridge_of_Spies (film).
- Vandersea, M.W., Kibler, S.R., Tester, P.A., Holderied, K., Hondolero, D.E., Powell, K., Baird, S., Doroff, A., Dugan, D., Litaker, R.W. *Harmful Algae.* 77, 81-92.

Integrated management of Harmful Algal Blooms (HABs) along the French Channel area. A system approach to assess and manage socio-economic impacts of HABs

Pascal Raux¹*, José Pérez Agundez² and Sarra Chenouf¹

¹ Université de Bretagne Occidentale, IUEM, UMR AMURE, rue Dumont d'Urville, 29280 Plouzané, France;

² Ifremer, IUEM, UMR AMURE, rue Dumont d'Urville, 29280 Plouzané, France;

* corresponding author's email: pascal.raux@univ-brest.fr

Abstract

HABs occur naturally, but human activities that disturb ecosystems seem to play a role in their more frequent occurrence, intensity and spatial extent (Hallegraeff et al., 2004). Increased nutrient loadings and pollution, food web alterations, non-native species, current modifications and climate change all play a role (NOAA, 2018). Regarding impacted economic activities, HAB events are managed on a crisis basis, leading to closures of contaminated areas and/or ban commercial products based on *in situ* monitoring and alert systems. Developments in remote sensing science can bring a significant added value to existing monitoring systems. For instance, remote sensing can support the development of an alert system that could result in much faster response times. To assess to which extent it can mitigate the socio-economic impacts of HABs (monitoring and management costs, avoided economic losses, risk management by stakeholders), but also to understand the adaptation dynamics of economic activities to HAB events and the way they are managed, a system approach has been implemented to describe the HAB socio-ecosystem of the French-administrated part of the English Channel. It will help to address the intrinsic complexity of HABs and their impacts.

Keywords: marine toxins, system approach, economic impact, French part of English Channel, scallop fishery

Introduction

Economic and human health impacts of HABs increased over the last decades in relation with increased nutrient loadings and pollution, food web alterations, non-native species, current modifications and climate change. Growth of economic activities attached to the exploitation of coastal and marine resources (fisheries, aquaculture, tourism and recreational activities are most important ones) have also contributed to increasing impacts.

At the same time, research and knowledge about HABs and especially factors that contribute to HABs, have developed strongly, following the development of monitoring systems. Still, how these factors come together to create a bloom of algae is not well understood (NOAA, 2018). As a consequence, HAB events are managed on a crisis basis, leading to administrative closures of impacted areas to human activities relying on the use of contaminated resources. Existing monitoring and systems are often costly, spatially limited and not very responsive due to time constraints for toxicological analyses.

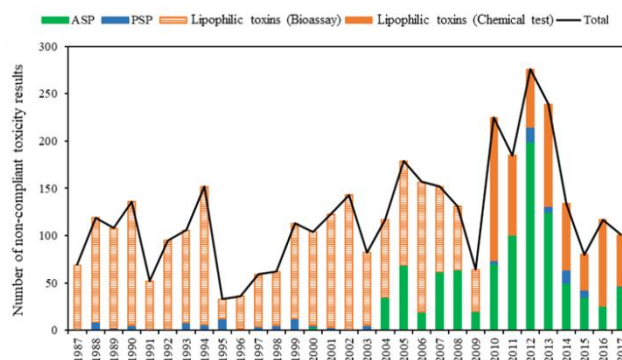


Fig. 1. Evolution of non-compliant results of toxicity/toxin testing over the 3 last decades (1987 – 2017) along the French Channel (data extracted from REPHYTOX monitoring network).

Remote sensing can thus bring a significant added value to existing monitoring systems. Using material from the Copernicus S-3 satellite, the Interreg France (Channel) England S-3 EUROHAB project is tracking the growth and spread of HABs in the Channel. These data will then be used to create a web-based system to alert

marine managers and fishing industries to the growth of potentially damaging algal blooms. The alert system should result in much faster response times. Data gathered will also help to better understand why, how and when HABs occur.

Facing HAB complexity, a system approach is implemented as a holistic and integrated approach to better assess and map HAB impacts over the Channel socio-ecosystem and their management, to address how far the proposed Web based alert system is able to mitigate these socio-economic impacts, and how economic activities are able to adapt to occurrences of HABs. Results will be used to feed and calibrate a regional economic model (I/O model) that will quantitatively assess the socio-economic costs of HABs along the French part of the English Channel for all potential affected activities. It will be also later used to explore scenarios for alternative management and refine the design of the web-based alert system.

Materials and Methods

Mapping of management processes, activities and impacts of HABs along the French Channel

An identification of economic activities impacted by HAB events was implemented in order to better understand HAB process from a monitoring and socio-economic point of view. This allows for mapping a first draft of the HAB system along the French part of the English Channel.

A DPSIR (Driver, Pressure, State, Impact, Response) framework was used to help building and mapping the system. It allows for an exhaustive and holistic view of HAB issues. Updates of mapping were made according to feedbacks from participative stakeholder workshops and interviews based on a shared and common view of the HAB system. Stakeholders were representatives of all potentially affected users as well as stakeholders in charge of the management of HAB events.

A system approach to address socioeconomic dimensions of HABs: beyond the assessments of impacts

The socio-economic dimensions of HABs go beyond the assessment of economic impacts. There is a lack of detailed information on human activities, especially regarding recreational ones. There are still ongoing debate and controversy about methods used for the assessments of economic impacts (mainly for non-market use). Sector-based assessments do not take in account cascade effects to other sectors. There is an important heterogeneity of individuals and companies rendering global evaluation complex.

There are different sensibilities to risk exposure and then different coping capacities and adaptation strategies. This results in different vulnerability profiles. There is also the need to take into account feed-back mechanisms and dynamics through adaptation strategies (individual and collective actions) and changes in regulation. To address this complexity and integrate the different socio-economic dimensions of HABs, a system approach is then applied (Bertalanffy 1968, Checkland 1999, Forrester 1961).

Application of the System Approach to the scallop fishery in the eastern Channel

The scallop fishery in the eastern Channel is the most important shellfish fishery in France. It counts for more than 250 fishing vessels, operating from October to May (legal fishing season). The annual production in 2017 was about 22,000 tons for a turnover of € 70 million. The fishery is strongly regulated in terms of fishing calendar, production areas, quotas, fishing trips and a minimum legal size of catch (11 cm). Due to the occurrences of HAB events, production areas can be closed leading to losses in production or additional cost to reach other remote and open production areas. The application of the System Approach to the scallop fishery proceeds with the characterisation of the monitoring subsystem and its spatial confrontation to the characterisation of the fishery subsystem (Figure 2).

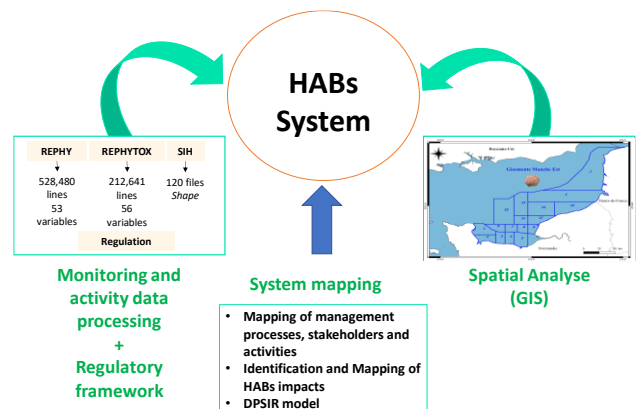


Fig. 2. Spatial confrontation of scallop fishery to HAB occurrences and the regulatory framework.

Data used for the spatial analysis are Phytoplankton cells count per litre and Phycotoxins concentration in shellfish from the REPHY and REPHYTOX monitoring networks managed by Ifremer, and production and value of scallops from the fisheries information system of Ifremer (SIH).

Assessment protocol of HAB risks over the fishing activity

The confrontation of monitoring data to the regulatory framework leads to the definition and construction of a protocol to derive a theoretical number of bans from HAB events integrating all toxins relevant to scallops. Using the R software, an algorithm was built to convert the abundance of toxic phytoplankton into a number of bans and duration of ban for each production areas (18 production areas). The script relies on a logical framework integrating regulatory information for each toxin and exploited species. A calendar of closures/openings was generated based on the results of the REPHYTOX monitoring network analysis. This calendar was then crossed with the fishing calendar, which is used for resource management purposes. Results from this cross-checking was finally used to generate the duration of bans expressed in days (Chenouf et al. 2020). This was later expressed through an indicator of loss rate of access days to fishing areas (Figure 3).

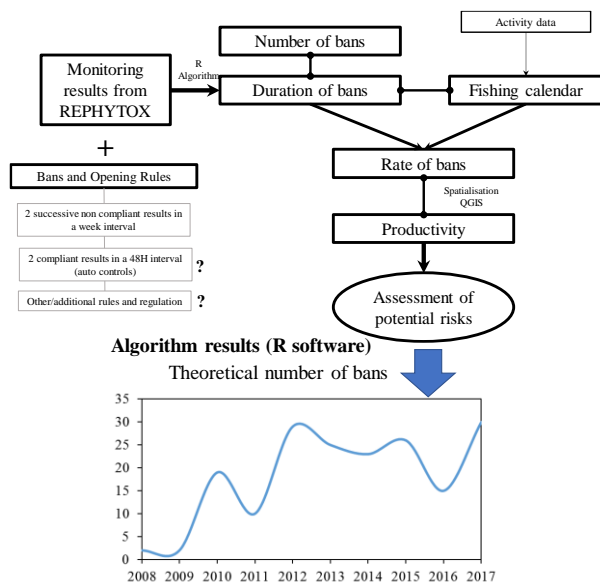


Fig. 3. Assessment protocol of HAB risks over the fishing activity

From 1988 to 2017, data used were:

- the abundance of toxic phytoplankton
- the number of alerts (evidence of phycotoxins impacting scallop species)
- the number of non-compliant results (results above the legal threshold)
- the number of bans and duration of bans per production area obtained from the R Algorithm.

The processed loss rate of access days to production areas was then confronted to the inter-annual production of scallop per production area to assess the risk exposure of the scallop fishery to HAB events. From the superposition of the two pieces of information a map of exposure to the HAB risk, based on the previous observation decade (2008-2017), was produced for each month of the fishing season (8).

Results and Discussion

The 8 monthly maps of exposure to the HAB risk form an atlas of HAB risk for the scallop fishery (Figure 4).

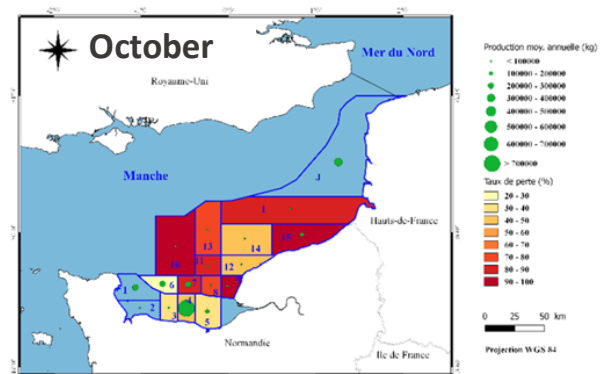


Fig. 4. Exposure map to the HAB risk for the October month.

The maps underline a strong exposure risk for the most important fishing period (from October to December) when production and prices are the most important. The potential for a web-based alert system seems to be quite important for this key period of the fishing season. The maps could be provided at a lower time scale, e.g. to assess the risk on a weekly basis, allowing fishermen to avoid risky areas. The web-based alert system would support fishermen by providing them with more detailed spatial information and almost real-time information to reduce potential losses of production due to contaminated areas.

But if threats in terms of HABs are naturally expressed in terms of negative impacts, the maps can also underline or question other impacts that could be positive. First when a HAB event occurs leading to a ban of one or several production areas, there are often no real losses of production for fishermen as they can redeploy their fishing effort to other production areas as underlined by the maps. This is particularly true for the eastern Channel where production areas are numerous (18). As a number of alternatives, some neighbouring production areas can remain opened

and accessible, fishing vessels can also be polyvalent and switch to other gears and species.

Reallocation of fishing effort over other production areas following occurrences of HAB events may then have consequences. Some of them could be either positive or negative. For instance, the closure of a production area can act as a biological rest and support stock dynamics. When the area is reopened after a long period, catches can also reach a premium market size with a significant added value for fishermen. Similarly, a more limited production due to HAB events can also be balanced by increasing prices at auctions for a scarce resource. But at the same time, the reallocation of fishing effort to other areas can lead to an overexploitation in these areas and to potential conflicts with other fishermen. The increase in production due to alternatives can also lead to decreasing prices.

There could be a balance between negative and positive impacts of HABs and they may act as a regulator of the scallop fishery in the eastern Channel.

There is thus a need to take into account the dynamics induced by the reallocation of fishing effort. This would require to work at a daily time scale and at the fishing vessel unit, to couple bio-economic models to HAB occurrences in order to assess the threshold above which HABs act as regulators or destructors of economic activities.

This potential regulator role of HABs can significantly impact the support from remote sensing through the proposed web-based alert system. Such an alert system can be positive if it contributes to alleviate the HAB constraints and the monitoring and control costs: mitigation of bans and associated costs, optimizing own checks, storage... But it questions the operational time scale of the tool (adverse effects for management purpose) and alleviating HAB constraints could also contribute to increase the fishing effort over the stocks.

The HAB system is a complex and dynamic system with a multivariate risk level. The System

Approach to HABs is a useful, holistic and shared representation of HABs, allowing to reveal hidden impacts of HABs. The definition and construction of an analysis protocol to translate monitoring and surveillance data into a risk exposure atlas through management measures can be replicated to other species, activities and areas. This a first use of data from the REPHY/REPHYTOX networks to a management purpose.

Acknowledgements

This study was carried out under the S-3 EUROHAB project funded through the French Channel English Interreg programme and led by the Plymouth Marine Laboratory.

References

- Bertalanffy, L. von. (1968). *General System Theory: Foundations, Development, Applications*, Revised ed. New York, NY, USA: Braziller.
- Chenouf S., Merzereaud M., Perez J., Raux P. (2020). Determination of scallop production areas closures due to phycotoxins along the Eastern English Channel using data from REPHY and REPHYTOX monitoring networks. SEANOE. <https://doi.org/10.17882/71912>
- Checkland, P. 1999. *Systems Thinking, Systems Practice*. New York, NY, USA: John Wiley & Sons.
- Forrester, J. 1961. *Industrial Dynamics*. Cambridge, MA, USA: MIT Press.
- Hallegraeff, G. M. et al. (2004). *Manual on Harmful Marine Microalgae*, Second revised edition, Hallegraeff, G.M., Anderson, D.M., Cembella, A.D. (Eds), Intergovernmental Oceanographic Commission UNESCO Publishing, 793p.
- NOAA. (2018). https://oceanservice.noaa.gov/facts/why_habs.html



Optical sensors and drone systems for the monitoring of harmful blooms

Development of a low cost optical sensor and of a drone system for the monitoring of cyanobacteria in freshwater ecosystems

Gabriel Hmimina¹, Kamel Soudani^{1*}, Florence Hulot¹, Louise Audebert¹, Stéphane Buttigieg², Patrice Chatelier², Simon Chollet³, Beatriz Decencièrè³, François Derkx², Catherine Freissinet⁴, Yi Hong⁵, Bruno Lemaire⁵, Alexis Millot³, Aurélien Perrin⁴, Catherine Quiblier⁶, Gonzague Six², Jean-Luc Sorin², Kevin Tambosco⁷, Viet Tran Khac⁵, Brigitte Vinçon-Leite⁵, Jean-François Humbert⁷

¹ ESE-Université Paris-Sud, Orsay ;

² IFSTTAR Nantes & Champs/Marne, Nantes ;

³ CEREEP, Foljuif ;

⁴ ARTELIA Grenoble, Grenoble ;

⁵ LEESU-ENPC Champs/Marne, Marne La Vallée,

⁶ MNHN Paris, Paris, France, ⁷ iEES Paris, Sorbonne Université

* corresponding author's email: kamel.soudani@u-psud.fr

Abstract

Cyanobacterial blooms frequently disturb the functioning of freshwater ecosystems and their uses, due to the harmful toxins that cyanobacteria are able to synthesize. Therefore, many countries have implemented monitoring programs aimed at reducing the risk of human exposure to these toxins. The main limitation is related to the heterogeneity of the spatial distribution of cyanobacteria. In the vertical dimension, these organisms can stay in different layers in the water column and in the horizontal scale, the cells may accumulate in some area of the water body, under the action of winds or currents. In an attempt to improve monitoring, many research projects have been undertaken in order to develop new tools, like buoys equipped with various underwater sensors. This tool is highly relevant but it does not allow assessing the horizontal distribution of cyanobacteria and its cost remains expensive. Moreover, if satellite remote sensing can be considered very useful for estimating biomass and horizontal distribution of cyanobacteria in a water body, the cost of this technology and the limited availability of satellites make it unaffordable for routine monitoring. In this context, our project named OSS-CYANO (Development of optical sensors and drone system for the survey of cyanobacteria) aims in a first time to develop and validate a new, low-cost aerial sensor. In this goal, we developed a framework for sensitive and selective estimation of phycocyanin concentration using a set of reflectance measurements over controlled mixes of phytoplankton cultures. The next part of our work aimed at developing an inexpensive passive optical sensor to selectively track phycocyanin, and which could be used for both high-frequency monitoring and drone-based measurements.

Keywords: Cyanobacteria, monitoring, optical sensor, drone system

Introduction

Blooms of cyanobacteria are a growing issue in inland waters due to eutrophication and to climate changes (Jöhnk et al. 2008; Pearl and Huisman 2009; Markensten et al. 2010). Adverse effects of these cyanotoxins on human and animal health have been described (eg. Kuiper-Goodman et al. 1999, Carmichael et al. 2001, Briand et al. 2003, Codd et al. 2005). The prevention of these effects requires frequent monitoring which currently involves regular field sampling followed by laboratory analysis, and identification and enumeration of phytoplankton. The cost-efficiency of such methods is limited by the spatial and temporal heterogeneity of cyanobacteria (Porat et al. 2001, Welker et al. 2003, Cuypers et al. 2011; Pobel et al. 2011).

Remote-sensing could be a suitable tool to address this issue, and several methods have been developed in order to track cyanobacteria-specific pigments (Li et al. 2015). Semi-empirical remote-sensing approaches are particularly promising as they explicitly tackle the issue of overlaps in pigments spectral features (Dekker et al. 1991; Simis et al. 2005). The major drawbacks of these approaches are that they require expensive instrumentation, extensive calibration and heavy computations. Most of the currently used optical sensors are active sensors (measuring signals transmitted by the sensor that are reflected, refracted or scattered by the Earth's surface), which are expensive and perform badly in turbid water.

To answer these issues, the OSS-CYANO project aimed at developing a framework and inexpensive sensor for quantitative passive optical detection of cyanobacteria. The main issues which needed to be addressed are the following:

- Deriving selective metrics using a limited number of bands.
- Limiting the effects of environmental factors in order to provide sensitive metrics in a wide range of conditions
- Providing an inexpensive and scalable way to measure the developed metrics.

A framework using mixes of phytoplankton cultures to derive selective metrics has been published (Hmimina et al. 2019) and was used to define a set of 6 spectral bands which could be used to selectively track concentrations in chlorophyll-a, phycocyanin and phycoerythrin. This work focuses on the development and validation of a sensor platform designed to accurately measure this spectral information.

Materials and Methods

Evaluation of the stability of optical indices in a changing light environment

A mesocosm experiment was run from July to November 2015 at the Foljuif CEREEP-Ecotron station (Ile-de-France, Equipex Planaqua, St-Pierre-les-Nemours). Three wave tank mesocosms (Blottiere et al. 2016) were coated with a fast-cure black silicon elastomer (Sylgard 170, Dow Corning, USA, Midland MI) and equipped with a set of four spectrometers (ASEQ, LR1-T spectrometer, 300–1000 nm, 0.6 nm resolution, thermoelectric cooler (TEC) module, Vancouver, Canada). Each tank was equipped with a nadir-looking spectrometer installed 50 cm above the water (FOV: 44 degrees, 40 cm diameter). The fourth spectrometer was equipped with a cosine corrector (CCSA1, Thorlabs, USA, Newton NJ). The four spectrometers were synchronized to acquire data simultaneously, and their integration time was optimized in order to obtain a constant signal versus noise ratio. The acquired spectra were used to derive six 10 nm wide gaussian bands centered on 450 nm, 515 nm, 610 nm, 676 nm, 696 nm and 750 nm. A phycocyanin index was then computed as:

$$PC = \frac{R_{610} - R_{515}}{R_{610} + R_{515} - 2 \times R_{750}}$$

Following the Figure 1, with R_x the reflectance within the band x.

One mesocosm was kept free of phytoplankton while the two others were primed with a

cyanobacteria culture (*Microcystis* sp. PMC 816.12) the 26 August. The spectrum of the mesocosm exhibiting the highest growth as measured with a BBE Fluoro Probe spectrofluorometer (bbe Moldaenke GmbH, Schwentimental) was computed knowing that this probe allowed to estimate the cyanobacterial biomasses (expressed in $\mu\text{g L}^{-1}$) (e.g. Le Boulanger et al., 2002).

Sensor design and validation

A passive optical sensor was designed to quantify the reflectance in the previously mentioned bands. Six 10 nm FWHM optical bandpass filters (Beijing Bodian Optical Tech, China, Beijing) were placed within a 4 cm diameter white silicon integrative sphere, on top of six photodiodes (TEMD5080X01, Vishay, USA, Malvern PA) whose signals were amplified (OPA2380, Texas Instruments, USA, Dallas TX) then converted into digital signals and stored every second. The gain was continuously increased following a saw-tooth function using an adjustable potentiometer (AD5206, Analog Devices, USA, Norwood MA), and the measured radiance was computed using the slope between the gain and resulting signal after calibration in an integrative sphere.

The sensor PCB was designed using KiCad EDA (<http://www.kicad-pcb.org>), the mechanical parts were designed under OpenScad EDA (<http://www.openscad.org>) and 3D printed. The optical parts were molded in optical silicon (Sylgard 184 and MS-2002, Dow Corning, USA, Midland Mi).

One sensor was installed over a water body in Champs-sur-Marnes, Ile de France, France in 2017, along with a BBE Fluoro Probes spectrofluorometer (bbe Moldaenke GmbH, Schwentimental).

Results and Discussion

Evaluation of the stability of optical indices in a changing light environment

The spectrum of the measured reflectance over one of the mesocosms as a function of the wavelength is shown in Figure 1.

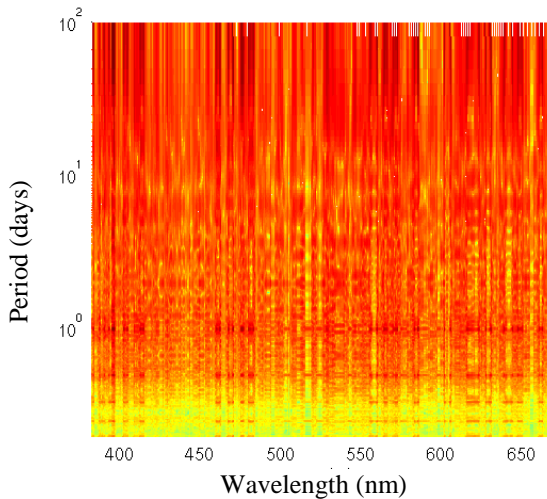


Fig. 1. Power spectral density of reflectance as a function of wavelength (x axis) and temporal scale (period in days, y axis).

Lines of high power densities can be seen for low periods (between 5 min and 1 day), indicating that the reflectance is sensitive to a high frequency phenomenon which affects all wavelength, with varying intensity. This can be explained by angular effects resulting from the interaction between waves and the solar angle.

Figure 2 shows the spectrum of the phycocyanin index.

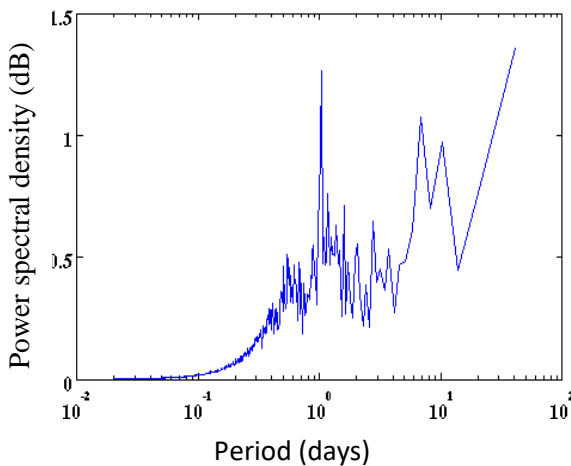


Fig. 2. Power spectral density (dB) of the phycocyanin index as a function of temporal scale (period in days, y axis).

High spectral densities can be seen for periods equal and lower than one day, and account for around one third of the total signal, indicating that the computation of a normalized optical index does not suppress the noise due to angular effects. To answer this issue, the high-frequency noise due to waves need to be filtered, and the high-frequency noise due to angular effects need to be addressed using observations made under comparable light conditions.

Sensor design and validation

The resulting sensor and its component are shown in Figure 3.



Fig. 3. Components and assembled optical sensor.

It was designed as a fully integrated sensor and datalogger, able to record water reflectance over a wide range of gain. The final production cost was lower than 500\$ per unit, and it was able to continuously record series of incident and reflected radiances in six spectral bands over a range of 256 gain values spanning 5 min each. The use of a gain versus radiance linear relationship fitted over a moving window spanning more than 5 min enable an automatic filtering of high-frequency noise due to waves and sudden changes in light environment. The obtained measurements of the phycocyanin index were related to cyanobacterial biomasses estimated by using the BBE-Spectrofluorometer as shown over the course of 12 days in Figure 4.

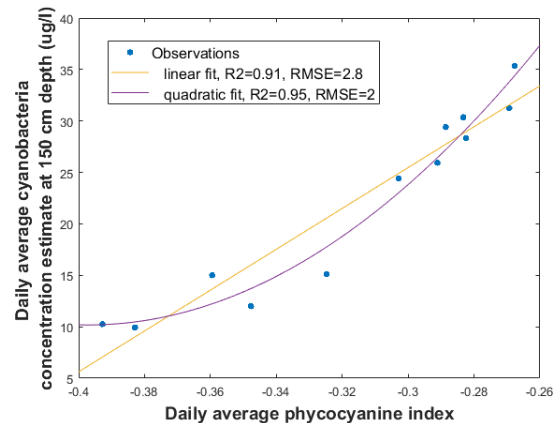


Fig. 4. Relationship between daily average phycocyanin index measurements and daily average

phycocyanin concentration derived from BBE measurement over the course of one of 12 days.

Significant relationships were obtained, indicating that the new passive sensor can provide a reliable estimation of phycocyanin concentration. Future efforts will focus on testing the sensor suitability for spatial sampling, and its ability to track phycocyanin concentration over a wider range of different aquatic ecosystems.

Acknowledgements

This work was supported by the ANR OSS-CYANO project ANR-13-ECOT-0001, grant ANR-2013-Ecotechnologies & EcoServices (ECO-TS) of the French Agence Nationale de la Recherche. This project has also benefited from technical and human resources provided by CEREEP-Ecotron Ile De France (CNRS/ENS, UMS 3194). Sampling was done in cooperation with the technical team of the Champs-sur-Marne area.

References

- Blottière, L., Jaffar Bandjee, M., Jacquet, S., Millot, A. and Hulot, F. D. (2017). *Freshw Biol*, 62: 161-177.
- Briand, J.-F., Jacquet, S., Bernard, C., & Humbert, J.-F. (2003). *Veterinary Research*, 34(4), 361–377.
- Carmichael, W. W., Azevedo, S. M. F. O., An, J. S., Molica, R. J. R., Elise, M., Lau, S., ... Renato, J. R. M. (2001). *Environ. Heal.*, 109(7), 663–668.
- Codd, G., Lindsay, J., Young, F., Morrison, L., & Metcalf, J. (2005). *Harmful Cyanobacteria*, 3, 1–23.
- Cuypers, Y., Vinçon-Leite, B., Groleau, A., Tassin, B., & Humbert, J.-F. (2011). *The ISME Journal*, 5(4), 580–589.
- Dekker, A. G., Malthus, T. J., & Seyhan, E. (1991). *IEEE Transactions on Geoscience and Remote Sensing*, 19(1), 89–95.
- Hmimina, G., Hulot, F. D., Humbert, J. F., Quiblier, C., Tambosco, K., Lemaire, B. J., Vinçon-Leite, B., Audebert, L., Soudani, K. (2019). *Water Research*, 148, 504-514.
- Jöhnk, K. D., Huisman, J., Sharples, J., Sommeijer, B., Visser, P. M., & Stroom, J. M. (2008). *Global Change Biology*, 14(3), 495–512.
- Kuiper-Goodman, T., Falconer, I., & Fitzgerald, J. (1999). *Human Health Aspects*. London: Taylor & Francis.
- Leboulanger, C., Dorigo, U., Jacquet, S., Le Berre, B., Paolini, G., Humbert, J.F. (2002) *Aquatic Microbial Ecology*, 30, 83-89.
- Li, L. H., Li, L., Song, K., Li, Y., Tedesco, L. P., Shi, K., & Li, Z. C. (2013). *Remote Sensing of Environment*, 135, 150–166.
- Markensten, H., Moore, K., & Pearson, I. (2010). *de Figueiredo, D. R., A. M. M.*
- Paerl, H. W., & Huisman, J. (2008). *Science*, 320(5872), 57–58.
- Pobel, D., Robin, J. J., & Humbert, J.-F. F. (2011). *Water Research*, 45(3), 1005–1014.
- Porat, R., Teltsch, B., Perelman, A., & Dubinsky, Z. (2001). *Journal of Plankton Research*, 23(7), 753–763.
- Simis, S. G. H., Peters, S. W. M., & Gons, H. J. (2005). *Limnology and Oceanography*, 50(1), 237–245.
- Welker, M., Von Döhren, H., Täuscher, H., Steinberg, C. E. W., & Erhard, M. (2003). *Archiv Für Hydrobiologie*, 157(2), 227–248.

Coupling high-frequency measurements and predictive modelling for monitoring and an early warning system of cyanobacteria blooms

Brigitte Vinçon-Leite*¹, Francesco Piccioni¹, Yi Hong¹, Viet Tran Khac¹, Bruno J. Lemaire¹, Denis Furstenuau Plec¹, Chenlu Li¹, Philippe Dubois¹, Mohamed Saad¹, Gabriel Hmimina², Kamel Soudani², Catherine Quiblier³, Kévin Tambosco⁴, Gonzague Six⁵, Catherine Freissinet⁶, Brigitte Decencièrre⁷, Jean-François Humbert⁴

¹ LEESU, Ecole des Ponts ParisTech, AgroParisTech, UPEC, Université Paris Est, Marne La Vallée, France

² Ecologie Systématique Evolution, CNRS, AgroParisTech, Université Paris-Saclay, Orsay, France

³ Museum National d'Histoire Naturelle, UMR 7245 MNHN-CNRS, 75231 Paris, France

⁴ iEES Paris-INRA, Sorbonne Université, 75005 Paris, France

⁵ IFSTTAR, Université Paris Est, Marne La Vallée, France

⁶ ARTELIA, 6 Rue Lorraine, F-38130 Echirolles, France

⁷ ENS, CNRS, CEREEP Ecotron IDF, UMS 3194, St Pierre Les Nemours, France

* corresponding author's email: b.vincon-leite@enpc.fr

Abstract

In urban watersheds, anthropogenic activities have major impacts on the ecological quality of water bodies. The degradation of water quality can result in toxic cyanobacteria blooms, which in turn may cause serious health risks to people in contact with water, *e.g.* when doing water sports. Due to the complexity of natural processes in water bodies, physically-based and spatially distributed models are valuable tools for better understanding the interactions between variables driving cyanobacteria blooms, as well as for helping stakeholders determine management strategies. However, traditional *in situ* measurements are limited by temporal and spatial resolution to make such numerical models reliable. Continuous *in situ* measurements provided by automated high-frequency monitoring can significantly improve adaptive decision-making. The main objectives of this work were to (i) set up a full-scale experimental site for high-frequency monitoring of cyanobacteria biomass in an urban lake; (ii) couple the high-frequency measurements and a physically-based three-dimensional hydro-ecological model for predicting cyanobacteria blooms; (iii) implement a transfer platform for real-time data management; and (iv) develop a web platform for communicating information to lake managers, other stakeholders and the public. These steps were conducted in the framework of the *OSS-cyano* project, funded by the French Research Agency (ANR). The study site is Lake Champs-sur-Marne (0.12 km² surface, 3.5 m maximum depth), located in Greater Paris. The field monitoring includes measurements of water temperature, dissolved oxygen, chlorophyll-a fluorescence and phycocyanin fluorescence at 10 min time steps, and regular vertical profiles of temperature and fluorescence of the main phytoplankton groups. The Delft3D hydrodynamic and ecological modules, *Flow* and *Bloom* respectively, were implemented. Using continuous measurements and short-term meteorological forecast, a predictive modelling of the cyanobacteria biomass evolution over four days was performed. Simulation results can then be communicated to the lake manager and the public through a web platform for health risk warning.

Keywords: urban lakes, forecasting, 3D modelling, web platform

Introduction

Urban lakes provide essential ecosystem services. They are important recreational areas and hotspots of biodiversity (*e.g.* Hill et al., 2015). Many urban lakes can also be considered as key elements in the drainage network as they retain storm water and prevent floods and also reduce associated pollutant loadings (*e.g.* Hassall and Anderson, 2015). Their role in the hydrological cycle and the fate of pollutants in urban watersheds must be better

understood (Birch and McCaskie, 1999). Most urban lakes react rapidly to external hydrological and meteorological forcings and are directly affected by climate change. Efficient monitoring systems are increasingly required for the management of lake ecosystems.

High nutrient loads from anthropogenic activities in the watershed can boost aquatic primary production. Due to global warming the risk of toxic

cyanobacteria blooms increases and so do public health problems (Lürling et al., 2017; O'Neil et al., 2012). For bathing areas, threshold levels of cyanobacteria biomass and toxin concentrations are provided by the European Union bathing water directive 2006-7 EC or the World Health Organization (WHO) guidelines which require that cyanobacteria biomass is monitored to avoid health risks. The EU directive in each member country is implemented by monitoring schemes based on cyanobacteria cell numbers. The regulation application is hampered by the delay between water sampling and the availability of the laboratory results which can take more than one week. This can lead to wrong decisions: swimming should have been banned some days earlier or conversely, the bathing prohibition decided on before getting the lab results was not necessary. In this context, the *Oss-Cyano* project (Development of optical sensors and drone system for the survey of cyanobacteria) was instigated with the aim to develop and validate a low cost, adaptive and efficient monitoring system of cyanobacteria blooms. In parallel with the development of a new aerial sensor (Hmimina et al., 2018), part of the project was dedicated to cyanobacteria bloom forecasting, through the coupling of high-frequency ground-truthing measurements to a physically-based three-dimensional hydro-ecological model. Six public research laboratories and one private company were involved in this project, funded by the French Research Agency (ANR).

During the last decade, specialized sensors that make it possible to measure *in situ* proxies of cyanobacteria biomass were developed. Nevertheless, operational measuring systems of the cyanobacteria specific pigment, phycocyanin, are not widely used and seldom *in situ* validated with reference methods. Warning stations using these sensors are even less common in freshwater bathing areas. In this paper we present (i) the design of a high-frequency monitoring of cyanobacteria biomass in a recreational urban lake; (ii) the field survey implemented for validating the real-time monitoring system and the predictive modelling; (iii) the dataset obtained and the results of the hydro-ecological model and (iv) the web platform for communicating information to lake managers, other stakeholders and the public.

Materials and Methods

Study site

Lake Champs-sur-Marne (48°51'50"N, 2°35'53"E) is located in the eastern Great Paris area, France. It is a sand-pit lake fed by the water table from the

nearby Marne River (Fig. 1). The lake is small (12 ha) and shallow (mean depth 2.4 m). It is a recreational area offering diverse outdoor activities (bathing, kayaking, sailing). Every summer, more than 5000 children from the neighbourhood visit the lake. Toxic cyanobacterial blooms, mainly *Aphanizomenon*, *Dolichospermum* and *Microcystis*, frequently occur.

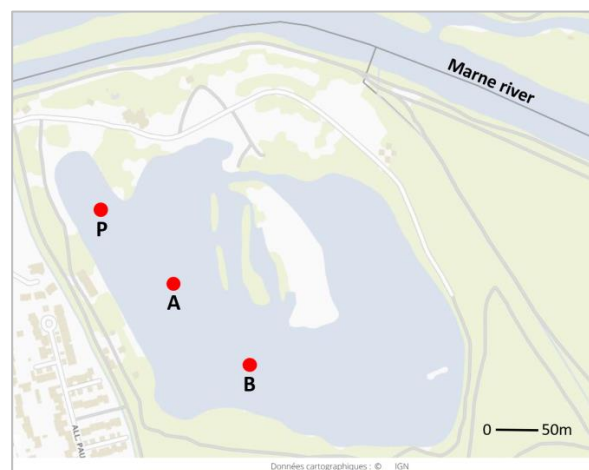


Fig. 1 Location of the monitoring sites

High-frequency monitoring system

High frequency measurements (every 10 min) of physical-chemical variables (water temperature, conductivity, pH, O₂), chlorophyll-a fluorescence (Chl_a hereafter), as a proxy of total phytoplankton biomass, and phycocyanin fluorescence, as a proxy of cyanobacteria biomass, were performed at three different sites (P, A and B, Figure 1). At each site, the continuous monitoring was performed at three depths for sites A and B and two depths for site P using a set of different underwater sensors. At sites A and B two thermal sensors were installed at 0.5 and 2.5 m depths; at site P only at 0.5 m depth. At the three sites a multi-parameter sensor was located at 1.5 m depth for measuring water temperature, pH, conductivity, dissolved oxygen, Chl_a and additionally phycocyanin at site B. The detailed technical characteristics of the sensors are presented in Tran Khac et al. (2018). At site B the data were measured at 1.5 m with a multiparameter probe (nke Sambat) and transmitted by a GPRS system to an onshore server once a day.

Field sampling

Fortnightly (in summer and autumn) to monthly (in spring and winter) field profiles were measured for four years, from mid-2015 to 2018 (75 samplings). Four phytoplankton groups (green algae, diatoms, cryptophytes and cyanobacteria) were measured with a spectrofluorimetric probe (BBE

Fluoroprobe), temperature, conductivity, dissolved oxygen and pH with a multi-parameter probe (Seabird SBE19). Laboratory analysis of Chla and phycocyanin were done in 2017 and 2018 (20 campaigns).

The model

Within the three-dimensional modelling suite Delft3D (Deltares, 2019) *Flow* and *Bloom* modules were used to simulate the hydrodynamics and the chlorophyll concentration used as a proxy of the total phytoplankton biomass, possibly including cyanobacteria. The physical domain features 801 cells (10 m x 10 m), in 12 horizontal layers (0.35 m thick) on the vertical axis. The $k-\epsilon$ turbulence closure model was used. The ecological module included 4 classes of phytoplankton: green algae, diatoms, flagellates and cyanobacteria.

Results and Discussion

Design of the warning system

The monitoring and warning systems were respectively based on the on-line measurements of water temperature, Chla and phycocyanin fluorescence collected at 1.5 m depth at site B and on the predictive modelling of cyanobacteria biomass during the 3 following days (Fig.). The data were validated through an automated script chain and stored in an onshore database (Tran Khac et al., 2018). In parallel a three-day progressive weather forecast was also provided to the database. On the one hand, the data were displayed for a visual assessment and on the other hand, they supplied the model initial concentrations of Chla and cyanobacteria. The model provides a space and time prediction of water temperature, Chla and cyanobacteria concentrations, in particular in the region of interest, the bathing area near site P (Figure 1).

Validation of the real-time monitoring data

It was necessary to assess the reliability of the realtime data of Chla and phycocyanin at site B before using them in the warning system. For doing this, the continuous measurements at 1.5 m depth at site B were compared to the measurements of the same variables at the other sites A and P and at other depths, with different sensors and with lab analysis. The automatic correction and validation algorithms were based on the comparative analysis of these data.

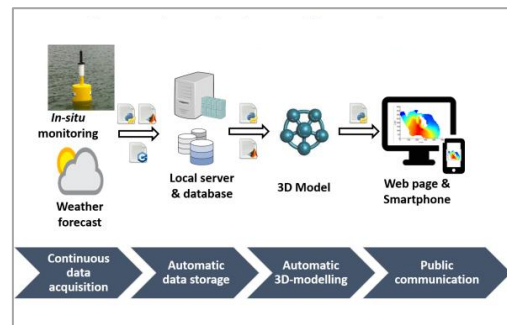


Fig. 2. Monitoring and warning system design

Modelling results

Hydrodynamics - The performance of the hydrodynamic model was first assessed. Beyond water temperature, the hydrodynamic model provides the biological module with the alternation of stratification and mixing of the water column, which drives the water motion and has a strong impact on cyanobacteria growth and transport. *Delft3D-Flow* was calibrated with a dataset collected in July 2015 and validated against the 2016 data. The hourly simulated and observed temperature at the measuring sites (0.5, 1.5 and 2.5 m depth) for the years 2016, 2017 and 2018 were compared. The agreement between modelling results and data, assessed through the Root Mean Square Error (RMSE) value (0.8°C) can be considered excellent and comparable to modelling results obtained in a neighbour shallow urban lake (Soulignac et al., 2017). The hydrodynamic model is able to satisfactorily simulate the changing hydrodynamics in Lake Champs and its impact on cyanobacteria biomass.

Cyanobacteria biomass - The biological module *Delft3D-Bloom* was then calibrated with a dataset collected for two weeks in July 2015. The results of a simulation performed over another 2 week period in 2018 (July 25th to August 8th) are presented on Figure 3. This period featured a sequence of thermal stratification of the water column (25th to 28th July), a mixing period from 29th to 31st July and a new stratification period from August 1st. The biological model was able to capture the timing and intensity of the observed Chla peak on July 29th (Figure 3). However, the simulated Chla concentration was overestimated, reaching a peak on July 31st. The following decreasing trend was then correctly represented. The cyanobacteria biomass also slightly increased until July 29th and then remained at this level. The model was able to simulate the cyanobacteria dynamics.

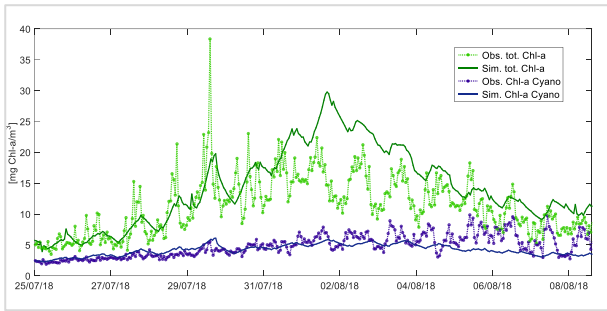


Fig. 3. Simulated and observed total and cyanobacteria chlorophyll (site B Jul-Aug 2018)

On-line warning system

The monitoring data and short-term predictive chain were embedded in a prototype of the warning system. An example of the short-term forecast (01-05/08/2018) is displayed in Fig. . The predictive results can be afterwards compared with the measured concentrations in order to check the validity of the forecast. In this case, the model forecast was close to the lower threshold of chlorophyll concentration in recreational waters considered as a moderate health risk level by the WHO (Chorus et al., 2000). This forecast, based on predicted chlorophyll concentration, would have drawn a moderate attention at the development of cyanobacteria. The lake managers would not need to collect samples for species identification and toxin analysis.

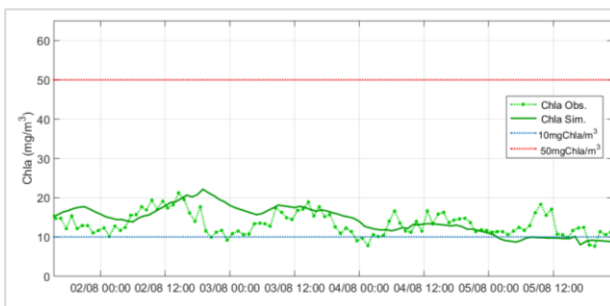


Fig. 4. Short-term forecast (4 days) of chlorophyll concentration. The blue and red lines indicate the threshold according to the WHO guidelines for low (10 $\mu\text{g/L}$) and moderate (50 $\mu\text{g/L}$) cyanobacteria health risk levels.

The website for displaying the monitoring data and the short-term forecast is under construction. The prototype webpage (<https://balneau-leeusu-rec.enpc.fr/#!/dashboard>) of the forecast display is presented in Fig. .

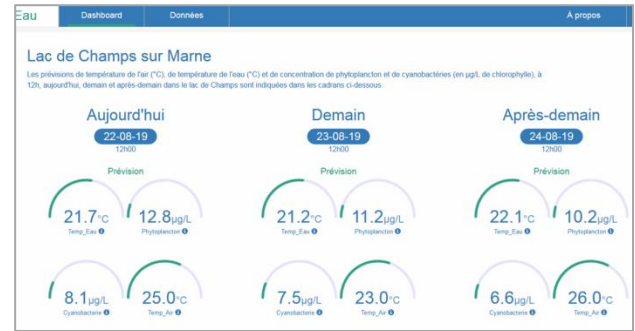



Fig. 5. Website page of the short-term forecast

Acknowledgements

This study was carried out under the ANR *OSS-Cyano* project (ANR-13-ECOT-0001). The authors would like to thank M.-A. Augé, A. de Bois and the DSI department of Ecole des Ponts ParisTech for their work in the development of the website prototype. The environmental observatories OSU EFLUVE and SOERE OLA contributed to the financial support for equipment maintenance. The authors also acknowledge the Département de Seine-Saint-Denis (CD93) and the Base de loisirs du lac de Champs/Marne for their logistical support in the field campaigns and fruitful discussion.

References

- Chorus I., Falconer I.R., Salas H.J., Bartram J., 2000. J. Toxicol. Environ. Health-Part B-Crit. Rev. 3, 323–347.
- Deltares, 2019. Delft3D No. V 5.06 Rev: 60089
- Hmimina G., Hulot F.D., Humbert J.F., Quiblier C., Tambosco K., Lemaire B., Vinçon-Leite B., Audebert L., Soudani K., 2019. Water Research 148, 504–514.
- Lüring M., M. Van Oosterhout F., Faassen E., 2017. Toxins, 9, 64.
- O’Neil J.M., Davis T.W., Burford M.A., Gobler C.J., 2012. Harmful Algae, 14, 313–334.
- Soullignac F., Vinçon-Leite B., Lemaire B., Martins J.R., Bonhomme C., Dubois P., Mezemate Y., Tchiguirinskaia I., Schertzer D., Tassin, B., 2017. Environ. Model. Assess. 1–14.
- Tran Khac V, Hong Y, Plec D, Lemaire B., Dubois, P., Saad, M., Vinçon-Leite, B., 2018. Processes 6, 11.



**Networking activities
around HABs: global HAB,
global HAB status report,
ICES-WGs and other
initiatives**

Overview of New Zealand HAB species and HAEDAT Events, with a comparison to Australian events

Enora Jaffrezic^{1,2,*}, Lesley Rhodes², Lincoln Mackenzie², Laura Schweibold^{1,3}, Gustaaf Hallegraeff³

¹Institut Universitaire Européen de la Mer, Plouzané, France

²Cawthron Institute, Nelson, New Zealand

³University of Tasmania, Hobart, Australia

* corresponding author's email: enora.j@outlook.fr

Abstract

As part of the preparation of a Global Harmful Algal Blooms Status Report, and to complete missing event data for the Australasian region, New Zealand harmful algal bloom (HAB) events with negative impacts on human society up to April 2018 were added to the IOC-ICES Harmful Algae Event Database (HAEDAT). The New Zealand occurrences of toxic microalgae species appearing on the reference list of IOC-UNESCO have also been catalogued. The similarities and differences of HAB events and species between Australia and New Zealand are reported and potential key factors that could explain highlighted to demonstrate the observed differences are suggested. The first referenced HAB event in New Zealand was a 'slime event' in the 1860s. Since then, many harmful and/or toxic events with varied impacts have occurred in New Zealand coastal and freshwater areas. One of the biggest toxic events, in terms of distribution, number of reported illnesses, and economic losses, was an unexpected neurotoxic shellfish poisoning (NSP) outbreak at the beginning of 1993 in the Hauraki Gulf. Since this event, weekly monitoring of harmful phytoplankton and biotoxins has been carried out. Overall, there are 110 Australasian HAB events catalogued in HAEDAT, 65 for Australia and 45 for New Zealand. In New Zealand, paralytic shellfish poisoning (PSP) is a predominant syndrome and has caused 35 human illnesses; PSP has also caused either illnesses or shellfish harvesting closures in Australia. NSP reports, including illnesses caused by *Karenia brevisulcata* aerosols, have caused 617 reported human cases in New Zealand, while no NSP events have been reported in Australia. In Australia, ciguatera fish poisoning (CFP) is the major reported syndrome and has caused 96 human illnesses, but no CFP has been recorded from consuming New Zealand fish. Also in Australia, 200 diarrhetic shellfish poisoning (DSP) illness events have been recorded whereas in New Zealand only 4 illnesses have been recorded.

Keywords: New Zealand, HAEDAT, harmful microalgae

Introduction

Harmful Algal Blooms (HABs) are a global phenomenon requiring an international approach for monitoring, management and improved understanding. In 2013, the IOC Intergovernmental Panel on HABs (IOC/IPHAB) and its partners launched the development of a Global HAB Status Report (GHSR) initiative (Hallegraeff *et al.*, 2017). The aim of these report series is to have a reference of HAB occurrences and events worldwide and their impacts on human health and ecosystem services. To achieve this, the occurrences of toxic algae are recorded per country and per harmful event in the Ocean Biogeographic Information System (OBIS), and in the Harmful Algae Event Data Base (HAEDAT) of the IOC International Ocean Data Exchange (IODE). Australia and New Zealand constitute one of the 13 designated OBIS

regions, named Australasia. Toxic species listed in OBIS and 60 HAEDAT events for this region were recorded in 2017. However, only the data of Australia had been recorded, introducing a bias in data processing for the Australasian region. In New Zealand, the first written record of a harmful event was a "slime event" in the 1860s, possibly caused by a *Gonyaulax* species (Washbourn, 1937). Since then, many harmful and/or toxic events with greater or lesser impacts have occurred in New Zealand coastal and freshwater areas. One of the biggest toxic events, in terms of distribution, victim number, and economic losses, was an unexpected NSP event in late of 1992/early 1993 in the north-eastern Hauraki Gulf (Jasperse, 1993). Since this event, weekly monitoring of the phytoplankton and also biotoxins in shellfish has been carried out.

The main objectives of this study were to [1] obtain an overview of the occurrences of toxic microalgae species and HAB events which have caused impacts on human society in New Zealand, and [2] compare HAEDAT events between Australia and New Zealand.

Materials and Methods

New Zealand toxic microalgae species

The first aim was to contribute to the distribution of New Zealand genus/species in the Taxonomic Reference List of Harmful Microalgae of IOC-UNESCO (Moestrup *et al.*, 2009). This list contains the valid taxonomic names and information about marine microalgae and freshwater cyanobacteria which produce toxins or which have toxic effects, and also species suspected to produce toxins.

Toxic microalgae occurrences in New Zealand, referenced in the published literature were catalogued. The scientific literature included referenced papers and reports about a toxic event, a toxic genus or species, or event due to biotoxin. The “grey literature” included conference proceedings and the online culture collection of microalgae of the Cawthron Institute (cultures.cawthron.org.nz) was also used.

New Zealand HAEDAT events

HAEDAT is an online meta database containing records of harmful algal events (in marine and freshwater bodies). Harmful algal events are recorded in HAEDAT by national focal points.

A harmful algal event is defined as (as per *Editors instructions for ON-LINE submission of data to HAEDAT*):

- (i) a water discoloration, scum or foam causing a socio-economic impact due to the presence of toxic or harmful microalgae,
- (ii) biotoxin accumulation in seafood above levels considered safe for human consumption,
- (iii) any event where humans, animals or other organisms are negatively affected by algae.

Before entering the New Zealand HABs events into HAEDAT, 11 grids were created, partly based on the location of aquaculture farms in New Zealand. New Zealand HAB events referenced in literature were entered into HAEDAT and the file was uploaded in April 2018. No events recorded after this date were entered.

Australia and New Zealand were compared according to seafood contamination and aerosol events. Different key factors which could explain the obtained results are presented. It is important to

emphasize that available information in HAEDAT on individual events or on species occurrences in OBIS varies greatly from event to event or country to country. Areas with numerous recorded events but with efficient monitoring and management programs, may have low risk of intoxications, whereas rare events in other areas may reflect severe problems and represent significant health risk.

Results and Discussion

Overview of the occurrence of toxic microalgae species and harmful events in New Zealand

From an analysis of the literature available, it was found that New Zealand waters host a total of 56 harmful marine microalgae species and 9 freshwater toxic species from the toxic species reference list of IOC-UNESCO. In total, 101 occurrences of toxic species have been recorded in New Zealand, and there are now 236 occurrences recorded for the Australasian region. Among the 56 species, 38 are toxic or potentially toxic to humans, meaning that they can cause poisoning or closures of commercial and recreational harvesting.

Eighteen species of recorded microalgae are ichthyotoxic or potentially ichthyotoxic, or can lead to anoxic conditions following high biomass decay. The location of these species and their impacts are presented in Figure 1. The majority of these species have been recorded in the Hauraki Gulf, Marlborough region and Tasman and Golden Bays, regions which contain many aquaculture farms. The high use of these coastal areas for aquaculture in New Zealand could explain the massive mortalities of caged fish and shellfish by direct toxic/physiological effects (mostly due to gill damage).

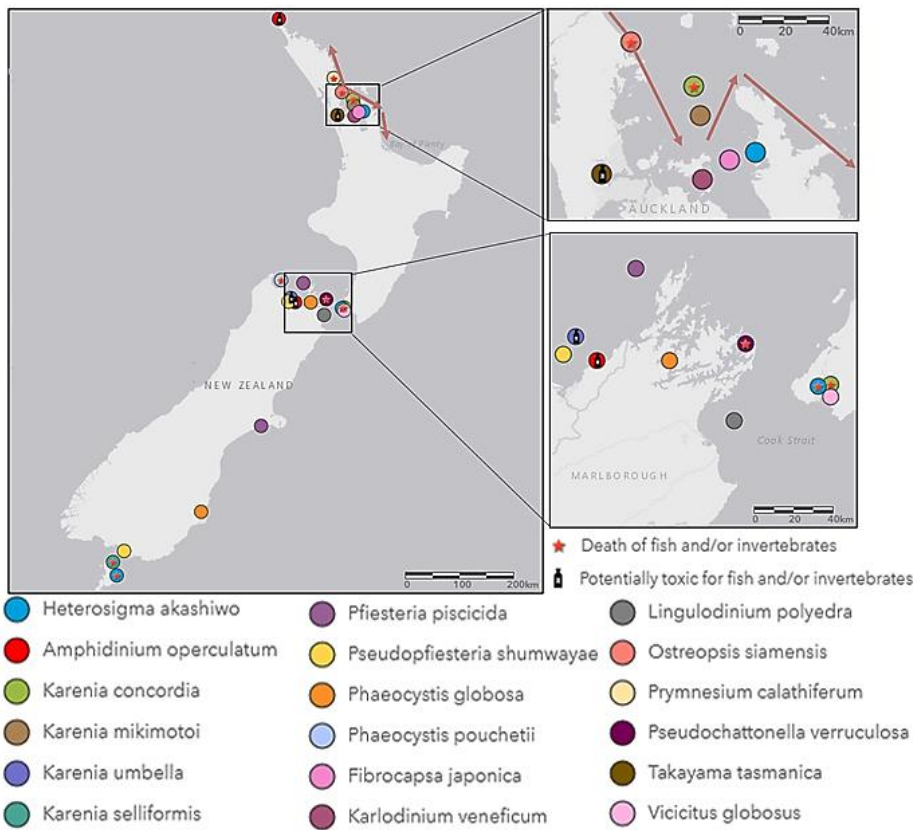


Fig. 1. Location of listed species lethal for fish and/or invertebrates by anoxia or by release of toxic compounds/mucus. Blooms with mortalities of fish and/or invertebrates are represented by a red star and potentially toxic species for fish and/or invertebrates are represented by a black bottle. The spread of an *Ostreopsis siamensis* bloom is represented by arrows. Inserts correspond to the Hauraki Gulf and Marlborough Sounds regions. Absence of events in a given location does not necessarily mean absence of toxicity or mortalities but reflects lack of monitoring or data.

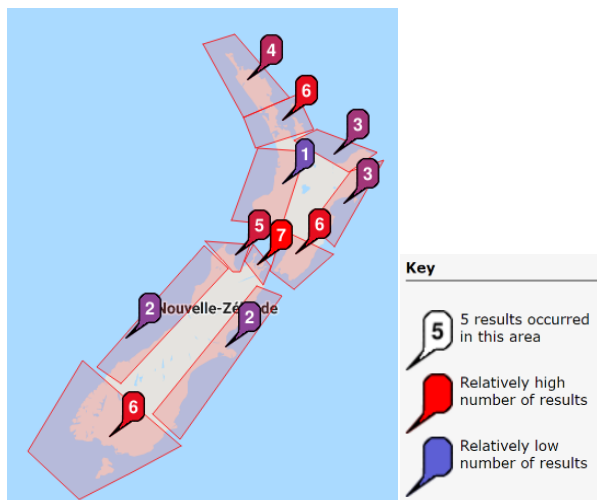


Fig. 2. Number of harmful algal events per grids in New Zealand (Source: Données cartographiques ©2018 Google, INEGI)

According to the HAEDAT website (downloaded in April 2018) New Zealand records include a total of 45 harmful events (Figure 2) whereas Australia records include a total of 65 harmful events. Most New Zealand HAEDAT events occurred in coastal areas which are highly used for aquaculture.

Differences between New Zealand and Australia in terms of seafood contamination events

Australia and New Zealand differ regarding the syndromes associated to seafood toxins (Fig. 4.). There were no Ciguatera Fish Poisoning (CFP) events in New Zealand whereas it is the main toxic

syndrome in Australia. This can be explained by the large quantity of tropical coral reef fish which can ingest and bioaccumulate toxic *Gambierdiscus* causing CFP in Australia, mainly in the Great Barrier Reef. The potential risk of CFP in New Zealand is through tropical fish which could transmit ciguatera migrating from subtropical regions to the New Zealand mainland (Rhodes *et al.*, 2017). NSP illnesses, including those caused by *Karenia brevisulcata* aerosols, have reached 617 reported human illnesses in New Zealand, but none have been reported in Australia. The two countries are similar in other regards. The same proportion of

paralytic shellfish toxin contamination has been reported in both countries, associated with either *Gymnodinium catenatum* or *Alexandrium* species. More human illnesses have been reported in New Zealand, mainly due to recreational shellfish gatherers, which are more common in New Zealand and who have not heeded warning signs of closures to harvesting (MacKenzie, 2014). Also, no amnesic shellfish poisoning events have occurred in either country, despite a number of toxic *Pseudo-nitzschia* species occurring in both countries. In New Zealand, amnesic shellfish toxin (AST) contamination risk is low despite many blooms, because the majority of *Pseudo-nitzschia* species that bloom only produce toxins in extremely low concentration (Rhodes *et al.*, 1998). In Australia, 200 DSP illness events have been recorded whereas only 4 illnesses have been recorded in New Zealand. The Australian event occurred in 1997 in an area with no prior biotoxin monitoring, while New Zealand has had a comprehensive monitoring program in place since 1993.

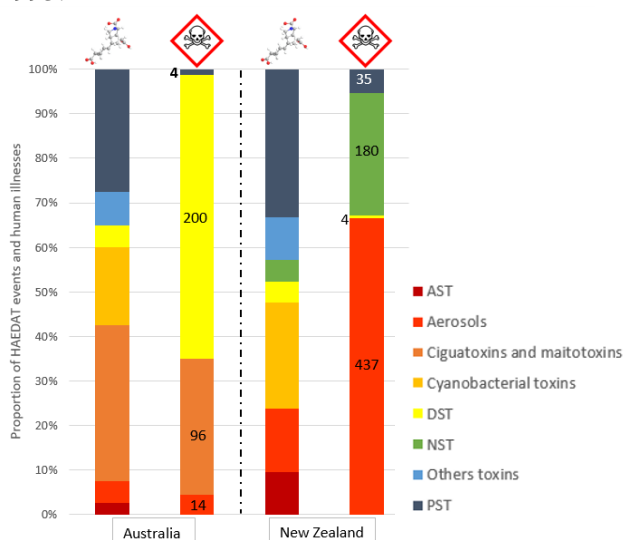


Fig. 4. Percentage of seafood contamination events above the safe toxic level among all the seafood contamination events recorded in HAEDAT in Australia and in New Zealand (left column) with the percentage of reported human illnesses associated with each toxin (right column)

Conclusion

The first objective of this work was to contribute to the GHSR by completing data recording of toxic microalgae occurrences and HAB events for New Zealand and thus for the Australasian region. Data sets still requires refining, especially for HAEDAT, such as the need for inclusion of more recent monitoring data for New Zealand. This will allow variation in the number of events and the number of human illnesses to be analysed over time to

determine the long-term benefits of the monitoring program. The second objective was to compare Australia and New Zealand in terms of HAEDAT events – in this case seafood contamination and aerosols events – and to determine factors which can explain the differences and similarities between the countries. In summary, the differences between Australia and New Zealand can be partially explained by a difference in the intensity of the monitoring programs, a different use of coastal areas for aquaculture (shellfish being a major export industry for New Zealand) and the different regional climatic conditions experienced by the two countries. (for example, tropical coral reefs contributing to CFP in Australia). A full account of this work will appear as part of a special issue of the journal *Harmful Algae* in preparation.

Acknowledgments

This paper is a part of work that has been achieved during the Master degree internship at Cawthron Institute by EJ between January and June 2018. I would like to thank Lesley Rhodes, my supervisor, for enabling me to participate at the 18th ICHA, Gustaaf Hallegraeff for this project on GHSR and Lincoln Mackenzie for his invaluable assistance in adding data.

References

- Hallegraeff, G.M., Bresnan, E., Enevoldsen, H., Schweibold, L., Zingone, A. (2017). *Harmful Algae News*, 58, 1-3.
- Jasperse JA (1993). Proceedings of a workshop on research issues, June 1993. The Royal Society of New Zealand, Misc. Ser. 24.
- MacKenzie, A. L. (2014). *New Zealand Journal of Marine and Freshwater Research*, 48(3), 430-465.
- Moestrup, Ø.; Akselmann, R.; Fraga, S.; Hoppenrath, M.; Iwataki, M.; Komárek, J.; Larsen, J.; Lundholm, N.; Zingone, A. (Eds) (2009 onwards). IOC-UNESCO Taxonomic Reference List of Harmful Micro Algae. Accessed at <http://www.marinespecies.org/hab> on 2018-04-24
- Rhodes, L., Scholin, C., & Garthwaite, I. (1998). *Natural Toxins*, 6(3-4), 105-111.
- Rhodes, L. L., Smith, K. F., Verma, A., Murray, S., Harwood, D. T., & Trnski, T. (2017). *New Zealand Journal of Marine and Freshwater Research*, 51(4), 490-504.
- Washbourn, H.P., 1936. Further reminiscences of early days. AG. Betts and Son, Nelson.



Proceedings of the 18th International Conference on Harmful Algae

www.issha.org

ISBN 978-87-990827-7-3

